

Hydroacoustic remote sensing of human impacted tidal and shallow water marine environments

Dissertation zur Erlangung des Doktorgrades der Naturwissenschaften (Dr. rer. nat.)
am Fachbereich Geowissenschaften der Universität Bremen

vorgelegt von
Ruggero Maria Capperucci

Bremen, October 2020

Betreuer der Promotion

Prof. Dr. Dierk Hebbeln

Dr. Alexander Bartholomä

Gutachter der Dissertation

Prof. Dr. Dierk Hebbeln

Prof. Dr. Verner Brandbyge Ernstsen

Prüfungsausschuss

Prof. Dr. Dierk Hebbeln

Prof. Dr. Verner Brandbyge Ernstsen

Dr. Alexander Bartholomä

Prof. Dr. Elda Miramontes Garcia

Dr. Daniel Hepp

Francis Ojukwu

Tag des Dissertationsskolloquiums

18. Februar 2020

Versicherung an Eides Statt

gem. § 5 Abs. 5 der Promotionsordnung vom 18.06.2018

Ich Ruggero Maria, Capperucci, Schlieffenstraße 49, 26123 Oldenburg,
Deutschland

(Vorname, Name, Anschrift)

versichere an Eides Statt durch meine Unterschrift, dass ich die vorliegende Dissertation selbständig und ohne fremde Hilfe angefertigt und alle Stellen, die ich wörtlich dem Sinne nach aus Veröffentlichungen entnommen habe, als solche kenntlich gemacht habe, mich auch keiner anderen als der angegebenen Literatur oder sonstiger Hilfsmittel bedient habe und die zu Prüfungszwecken beigelegte elektronische Version (PDF) der Dissertation mit der abgegebenen gedruckten Version identisch ist.

Ich versichere an Eides Statt, dass ich die vorgenannten Angaben nach bestem Wissen und Gewissen gemacht habe und dass die Angaben der Wahrheit entsprechen und ich nichts verschwiegen habe.

Die Strafbarkeit einer falschen eidesstattlichen Versicherung ist mir bekannt, namentlich die Strafandrohung gemäß § 156 StGB bis zu drei Jahren Freiheitsstrafe oder Geldstrafe bei vorsätzlicher Begehung der Tat bzw. gemäß § 161 Abs. 1 StGB bis zu einem Jahr Freiheitsstrafe oder Geldstrafe bei fahrlässiger Begehung.

Bremen, 11.10.2019

Ort, Datum

Unterschrift

A Clara e Gaia.

E a Serena, che ha reso possibile tutto.

Κι ἄν πτωχική τὴν βρεῖς, ἢ Ἰθάκη δὲν σὲ γέλασε.
Ἔτσι σοφὸς ποῦ ἔγινες, μὲ τόση πείρα,
ἤδη θὰ τὸ κατάλαβες ἢ Ἰθάκες τί σημαίνουν.

Κ. Π. ΚΑΒΑΦΗΣ

Abstract

Coastal areas are among the most ecologically diverse, economically valuable and fragile ecosystems in nature: human pressure on coasts is higher than on any other natural environment and it keeps growing; climate changes are also adversely affecting the coastal marine habitats. Tidal environments, with their peculiar combination of terrestrial, palustrine, and aquatic habitats are considered of extreme importance for biodiversity. Nevertheless, they are vanishing faster than any other complex ecosystem on Earth. In the past decades, national and international regulations were issued for mapping and protecting coastal and marine habitats. Therefore, the scientific community has been involved in finding efficient and effective methods for producing seafloor habitat maps, which could be used, then, as basis for habitat monitoring, protection, restoration, and for managing the sustainable development of coastal areas.

Among the possible different tools for habitat mapping, remote sensing and in-situ techniques represent a useful combination for characterizing large areas. Hydroacoustic sources have been used since decades for seafloor mapping and still represent the best tool for investigating the nature and the dynamics of underwater habitats. The large amount of different available acoustic systems and the variety of possible processing approaches led to a lack in standards about the optimal use of such systems for habitat mapping, thus in the last 10 years many programs were launched to bridge such gap. Nevertheless, many aspects are still unclear.

Seafloor roughness is among the most relevant parameters that influence the acoustic signal. Roughness is a product of multiple factors, including sediment composition and distribution (“*sediment roughness*”), seafloor morphology (“*topographic roughness*”), and biological communities (“*benthic roughness*”). Direct human disturbance (e.g. from dredging and dumping activities) further complicate the natural seafloor roughness.

The present research made use of multiple hydroacoustic sources (singlebeam and multibeam echosounders, sidescan sonars, ADCP) coupled with in-situ techniques, in order to study the role of the different roughness components in influencing the backscatter, both when automatic and expert-

based classification strategies are adopted. The results were used for assessing the impact of a deep-water terminal construction (JadeWeserPort, in the Jade Channel) on sediments and biocommunities. Five research sites within three areas (the backbarrier system of Norderney Island, the Jade Channel, and the seafloor in vicinity of the Helgoland Island) were selected in the German Bight (southern North Sea), in order to represent intertidal and subtidal environments characterized by the presence of both crisp and fuzzy habitat boundaries, hard and soft grounds, and affected by different degrees of human disturbance.

The results show that automatic classification tools allow to highlight the roughness factors that play the primary role in influencing the backscatter at specific sites. The multiple generations of dredging marks present in the Jade Channel dominated the classification outcomes (*topographic roughness* >> *sediment and benthic roughness*). As a result, the acoustic classes corresponded to the main morphological regions, rather than to the sediment bottom characteristics. For the habitat mapping of the strongly impacted area nearby the JadeWeserPort, an expert-based approach was therefore preferred. The impact of the port construction produced a redistribution of sediments and the development of new benthic assemblages (mainly made by opportunistic and highly mobile species), which replaced the existing ones.

On the less disturbed seafloor in the nearby of Helgoland, the crisp boundary between the soft and hard ground regions was correctly identified by the automatic classification tools (*topographic roughness* >> *sediment and benthic roughness*). In addition, the acoustic data showed that in the soft ground area characterized by homogeneous sediment composition and by the absence of seafloor morphologies, the presence of a dense colony of soft, centimetre-sized brittle stars (devoid of rigid structure) was able to modify the backscatter values (*benthic roughness* >> *topographic and sediment roughness*). Such fuzzy boundary was also successfully mapped on the automatic classification outcomes. However, within the hard ground regions the detection of two different population of bryozoan resulted to be difficult (*topographic and sediment roughness* >> *benthic roughness*).

In the Norderney intertidal and subtidal areas, the complex interplay of all the roughness components made it difficult to use automatic classification tools (*topographic* \approx *sediment* \approx *benthic roughness*), which were at most able to identify the main tidal-flat drainage system. On the contrary, the expert-based approach allowed the segmentation of the sidescan-sonar backscatter in several morpho-sedimentary and benthic classes. A comparison with an existing seafloor classification based on satellite data (RapidEye) showed the superior ability of

sidescan sonar in resolving seafloor structures, sediment classes, and shellfish beds.

The outcomes of the present research offered a contribution to the development of recommendations and guidelines for mapping and monitoring the German coastal waters (WIMO Project – Scientific monitoring concepts for the German Bight).

Page left intentionally blank

Zusammenfassung

Küsten gehören in der Natur zu den ökologisch vielfältigsten, komplexesten und gleichzeitig auch zu den sehr empfindlichen Ökosystemen. Besonders einzigartig ist die hohe Biodiversität der Gezeitemsysteme mit ihrer großen Bandbreite von Faziestypen, die von voll marin bis hin zu voll terrestrisch reichen. Natürliche Veränderungen bedingt durch den Klimawandel und die intensive wirtschaftliche Nutzung durch den Menschen lassen den Existenzdruck auf dieses Ökosystem immer stärker werden, mit der Gefahr, dass dieses System nachhaltig gestört, beziehungsweise in Teilen gänzlich verloren geht.

Für die Bewertung des ökologischen Zustandes des Wattenmeeres wurden während der letzten Jahrzehnte eine Reihe nationaler und internationaler Regelwerke entwickelt, die den Zustand einerseits bewerten und andererseits schützen. In diesem Rahmen war die Wissenschaft immer wieder gefordert, sinnvolle und effiziente Methoden zur Seeboden- bzw. Habitat-Kartierung zu entwickeln, die für das Monitoring, für die Erstellung von Schutzbestimmungen, für die Rückgewinnung bereits verlorener Gebiete und für das Management einer nachhaltigen Nutzung herangezogen werden können.

Unter den zahlreichen Verfahren zur Habitatkartierung haben sich Fernerkundungsmethoden in Verbindung mit in-situ-Verfahren für Kartierung und Charakterisierung besonders weiträumiger Habitate an Land und im Intertidal/Eulitoral bewährt. Für die häufig hoch dynamischen Habitate im Subtidal/Sublitoral wurde die hydroakustische Seebodenklassifizierung als alternative Methodik für in der akustischen Unterwasserfernerkundung entwickelt. In den letzten zehn Jahren wurde immer wieder versucht, die Verfahren aus der Unterwasserfernerkundung mit denen der terrestrischen Fernerkundung zu koppeln, um eine möglichst vollständige Erfassung vom Subtidal bis ins Supratidal zu erreichen. Doch leider bestehen hier immer noch einige Lücken in der Verfahrensanpassung.

Die Rauheit des Meeresbodens in ihrer Gesamtheit ist das Hauptmerkmal im akustischen Rückstreusignal in der Unterwasserfernerkundung. Es stellt die Summe aus vielen Einzelfaktoren wie der Sedimentzusammensetzung und Sedimentverteilung („*sediment roughness*“), sowie dem Meeresbodenrelief

(„*topographic roughness*“) und den benthischen Besiedlungsstrukturen („*benthic roughness*“) dar. Überprägt werden diese Faktoren durch künstliche, vom Menschen verursachte Rauheit wie das Relief von Baggerspuren.

Für die in dieser Arbeit vorstellten Forschungsarbeiten wurden mehrere akustische Signalquellen (Einstrahlecholot, Fächerecholot, Seitensichtsonar und akustischer Strömungsmesser ADCP) in Verbindung mit visuellen und in-situ-Beprobungen auf ihr unterschiedliches, akustisches Ansprechverhalten verschiedener Meeresbodentypen hin untersucht. Dabei wurden für die Bewertung der verschiedenen Rückstreucharakteristika manuelle und automatische Klassifizierungsverfahren genutzt.

Im Bereich des Tiefwasserhafens JadeWeserPort wurden die Verfahren für die Erfassung der anthropogen bedingten Veränderungen der Meeresbodenhabitate durch die dortigen Baumaßnahmen eingesetzt. Natürliche Veränderungen in der Habitatdynamik wurden an verschiedenen Lokalitäten in der südlichen Nordsee untersucht. Das Rückseitenwatt der ostfriesischen Insel Norderney stand dabei für sub- und intertidale Habitate des Wattenmeeres, die Bereiche um die Insel Helgoland für subtidale Offshore-Habitate. Schwerpunkte in der akustischen Detektion und Klassifikation stellten dabei scharfe und diffuse Übergänge von Habitatzonierungen in Weich- und Hartsubstraten sowie deren spezifischen Rauheitsmuster dar.

Die Auswertung mit automatisierten Klassifizierungsverfahren bildet deutlich die unterschiedlichen Rauheitsmerkmale in den verschiedenen Habitaten ab, die vorwiegend an die Substratzusammensetzung gekoppelt sind. In den wenig gestörten durch geringe Topographie gekennzeichneten Weichsubstraten um Helgoland, lassen sich die verschiedenen Rauheitsmerkmale deutlich abgrenzen. Massive Vorkommen von Schlangensterne sind hier als eigenes akustisches Signal zu erkennen. Die geringere Dichte von Bryozoen als Bewuchs auf den Hartsubstraten hingegen lassen sich nicht ohne weiteres automatisch klassifizieren.

Noch deutlich schwieriger gestaltet sich die Differenzierung stark anthropogen beeinflusster Gebiete wie dem JadeWeserPort. Hier dominiert die sekundär generierte Kleintopographie des Meeresbodens die Rückstreuung, Sedimente und Besiedlung treten im Rückstreusignal teilweise in den Hintergrund. Die Meeresbodenklassifizierung in solchen Gebieten lässt sich weitestgehend nur „händisch“ von Experten realisieren, die aktuellen automatischen Verfahren helfen in diesem Falle weniger. Die Bewertung der „Sekundärtopographie“ gewinnt in diesem Fall besonders an Bedeutung, da die Reorganisation der benthischen Gemeinschaften nach dem Baueingriff deutlich

die Topographie gebunden ist und erst im weiterer Entfernung vom Eingriff stärker mit den Sedimenten korrespondiert.

Die Wattmorphologie stellt ebenfalls eine Herausforderung an die automatische akustische Klassifizierung der Oberflächen dar. Charakteristisch sind die Rauheitsmuster von Muschelbesiedlungen und Entwässerungsstrukturen. Der direkte Vergleich von Satelliten-basierter Klassifizierung und Ergebnissen der Seitensichtsonar-Mosaikkarten im Intertidal zeigte jedoch deutliche Vorteile in der akustischen Klassifizierung. Sowohl die Möglichkeit einer durchgängigen Erfassung von Sub- und Intertidal ohne das Problem der Wasserbedeckung als auch die höhere Auflösung und bessere Identifikation von räumlichen Sedimentverteilungsmustern, Entwässerungsstrukturen und Besiedlungsdichten durch Muschelkolonien sprechen für die hydroakustischen Verfahren. Lediglich die deutlich größere Flächenabdeckung spricht für die Satelliten basierte Fernerkundung.

Page left intentionally blank

Table of Contents

Abstract	ix
Zusammenfassung	xiii
Table of Contents	xvii
List of Figures	xxiii
List of Tables	xxix
Aknowledgements	xxxiii
<i>Chapter 1</i> Introduction	1
1.1. <i>General introduction</i>	1
1.2. <i>Physical settings: tide-dominated coasts and the Wadden Sea</i>	5
1.3. <i>State of the art and open questions</i>	8
1.3.1. <i>Habitat, Habitat surrogates, and Seafloor roughness</i>	9
1.3.2. <i>From habitat mapping to habitat monitoring</i>	11
1.3.3. <i>Disturbance, Impact, and Habitat patchiness</i>	13
1.4. <i>Objectives</i>	15
1.5. <i>Thesis outline</i>	15
1.6. <i>References</i>	17
1.7. <i>Research funding</i>	27
1.8. <i>Declaration of contribution</i>	27
<i>Chapter 2</i> Marine Habitat Mapping: stretching the blue marble on a map	31
2.1. <i>Abstract</i>	31
2.2. <i>Introduction</i>	32
2.3. <i>What is Marine Habitat Mapping</i>	32
2.4. <i>Why Marine Habitat Mapping</i>	34
2.5. <i>How to map the marine habitat</i>	35
2.5.1. <i>In situ techniques</i>	35
2.5.2. <i>Remote sensing techniques</i>	36
2.5.3. <i>Hydroacoustic techniques</i>	37

2.6.	<i>Facing the challenge</i>	37
2.7.	<i>Finding a common strategy</i>	38
2.8.	<i>The 4th dimension of Marine Habitat Mapping: when?</i>	39
2.9.	<i>References</i>	40
Chapter 3 Sediment vs. topographic roughness: anthropogenic effects on acoustic seabed classification		47
3.1.	<i>Introduction</i>	47
3.2.	<i>Study area and methods</i>	48
3.2.1.	Data processing	50
3.3.	<i>Results</i>	50
3.3.1.	Sedimentary data	50
3.3.2.	Acoustic data	51
3.4.	<i>Discussion and conclusions</i>	53
3.5.	<i>References</i>	55
Chapter 4 Tools to evaluate seafloor integrity: comparison of multi-device acoustic seafloor classifications for benthic macrofauna-driven patterns in the German Bight, southern North Sea		57
4.1.	<i>Abstract</i>	57
4.2.	<i>Introduction</i>	58
4.3.	<i>Study area</i>	59
4.4.	<i>Materials and methods</i>	62
4.4.1.	Acoustic data	62
4.4.2.	Grab sampling	65
4.4.3.	Macrofauna and sediments	65
4.5.	<i>Data analyses</i>	66
4.5.1.	RoxAnn- and EchoPlus-based seafloor classification	66
4.5.2.	QTC-based acoustic seafloor classification	67
4.5.3.	Macrofauna	68
4.6.	<i>Results</i>	69
4.6.1.	Acoustic backscattering	69
4.6.2.	Derivates from bathymetry	69
4.6.3.	Acoustic seafloor classification	71
4.6.3.1.	QTC Swathview™ sidescan sonar	71
4.6.3.2.	QTC Swathview™ multi-beam echosounder	71

4.6.3.3. RoxAnn	72
4.6.3.4. QTC View 5.5™/QTC Impact™ single-beam echosounder	73
4.6.4. Sediments	73
4.6.5. Macrofauna	75
4.6.6. Brittle star abundance vs. side-scan sonar grey values	78
4.7. <i>Discussion</i>	79
4.7.1. Acoustic seafloor classification comparison	79
4.7.2. Influence of macrobenthos	80
4.8. <i>Conclusions</i>	82
4.9. <i>Acknowledgements</i>	83
4.10. <i>References</i>	83
Chapter 5 Sidescan sonar meets airborne and satellite remote sensing: challenges of a multi-device seafloor classification in extreme shallow water intertidal environments.	89
5.1. <i>Abstract</i>	89
5.2. <i>Introduction</i>	90
5.3. <i>Physical settings</i>	93
5.4. <i>Methods</i>	95
5.4.1. Sidescan sonar data collection and processing	95
5.4.2. Sediment samples data collection and processing	96
5.4.3. Lidar data	98
5.4.4. Seafloor classification	98
5.4.5. Comparison with RapidEye-TerraSAR-X seafloor classification	99
5.4.6. Geographic Information System (GIS)	99
5.5. <i>Results</i>	99
5.5.1. Morphology (Lidar data)	99
5.5.2. Sediment grain size distribution	100
5.5.3. Sidescan sonar 2013	101
5.5.4. Seafloor classification	105
5.5.5. Comparison sidescan sonar 2013 and 2014	107
5.6. <i>Discussion</i>	107
5.6.1. Seafloor classification	107
5.6.2. Tidal drainage system	108
5.6.3. Shellfish beds	108
5.6.4. Tidal flat deposits	110

5.6.5.	Comparison sidescan sonar 2013 and 2014	112
5.6.6.	Comparison with RapidEye-TerraSAR-X seabed classification	112
5.7.	<i>Conclusions</i>	114
5.8.	<i>Acknowledgments</i>	115
5.9.	<i>References</i>	116
Chapter 6 Hydrodynamics and hydroacoustic mapping of a benthic seafloor in a coarse grain habitat of the German Bight		121
6.1.	<i>Abstract</i>	121
6.2.	<i>Introduction</i>	122
6.3.	<i>Physical settings</i>	124
6.4.	<i>Data collection and processing</i>	125
6.4.1.	Bathymetry and Acoustic Seafloor Mapping - Singlebeam echosounder (SBES), Subbottom profiler (SBP), and Multibeam echosounder (MBES)	126
6.4.2.	Acoustic Seafloor Mapping - Sidescan Sonar (SSS)	127
6.4.3.	Groundtruthing – Bottom samples	127
6.4.4.	Groundtruthing – Underwater videos	128
6.4.5.	Hydrography – Acoustic Doppler Current Profiler (ADCP)	128
6.5.	<i>Results</i>	129
6.5.1.	Bathymetry and Morphology	129
6.5.2.	Bottom samples	129
6.5.3.	Underwater video analysis	130
6.5.4.	Hydroacoustics - Sidescan sonar (SSS)	132
6.5.5.	Hydroacoustics – Singlebeam (SBES)	133
6.5.6.	Hydrography – Acoustic Doppler Current Profiler (ADCP)	133
6.6.	<i>Discussion</i>	136
6.7.	<i>Conclusion</i>	139
6.8.	<i>Acknowledgments</i>	140
6.9.	<i>References</i>	140
Chapter 7 Benthic biodiversity changes in response to dredging activities during the construction of a deep-water port		145
7.1.	<i>Abstract</i>	145
7.2.	<i>Introduction</i>	146
7.3.	<i>Material and methods</i>	149
7.3.1.	Study area	149

7.3.2.	Dredging and dumping data	150
7.3.3.	Bathymetric data	152
7.3.4.	Sampling and sample procedure	152
7.3.5.	Statistical data analyses	154
7.4.	<i>Results</i>	155
7.4.1.	Dredging and dumping	155
7.4.2.	Changes in seabed morphology	155
7.4.3.	Changes in sediment composition and distribution	156
7.4.4.	Changes in macrofauna diversity and abundance	156
7.4.5.	Changes in distribution and abundance of taxa between 2002 and 2010	158
7.4.6.	Macrofauna community structure in 2002	159
7.4.7.	Macrofauna community structure in 2010	162
7.4.8.	Changes in macrofauna community structure between 2002 and 2010	164
7.5.	<i>Discussion</i>	167
7.5.1.	Physical effects of the construction work	167
7.5.2.	Changes in macrofauna community structure	169
7.5.3.	Direct dredging effects on the macrofauna community structure in 2010	169
7.5.4.	Indirect dredging effects on the macrofauna community structure in 2010	170
7.6.	<i>Conclusion</i>	172
7.7.	<i>Acknowledgements</i>	172
7.8.	<i>References</i>	173
Chapter 8 Relationships between spatial patterns of macrofauna communities, sediments and hydroacoustic backscatter data in a highly heterogeneous and anthropogenic altered environment		179
8.1.	<i>Abstract</i>	179
8.2.	<i>Introduction</i>	180
8.3.	<i>Material and methods</i>	182
8.3.1.	Study area	182
8.3.2.	Acoustic seafloor classification	183
8.3.3.	Sampling	184
8.3.4.	Sediment sample procedure	185
8.3.5.	Macrofauna sample procedure	186

8.3.6.	Data analysis	186
8.4.	<i>Results</i>	188
8.4.1.	Classification of SSS backscatter data	188
8.4.2.	Sediment composition and distribution	190
8.4.3.	Macrofauna	192
8.4.4.	Comparison of spatial patterns	196
8.4.5.	Relationship between environmental variables and macrofauna community structure	196
8.5.	<i>Discussion</i>	199
8.5.1.	Hydroacoustic classification versus sediment distribution and seabed roughness	200
8.5.2.	Hydroacoustic classification and sediments versus macrofauna community structure	201
8.5.3.	Environmental factors structuring the macrofauna communities	202
8.6.	<i>Summary</i>	203
8.7.	<i>Acknowledgement</i>	203
8.8.	<i>References</i>	204
Chapter 9	Synthesis and future perspectives	211
9.1.	<i>Jade</i>	211
9.2.	<i>Norderney</i>	213
9.3.	<i>Helgoland</i>	214
9.4.	<i>References</i>	215

List of Figures

- Figure 1.1. The influence of system geometry, acoustic footprint, seafloor roughness, and morphology on acoustic backscatter. a) Different hydroacoustic systems used for seafloor classification, and related beams/footprints (in orange). b) The same topographic roughness (black line on the top-left side) can be the result of different grain size composition. The backscattered information will be influenced by the seafloor pattern and by its footprint size. c) seafloor morphologies (e.g. dunes) can give different backscatter signatures, depending on the data acquisition direction. 10
- Figure 3.1. a) The Jade region, with the Jade Weser Port and, in red, the study area. b) Location map of the Jade system. c) close up un the research site; white lines: main acoustic transects, red crosses: sampling stations. 49
- Figure 3.2. DTM of the research area (a) and main morphological domains (b). 52
- Figure 3.3. Clustering analysis, Euclidean similarity measure (a). SBES acoustic classification (b), overlaid by the sediment data. 53
- Figure 3.4. MBES acoustic classification (a) and SSS acoustic classification (b).. 53
- Figure 4.1. Location of the study area west of Helgoland, with the subarea (hatched box) selected for detailed surveying. 60
- Figure 4.2. Study area. Left panel: Bathymetry (RoxAnn) and sample locations (with corresponding mean grain size). Right panel: Interpreted and interpolated results of RoxAnn data analysis: colour categories see Figure 4.5; A-C benthic communities (modified after Hass et al. 2016). Rectangle in both panels: subarea selected for detailed surveying. 61
- Figure 4.3. Subarea: bathymetry (2012) from multi-beam echosounder a) and backscatter (2011) from sidescan sonar b) with positions of 2011 grab samples and macrobenthos communities. c–f Seafloor classification: c) single-beam echosounder, RoxAnn GD-X (HE 364, 2011); d) multi-beam echosounder (2012), QTC swathview; e) sidescan sonar (2011), QTC swathview; f) single-beam echosounder (2012), QTC 5.5/QTC Impact.

Lower tables: corresponding areal percentages of seafloor classes and percentages of macrobenthic communities.	63
Figure 4.4. Subarea. Broad-scale bathymetric position index (BPI, upper left), fine-scale BPI (upper right), bottom slope (lower left) and terrain ruggedness (lower right).....	70
Figure 4.5. Study area. RoxAnn box of roughness (E1) vs. hardness (E2). I–V Classes mentioned in the text. Inset E1 vs. E2 plotted as black dots superimposed on the chosen colour scheme (modified after Hass et al. 2016).....	73
Figure 4.6. Subarea. Grain size distributions along the transect of 2013 from the northwest (sample 2013_20) to the southwest (sample 2013_02).....	75
Figure 4.7. Subarea. Grain size distributions along the transect of 2011 from the northwest (sample 2011_02) to the southwest (sample 2011_86).....	75
Figure 4.8. Subarea. Percentage of major fauna groups to total taxa along transects T1 to T4 (for location of T1-T4, see Figure 4.3b).....	76
Figure 4.9. Subarea. Hierarchical clustering of macrofauna samples.....	77
Figure 4.10. Subarea. Correlations (Spearman rank order) between grey values (0 = black, 255 = white) from sidescan sonar mosaic and total abundance of the brittle star <i>A. filiformis</i> in 2013 (upper panel) and 2011 (lower panel).	78
Figure 5.1. Location map of the study site (in orange) with the names of the main geographical and morphological units used in the text.	94
Figure 5.2. Digital Terrain Model - DTM (a) and SSS mosaic (b) of the study area. The DTM was based on Lidar data collected in 2013; the blue color corresponds to the areas covered by water during the data acquisition. 32 sediment samples (black dots, in a) were collected along 5 north-south transects (T1 to T5, from west to east) in 2013 (orange dots, in b) and 2014 (blue dots, in b). Two transects (T1 and T3) are highlighted (black lines) and presented in details within the text.....	97
Figure 5.3. Backscatter mosaic of SSS data (a), overlaid by the sediment distribution pie charts (b). Seabed classification of the Lütetsburgerplate, based on SSS and sediment data (c). The pie charts were build using the three main grain size fractions (M: mud, VFS: very fine sand, FS: fine sand). The transects T1 and T3 are highlighted in red. The area was segmented into 10 classes, corresponding to different backscatter regions, morphologies (bedforms, shellfish beds etc.), and sediment characteristics. For the description of the classes, see the text.	102

- Figure 5.4. Sidescan sonar mosaics of 2013 (left) and 2014 (right) datasets, in 1 m resolution. Red (2013) and Orange (2014) lines correspond to the shellfish bed extension; green colors (dark green: 2013, bright green: 2014) correspond to the tidal drainage system (Riffgat channel and secondary channels). The regions corresponding to these classes were used for comparison. The vast majority of the area, corresponding to the intertidal flat deposits, is in 2014 strongly driven by the noise, which covers the seabed signal and affect the ability to segment the area into different morpho-sedimentological classes. The small boxed areas zoom into the three main tidal system components: intertidal deposits (1a and 1b); shellfish beds (2a and 2b); drainage system (3a and 3b)..... 103
- Figure 5.5. Comparison of SSS backscatter data (2013 and 2014), SSS-sediment classification, Lidar DTM bathymetry and sediment grain size fractions, along transects T1 and T3 (for the location of the transects, cf. Figure 5.2). These two transects were chosen to best represent the high variability of sediments, backscatter, and topographic features in the western and eastern regions of the study side, dominated by the association shellfish-mud (T1, west of the Wagengat) and by the typical intertidal mixed flat-sand flat sequence (T3, east of the Wagengat). For the details about the SSS-sediment classification, see Figure 5.3 and the body text..... 109
- Figure 5.6. Detection of shellfish banks and patches by means of different remote sensing device and classifications. SSS and Lidar data were exported at 0.5 m grid. Shellfish beds can be easily recognized and mapped both in the SSS and in the Lidar topographic data, although the extension of the banks is much more clear in the SSS datasets (even in the 2014, despite of the poor quality of the dataset). Similarly to the backscatter SSS data, Lidar intensity could be used for detection and mapping of shellfish beds, although similar intensity values and pattern are not univocally generated by the presence of such banks. 111
- Figure 5.7. Sediment classification of the Lütetsburger area by means of different remote sensing sources a) hydroacoustic data from SSS June 2013 and b) satellite data from RE June 2011. The area covered with water in the RE map was marked in the SSS classification and excluded from further computation. The 10 morpho-sedimentological SSS classes were grouped and reduced to 4 classes in order to match the RE classification, and the corresponding coverage (in %) was given for comparison..... 113

Figure 6.1. A) Location map of the study site “Helgoländer Steingrund”, east of the Helgoland Island, in the southern North Sea. B) Bathymetry map from Multibeam echo-sounder and Subbottom profiler data (SBP). Sampling stations are showed as yellow dots; the yellow lines (Profile 1 and Profile K5-K6) correspond to the transect showed in C. C) Elevation profiles in west-east (K5-K6 = Acoustic Doppler Current Profiler (ADCP) time series transect) and north-south directions. D) nautical chart with the survey lines for the Singlebeam echo-sounder (SBES, blue), underwater video (red), and ADCP (green). SBP survey lines correspond to the SBES ones..... 125

Figure 6.2. The three main sediment types and the sediment distribution map in the Helgoländer Steingrund area. The colored dots (and the related photos) correspond to sandy sediments (yellow), gravelly sediments (orange), and hard substrate (purple). The high-resolution morpho-bathymetric map in the background shows in detail the complex topography characterizing the half-moon shaped ridge, especially in its central and south-western parts..... 130

Figure 6.3. Seafloor classification based on underwater videos and acoustic data – A) Video classification: (1) Ripple-shaped sand, (2) Gravel and shell fragments, (3) Sand and gravel, (4) Colonized hard substrate, (5) Non-colonized hard substrate, (6) Mixed substrate – B) Segmentation of the video tracks into the six seabed types (see above), the zones of high abundance of the two bryozoan species have been highlighted with polygons: green = *F. foliacea* and brown = *A. diaphanum*. C) Singlebeam (SBES) acoustic classification (three classes); on the background: Sidescan sonar (SSS) backscatter mosaic (2016 dataset). D) SSS backscatter mosaic (2018 dataset), on top of the 2016 one. E) Acoustic seafloor classification of the 2018 SSS data. The color code of the three classes corresponds to the colors of the SBES ones. 131

Figure 6.4. Tidal curve recorded at the Helgoland harbour gauge during the Acoustic Doppler Current Profiler survey (transect K5-K6). The red dots correspond to the current velocity/direction measurements showed in Figure 6.5. 133

Figure 6.5. Averaged velocity vectors of the six Acoustic Doppler Current Profiler transects of November 2018 (positions in Figure 6.1D). Ebb flow 2 m above sea bottom (upper left) and over the entire water column

	(lower left). Flood flow 2 m above sea bottom (upper right) and over the entire water column (lower right).	134
Figure 6.6.	Time series of the transect K5-K6 (position in Figure 6.1D) during different tidal stages (shown in Figure 6.4). The left column shows the averaged velocity vector for the first 2 meters above sea bottom, the right column gives the velocity direction (in geographic orientation) over the entire water column.	135
Figure 6.7.	Time slots of the different tidal stages of Transect K5-K6 during ebb-flow, slack water and flood flow. The colored pattern shows the two flow direction perpendicular to the transect direction. In such a west-east-oriented transect, positive values indicate the north-directed component and negative values the south-directed component.	136
Figure 7.1.	Location of a) the study area in the German Bight of the southern North Sea and b) the main features related to the modified coastline (yellow: land), the construction activities for the “JadeWeserPort” (JWP), and the regularly dredged old fairway (pointed lines). Along the transects (T1-T4) the location of the sampling stations (black dots) are shown in relation to the dredging and dumping activities for the JWP.	150
Figure 7.2.	Bathymetry of the study area (depths in m referred to Normalhöhenull (NHN)) and mud content (percentage by weight) at the sampling stations in a) 2002 and b) 2010.	151
Figure 7.3.	Macrofauna taxa number per sampling station (0.1m ²) in a) 2002 and b) 2010, abundance of macrofauna (individuals/m ²) per sampling station in c) 2002 and d) 2010, and biomass (wet weight in g) per sampling station in e) 2010 (no biomass data for 2002).	157
Figure 7.4.	Cluster analyses of macrofauna data in a) 2002 and b) 2010, based on Bray-Curtis similarity, using fourth-root transformed taxa abundance data, black lines indicate the significantly different cluster according to the SIMPROF test ($p < 0.05$), and the concerning spatial alignment of the macrofauna communities in c) 2002 and d) 2010 in the study area.	161
Figure 7.5.	Relative and absolute dominance of the different feeding types in the macrofauna communities A-F.	162
Figure 7.6.	Combined cluster analyses (a) and MDS (b) of macrofauna data in 2002 and 2010, based on Bray-Curtis similarity, using fourth-root transformed taxa abundance data.	166

Figure 7.7. Abundance of characteristic macrofauna taxa (individuals/m ²) in 2002 and 2010, 1 Anthozoa spp.; 2 Corophium volutator; 3 Gastrosaccus spinifer; 4 Macoma balthica; 5 juvenile Mytilidae sp.; 6 Nephtys hombergii; 7 juvenile Nephtys spp.; 8 Peringia ulvae; 9 Petricolaria pholadiformis; 10 Pygospio elegans; 11 Scoloplos (Scoloplos) armiger.	167
Figure 8.1. Location of a) the study area in the German Bight of the southern North Sea and b) bathymetry of the study area (depths in meter refer to Normalhöhennull (NHN)) and main features related to the new coastline (grey land), location of the sampling stations (black dots), the regularly dredged old navigation channel (dashed line), and the dredging (red line) and dumping (yellow line) activities for the JadeWeserPort (JWP).	183
Figure 8.2. a) Sidescan sonar (SSS) mosaic (1 m resolution). High backscatter intensity in dark grey, low backscatter in white. b) Acoustic classes (black lines) on top of the SSS mosaic. c) Final classification of the SSS data in 10 acoustic classes (see Table 8.2 for the description).	187
Figure 8.3. Sediment and macrofaunal composition in relation to the acoustic classification. a) the main sediment components (gravel, sand, mud, and shell lag) are represented by pie charts, overlapped by dots which correspond to the textural classification (after Folk, 1954) of the samples. b) Spatial distribution of the 5 macrofaunal communities, as derived by the statistical analysis.	192
Figure 8.4. Top: Cluster analysis. Bottom: MDS of macrofaunal data, based on Bray Curtis similarity, using fourth-root transformed data; black lines indicate the significantly different cluster according to the SIMPOROF test ($p < 0.05$).	194
Figure 8.5. Sediment classification in textural groups (Folk, 1954) per acoustic class. Similar compositions can be observed between classes A and B (mS to S), and among classes C and E (sM) and D and F (mS). Only one sample defines Class E, while three samples are plotted for Class D (although very similar, therefore not clearly visible). Classes G, H, and J were not sampled.	197
Figure 8.6. dbRDA plot representing the model of spatial variation in macrofaunal community structure and the relationship to environmental parameters (“days after” = number of days after the last dredging/dumping activity for the JWP; HB = high backscatter, MB = medium backscatter, LB = low backscatter).	198

List of Tables

Table 3.1. Left: calculated (and average) distance among replications for each station. Right: sediment grain size analysis, expressed as dry weight percent on bulk sediment.	51
Table 4.1. Data acquisition in the working area between 2011 and 2014.	61
Table 4.2. Grey values (0=black, 255=white) for sidescan sonar mosaics from 2011 to 2014 in the subarea.....	69
Table 4.3. Similarity index of seafloor classification based on Bray-Curtis.....	79
Table 5.1. Technical specifications of the Starfish 452f and overview about SSS data collection and weather/sea conditions recorded during the two surveys in 2013 and 2014.....	96
Table 5.2. Sediment grain size distribution (in ϕ intervals, Wentworth scale) and relative sediment classes (after Folk, 1954).....	101
Table 5.3. Details of the 10 SSS-sediment classes. Greyscale histograms (on the right). X axis: 8-bit greyscale values, from 0 (black) to 255 (white), corresponding to high and low backscatter values, respectively. Y axis: number of counts per class (not the same scale for all the classes).....	104
Table 7.1. Areas of interest according to the categories of disturbance in the study area with the involved sampling stations.	152
Table 7.2. Comparison of the defined areas of interest (see Table 7.1) in 2002 and 2010 referring to the taxa number, macrofauna abundance (individuals/m ²), and effective number of taxa given as mean with standard deviation (sd), and the results of the performed ANOVAs; T17, T33, T41 were excluded, because at these stations no macrofauna was found in 2002; at T22 a high number of <i>Gastrosaccus spinifer</i> was found in 2010.....	158
Table 7.3. Changes in the presence of all macrofauna taxa, which were found in 2010 at a minimum of 3 stations (10%) less (↓) or more (↑) than in 2002 (30 stations in total). Presence at the stations, which were affected by the	

dredging activities for the JWP (2008-2010) and in the old fairway, was listed in comparison to the presence at the not dredged stations.	159
Table 7.4. Macrofauna communities of 2002 and 2010 with sediment categories at the concerning stations, total macrofauna taxa number per community, and macrofauna taxa number per station (0.1 m ²), abundance (individuals/m ²), and the diversity index effective number of taxa given as mean with standard deviation (sd).	160
Table 7.5. Characteristic macrofauna taxa in a) 2002 and b) 2010 with mean abundance of not transformed data and mean similarity and percentage of their contribution to the community, based on Bray-Curtis similarity, using fourth-root transformed taxa abundance data.	160
Table 7.6. Results of the BIOENV analysis with fourth-root transformed macrofauna abundance and biomass data of 2010 and normalized abiotic variables.....	164
Table 7.7. Results of the PERMANOVA and PERMDISP pairwise test of all macrofauna communities in 2002 and 2010, statistically significant differences ($p < 0.05$) are marked in bold.....	164
Table 7.8. Comparison of mean abundances (individuals/m ²) of 11 characteristic taxa at the 30 sampling stations in 2002 and 2010 with standard deviation (sd) and results of the performed ANOVAs.	165
Table 8.1. Number of dredging days for the JWP and number of days between the last dredging/dumping activity for the JWP and the sampling date for the JWP dredged stations (The regular dredging activities in the old navigation channel are not included here).....	185
Table 8.2. Acoustic classes and their characteristics, in relation with the sediment grain size composition and with the seabed roughness. A close up of the SSS image relative to each acoustic class is given in the last column, each box measuring approximately 90x120 m in size.....	189
Table 8.3. Summary of the sediment grain size composition per station. For each sampling locations, the relative acoustic class is given.	191
Table 8.4. Results of the PERMANOVA and PERMDISP pairwise test for all of the macrofauna communities, statistically significant ($p < 0.05$) are marked in bold.	193
Table 8.5. Taxa number per station (0.1m ²), abundance (individuals/m ²) and effective species number of all macrofaunal communities are given as	

mean with standard deviation (sd) with sediment categories (%), depth and number of dredging days for the JWP at the concerning stations. ... 193

Table 8.6. Characteristic macrofauna taxa with mean abundance of non-transformed data and mean similarity and percentage of their contribution to the community, based on Bray-Curtis similarity, using fourth-root-transformed taxa abundance data..... 195

Table 8.7. Results of the multivariate regression analysis (DistLM). Environmental variables were analysed individually (marginal test) and sequentially using a step-wise forward selection procedure (AIC = an information criterion). % Prop. is the proportion of variance in macrofauna taxa explained by each variable. Significant (<0.05) values are indicated in bold (“days after” = the number of days after the last dredging/dumping activity for the JWP)..... 198

Page left intentionally blank

Aknowledgements

Many thanks to my reviewers, Prof. Dr. Dierk Hebbeln and Prof. Dr. Verner B. Ernsten for their always very kind availability and encouragement. A special thanks to Prof. Dr. Dierk Hebbeln for his suggestions and corrections, which significantly improved the quality of this thesis.

For his continuous support, his expertise, his time, for his always positive confidence in my work, my greatest and deepest thanks to Dr. Alexander Bartholomä. Dear Alex, I have learnt a lot from you.

Thanks to the thesis committee members for their positive comments.

Over the years many persons helped me in my research. Thanks to all the PhD students, lab technicians, researchers, and professors who shared their knowledge with me. I am really grateful I had the opportunity to work in Germany and New Zealand with so many professional, friendly, and hearty people. The time spent in New Zealand will stay as a milestone in my life. In particular, I want to acknowledge my coauthors, my fantastic colleagues at the Senckenberg am Meer Institute of Wilhelmshaven, and the crew members of the RV Senckenberg.

Extra moenia

Quel che viene dal cuore può essere scritto solo con la lingua del cuore.

I ringraziamenti sono sempre, inevitabilmente, una lista di volti e di nomi, un riassunto di rapporti coltivato negli anni, una trama fatta di filo e di vuoti che lasciano passare parole ed emozioni. Di tale tessuto Serena è l'ordito. Se la qualità di un ricamo si giudica in base alla preziosità degli intrecci e alla finezza del disegno, tutto è possibile

solo grazie all'ordito. Serena non è mai stata "stella guida" ma, al contrario – e per dirla con Tolkien – compagna nelle sfide quotidiane della vita, donna con bisogni, desideri e fragilità. Per me, soprattutto, capace di amore profondissimo.

Clara e Gaia: siete state l'emozione più intensa e sorprendente della mia vita e continuate ad esserlo. Mi avete cambiato, continuate a farlo giorno dopo giorno. Non siete il mio futuro: siete il vostro; e già mi diverto ad immaginare quello di cui sarete capaci.

Siamo una somma inscindibile di ciò che siamo stati e dei nostri progetti futuri. Le nostre radici non solo ci seguono, ma ci permeano; sono carne e pensieri, esperienze ad affetti altrettanto reali quanto la chimica del nostro corpo. Grazie alla mia famiglia: a chi c'è stato dall'inizio, a chi c'è sempre stato, a chi è arrivato col tempo, a chi è già ripartito. Mi mancano coloro da cui sono distante, anche se posso telefonarvi. Mi mancano quelli che non posso più chiamare. Mi mancate tantissimo.

Ci sono persone speciali che, durante la vita, ci troviamo a fianco e finiscono sul nostro stato di famiglia, sebbene non all'anagrafe. Amiche ed amici, fratelli che ritrovo sempre (anche senza sentirli) in un angolo del mio cuore. Come tutte le cose veramente preziose: rare e gratuite.

Tra le molte persone che hanno percorso pezzi di strada con me ce ne sono alcune capaci di farmi guardare in modo diverso la mia vita. Cantori, cantastorie, che hanno annodato a quattro mani fili narrativi prima sconosciuti eppure presenti al mio telaio; che mi hanno mostrato la bellezza dietro i buchi, la potenzialità dei nodi senza i quali la trama scivola.

In questo lungo viaggio ho conosciuto Paesi, persone, ho raggiunto più volte alcuni dei luoghi più lontani al mondo. Ogni compagno di viaggio ha lasciato la sua nota sul mio diario, ciascuno con la sua grafia e col suo stile. A tutti voi, colleghi e amici che ho incrociato su qualche nave o che incontro giornalmente in corridoio, il mio grazie. Uno, in particolare, ha avuto la pazienza e la follia di continuare a crederci. Molte volte ho creduto in me sulla base della tua fiducia.

Chapter 1

Introduction

1.1. General introduction

“Human impact is poorly understood. (...) The greatest threat to the oceans from humans may simply be ignorance” (Harris 2012a)

Coastal systems represent 20% of the earth surface (Cicin-Sain et al. 2002). They are the interface between land and marine systems (Carter 1988) (although a minor part includes the transition to fresh water systems), each of these characterized by peculiar dynamics and related processes (Hinrichsen 1998). Any process that occurs in peri-coastal regions, both from land- and seaside, has an effect on the coasts (e.g. Burke et al 2001, Martinez et al. 2006), which are therefore continuously changing and – in terms of conservation – fragile and sensitive to those changes.

Coastal systems include a variety of different tidal and non-tidal environments, from rocky- to sandy coasts, from beaches to brackish lagoons, from subtidal to intertidal mud flats (Schwartz 2005), each of them linked to specific geological, morphological, physical, and biological processes.

Human pressure on coastal ecosystems is higher than on any other natural environment (Valiela 2006), and it keeps growing (Lindeboom 2002). Over 40% of the world population live within 100 km from the sea and 64% of the world’s megacities lie in coastal zones (Martinez et al. 2006, Brown et al. 2013). Besides, they represent the most important capital stock of the total economic value of the planet (Costanza et al. 1997), as 77% of the global ecosystem-services value comes from coastal areas (Costanza et al. 2014).

The anthropization of the coasts includes urbanization, fishing, farming, oil and gas exploitation, mining, wind farms, marine traffic, tourism, and recreational activities (McLachlan and Brown 2006). Each of these factors produces an impact on local ecosystems. Among the multiple anthropogenic stresses (which bring to “**cumulative human impacts**”, Harris 2012a), activities like construction/expansion of ports (e.g. Boulay 2012, Erfteemeijer et al. 2013),

land reclamation and beach nourishment (e.g. McLachlan and Brown 2006, Petersen and Bishop 2009), dredging and dumping (e.g. Newell et al. 2002, Simonini et al. 2007) for the maintenance of shipping lines and/or for underwater mining (mainly sand and gravel, e.g. Boyd et al. 2006) produce direct physical modifications on coastal habitats in terms of seafloor geometry/morphology, sediments, and benthic communities. Human-induced changes in seafloor morphology and/or in sediment composition modify the hydraulic conditions and have direct impacts on the bio-communities (Sardà et al. 2000, Sutton and Boyd 2009).

On the other hand, biological changes (e.g. bioinvasion) produce effects on the seafloor morphology, which in turn may have an impact on the hydraulic conditions and hence on the sediment composition and/or distribution. For instance, the recent invasion of pacific oysters (*Crassostrea gigas*) along the North Sea coast produced modifications in nature and morphology of the seabed (with the appearance of large reef-like structures), in the sediment dynamics (from mobile siliciclastic soft ground to firm carbonate hard ground), and in the native bio-communities (Markert et al. 2010). Therefore, there is a complex interplay between the biotic and the abiotic components, and the cause-effect relationship is not always clear.

Coastal zones are affected by **climate changes** (Harley et al. 2006): in particular, sea level rise influences the near shore dynamics, modifying the hydraulic conditions, raising the risk of coastal flooding (Neumann et al. 2015) and, at the end, causing a change or a shift in the sediment/bio-communities patterns. Climate changes have been also connected to an increase in the energy, frequency, and duration of natural extreme events, such as storm surges and tropical cyclones (Webster et al. 2005, Mann and Emanuel 2006, Kossin 2018). As a large portion of the human population lives in coastal regions (Small and Nicholls 2003) and this percentage will increase in the future (Hugo 2011, Seto 2011), the consequences of such changes cannot be simply accepted as a natural step towards a new dynamic equilibrium of the environment, and actions have to be taken on global and local levels for mitigating the hazards connected to sea level rise (flooding, contamination of fresh water coastal reservoirs, erosion, etc.). Sterr (2008) estimated in 300 million US\$ (1995 values) the costs for damages caused by flooding and erosion along the German coast, associated to 1 m sea level rise. Human interventions on habitat communities of near shore environments can amplify or mitigate such climatic-related effects (e.g. Duarte et al 2013), and therefore the management of coastal areas is strategic for facing the hazards connected to climate changes.

Over the last decades, several national and international programs on coastal marine habitat protection were promoted both by governmental and non-governmental institutions (e.g. Connor et al. 2004, Pickrill and Kostylev 2007, Lucieer et al. 2019). The European Union (hereafter EU) issued **new regulations** for monitoring the quality of marine environments and defending the associated habitats. Back in 1979 with the first Bird Protection law (Council Directive 79/409/EEC), the EU pointed out the need of a better understanding of threatened habitats as a key for protecting endangered species and ecosystems. The same year, the Bern Convention gathered European and African countries with the aim of defending natural habitats, promoting conservation strategies, fighting pollution and establishing common policies among the countries. As a consequence, in 1992 the EU adopted the Habitat Directive (Council Directive 92/43/EEC) on “Conservation of natural habitats and of wild fauna and flora”. Pursuant to this Directive, a network of protected sites was designed (Natura 2000) and a specific habitat classification system (European Nature Information System, EUNIS, EEA 2012) was adopted, with a particular regard to threatened habitats. The Water Framework Directive (WFD, Directive 2000/60/EC) and the Marine Strategy Framework Directive (MSFD, Directive 2008/56/EC), with main focus on surface and ground waters (WFD) and more specifically on marine waters (MSFD), set the legal grounds for an extensive water quality assessment and laid down deadlines for achieving the Good Environmental Status (GES) for the EU’s marine waters by 2020. Therefore, the original request of attention to habitat quality and conservation led to binding international obligations and legal duties to be fulfilled by each EU country.

Since then, new programs were launched for mapping marine habitats and defining their quality status (see ICES 2014 for a summary of the international and national mapping programs in the EU; e.g. for the German marine territory: WIMO - Wissenschaftliche Monitoringkonzepte für die Deutsche Bucht/Scientific Monitoring Concepts for the German Bight, Winter et al. 2016; AskAWZ - Acoustic Seafloor Classification of the German Exclusive Economic Zone, BSH 2016), with the aim of using the information derived by such basemaps for planning the future environmental protection, maintenance, and sustainable development of coastal areas. The definition of a habitat and the assessment of its current environmental status are done through the simplification of the reality into significant discrete descriptors (e.g. physical, geological, biological components, etc., Kostylev 2012). The process of data collection, analysis, simplification, and the geographical representation of habitats on a map goes under the name of **habitat mapping**.

Habitat mapping is commonly carried out with a combination of remote sensing and in-situ techniques (Costello 2009), which allows to spatially extend the point information to a broader area. Remote sensing in marine environments includes both airborne/satellite imaging and underwater hydroacoustics (“acoustic remote sensing”, in Huff 2008). While the former uses electromagnetic waves and their interaction with the ground to gather information (e.g. Lillesand and Kiefer 1994, Elachi and van Zyl 2006), the latter is based on acoustic waves (e.g. Anderson et al. 2008, Blondel 2008). In-situ techniques (MESH 2008) consist of field observations (including the use of underwater photo or video systems), sediment and biological sampling, and physical measurements (e.g. currents, suspended load, temperature, salinity, nutrients, light wave spectra, etc.).

In the past, the limited amount of available satellite sensors (Cracknell 2018, Zhu et al. 2018) forced the habitat mapping based on such sources to some kind of standards, where the main variable was represented by the specific approach used for the data processing. At the same time, the **hydroacoustic sources** used for habitat mapping were (and still are) extremely heterogeneous (Jonsson et al. 2009) in terms of geometry, frequencies, manufactures, spanning from sediment sub-bottom profilers to extreme shallow water bathymetric systems (Kenny et al. 2003, Brown et al. 2011). The basic physical principles ruling the behaviour of sound waves in water and their interaction with the seafloor are well known (e.g., Lurton 2010, Jackson and Richardson 2007). Although there are still hydro-acoustic devices based on signal reflection (e.g. single beam echo-sounders systems), most of the tools use backscattered waves as source of information for classifying the seabed (e.g. sidescan-sonar and multibeam echo-sounder systems; see Brown et al. 2011 for a review).

However, the understanding of the role of single abiotic and biotic components on the generation of backscatter is still unclear. Moreover, there is a lack of standards about procedures for collecting, processing, analysing data, and producing maps (Lurton and Lamarche 2015). National and international mapping and monitoring programs pushed the scientific communities towards this direction, and over the last 10 years some guidelines have been published (e.g., BSH 2016, Lamarche and Lurton 2018).

The segmentation of the seabed in classes based on backscatter data forms the basis for the so-called **Acoustic Seafloor Classification**, and the groundtruthing of the acoustic classes by means of data derived from bottom samples is the **Seabed characterization**. **Chapter 2** of this doctoral thesis provides an overview about the available remote sensing techniques and, specifically, about acoustic seabed classification systems.

1.2. Physical settings: tide-dominated coasts and the Wadden Sea

“Although there is an increase in scientific knowledge of many coastal ecosystems (...), these ecosystems are vanishing fast” (Miththapala, 2013)

The role of interface between land and sea is particularly evident in tidal environments, where large regions (intertidal areas) are cyclically covered by water and exposed to air; the ecosystem offers a unique mixture of aquatic (both fresh- and marine waters), palustrine, and terrestrial habitats and it is considered of extreme importance for biodiversity (Gopal et al. 2000, 2001). Among all the different coastal systems, **tidal flats** (also called “tidal wetlands”, e.g. Yang et al. 2008; or, less commonly, naming a part for the whole, “mud flats”, e.g. Dalrymple et al. 1991) are present worldwide, although there is no exact quantification of their coverage (Flemming 2012). In 1999 the Common Wadden Sea Secretariat commissioned a report to list the extension of tidal flats around the globe (Deppe 1999), which produced an inventory of 350 wetland sites; however, no mention about the total coverage was provided.

Several classifications were developed for categorising the tidal environments, based on tidal regime (e.g. Davies 1972) or on tidal range. The most commonly used (Davies 1964, Davies 1972, Bird 1970, Hayes 1975) includes three classes: microtidal (tidal range: 0-2 m), mesotidal (tidal range: 2-4 m), and macrotidal systems (tidal range >4 m). A more refined subdivision in five classes was adopted by Hayes (1979): <1 m: microtidal; 1-2 m: lower mesotidal; 2-3.5 m: upper mesotidal; 3.5-5 m: lower macrotidal; > 5 m: Upper macrotidal. The regions with tidal range < 5 cm were named as “tideless enclosed seas” by Eisma (1998).

Although considered in the past as unhealthy and unsafe places (particularly in tropical latitudes), tidal wetlands offered several advantages for human settlers, like access to waterways, fertile lands for farming, and proximity to waters for fishing (Knottnerus 2005). The development of strategies for coping with sea level rise and storm events led to a stable human presence on tidal coasts, and even to an intense process of land reclamation by means of drainage networks and dike systems (e.g. Reise 2005, An et al. 2007, Balbo et al. 2017).

Nowadays, wetlands are accounted as particularly vulnerable and have been described as the most endangered complex ecosystem on Earth (Finlayson et al 2005). Davidson (2014) reviewed 189 studies and reports dealing with wetland habitat lost, finding that between 64-71% of the world wetland coverage

vanished since 1900 AD, and Barbier et al. (1997) estimated in 57% the loss of wetlands in Germany for the period 1950-1985. More specifically, tidal wetlands are globally facing a rapid decrease in areal coverage and habitat quality (e.g. Callaway et al. 2012, Murray et al. 2014, Brophy et al. 2019).

The **Wadden Sea** is the world's largest continuous meso-tidal system (Reise et al. 2010), which extends throughout the Netherlands, Germany, and Denmark. It includes unique ecological and cultural sites, which have gathered the status of biosphere reserve (UNESCO, 1986) and of UNESCO World Heritage Site in 2009 (2014, for the Danish part). It extends over more than 10000 km², including 25 islands and a few mobile sandbanks, and a total of 30 tidal inlets.

The Wadden Sea is the result of coastal evolution following the Holocene sea level rise (Behre 1987, Ehlers 1988, Streif 1990), later on shaped by the human attempt to gain low-standing coastal areas for farming, and to defend them from floods and storm surges by means of dike systems (Flemming and Davies 1994, Flemming 2002). Thus, it represents:

- a unique example of coastal dynamics in response to sea level change (e.g. CPSL 2001, CPSL 2010, Reise 2005);
- an extraordinary archive for archaeological and historical evidences testifying the human strategies coping with a rising sea level (e.g. Behre 2004, Lotze 2005);
- an important model for studying the adaptation of a natural wetland environment to long term human disturbance (Flemming and Bartholomä 1997, Lotze et al. 2005) and for modelling its future development (Benninghof and Winter 2019).

In the Wadden Sea region (i.e. including the adjacent inland marsh and beach areas) different, sometimes opposite interests coexist:

- it is a *most protected international natural park* for mammals and birds; its access and use are strictly regulated by environmental restrictions and international laws (Trilateral Cooperation on the protection of the Wadden Sea);
- it is traditionally exploited since centuries for *fishing, agriculture, and farming* (e.g. Smit et al. 1998, Lotze 2007);
- it is a place for *recreational activities*; in particular, the Frisian Islands are facing a continuous growth in tourism (Ehlers 1988, Brand and Wollesen 2009), with over 23 million overnight stays in 2013 only for the German Wadden Sea area, (Klöpffer et al. 2017);

- it borders the main *international shipways* across the German North Sea and three of the *largest container ports* in Europe (Amsterdam, Bremerhaven, Hamburg) as well as the only deep-water container terminal of Germany (JadeWeserPort in Wilhelmshaven).

The management of such a complex, dynamic, and threatened area requires therefore balancing among different needs, expectations, and legal requirements. The ability of mapping the habitats in tidal environments and documenting their ecological status-quo, represents, therefore, a key factor for understanding their natural dynamics, for assessing the impacts caused by humans and sea level rise, and for modeling the effects of habitat changes on human society. Moreover, it offers an indispensable basis for planning the conservation, restoration, and managing the future development of such vulnerable habitats.

The hybrid nature of tidal systems (marine and terrestrial, with their large intertidal regions) consents the use of satellite/airborne and hydroacoustic sources for investigating the seafloor, although with strong limitations. In fact, the high turbidity of the water (given by the amount of fine material in suspension, up to 120 mg/l in the Wadden Sea, e.g. Badewien et al. 2009, Bartholomä et al. 2009) makes it impossible for radiometric and optical sensors to penetrate the water column (light penetration < 0.5 m, Staneva et al. 2009), limiting the data collection to the intertidal areas and during low-tide time windows. Even so, water can still cover intertidal regions during low-tides (due to a combination of the low-angled tidal flat slope and of adverse wind/sea conditions), affecting the records. On the other hand, the use of hydroacoustic sources for seafloor data collection is limited to high-tide time windows and, more in general, by the water depth, related to the local maximum tidal range (1 to 4 m in the German Wadden Sea, Flemming and Davis 1994). As a result, only a very few studies have been published showing applications of hydroacoustic systems in extreme shallow water conditions, e.g. for mussel bed recognition (van Overmeeren et al. 2009), seagrass mapping (Greene et al. 2019), boulders detection (von Rönn et al. 2019), and sediment classification (Biondo and Bartholomä 2017).

The present doctoral thesis offers an innovative contribution to investigate the habitats of disturbed and less disturbed tidal environments, by means of an efficient and effective use of hydroacoustic systems and in-situ techniques for habitat mapping and monitoring. The research focussed on both intertidal areas (where a hydroacoustic-based habitat classification was compared with a satellite-based one) and subtidal regions. Both sharp and gradational

transitions among different habitats were present in the research sites. Gradational transitions were due to changes in the abiotic seafloor characteristics (i.e. sediments and seabed morphologies) and to the composition and distribution of the benthic communities. The ability of the hydroacoustic systems to detect such variations and, therefore, to distinguish different habitats is among the goals of the present work. In particular, the influence of benthic component on the acoustic signal was investigated, both on soft- and hard grounds. Different hydroacoustic systems were tested, in order to contribute to the definition of guidelines for scientific mapping and monitoring of coastal waters (WIMO Project). Besides, the impact of large port construction on disturbed environments and the relevance of such disturbance for the habitat classification process were addressed.

The study sites of **Chapters 3, 5, 7, and 8** are located within the Wadden Sea area or in the immediate nearby: the Norderney tidal flat and the seafloor around the JadeWeser deep-water container terminal (for details, see the introductions of the single chapters). **Chapters 4 and 6** investigate the relatively undisturbed seabottom in the vicinity of the Helgoland Island, characterized by both hard and soft grounds.

1.3. State of the art and open questions

Over the last decades the scientific community benefited from the aforementioned national and international programs and agreements for preserving and restoring vulnerable ecosystems, and launched or took part in new projects for developing scientific methods and standards for mapping and monitoring coastal habitats.

A literature research on Google Scholar for the words “marine habitat mapping” limited to the year 2000 returned 19900 results, whereas for the time window relative to the last decades (2000-2018) the number of publications is more than doubled (47700). Even using more restrictive search criteria the result does not change: up to the year 2000 only 75 indexed papers/reports included the words “Acoustic seafloor/seabed classification” in the title or keywords. The number rose to 1227 publications until the year 2017. The lack of standards about terminology and the use of different terms with the same meaning often cause confusion. A short explanation about the **keywords used in the present study** is given in this paragraph in order to:

1. better introduce the background of the present work;

2. point out the open research gaps, some of which will be addressed in the following chapters.

1.3.1. *Habitat, Habitat surrogates, and Seafloor roughness*

“A benthic habitat can (...) be defined as an area of the seabed that is distinct from its surroundings in terms of physical, biological, and chemical variables” (Lecours et al. 2015)

Scientific literature is rich of expressions borrowed from common language, where univocal definitions are not always needed. The use of synonyms in order to avoid repetitions can generate confusion, as the same concept can be defined by different terms, which are used elsewhere with different degree of overlapping meanings. “Habitat” is one of those words, which partially overlaps with others like ecosystem, ecotope, biotope, ecological niche, etc., with no univocal scientific definition.

The word “**habitat**” has been used both, *stricto sensu*, in reference to the place which is suitable for a species or an assemblage of species (biocommunity) and, in a broader sense, with regards to the physical place and the biological component together (e.g. Foster-Smith et al. 2007). These two components are often referred to as “**abiotic**” and “**biotic**”, respectively. McDermid et al. (2005) offers a review about the ambiguous use of the word “habitat” in the scientific literature. However, it is widely accepted that the definition of a habitat is based necessarily on the description of the factors that make possible (or potentially possible) the presence of living beings. Those factors are defined as “**surrogates**” (e.g. Post 2008) since they can be used – alone or in combination – for describing a habitat, regardless to the actual presence of organisms. Some authors, thus, refer to this practice as “potential habitat mapping” (Greene et al. 2007).

In marine environments, the abiotic factors (“physical surrogates”; Post 2008) defining a specific habitat can be divided in two groups (Harris 2012b): a) seafloor properties (morphology and its derivatives, exposure, depth, nature of the seafloor – hard or soft ground -, sediment characteristics), and b) physical parameters connected to the water column (e.g. temperature, salinity, suspension load, exposure time - in tidal environments -, current speed, oxygen content, light, food availability, etc.). The characterization and quantification of at least some of such parameters and their representation within a geographic framework is the goal of the habitat mapping. **Scaling** represents one of the most relevant and – at the same time – one of the most misunderstood factors in the definition of a habitat and its spatial extension (Greene et al. 2007).

Among the physical surrogates, the **seafloor roughness** plays a prominent role in the generation of acoustic echo and backscatter (Jackson and

Briggs 1992). While “hardness” and “roughness” are usually appointed as key controlling factors for reflection-based systems (i.e. single beam echo-sounders and first reflection of sub-bottom sources; Brekhovskikh and Lysanov 1982, Anderson et al. 2008, Mielk et al. 2014, Hass et al. 2016), the seafloor roughness is the main player in the backscatter generation (e.g. Briggs 1989, Pouliquen and Lurton 1992, Lurton and Lamarche 2015). As for many already mentioned terms, there is no unique definition and terminology for seafloor roughness, which is also referred to as surface roughness (e.g. Mulhearn 2000, Ferrini and Flood 2006), seabed roughness (e.g. Ferrini and Flood 2006, Steininger et al. 2013, Pinson et al. 2018), bottom roughness (Jackson and Briggs 1992), and topographic (or micro-topographic) roughness (e.g. Matsumoto et al 1993). The seafloor roughness (Figure 1.1) can be referred to (in bold, the nomenclature adopted in this thesis):

- natural seafloor morphology
 - artificial seafloor morphologies
 - sediment characteristics (composition/distribution)
 - benthic features
 - any combination of the previous elements.
- } **Topographic roughness**

} **Sediment roughness**

} **Benthic roughness**

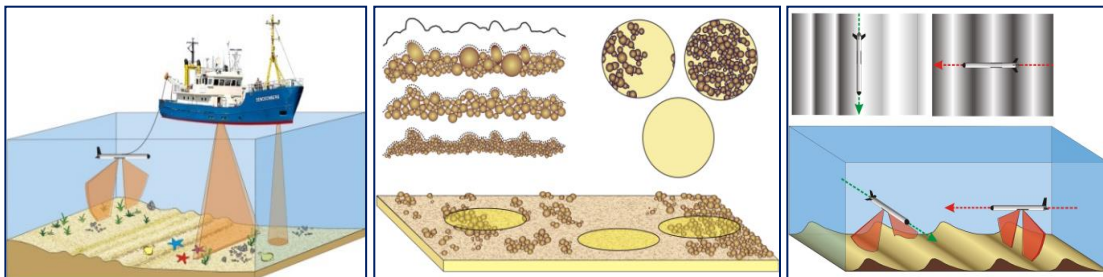


Figure 1.1. The influence of system geometry, acoustic footprint, seafloor roughness, and morphology on acoustic backscatter. a) Different hydroacoustic systems used for seafloor classification, and related beams/footprints (in orange). b) The same topographic roughness (black line on the top-left side) can be the result of different grain size composition. The backscattered information will be influenced by the seafloor pattern and by its footprint size. c) seafloor morphologies (e.g. dunes) can give different backscatter signatures, depending on the data acquisition direction.

The way all these elements relate to each other and the effect on the backscatter is not entirely clear, yet. The backscatter intensity, for example, is usually described as a function of the acoustic frequency, of the system/seafloor geometry (grazing angle), and of sediment grain size (e.g. Hines 1990, Collier and Brown 2005, Lurton 2010). However, the contribution of the abiotic and biotic components to the seafloor roughness and their influence on the acoustic signal is not fully understood.

The interplay of *topographic* (mainly human induced, e.g. dredging marks) and *sediment roughness* on the acoustic signal of multiple acoustic devices (multibeam, sidescan sonar, and single beam echo sounder) is addressed in **Chapter 3**, in which the effect of tides on sediment sampling were also investigated. In fact, in extremely dynamic environments, the near-to-surface sediments change constantly, due to the sediment carpet transported by the tidal currents (Svenson et al. 2009, Kubicki and Bartholomä 2011). Therefore, the acoustic data may potentially mismatch the sediment data, if they were collected during different tidal phases (for instance, groundtruthing acoustic data recorded during maximum ebb flow by means of sediment samples recovered during slack water). The influence of the benthic organisms to the acoustic backscatter intensity is specifically presented in **Chapter 4**, in which gradual and transitional backscatter changes observed on the soft and hard ground seabed types (see also the next paragraph) have been investigated in regards to the interaction between the seafloor roughness components.

1.3.2. *From habitat mapping to habitat monitoring*

“Our ability to map the physical spaces that organisms might utilize far exceeds our ability to measure the extent to which those spaces are actually occupied” (Harris and Baker 2012).

With the term “**habitat mapping**” is intended both the practical and intellectual process of data collection-analysis, and the delivery of a proper, classified product (habitat map; MESH 2008). Different approaches based on hydroacoustic systems and in-situ techniques are available: Eastwood et al. (2006) distinguishes between “top-down” (segmentation of the acoustic dataset into classes and characterization by means of bottom samples) and “bottom-up” approach (subdivision of the area into biological units, based on bottom samples, and spatial mapping of such assemblages by means of their related statistical environmental parameters). Independently from the strategy used, the workflow to generate a habitat map can be summarized as follows (modified after Brown et al. 2011):

1. *Data collection*: including both the gathering of the existing knowledge and the collection of new records by means of remote sensing and/or in-situ observations and sampling techniques).
2. *Data analysis*: characterization of the physical and/or biological components of the habitats. Simplification of the habitat into a set of significant descriptors by means of expert-based (“manual classification by scientists” in

-
- Reynolds et al. 2008) and/or statistical clustering algorithms (“supervised” and “unsupervised classification” in Reynolds et al. 2008).
3. *Habitat classification*: segmentation of the research area into different classes, based on the defined habitat descriptors and on the relative statistical thresholds.
 4. *Habitat mapping* (stricto sensu): geographic-based representation of the spatial extension of the habitats on a map.

The current practice pushes towards automatic/semi-automatic seafloor classification methods, based on remote sensing data, with minimal human input (Costa and Battista 2013). Such tools allow to classify the seabed using different degrees of man-supervision, aiming to minimize the subjective interpretation and, therefore, to produce expert-independent results and outcomes (Brown et al. 2011).

The classification process ends with the definition of distinctive areas (separated by boundaries), which differs for “physical, chemical, and biological conditions” (Kostylev et al. 2001). Nevertheless, natural systems rarely show sharp contacts among different environments, whereas changes occur often along transitional gradients (Cochrane 2008, Brown and Collier 2008). Harris (2012c) distinguishes between **crisp boundaries**, univocal and sharp, and **fuzzy boundaries**, where changes in habitats are expressed as transitional shifts in seabed characteristics. The definition of any habitat boundary is, to some degree, subjective (Brown et al. 2011); it can be supported by statistical factors, which help pointing out significant differences between adjacent habitats (e.g. based on backscatter values, waveform shapes, benthic organisms, etc.). Such factors, however, need to be interpreted, as they express statistical values that may – or may not – reflect real differences in terms of habitat. Habitat mapping of fuzzy environments is therefore particularly challenging, because of the large degree of personal interpretation required. How to define habitat boundaries in fuzzy natural environments, and how to use such boundaries in monitoring programs (without mixing up actual habitat changes and classification uncertainty) are still open questions, which demand more investigations.

Chapter 4, Chapter 5, and Chapter 6 of the present thesis address some of those topics, focussing on areas where both crisp and fuzzy boundaries are present. In **Chapter 5** the transitional changes are produced by shifts in sediment composition and seafloor morphologies in a typical tidal flat environment, and an expert-based seabed classification was preferred to an automatic approach. In **Chapters 4 and 6** the role of the biocommunities in delimiting different habitats is investigated (both on hard and soft grounds), specifically regarding the

influence of the benthic organisms on the acoustic signal and, consequently, the classification.

As a step forward in habitat mapping, time and spatial scales have to be considered as essential factors for understanding the dynamics of specific environments, forming the basis of the **habitat monitoring** concept. **Time-series**, in fact, are the only way to actually assess real changes in habitats composition and/or distribution. In most the cases, habitat monitoring is the main goal of the habitat mapping: 84% of the studies analysed by Harris (2012a) were carried out within the frame of a monitoring program; nevertheless, all of these studies aimed to set up baselines for specific habitats, rather than comparing different stages of the same habitats over time. In fact, if land-based time repetitions are common in satellite remote sensing studies, the acquisition of time-series data based on hydro-acoustic sources is not a standard practice, which leaves space to open research questions. For instance, depending on the environment dynamics, systems can change so rapidly that a single classification may not be representative of the status-quo of the habitats. Therefore, time-series data are necessary not only for assessing the dynamics of an ecosystem, but also for contributing to the validation of the initial habitat mapping products. The study presented in **Chapter 3** makes use of time-series data collected during a tidal cycle in order to check the variability of hydroacoustic records and sediment composition due to the tidal stage, in an extremely dynamic channel. A series of hydroacoustic records over four years time period are considered in **Chapter 4** in order to assess the stability of a hard and soft ground seabed and to validate the seafloor classifications based on different acoustic sources.

1.3.3. *Disturbance, Impact, and Habitat patchiness*

Disturbance is “any discrete event in time that disrupts ecosystems, communities or population structure and changes resources, substrate availability or the physical environment” (Pickett and White 1985)

The word “**disturbance**” has often been used in scientific literature as a synonym for “perturbation”, “stress”, or “impact” (Rykiel 1985, Borics et al. 2013). Pickett and White (1985) described the disturbance as the change of the environmental equilibrium of an ecosystem, which exceeds the natural variability of the system itself. However, the definition of natural variability is somehow arbitrary, as it strongly depends on the observation scale (Landres et al 1999). Likewise, scaling plays a role in the definition of “disturbed environments”; in fact, Pickett et al. (1989) specified that the concept of disturbance can only be described in relation to the temporal and spatial scale of a specific habitat.

Any attempt to include the time scale in the definition of a habitat and in the description of its changes requires a long-time observation of the system (at multiple time- and spatial scales), in order to define:

- The natural variability of the habitat (“baseline”, in Harris 2012a), which includes the physiological fluctuations of the system;
- The natural disturbance, related to:
 - High energetic or catastrophic events (e.g. storms, tsunamis, volcanic activities, seaquakes, tectonics, etc.);
 - Climate changes (e.g. sea level rise, changes in the geochemical conditions of seawater, etc.). This disturbance can, eventually, also be accounted as long-term human induced, although this point exceeds the focus of the present work;
- The human-induced (i.e. artificial or anthropogenic) disturbance.

The word “**impact**”, on the other side, can be specifically used to define the results of a disturbance (e.g. Rykiel 1985), i.e. the process which leads to some changes. In other words, the disturbance (process) causes an impact (result) on specific habitats. The impact is therefore a change in the environment and in its abiotic/biotic components, and the kind of disturbance (natural and/or human driven) is the controlling parameter for those changes.

Marine habitats are strongly impacted by human disturbance: Halpern et al. (2008) showed that the entire marine realm is, to some degree, affected by human disturbance. The ability of remote sensing techniques to map disturbed habitats and to distinguish between natural and human-driven disturbance is, in large parts, still questioned.

The Wadden Sea and surroundings present both directly cumulative disturbed and less disturbed areas (e.g. Lotze et al 2005, Kabat et al 2012). The **Chapter 7** focuses on the impact produced by the activities connected to the construction of a deep-water container terminal on sediments and bio-communities in the Jade area (JadeWeserPort), comparing the macro-zoobenthos composition and distribution before and during port construction. The extensive presence of dredging marks in the Jade Channel, their influence on the hydroacoustic backscatter (and on the related acoustic seafloor classification), and the ability of acoustic systems in assessing the human disturbance on sediment substrates and bio-communities are the foci of **Chapter 8**.

1.4. Objectives

For this study, different acoustic systems and in-situ sampling techniques were coupled and applied to disturbed and undisturbed environments, in intertidal and subtidal areas, in order to evaluate:

1. The role of topographic, sediment, and benthic roughness in modifying the backscatter signal and therefore in driving hydroacoustic-based seafloor classifications.
2. The ability of such acoustic systems in classifying transitional environments characterized by fuzzy boundaries, by means of both automatic and expert-based classification approaches.
3. The impact of human disturbance of deep-water port construction on sediments and benthic communities in tidal ecosystems.
4. The benefits and limitations of acoustic systems in comparison with satellite remote sensing sources for habitat mapping of intertidal and subtidal areas.

1.5. Thesis outline

The doctoral thesis is presented as a cumulative work, which sums up the results already published or accepted for publishing by the candidate in scientific journals and presented at conferences over the past years. Each chapter consists of a scientific paper, which investigates specific aspects of the remote sensing techniques applied for habitat mapping, and the human impact of large port construction activities on sediments and benthic fauna. The papers are presented following a scientific and topic-related thread, rather than their chronological order.

Chapter 1 Introduction.

Chapter 2 presents an overview about available habitat mapping and acoustic seabed classification systems, including a literature review. The paper is a chapter of a conference proceeding book (YouMares 2013), and it was written as an introduction for the “Marine Habitat Mapping” scientific session, proposed and headed by the PhD candidate as a chairman.

Chapter 3 looks into the influence of sediments and natural/artificial seabed morphologies on the backscatter signal, for different acoustic

sources (singlebeam echo-sounder, sidescan-sonar, multibeam echo-sounder). The use of different time windows for acoustic and sediment data collection, and the resulting mismatch between the acoustic seafloor classification and the sediment data are also addressed. A repeated series of sediment samples were taken, at the same location, in order to evaluate the tidal-related local variability of near-to-surface sediments. The study was carried out in the Jade Channel, when the first deep-water container terminal (JadeWeserPort, Wilhelmshaven, Germany) was under construction, therefore representing an optimal testing site for highly disturbed environments. The paper was presented at the Hydro 2012 conference in Rotterdam and was awarded with the “Best student paper award”.

Chapter 4 considers how the seafloor texture given by the sediment characteristics and the benthic fauna can modify the acoustic signal of four different seafloor classification systems, and how the semi-automatic classification software performs on both crisp- and fuzzy-bordered environments. The role of densely spaced brittle star communities in increasing the roughness and in influencing the acoustic backscatter intensity was also investigated. An area of approximately 100 km² western of Helgoland (German North Sea) was investigated.

Chapter 5 shows an application of sidescan sonars in classifying intertidal systems (backbarrier tidal flat of Norderney Island). Acoustic sources are generally not deployed in such extremely shallow water environments, where other remote sensing sources (i.e. satellite and air-borne) are usually preferred. The performance and limitations of the sidescan sonar are presented, together with a comparison to an existing classification based on satellite (RapidEye) data. The ability, limits and benefits of each system in detecting and resolving the abiotic (sediments) and biotic (shellfish beds) components in a transitional and highly dynamic environment are described.

Chapter 6 investigates a region of the Helgoländer Steingrund area, an end-moraine deposit characterized by the presence of both soft and hard grounds and the colonization by bryozoans. The study took

advantage by the use of underwater videos for improving the acoustic-based habitat classifications. The role of the morphology and of the hydrodynamic conditions triggered by tidal currents and by storm events in explaining the distribution of the different bryozoan communities was analysed by means of current measurements (ADCP).

- Chapter 7** analyses the effects of a deep-water container terminal construction (JadeWeserPort, Wilhelmshaven, Germany) on composition and distribution of sediments and benthic communities, by means of bathymetric (high-resolution DTM from multibeam echosounder), sedimentological, and biological data. Macrofauna and sediment records before and during the port construction (2002 and 2010, respectively) were compared. A set of statistical routines was used for understanding the modification of benthic community patterns in disturbed and non-disturbed areas.
- Chapter 8** in the same research area of Chapter 7, it makes use of an expert-based sidescan sonar classification and multivariate statistical tools in order to test the pattern congruence of the bio-communities structure with the acoustic classes, the number of days after dredging, and the sediment composition.
- Chapter 9** Synthesis and future perspectives. It offers a synthesis of the results and applications. It summarizes the open research gaps and suggests possible future investigations.

1.6. References

- An, S., Li, H., Guan, B., Zhou, C., Wang, Z., Deng, Z., Zhi, Y., Liu, Y., Xu, C., Fang, S., Jiang, J., Li, H., 2007. China's natural wetlands: past problems, current status, and future challenges. *Ambio* 36, 335-342, doi: 10.1579/0044-7447(2007)36[335:CNWPPC]2.0.CO;2
- Anderson, J. T., Holliday, D. V., Kloser, R., Reid, D. G., Simard, Y., 2008. Acoustic seabed classification: current practice and future directions. – *ICES Journal of Marine Science*, 65, 1004-1011, doi: 10.1093/icesjms/fsn061
- Badewien, T.H., Zimmer, E., Bartholomä, A., Reuter, R. 2009. Towards continuous long-term measurements of suspended particulate matter (SPM) in turbid coastal waters. *Ocean Dynamics*, 59 (2), 227-238, doi: 10.1007/s10236-009-0183-8

-
- Balbo, A.L., Martínez-Fernández, M., Esteve-Selma, M.-A., 2017. Mediterranean wetlands: archaeology, ecology, and sustainability, *WIREs Water* 2017, e1238, doi: 10.1002/wat2.1238
- Barbier, E.B., Acreman, M., Knowler, D. 1997. Economic valuation of wetlands, a guide for policy makers and planners. Ramsar Convention Bureau, Gland, Switzerland, 143 pp.
- Bartholomä, A., Kubicki, A., Badewien, T.H., Flemming, B.W. 2009. Suspended sediment transport in the German Wadden Sea—seasonal variations and extreme events. *Ocean Dynamics*, 59 (2), 213-225, doi: 10.1007/s10236-009-0193-6
- Behre, K.-E., 1987. Meeresspiegelbewegungen und Siedlungsgeschichte in den Nordseemarschen, *Vortr. Oldenburg. Landschaft*, 17, 1-47.
- Behre, K.-E., 2004. Coastal development, sea-level change and settlement history during the later Holocene in the clay district of Lower Saxony (Niedersachsen), northern Germany, *Quaternary International*, 112 (1). 37-53, doi: 10.1016/S1040-6182(03)00064-8.
- Benninghoff, M., Winter, C., 2019. Recent morphologic evolution of the German Wadden Sea, *Scientific Reports*, 9, Article number: 9293, doi: 10.1038/s41598-019-45683-1
- Biondo, M., Bartholomä, A. 2017, A multivariate analytical method to characterize sediment attributes from high-frequency acoustic backscatter and ground-truthing data (Jade Bay, German North Sea coast). *Continental Shelf Research*, doi: 10.1016/j.csr.2016.12.011
- Bird, E.C.F., 1970. *Coasts*. M.I.T. Press, Cambridge, MA, 310 pp.
- Blondel, P., 2008. A review of acoustic techniques for habitat mapping. *Hydroacoustics* 11, 29-38.
- Borics, G., Várбірó, G., Padisák, J., 2013. Disturbance and stress: different meanings in ecological dynamics? *Hydrobiologia*, 711 (1), 1-7, doi: 10.1007/s10750-013-1478-9
- Boulay, S.O.C., 2012. Analysis of multibeam sonar data for benthic habitat characterization of the Port of Tauranga, New Zealand. Thesis, Master of Science (MSc), University of Waikato, Hamilton, New Zealand, 200 pp.
- Boyd, S.E., Coggan, R.A., Birchenough, S.N.R., Limpenny, D.S., Eastwood, R.L., Foster-Smith, R.L., Philpott, S., Meadows, W.J., James, J.W. C., Vanstaen, K., Soussi, S., Rogers, S., 2006. The role of seabed mapping techniques in environmental monitoring and management. Science Series Technical Report no. 127, CEFAS, 215 pp.
- Brandt, A.C., Wollesen, A., 2009. Tourism and recreation. Thematic report No. 3.4. In: Marencic, H., Vlas, J. de (Eds), 2009. Quality Status Report 2009. Wadden Sea Ecosystem No. 25. Common Wadden Sea Secretariat, Trilateral Monitoring and Assessment Group, Wilhelmshaven, Germany.
- Brekhovskikh, L., Lysanov, Y., 1982. Fundamentals of ocean acoustics. Ed. L. Felsen. Springer Series in Electrophysics Volume 8. Springer-Verlag, Berlin
- Briggs, K.B., 1989. Microtopographical roughness of shallow-water continental shelves, *IEEE Journal of Oceanic Engineering*, 14, 4, 360-367, doi: 10.1109/48.35986
- Brophy, L.S., Greene, C., Hare, V.C., Holycross, B., Lanier, A., Heady, W.N., O' Connor, K., Imaki, H., Haddad, T., Dana, R. 2019. Insights into estuary habitat loss in the western United States using a new method for mapping maximum extent of tidal wetlands. *PLOS ONE*, 14 (8), 34 pp.: e0218558, doi: 10.1371/journal.pone.0218558.
- Brown, C.J., Collier, J.S. 2008. Mapping benthic habitat in regions of gradational substrata: an automated approach utilising geophysical, geological, and biological relationships. *Estuarine, Coastal and Shelf Science*, 78 (3), 203-214, doi: 10.1016/j.ecss.2007.11.026

- Brown, C.J., Smith, S.J., Lawton, P., Anderson, J.T., 2011. Benthic habitat mapping: A review of progress towards improved understanding of the spatial ecology of the seafloor using acoustic techniques. *Estuary, Coastal and Shelf Science*, 92, 3, 502-520, doi: 10.1016/j.ecss.2011.02.007
- Brown, S., Nicholls, R., Woodroffe, C., Hanson, S., Hinkel, J., Kebede, A.S., Neumann, B., Vafeidis, A.T., 2013. Sea-level rise impacts and responses: a global perspective. In: Finkl, C.W. (Ed), *Coastal Hazards*. Netherlands: Springer, 117-149, doi: 10.1007/978-94-007-5234-4_5
- BSH, 2016. Guideline for seafloor mapping in German marine waters using high-resolution sonars. BSH No. 7201, 147 pp.
- Burke, L., Kura, Y., Kasem, K., Revenga, C., Spalding, M., McAllister, D., 2001. *Coastal ecosystems*. Washington DC, World Resources Institute. 93 pp.
- Callaway, J.C., Borde, A., Diefenderfer, H.L., Parker, V.T., Rybczyk, J.M., Thom, R.M. 2012. Pacific Coast Tidal Wetlands. In Batzer, D.P., Baldwin, A.H. (Eds), *Wetland Habitats of North America: Ecology and Conservation Concerns*. University of California Press, 408 pp.
- Carter, R.W.G., 1988. *Coastal environments. An introduction to the physical, ecological and cultural systems of the coastlines*. Academic Press, New York, 617 pp.
- Cicin-Sain, B., Bernal, P., Veerle, V., Belfiore, S., Goldstein, K. 2002. *A Guide to Oceans, Coasts, and Islands at the World Summit on Sustainable Development*, Center for the Study of Policy, Newark, Delaware, August 2002, 41 pp.
- Cochrane, G.R., 2008. Video-supervised classification of sonar data for mapping seafloor habitat. In: *Marine habitat mapping technology*, Reynolds, J.R., Green, H.G. (Eds), doi: 10.4027/mhmta.2008.13
- Collier, J.S., Brown, C.J., 2005. Correlation of sidescan backscatter with grain size distribution of surficial seabed sediments. *Marine Geology*, 214, 4, 431-449, doi: 10.1016/j.margeo.2004.11.011
- Connor, D.W., Allen, J.H., Golding, N., Howell, K.L., Lieberknecht, L.M., Northen, K.O., Reker, J.B., 2004. The Marine Habitat Classification for Britain and Ireland Version 04.05. In: JNCC (2015) *The Marine Habitat Classification for Britain and Ireland Version 15.03*. jncc.defra.gov.uk/MarineHabitatClassification
- Costa, B.M., Battista, T.A. 2013. The semi-automated classification of acoustic imagery for characterizing coral reef ecosystems, *International Journal of Remote Sensing*, 13 doi: 10.1080/01431161.2013.800661
- Costanza, R., D'Arge, R., de Groot, R., Farber, S., Grasso, M., Hannon, B., Naeem, S., Limburg, K., Paruelo, J., O'Neill, R.V., Raskin, R., Sutton, P., van den Belt, M., 1997. The value of the world's ecosystem services and natural capital. *Nature*, 387, 253-260, doi: 10.1038/387253a0
- Costanza, R., de Groot, R., Sutton, P., van der Ploeg, S., Anderson, S.J., Kubiszewski, I., Farber, S., Turner, R.K., 2014. Changes in the global value of ecosystem services. *Global Environmental Change*, 26, 152-158, doi: 10.1016/j.gloenvcha.2014.04.002
- Costello, M.J. 2009. Distinguishing marine habitat classification concepts for ecological data management. *Marine Ecology Progress Series*, 379, 253-268, doi: 10.3354/meps08317
- Council Directive 79/409/EEC of 2 April 1979 on the conservation of wild birds.

-
- Council Directive 92/43/EEC of 21 May 1992 on the conservation of natural habitats and of wild fauna and flora. OJ L 206, 22.7.1992, p. 7–50. <http://data.europa.eu/eli/dir/1992/43/oj>
- CPSL 2001. Final Report of the Trilateral Working Group on Coastal Protection and Sea Level Rise. Wad-den Sea Ecosystem No. 13. Common Wadden Sea Secretariat, Wilhelmshaven, Germany.
- CPSL, 2010. CPSL Third Report. The role of spatial planning and sediment in coastal risk management. Wadden Sea Ecosystem No. 28. Common Wadden Sea Secretariat, Trilateral Working Group on Coastal Protection and Sea Level Rise (CPSL), Wilhelmshaven, Germany.
- Cracknell, A.P. 2018. The development of remote sensing in the last 40 years. *International Journal of Remote Sensing*, 39 (23), 8387-8427, doi: 10.1080/01431161.2018.1550919
- Davidson, N.C., 2014. How much wetland has the world lost? Long-term and recent trends in global wetland area, *Marine and Freshwater Research*, 65, 10, 934-941, doi: 10.1071/MF14173
- Dalrymple, R.W., Makino, Y., Zaitlin, B.A., 1991. Temporal and Spatial Patterns of Rhythmite Deposition on Mud Flats in the Macrotidal Cobequid Bay-Salmon River Estuary, Bay of Fundy, Canada. *Clastic Tidal Sedimentology - Memoir 16*, 137-160.
- Davies, L.J., 1964. A Morphogenic approach to the worlds' shorelines. *Zeitschrift für Geomorphologie*, 8, 127-142.
- Davies, L.J., 1972. Geographical variation in coastal development. Oliver and Boyd, Edinburgh, 204 pp.
- Deppe F., 1999. Intertidal Mudflats Worldwide. Practical course at the Common Wadden Sea Secretariat (CWSS) in Wilhelmshaven 1st June - 30th September 1999, 100.
- Directive 2000/60/EC of the European Parliament and of the Council of 23 October 2000 establishing a framework for Community action in the field of water policy. OJ L 327, 22.12.2000, p. 1-73. <http://data.europa.eu/eli/dir/2000/60/oj>
- Directive 2008/56/EC of the European Parliament and of the Council of 17 June 2008 establishing a framework for community action in the field of marine environmental policy (Marine Strategy Framework Directive) (Text with EEA relevance), OJ L 164, 25.6.2008, 19-40, <http://data.europa.eu/eli/dir/2008/56/oj>
- Duarte, C., Losada, I.J., Hendriks, I., Mazarrasa, I., Marba, N., 2013. The role of coastal plant communities for climate change mitigation and adaptation. *Nature Climate Change*, 3, 961-968, doi: 10.1038/nclimate1970.
- Eastwood, P.D., Souissi, S., Rogers, S.I., Coggan, R.A., Brown, C.J., 2006. Mapping seabed assemblages using comparative top-down and bottom-up classification approaches. *Canadian Journal of Fisheries and Aquatic Sciences*, 63, 1536-1548, doi: 10.1139/f06-058
- Elachi, C., van Zyl, J.J., 2006. Introduction to the Physics and Techniques of Remote Sensing. Hoboken, New Jersey, John Wiley & Sons, 584 pp.
- Ehlers, J., 1988. The morphodynamics of the Wadden Sea, A.A. Balkema, Rotterdam, 397 pp.
- Eisma, D., 1998. Intertidal Deposits: River Mouths, Tidal Flats, and Coastal Lagoons, 1st Edition, CRC Press, 525 pp.
- Erfteemeijer, P., Jury, M.J., Gabe, B., Dijkstra, J.T. Leggett, D., Foster, T.M., Shafer, D.J., 2013. Dredging, port- and waterway construction near coastal plant habitats. In: Australasian

- Port and Harbour Conference (14th : 2013 : Sydney, N.S.W.). Coasts and Ports 2013: 21st Australasian Coastal and Ocean Engineering Conference and the 14th Australasian Port and Harbour Conference. Barton, A.C.T.: Engineers Australia, 280-284.
- EEA (European Environmental Agency), European Topic Centre on Biological Diversity (ETC/BD), 2012. EUNIS Habitat Classification 2012 - a revision of the habitat classification descriptions. EEA (ETC/BD), 2013-01-01.
- Ferrini, V.L., Flood, R.D., 2006. The effects of fine-scale surface roughness and grain size on 300 kHz multibeam backscatter intensity in sandy marine sedimentary environments, *Marine Geology*, 228, 1, 153-172, doi: 10.1016/j.margeo.2005.11.010
- Finlayson, C.M., D'Cruz, R., Davidson, N.C. 2005. Ecosystems and Human Well-being: Wetlands and Water Synthesis: a report of the Millennium Ecosystem Assessment. Washington, DC: World Resources Institute, ISBN 978-1-56973-597-8, 80 pp.
- Flemming, B.W., 2002. Effects of climate and human interventions on the evolution of the Wadden Sea depositional system (Southern North Sea). In: Wefer G., Berger W.H., Behre KE., Jansen E. (Eds), *Climate Development and History of the North Atlantic Realm*. Springer, Berlin, Heidelberg, doi: 10.1007/978-3-662-04965-5_26
- Flemming, B.W., 2012. Siliciclastic Back-Barrier Tidal Flats. In: Davis, R.A. Jr, Dalrymple, R.W. (Ed.), *Principles of Tidal Sedimentology*, 231-267, doi: 10.1007/978-94-007-0123-6_10.
- Flemming, B.W, Bartholomä, A., 1997. Response of the Wadden Sea to a rising sea level: a predictive empirical model, *German Journal of Hydrography*, 49, 343-353, doi: 10.1007/BF02764043
- Flemming, B.W, Davis, R.A., 1994. Holocene evolution, morphodynamics and sedimentology of the Spiekeroog barrier island system (southern North Sea). *Senckenbergiana maritima*, 24, 117-155.
- Foster-Smith, R., Connor, D. & Davies, J., 2007. What is habitat mapping? In: *MESH Guide to Habitat Mapping*, MESH Project, 2007, JNCC, Peterborough.
- Gopal, B., Junk, W. J., Davis, J.A., 2000. Biodiversity in wetlands: assessment, function and conservation. Volume 1. Backhuys Publishers, Leiden, The Netherlands, 353 pp.
- Gopal, B., Junk, W. J., Davis, J.A., 2001. Biodiversity in wetlands: assessment, function and conservation. Volume 2. Backhuys Publishers, Leiden, The Netherlands, 311 pp.
- Greene, H & Bizzarro, Joseph & O'Connell, V.M. & Brylinsky, C.K., 2007. Construction of digital potential marine benthic habitat maps using a code classification scheme and its application. *Special Paper - Geological Association of Canada*, 141-155.
- Greene, A., Rahman, A., Kline, R., Rahman, M. 2018. Side scan sonar: A cost-efficient alternative method for measuring seagrass cover in shallow environments. *Estuarine, Coastal and Shelf Science*. 207. 10.1016/j.ecss.2018.04.017.
- Halpern, B. S., Walbridge, S., Selkoe, K. A., Kappel, C. V., Micheli, F., D'Agrosa, C., Bruno, J. F., Casey, K. S., Ebert, C., Fox, R. F., Heinemann, D., Lenihan, H. S., Madin, E. M. P., Perry, M. T., Selig, E., R., Spalding, M., Steneck, R., Watson, R., 2008. A Global Map of Human Impact on Marine Ecosystems. *Science*, 319 (5865), 948-952, doi: 10.1126/science.1149345
- Harley, C.D.R., Hughes, A., Hultgren, K.M., Miner, B.G., Sorte, C.J., Thornber, C.S., Rodriguez, L.F., Tomanek, L., Williams, S.L., 2006. The impacts of climate change in coastal marine systems. *Ecol Lett*, 9, 228-241, doi: 10.1111/j.1461-0248.2005.00871.x

-
- Harris, P.T., 2012a. Anthropogenic threats to benthic habitats. In: Harris, P.T. and Baker, E.K. (Eds.), *Seafloor geomorphology as benthic habitat*, Elsevier, 39-60, doi: 10.1016/B978-0-12-385140-6.00003-7
- Harris, P.T., 2012b, Surrogacy. In: Harris, P.T. and Baker, E.K. (Eds.), *Seafloor geomorphology as benthic habitat*, Elsevier, 93-108, doi: 10.1016/B978-0-12-385140-6.00005-0
- Harris, P.T., 2012c. Biogeography, benthic ecology, and habitat classification schemes. In: Harris, P.T. and Baker, E.K. (Eds.), *Seafloor geomorphology as benthic habitat*, Elsevier, 61-91, doi: 10.1016/B978-0-12-385140-6.00004-9
- Harris, P., Baker, E., 2012. Why Map Benthic Habitats? In: Harris, P.T. and Baker, E.K. (Eds.), *Seafloor geomorphology as benthic habitat*, Elsevier, 3-22, doi: 10.1016/B978-0-12-385140-6.00001-3.
- Hass, H. C., Mielck, F., Fiorentino, D., Papenmeier, S., Holler, P., Bartholomä, A., 2016. Seafloor monitoring west of Helgoland (German Bight, North Sea) using the acoustic ground discrimination system RoxAnn, *Geo-Marine Letters*, 37, 125-136, doi: 10.1007/s00367-016-0483-1
- Hayes, M., 1975. Morphology of sand accumulation in estuaries: an introduction to the symposium. In Cronin, L.E. (Ed.), *Estuarine Research*, vol. II, Academic Press, 3-22.
- Hayes, M.O., 1979. Barrier island morphology as a function of tidal and wave regime, In: Leatherman, S.P. (Ed.), *Barrier islands*, Academic, New York, 1-27.
- Hines, P.C., 1990, Theoretical model of acoustic backscatter from a smooth seabed, *The Journal of the Acoustical Society of America*, 88, 324-334, doi: 10.1121/1.399954
- Hinrichsen, D., 1998. *Coastal waters of the world: trends, threats and strategies*. Washington DC, Island press, 275 pp.
- Huff, L.C. 2008. Acoustic remote sensing as a tool for habitat mapping in Alaska waters. In: Reynolds, J.R., Greene, H.G. (Eds), *Marine Habitat Mapping Technology for Alaska*, Alaska Sea Grant College Program, University of Alaska Fairbanks, 29-45, doi: 10.4027/mhmta.2008.03.
- Hugo, G., 2011. Future demographic change and its interactions with migration and climate change. *Global Environmental Change*, 21, Supplement 1, 21-33, doi: 10.1016/j.gloenvcha.2011.09.008
- ICES. 2014. Report of the Working Group on Marine Habitat Mapping (WGMHM), 19–23 May 2014, San Sebastian, Spain. ICES CM 2014/SSGSUE:07, 59.
- Jackson, D.J., Briggs, K.B., 1992. High-frequency bottom backscattering: Roughness vs. sediment volume scattering, *Journal of the Acoustical Society of America*, 92, 2, 962-977, doi: 10.1121/1.403966
- Jackson, D., Richardson, M., 2007. *High-Frequency Seafloor Acoustics*, The Underwater Acoustic Series, Springer, 616 pp.
- Jonsson, P., Sillitoe, I., Dushaw, B., Nystuen, J., Heltne, J. 2009. Observing using sound and light – A short review of underwater acoustic and video-based methods. *Ocean Science Discussion*, 6, 819-870.
- Kabat, P., Bazelmans, J., van Dijk, J., Herman, P.M.J., van Oijen, T., Pejrup, M., Reise, K., Speelman, H., Wolff, W.J., 2012. The Wadden Sea Region: towards a science for sustainable development. *Ocean and Coastal Management*, 68, 4-17, doi: 10.1016/j.ocecoaman.2012.05.022

- Kenny, A.J., Cato, I., Desprez, M., Fader, G., Schüttenhelm, R.T.E., Side, J., 2003, An overview of seabed-mapping technologies in the context of marine habitat classification, *ICES Journal of Marine Science*, 60, 2, 2003, 411–418, doi: 10.1016/S1054-3139(03)00006-7
- Klopper, S., Baptist, M.J., Bostelmann, A., Busch, J., Buschbaum, C., Gutow, L., Janssen, G., Jensen, K., Jørgensen, H., de Jong, F., Lüerßen, G., Schwarzer, K., Stempel, R., Thieltges, D., 2017. Wadden Sea Quality Status Report 2017, Common Wadden Sea Secretariat, Wilhelmshaven, Germany [Miscellaneous], hdl:10013/epic.cbae88a7-2b8f-4847-bf8b-edfafbf0359d
- Knottnerus, O.S., 2005. History of human settlement, cultural change and interference with the marine environment, *Helgoland Marine Research*, 59, 2-8, doi: 10.1007/s10152-004-0201-7
- Kossin, J.P., 2018. A global slowdown of tropical-cyclone translation speed, *Nature*, 558, 104-107, doi: 10.1038/s41586-018-0158-3
- Kostylev, V., Todd, B.J., Fader, G.B.J., Courtney, R.C., Cameron, G.D.M., Pickrill, R.A. 2001. Benthic habitat mapping on the Scotian Shelf based on multibeam bathymetry, surficial geology and sea floor photographs. *Marine Ecology Progress Series*, 219, 121-137, doi: 10.3354/meps219121
- Kostylev, V., 2012. Benthic habitat mapping from seabed acoustic surveys: do implicit assumptions hold?, *International Association of Sedimentologists Special Publication*, 44, doi: 10.1002/9781118311172.ch20.
- Kubicki, A., Bartholomä, A., 2011. Sediment dynamics in the Jade tidal channel prior to port construction, Southeastern North Sea. *Journal of Coastal Research*, 64, 771-775.
- Lamarque, G., Lurton, X., 2018. Recommendations for improved and coherent acquisition and processing of backscatter data from seafloor-mapping sonars, *Marine Geophysics Research*, 39, 5-22, doi: 10.1007/s11001-017-9315-6
- Landres, P.B, Morgan, P., Swanson, F.J., 1999. Overview of the use of natural variability concepts in managing ecological systems. *Ecological Application*, 9 (4), 1179-1188, doi: 10.1890/1051-0761(1999)009[1179:OOTUON]2.0.CO;2
- Lecours, Vincent & Devillers, Rodolphe & Schneider, David & Lucieer, Vanessa & Brown, Craig & Edinger, Evan., 2015. Spatial scale and geographic context in benthic habitat mapping: Review and future directions. *Marine Ecology Progress Series*. 535. 259-284. 10.3354/meps11378, doi: 10.3354/meps11378
- Lillesand, T.M., Kiefer, R.W., 1994. *Remote Sensing and Image Interpretation*, 3rd ed. Toronto, John Wiley & Sons, 750 pp.
- Lindeboom, H., The coastal zone: an ecosystem under pressure. In: Field, J.G., Hempel, G., Summerhayes, C.P. (Eds), 2002. *Oceans 2020: science, trends, and the challenge of sustainability*. Island Press, 365 pp.
- Lotze, H.K., 2005. Radical changes in the Wadden Sea fauna and flora over the last 2,000 years, *Helgoland Marine Research*, 59, 71-83, doi: 10.1007/s10152-004-0208-0
- Lotze, H.K., 2007, Rise and fall of fishing and marine resource use in the Wadden Sea, southern North Sea. *Fisheries research*, 87 (2-3), 208-218, doi: 10.1016/j.fishres.2006.12.009
- Lotze, H.K., Reise, K., Worm, B., van Beusekom, J., Busch, M., Ehlers, A., Heinrich, D., Hoffmann, R.C., Holm, P., Jensen, C., Knottnerus, O.S., Langhanki, N., Prummel, W., Vollmer, M., Wolff, W.J., 2005. Human transformations of the Wadden Sea ecosystem

-
- through time: a synthesis, *Helgoland Marine Research*, 59, 84-95, doi: 10.1007/s10152-004-0209-z
- Lucieer, V., Johnson, C., Barrett, N., 2019. Making the first national seafloor habitat map, *Eos*, 100, doi: 10.1029/2019EO116965
- Lurton, X., 2010. An introduction to underwater acoustics. Principle and applications, Springer, 680 pp.
- Lurton, X., Lamarche, G., (Eds), 2015. Backscatter measurements by seafloor-mapping sonars. Guidelines and Recommendations. Geohab Report, 200 pp. <http://geohab.com/wp-content/uploads/2014/05/BSWG-REPORT-MAY2015.pdf>
- Mann, M.E., Emanuel, K.A., 2006. Atlantic hurricane trends linked to climatic change. *Eso*, *Trans. Amer. Geophys. Union*, 87, 233-241, doi: 10.1029/2006EO240001
- Markert, A., Wehrmann, A., Krohncke, I., 2010. Recently established *Crassostrea*-reefs versus native *Mytilus*-beds: differences in ecosystem engineering affects the macrofaunal communities (Wadden Sea of Lower Saxony, southern German Bight). *Biol Invasions*, 12, 15–32, doi: 10.1007/s10530-009-9425-4
- Martínez, M.L., Intralawan, A., Vázquez, G., Pérez-Maqueo, O., Suttond, P., Landgrave, R., 2006. The coasts of our world: Ecological, economic and social importance, *Ecological Economics*, 63 (2–3), 254-272, doi: 10.1016/j.ecolecon.2006.10.022
- Matsumoto, H., Dziak, R.P., Fox, C.G., 1993. Estimation of seafloor microtopographic roughness through modeling of acoustic backscatter data recorded by multibeam sonar systems, *The Journal of the Acoustical Society of America*, 94, 2776-2878, doi: 10.1121/1.407361
- McDermid, G. J., Franklin, S. E., LeDrew, E. F. (2005). Remote sensing for large-area habitat mapping. *Progress in Physical Geography*, 29(4), 449-474, doi: 10.1191/0309133305pp455ra
- McLachlan, A., Brown, A.C., 2006. *The Ecology of Sandy Shores (Second Edition)*, 14 - Human Impacts, 273-301.
- MESH, 2008. MESH (Mapping European seabed habitats): review of standards and protocols for seabed habitat mapping.
- Mielck, F., Bartsch, I., Hass, H. C., Wölfl, A. C., Bürk, D., Betzler, C., 2014. Predicting spatial kelp abundance in shallow coastal waters using the acoustic ground discrimination system RoxAnn, *Estuarine Coastal and Shelf Science*, 143, 1-11, doi: 10.1016/j.ecss.2014.03.016
- Miththapala, S., 2013. Tidal flats. *Coastal Ecosystems Series (Vol 5)*. iii + 48pp. Colombo, Sri Lanka: IUCN.
- Mulhearn, P.J., 2000. Modelling acoustic backscatter from near-normal incidence echosounders - Sensitivity Analysis of the Jackson Model (No. DSTO-TN-0304). Defence Science and Technology Organisation Melbourne (Australia).
- Murray, N.J., Clemens, R.S., Phinn, S.R., Possingham, H.P., Fuller, R.A. 2014. Tracking the rapid loss of tidal wetlands in the Yellow Sea. *Frontiers in Ecology and the Environment*, 12 (5), 267-272, doi: 10.1890/130260
- Neumann, B., Vafeidis, A.T., Zimmermann, J., Nicholls, R.J., 2015. Future coastal population growth and exposure to sea-level rise and coastal flooding - A global assessment. *PLoS ONE* 10(3): e0118571, doi: 10.1371/journal.pone.0118571

- Newell, R.C., Seiderer, L.J., Simpson, N.M., Robinson, J.E., 2002. Impact of marine aggregate dredging and overboard screening on benthic biological resources in the central North Sea: production licence area 408. Coal Pit Marine Ecological Surveys Limited Technical Report No 1/4/02 to the British Marine Aggregate Producers Association (BMAPA), 72 pp.
- Petersen, C.H., Bishop, M.J. 2009. Assessing the Environmental Impacts of Beach Nourishment. *BioScience*, 55, 887-896, doi: 10.1641/0006-3568(2005)055[0887:ATEIOB]2.0.CO;2
- Pickett, S.T.A., White, P.S., 1985. The Ecology of Natural Disturbance and Patch Dynamics, 472, doi: 10.1016/C2009-0-02952-3
- Pickett, S.T.A., Kolasa, J., J.J. Armesto, J. J., Collins, S.L., 1989. The Ecological Concept of Disturbance and Its Expression at Various Hierarchical Levels. *Oikos*, 54(2), 129-136, doi: 10.2307/3565258
- Pickrill, R.A., Kostylev, V.E., 2007, Habitat mapping and national seafloor mapping strategies in Canada, In: Todd, B.J., and Greene, H.G. (Eds.), *Mapping the seafloor for habitat characterization: Geological Association of Canada, Special Paper 47*, 483-495.
- Pinson, S., Barbier, B. Holland, C., Stephan, Y., 2018. Seabed roughness measurement using the multibeam-subbottom-profiler SBP120, *The Journal of the Acoustical Society of America*, 144(3), 1972-1972, doi: 10.1121/1.5068619
- Post, A.L., 2008. The application of physical surrogates to predict the distribution of marine benthic organisms, *Ocean & Coastal Management*, 51 (2), 2008, 161-179, doi: 10.1016/j.ocecoaman.2007.04.008
- Pouliquen, E., Lurton, X., 1992. Sea-bed identification using echo-sounder signals, in European conference on underwater acoustics. In: Weydert, M. (Ed.), *Proceedings of the European Conference on Underwater Acoustics*, Elsevier Applied Science, London, pp. 535-539.
- Reise, K., 2005. Coast of change: habitat loss and transformations in the Wadden Sea, *Helgoland Marine Research*, 59, 9-21, doi: 10.1007/s10152-004-0202-6.
- Reise, K., Baptist, M., Burbridge, P., Dankers, N., Fisher, L., Flemming, B., Oost, A.P., Smit, C. 2010. The Wadden Sea – a universal outstanding tidal wetland. *Wadden Sea Ecosystem*, 29, Common Wadden Sea Secretariat, Wilhelmshaven Germany, 7-24.
- Reynolds, J., Greene, H.G., Woodby, D., Kurland, J., Allee, B. 2008. Overview: Marine Habitat Mapping Technology for Alaska. In: Reynolds, J.R., Greene, H.G. (Eds), *Marine Habitat Mapping Technology for Alaska*, Alaska Sea Grant College Program, University of Alaska Fairbanks, 1-11, doi: 10.4027/mhmta.2008.01.
- Rykiel, E.J. JR, 1985. Towards a definition of ecological disturbance, *Australian Journal of ecology*, 10, 361-365, doi: 10.1111/j.1442-9993.1985.tb00897.x
- Sardà, R., Pinedo, S., Gremare, A., Taboada, S., 2000. Changes in the dynamics of shallow sandy-bottom assemblages due to sand extraction in the Catalan Western Mediterranean Sea. *ICES Journal of Marine Science*, 57, 1446–1453, doi: 10.1006/jmsc.2000.0922
- Seto, K.C., 2011. Exploring the dynamics of migration to mega-delta cities in Asia and Africa: Contemporary drivers and future scenarios. *Global Environmental Change* 2011, 21, Supplement 1, 94-107, doi: 10.1016/j.gloenvcha.2011.08.005
- Simonini, R., Ansaloni, I., Bonini, P., Grandi, V., Graziosi, F., Iotti, M., Massamba-N'Siala, G., Mauri, M., Montanari, G., Preti, M., De Nigris, N., Prevedelli, D., 2007. Recolonization

-
- and recovery dynamics of the macrozoobenthos after sand extraction in relict sand bottoms of the Northern Adriatic Sea, *Marine Environmental Research*, 64, 574–589, doi: 10.1016/j.marenvres.2007.06.002
- Small, C., Nicholls, R.J., 2003. A global analysis of human settlement in coastal zones. *Journal of Coastal Research*, 19, 584-599.
- Smit, C.J., Dankers, N., Ens, B.J., Meijboom, A. 1998. Birds, mussels, cockles and shellfish fishery in the Dutch Wadden Sea: how to deal with low food stocks for eiders and oystercatchers? *Senckenbergiana maritima*, 29 (1-6), 141-153.
- Staneva J, Stanev E, Wolff J-O, Badewien T, Reuter R, Flemming BW, Bartholomä A, Bolding K (2009) Hydrodynamics and sediment dynamics in the German Bight: A focus on observations and numerical modelling. *Continental Shelf Research*, 29 (1), 302-319, doi: 10.1016/j.csr.2008.01.006
- Steininger, G., Holland, C.W., Dosso, S.E., Dettmer, J., 2013. Seabed roughness parameters from joint backscatter and reflection inversion at the Malta Plateau, *The Journal of the Acoustical Society of America* 134 (3), 1833-1842, doi: 10.1121/1.4817833
- Sterr, H., 2008. Assessment of Vulnerability and Adaptation to Sea-Level Rise for the Coastal Zone of Germany. *Journal of Coastal Research* 24(2), 380 – 393, doi: 10.2112/07A-0011.1
- Streif, H., 1990. Das ostfriesische Küstengebiet: Nordsee, Inseln, Watten und Marschen. Reihe: Sammlung geologischer Führer, Bd. 57. Berlin Stuttgart, 1990.
- Sutton, G., Boyd, S., 2009. Effects of extraction of marine sediments on the marine environment 1998-2004, ICES Cooperative Research Report, 297, 180 pp.
- Schwartz, M. (Ed.), 2005. *Encyclopedia of coastal science*. Springer, 1211 pp.
- Svenson, C., Ernstsen, V.B., Winter, C., Bartholomä, A., Hebbel, D., 2009. Tide-driven Sediment Variations on a Large Compound Dune in the Jade Tidal Inlet Channel, Southeastern North Sea, *Journal of Coastal Research*, 56, 361-365.
- Valiela, I. 2006. *Global Coastal Changes*. Blackwell Publishing, 367 pp.
- van Overmeeren, R., Craeymeersch, J., van Dalen, J., Fey, F., Heteren, S., Meesters, E., 2009. Acoustic habitat and shellfish mapping and monitoring in shallow coastal water. Sidescan sonar experiences in The Netherlands. *Estuarine, Coastal and Shelf Science*. 85. 437-448, doi: 10.1016/j.ecss.2009.07.016.
- von Rönn, G., Schwarzer, K., Reimers, H.-C., Winter, C. 2019. Limitations of Boulder Detection in Shallow Water Habitats Using High-Resolution Sidescan Sonar Images. *Geosciences*, 9(9), 390, doi: 10.3390/geosciences9090390.
- Webster P.J., Holland, G.J., Curry, J.A., Chang, H.-R., 2005. Changes in tropical cyclone number duration and intensity in a warming environment, *Science*, 309, 5742, 1844-1846, doi: 10.1126/science.1116448.
- Winter, C., Backer, V., Adolph, W., Bartholomä, A., Becker, M., Behr, D., Callies, C., Capperucci, R.M., Ehlers, M., Farke, H., Geimecke, C., Grayek, S., Hass, C.H., Heipke, C., Herrling, G., Hillebrand, H., Hodapp, D., Holler, P., Jung, R., Krasemann, H., Kröncke, I., Kwohl, E., März, J., Meyerdierks, D., Mielck, F., Millat, G., Reimers, H.C., Reuter, R., Schmidt, A., Staneva, J., Stanev, E., van Beusekom, J., Wirtz, K. 2016. WIMO -Wissenschaftliche Monitoringkonzepte für die Deutsche Bucht - Abschlussbericht, 158 pp.

- Yang, S.L., Li, H., Ysebaert, T., Bouma, T.J., Zhang, W.X., Wang, Y.Y., Li, P., Li, M., Ding, P.X., 2008. Spatial and temporal variations in sediment grain size in tidal wetlands, Yangtze Delta: On the role of physical and biotic controls, *Estuarine, Coastal and Shelf Science*, 77, 4, 657-671, doi: 10.1016/j.ecss.2007.10.024.
- Zhu, L., Suomalainen, J., Liu, J., Hyyppä, J., Kaartinen, H., Haggren, H., 2018. A review: remote sensing data. In: Rustamov, R.B., Hasanova, S., Zeynalova, M.H. (Eds), *Multi-purpose application of geospatial sensors*. IntechOpen Publication, 224 pp, doi: 10.5772/intechopen.69713

1.7. Research funding

This research has been carried out within the INTERCOAST Project (Integrated Coastal Zone and Shelf Sea Research), an International Research Training Group funded by Deutsche Forschungsgemeinschaft DFG (German Research Foundation) and supported by the Universities of Bremen (Germany) and Waikato (New Zealand). Part of the activities have been funded by the Lower Saxony Ministry of Environment, Energy and Climate Protection (“Niedersächsische Ministerium für Umwelt, Energie und Klimaschutz”), and by the Lower Saxony Ministry of Science and Culture (“Niedersächsische Ministerium für Wissenschaft und Kultur”), within the WIMO Project (“Wissenschaftliche Monitoringkonzepte für die Deutsche Bucht”, Scientific Research Concepts for the German Bight).

1.8. Declaration of contribution

Chapter 2 *Capperucci, R.M. 2013. Marine habitat mapping: stretching the blue marble on a map. In: Recent impulses to Marine Sciences and Engineering. From coast to deep sea: multiscale approaches to marine sciences, Einsporn, M., Wiedling, J., Schöttener, S. (Eds.), DGM and ICBM, 178-189*

The paper was published as a chapter of a conference book. The conference (YouMares2013) hosted a “Marine Habitat Mapping” scientific session, proposed and chaired by R.M. Capperucci. As chairman of a session, the author was invited to write an introduction to the topic and a literature review. The chapter was reviewed by the Scientific Committee of the YouMares Conference before its acceptance.

Chapter 3 ***Capperucci, R.M., Bartholomä, A. 2012. Sediment vs Topographic Roughness: Anthropogenic Effects on Acoustic Seabed Classification. In: Hydro12 - Taking care of the sea, Conference Proceedings, 13 November 2012 - 15 November 2012, Rotterdam, 23-28.***

The specific research topic and the survey plan (geophysical measurements and sediment sampling) were designed by R.M. Capperucci in accordance with Dr. A. Bartholomä. The collection and the processing of the hydroacoustic data and sediment samples were done by R.M. Capperucci (with contributions by a Senckenberg lab assistant, for the sediment processing). The analysis and interpretation of the data, as well as the writing of the paper were done by R.M. Capperucci. Dr. A. Bartholomä supervised the work and reviewed the manuscript. The study was presented at the Hydro 2012 Conference, was selected among the best student works and was finally awarded with the “Best Student Paper Award” by the conference Scientific Board.

Chapter 4 *Holler, P., Markert, E., Bartholomä, A., **Capperucci, R.**, Hass, C.H., Kröncke, I., Mielke, F., Reimers, C.H. 2017. Tools to evaluate seafloor integrity: comparison of multi-device acoustic seafloor classifications for benthic macrofauna-driven patterns in the German Bight, southern North Sea. Geo-Marine Letters, 37 (2), 93-109, doi: 10.1007/s00367-016-0488-9*

The data collection and processing were done on different cruises by all the authors. R.M. Capperucci processed and analyzed part of the hydroacoustic data and took part in the manuscript editing and revision (both for text and figures).

Chapter 5 ***Capperucci, R.M., Kubicki, A., Holler, P., Bartholomä, A. 2020. Sidescan sonar meets airborne and satellite remote sensing: challenges of a multi-device seafloor classification in extreme shallow water intertidal environments. Geo-Marine Letters, <https://doi.org/10.1007/s00367-020-00639-7>.***

The concept of the research topic and the design of the survey were developed by R.M. Capperucci, under the supervision of Dr. A. Bartholomä. The collection of the hydroacoustic and sedimentological data was done during multiple surveys by all the authors. The processing, analysis and interpretation of the data were done by R.M. Capperucci, with contributions by the co-

authors. The paper was conceived and written mostly by R.M. Capperucci, the other authors made significant contributions helping to improve the text.

- Chapter 6** Bartholomä, A., **Capperucci, R.M.**, Coers, S.I.I., Becker, L.R., Battershill, C.N. 2019. *Hydrodynamics and hydroacoustic mapping of a benthic seafloor in a coarse grain habitat of the German Bight. Geo-Marine Letters*, doi: <https://doi.org/10.1007/s00367-019-00599-7>

The field measurements were carried out by all the authors (except for Prof. C. Battershill) on different cruises. Data processing and interpretation were done by Dr. A. Bartholomä, R.M. Capperucci, and S. Coers. The concept of the paper was designed by Dr. A. Bartholomä, while the writing and editing were done by Dr. A. Bartholomä and R.M. Capperucci, with contributions from the other authors.

- Chapter 7** Gutperlet, R., **Capperucci, R.M.**, Bartholomä, A., Kröncke, I. 2015. *Benthic biodiversity changes in response to dredging activities during the construction of a deep-water port. Marine Biodiversity*, 45 (4), 819-839, doi: [10.1007/s12526-014-0298-0](https://doi.org/10.1007/s12526-014-0298-0)

The design of the survey was done by R.M. Capperucci with regards to the hydroacoustic data acquisition plan. Sampling locations were selected in cooperation with the other research partners. On board activities (hydroacoustic and sediment sampling) were run by R.M. Capperucci, as well as the related data processing and analysis. The parts of the paper dealing with hydroacoustic and the sedimentological topics were written by R.M. Capperucci, with significant contributions to the introduction, methodological and discussion parts.

- Chapter 8** Gutperlet, R., **Capperucci, R.M.**, Bartholomä, A., Kröncke, I. 2017. *Relationships between special patterns of macrofauna communities, sediments and hydroacoustic backscatter data in a highly heterogeneous and antropogenic altered environment. Journal of Sea Research*, 121, 33-46, doi: [10.1016/j.seares.2017.01.005](https://doi.org/10.1016/j.seares.2017.01.005)

The design of the survey was done by R.M. Capperucci with regards to the hydroacoustic data acquisition plan. Sampling locations were selected in cooperation with the other research

partners. On board activities (hydroacoustic and sediment sampling) were run by R.M. Capperucci, as well as the respective data processing and analysis. The concept of the paper was conceived and structured together with Dr. R. Gutperlet. The parts of the paper relative to the acoustic and the sedimentological topics (introduction, research gaps, methods, results and discussion) were written by R.M. Capperucci, as well as the figures and tables related to the hydroacoustic and sedimentological topics.

Chapter 2

Marine Habitat Mapping: stretching the blue marble on a map

Ruggero Maria Capperucci^{1,2}

¹MARUM – Center for Marine Environmental Sciences, University of Bremen, Leobener Strasse, 28359 Bremen, Germany

²Marine Research Department, Senckenberg am Meer, Südstrand 40, 26382 Wilhelmshaven, Germany

Keywords: *Remote sensing, Hydroacoustic, Benthic, Habitat mapping, Monitoring*

2.1. Abstract

Marine Habitat Mapping (MHM) can be described as a process to simplify the marine environment in a discrete amount of parameters. It is a key tool for environmental analysis, policy making and future development planning. It gathers expertise from a wide range of disciplines, e.g.: geosciences, engineering, biology, physics, ecology, and modeling. The increasing demand for versatile uses of marine environments makes the outcomes even more relevant for legal and socio-economic applications. The integration of multiple remote-sensing techniques (acoustics, aerial and satellite images) coupled with punctual ground-truthing (sediment and/or biological samples, video/photo analysis) and with statistical/GIS analysis is becoming a standard tool. Nevertheless, relevant questions are still open, particularly regarding the protocols for mapping and the reliability/repeatability of the outcomes. The review offers an introduction to the concept of MHM and a glimpse summary about the main principles and methods used for it, with a focus on the integration of remote sensing and hydroacoustic approaches with *in situ* techniques for mapping and monitoring coastal areas.

Capperucci, R.M., 2013. Marine Habitat Mapping: stretching the blue marble on a map. In: Recent Impulses to Marine Science and Engineering. From coast to deepsea: multiscale approaches to marine sciences. YouMares 4 Glimpse Review. Einsporn, M., Wiedling, J., Schöttener, S. (Eds), DGM-ICBM, 178-189.

2.2. Introduction

Marine Habitat Mapping (hereafter MHM) can be described as a process to simplify the marine environment in a discrete amount of parameters and presenting them in a thematic map (Foster-Smith et al. 2007). For a long time the definition of habitat itself and its application to seafloor mapping has been an issue restricted to scientists (Mitchel 2005). However, the increase of human pressure on marine - and particularly coastal - systems (Halpern et al. 2008) raised the interest on MHM principles and techniques, which are nowadays considered a key tool for environmental analysis, policy making and future development planning (Baker and Harris 2012).

As marine environments are independent from political boundaries, in recent times different countries have been required to cooperate in describing and monitoring common habitats. Thus, a greater number of international projects aimed to define protocols, standard and techniques to univocally map marine ecosystems have been developed (e.g. ICES 2012).

The present study offers an introduction to the concept of MHM and a glimpse summary about the main principles and methods used for it, with a particular focus on the integration of remote sensing and hydroacoustic approaches coupled with point sampling techniques for mapping and monitoring coastal areas.

2.3. What is Marine Habitat Mapping

Habitat comes from the Latin verb “*habitare*”, meaning “to live”. Despite the crucial relevance of this concept, there is not a unique definition for it (Hall et al. 1997; Corsi et al. 2000). The most common definition refers to the place where an organism lives or could potentially live (Begon et al. 1996; Blondel 2008), which is a concept based on the ecological definition of niche (Grinnell 1917; Hutchinson 1957). From this perspective, even though the term habitat is clearly organism-centered (MacMahon et al. 1981; Kostylev 2012), the subject lays within the word “place”, which is defined purely by abiotic descriptors (“Physical and chemical aspects”, Whittaker et al. 1973, p. 326).

A slightly different interpretation stresses much more the role of the actual presence of living organism in defining a specific habitat (Dauvin et al. 2008). In this sense, “A habitat is defined as plant and animal communities as the characterizing elements of the biotic environment, together with abiotic factors

(soil, climate, water availability and quality, and others), operating together at a particular scale” (Davies et al. 2004, p. 286).

During the last decades, the urgent need to integrate ecological information into policy making (Cohen 1996) shifted the “habitat definition issue” from a scientific board to a social, economic and political discourse (Leaf and Pamuk 1997). In this sense, the previous definition had to be reviewed and integrated with a new perspective which includes human beings and their settlements (i.e. habitats; Cohen 1996).

Similarly, the concept of Habitat Mapping applied to the marine realm has been defined differently over the time (Blondel 2008; Brown et al. 2011) depending on the purpose of mapping (e.g. fishery resource management, potential hazard assessment, etc.; Harris and Baker 2012), on the technique used (e.g. point sampling methods, remote sensing approaches etc.), on the scale (from single organism to biotopes; Harris 2012), and on the main discipline behind the investigation (e.g. ecology, geology, biology, etc.).

The European MESH project described the MHM as “Plotting the distribution and extent of habitats to create a map with coverage of the seabed showing distinct boundaries separating adjacent habitats” (Foster-Smith et al. 2007, p. 1). Brown et al. (2011) pointed out the limitation of this description: although a boundary is needed to distinctly discriminate a specific area from the surrounding environment (Kostylev et al. 2001), the actual seafloor presents often gradational and continuous changes rather than sharp discontinuities (Brown and Collier, 2008; Cochrane 2008). Therefore Brown et al. (2011) prefer a different definition that includes “The use of spatially continuous environmental data sets to represent and predict biological patterns on the seafloor (in a continuous or discontinuous manner)” (p. 503).

When applied to marine realm, habitat mapping is often named as Seabed or Benthic Habitat Mapping (e.g. Kostylev et al. 2001; Purkis and Pasterkamp 2004; Ierodiaconou et al. 2007). It could be defined, in a broad sense, as the process of segmenting the seabed into discrete information that can be univocally represented on maps, to be used for describing or predicting the spatial and – in same case - temporal distribution and composition of a specific habitat and the connection between different habitats. Thus, rather than pointing out a specific methodology, this term gathers together information from a wide spectrum of disciplines and techniques (from geology to ecology, from biology to computer modeling, etc.) with the aim of translate the complexity of the habitat issue (as described before) in a way that is scientifically correct, reliable, repeatable, and usable for socio-economic and management decisions (Baker and Harris 2012).

2.4. Why Marine Habitat Mapping

The use of visual concepts (for structuring, decoding, describing, and communicating the world) traces back to the nature itself of human beings. The visual understanding and memory plays a fundamental role in both the learning and the communication processes. In addition, geographical information is meant to be spatially structured and visualized on maps. Together with geographical and nautical charts (Blake 2004), thematic maps (e.g. sedimentological and geological maps) have been largely used in science all the way back to the early stages of these disciplines, mainly but not only for scientific reasons (Laban 1998).

The world population growth is a well-documented and studied phenomenon (see Livi-Bacci 2012, for an analytical introduction to the theme) and one of the most relevant aspects is where the growth concentrated (Hinrichsen 1999; Seto et al. 2011). Vulnerable areas such as coasts and wetlands have been particularly stressed by the so-called “skewed growth” (Seto et al. 2011). Different studies calculate that 40-44% of population live within 100 km from the coast (GESAMP 2001; SEDAC 2010; see Crowell et al. 2007, for a critical analysis of these values) and around 10% in the low elevation coastal zone (<10 m, McGranahan et al. 2007). It is a loop, where the population grows, and so does its dependence on the ecosystem (as primary economic source), as well as the human pressure on the environment itself and the need of minimizing potentially harmful changes.

As a consequence, over the last decades the interest for the habitat shifted from a purely scientific (and only secondly economic) board to more sociological and political sciences (similarly to what has happened for the sea level rise and global warming discussions) (Harris and Baker 2012).

European legislations offer a good example of this process. Due to public awareness of environmental issues and to the economic, political and civil interests, the EU Agencies have been urged to pass new regulations (e.g Council Directive 92/43/EEC; European Parliament and Council Directive 2000/60/EC; European Parliament and Council Directive 2008/56/EC) that commit every EU member in defining, monitoring, and protecting their national habitats. These obligations have catalyzed 1) A new pulse in surveying the seafloor and therefore a gain in knowledge (Evans, 2006) and 2) The rise of several international projects (e.g. MESH, EuSeaMAP, HERMIONE). In fact, as the environment is independent from political boundaries, different countries have been implicitly forced to find a common strategy to map the marine habitat. For example, the Wadden Sea has undergone this process with the institution of

a Common Secretariat and a Trilateral Act (among Germany, The Netherlands and Denmark) for the monitoring and the drawing of a quality status report.

Consequently, MHM and its outcomes play nowadays a key role in quantitative translating the complexity of the environment into visual- thematic maps which are used for a wide range of management and industry purposes (Kurland and Woodby 2008; Cogan et al. 2009; Baker and Harris 2012; Copeland et al. 2013). As a result of a survey, Harris and Baker (2012) found that the gain of new scientific knowledge is only the 3rd of the main purposes of MHM, after the support to Governments for marine planning and the definition of marine protected areas.

2.5. How to map the marine habitat

Offering a complete introduction about methods and techniques used for MHM goes beyond the aim and scope of this review. A number of text books and literature reviews have been already published, both about MHM practices (e.g. Boyd et al. 2006; Anderson et al. 2007; Franklin 2009; Brown et al. 2011) and specific aspects of each method. Nevertheless, hereinafter a short summary is given about the main approaches to Benthic Habitat Mapping. For a general overview about the techniques for marine investigations, see the glimpse review by Gottshall and Heckmann (2013).

2.5.1. *In situ* techniques

In situ techniques are between the most commonly used in the MHM realm (e.g. Boyd et al. 2006; Anderson et al. 2007). They consist in surveying a small portion of the seafloor by means of direct investigations that can include a proper physical contact with the seabed (e.g. sampling) and/or a close-up of its surface component (video or still frame; Coggan et al. 2007b). Several different samplers are used (Eleftheriou 2013), mainly depending on the purpose of the research (epifauna, sediments, water samples etc.) and on the nature of the seabed (e.g. rock outcrops, soft mud layers, mussel beds). In situ techniques offer the advantage of a quantitative measurement of a number of environmental parameters (biological, geological, oceanographic) and the disadvantage of being time consuming and single-point based (Diesing et al. 2009).

In fact, in order to infer spatial information, a process of interpolation is required (implying some uncertainty, Brown et al. 2002). Point sampling techniques are based on the assumption that the sample collected is statistically representative of the actual characteristics (physical, biological, geotechnical etc.)

of the seafloor. Moreover, despite the technical advance of positioning systems, the impossibility of precisely controlling the location of a sampling device underwater can severely affect the final results, especially in naturally highly-heterogeneous and/or highly disturbed environments (Capperucci and Bartholomä 2012). The use of under-water video devices fills some of these gaps (Diesing et al. 2009), with the possibility of tracking in real time the underwater tools (or to calculate its position by means of the offsets) and the gain in a continuous spatial coverage rather than a point-sampling grid.

In situ techniques are commonly used for the ground-truthing of data collected by means of indirect techniques (see below).

2.5.2. Remote sensing techniques

In a broad sense, remote sensing includes any techniques which investigate the environment without any direct contact with it (Lillesand and Kiefer 1994; Elachi and van Zyl 2006) i.e. both airborne/satellite methods and hydro-acoustic technologies.

Most commonly, however, remote sensing is meant for indirect measurements collected by means of devices which use electro-magnetic sources (passive and/or active, e.g. Campbell, 2002).

Airborne and satellite techniques have been widely employed for habitat description and documentation (McDermid et al. 2005) both in terrestrial and marine realms. The applications range from vegetation detection (see Xie et al. 2008, for a review) to human related target definition (e.g. Schott 2007). However, the use of such techniques in the marine environment (Dekker et al. 2007) is physically limited by the penetration of electromagnetic signals into the water (Gordon and McCluney 1975). Therefore, most published literature relates to extremely shallow water environments and - anyway - to areas where water transparency assures a good penetration down to the seafloor. Remote sensing systems present the advantage of a time- and cost-efficient technology that can be periodically deployed on the same area. Satellite-based systems, in particular, offer the unique advantage of being dependent (i.e. limited) to the actual constellation of satellites orbiting over the Earth, which makes easier to reach a common standard (all the research groups have to use the same data sources). In addition to satellite and airborne image analysis, LiDAR systems are becoming widely used in MHM because of the capability of coupling electromagnetic-based information to high resolution topographic measurements.

2.5.3. *Hydroacoustic techniques*

Hydroacoustic sources have been used since decades for the investigation of the seafloor; the relative literature can be named as uncountable. Besides the historical uses (for depth measurements, sediment visual segmentation, etc., e.g. Lurton 2010; Blondel 2009), a new disciplines arose in the last 20 years, based on the analysis of the shape of the signal backscattered from the seabed. Despite the remarkable differences among the acoustic systems (due to constructional details, geometry of the device, etc.) there is a common principle: the interaction with the seafloor surface and subsurface modifies the echo shape so that the returned signal can be decomposed and analyzed to gather information about the nature of the seabed (Hamilton 1999). The use of multiple acoustic devices for the definition and mapping of seabed types and habitats goes often under the name of Acoustic Seabed Classification (ASC, e.g. Anderson et al. 2007; 2008; Brown and Blondel 2009).

In addition to the manual interpretation (which has been largely used since the early stage of this discipline), in recent years a new generation of Acoustic Ground Discrimination Systems (AGDS, Kenny et al. 2003) has been developed, with the aim of making the mapping technique less expert-based and more replicable (Brown 2007).

Although it is not possible to offer a complete review of the publications which link the hydroacoustic techniques to the MHM science, some authors covered aspects of this topic with specific reviews which are fundamental for a good understanding of the state of the art and future perspective of this discipline (e.g. Kenny et al. 2003; Coggan et al. 2007a; Hamilton 2005; Boyd et al. 2006; Brown et al. 2011).

2.6. Facing the challenge

The above mentioned international projects and regulations about MHM and its applications go toward the same direction, which can be summarized in 4 main steps:

1. Establishing international and multi-disciplinary working groups for defining standards and protocol for mapping;
2. Measuring and mapping for describing the current state of the habitat;
3. Predicting and modeling habitat composition and distribution, including future scenarios that take into account the human effects and providing measures for mitigating negative impacts;

-
4. Monitoring the environment (in both middle- and long-term terms) in order to validate the models and documenting the changes, while improving the knowledge about ecosystem dynamic.

The outcomes should act as guidelines for any policy decision, which can interfere with the preservation of the habitat as a resource for the environment and for the human being itself.

The monitoring aspect, in particular, opens new scenarios in the MHM discipline, pointing out the fundamental need of having reliable and repeatable tools for releasing products that can consistently be compared over the time. This point is strictly link to two other aspects which represent the real challenge for the future of the MHM discipline.

2.7. Finding a common strategy

The call for common standards is a relatively new concept in the MHM community (McDermid et al. 2005; Coggan et al. 2007a; Vanden Borre et al. 2011, Brown et al. 2011). As a recently born discipline, most of the efforts have been spent in shifting existing technologies into a new application and understanding how they were able to render the actual world on a map. And the way to answer this question is far but ended.

In fact, even considering the same methodology (i.e. hydroacoustic methods) the variety of the devices (e.g. technical details, ways of deployment, environmental conditions, processing) is wide enough to force the scientific community to focus firstly on single aspects of specific devices (for example the ability of a specific acoustic source in discriminating between sediments types, e.g. Anderson et al. 2002; Collier and Brown 2005, Bartholomä 2006). Only recently there has been a shift toward a multi-devices comparison. Yet, these attempts aim primarily to test different acoustic sources (for example, multibeam vs. sidescan-sonar or singlebeam, e.g. Bartholomä 2006; Holler and Bartholomä 2010; Schimel et al. 2010a), whereas a very few publications focused on testing a single class of devices over the same targets (e.g. different sidescan sonars on the same seabed area, Hass et al. 2012). This is an essential aspect if we consider that even the maps from the same country are produced by a pool of working groups using different devices.

However, in the scientific community there is an increasing effort to merge different experiences and to find a common approach that allows the delivery of consistent products (e.g. Capperucci et al. 2013a). Important steps have been recently undertaken in this direction. For the 6th Shallow Water

Conference, a multibeam record (called “Common Dataset”) has been made available to the scientific community with the aim of comparing the results of different approaches and processing techniques. Afterwards, the same dataset has been used as training and testing one for the attendants of the 12th International Symposium GeoHab 2013. From this experience, a working group (Working Group on Multibeam Sonar Backscatter Data Acquisition and Processing, SOBAP) has been launched “to discuss and propose a series of best practice or standards for acquisition and processing of multibeam sonar backscatter data” (SOBAP, 2013, p.1).

2.8. The 4th dimension of Marine Habitat Mapping: when?

An extremely limited literature has been published about the 4th dimension of MHM: the timing. It is not uncommon to ground-truth remote sensing data with samples collected in different surveys (e.g. Whitmire et al. 2007; Schimel et al. 2010b), assuming a relative stability of the systems (which can be the case, but only under specific circumstances and for certain scales, conditions which are not known *a priori*). Similarly, a very few studies face the challenge of a time-series analysis of the same area, especially for ASC systems (e.g. Gleason et al. 2005). Most of these researches focus on specific aspects related to highly disturbed environments, like dredging/disposal sites (e.g. Wienberg and Bartholomä 2005), addressing the recovery time of sediments and/or benthic communities (e.g. Bolan and Rees 2003; Boyd et al. 2005).

The research gaps raise some questions: What we map today will be meaningful in the future? How can we set up standards and practices if we do not assess their reliability on a temporal scale? Where feasible, the integration of different techniques can potentially help filling the gaps, for example combining the high-resolution of the *in situ* data and the spatial extension of the acoustic methods for setting up the scene and validate remote sensing based maps.

In this sense, the monitoring of tidal systems, where wide intertidal areas are periodically exposed, represents a very good laboratory for satisfying the need of temporal representation. In fact, satellite images are an efficient and effective method for repeated acquisitions in standard configuration (e.g. Jung et al. 2013), whereas LiDAR data can provide high-resolution topographic information, coupled with roughness-based classifications (e.g. Schmidt et al. 2013). Remote sensing data can be then compared with the acoustic ones, collected in extreme shallow water conditions during high-tide periods, integrating subtidal sectors, too. *In situ* techniques can contribute to the identification and definition of the

habitats and to ground-truth remote data. The tidal flat areas in the Wadden Sea provide a good example. In the framework of the WIMO Project (Wissenschaftliche Monitoring Konzepte für die Deutsche Bucht, “Scientific monitoring concepts for the German Bight”), an interdisciplinary group is working in this direction, producing the first promising results (Capperucci et al. 2013b).

2.9. References

- Anderson, J. T., Gregory, R. S., Collins, W. T. 2002. Acoustic classification of marine habitats in coastal Newfoundland. *ICES Journal of Marine Science*, 59 (1), 156-167.
- Anderson, J. T., Holliday, D. V., Kloser, R. J., Reid, D., Simard, Y. (ed.) 2007. Acoustic seabed classification of marine physical and biological landscapes. *ICES Cooperative Research Report*, 286, ICES, Copenhagen, 185 pp.
- Anderson, J. T., Holliday, D. V., Kloser, R., Reid, D. G., Simard, Y. 2008. Acoustic seabed classification: current practice and future directions. *ICES Journal of Marine Science*, 65, 1004–1011.
- Bartholomä, A., 2006, Acoustic bottom detection and seabed classification in the German Bight, southern North Sea. *Geo-Marine Letters*, 26 (3), 177-184.
- Begon, M., Harper, J. L., Townsend, C. R. 1996. *Ecology: Individuals, Populations and Communities*, 3rd ed. Oxford, Blackwell Science Ltd, 1068 pp.
- Baker, E. K., Harris, P. T., 2012. 2 - Habitat Mapping and Marine Management In: *Seafloor Geomorphology as Benthic Habitat* ed. by Harris, P. T., Baker, E. K., London, Elsevier, 23-38.
- Blake, J. 2004. *The Sea Chart: The Illustrated History of Nautical Maps and Navigational Charts*. London, Conway Maritime Press, 160 pp.
- Blondel, P. 2008. A review of acoustic techniques for habitat mapping. *Hydroacoustics*, 11, 29-38.
- Blondel, P. 2009. *The Handbook of Sidescan Sonar*. Berlin; Heidelberg; New York: Springer, 324 pp.
- Bolam, S. G., Rees, H. L. 2003. Minimizing Impacts of Maintenance Dredged Material Disposal in the Coastal Environment: A Habitat Approach. *Environmental Management*, 32 (2), 171-188.
- Boyd, S. E., Coggan, R. A., Birchenough, S. N. R., Limpenny, D. S., Eastwood, R. L., Foster-Smith, R. L., Philpott, S., Meadows, W. J., James, J. W. C., Vanstaen, K., Soussi, S., Rogers, S. 2006. The role of seabed mapping techniques in environmental monitoring and management. *Science Series Technical Report no. 127, CEFAS*, 215 pp.
- Boyd, S. E., Limpenny, D. S., Rees, H. L., Cooper, K. M. 2005. The effects of marine sand and gravel extraction on the macrobenthos at a commercial dredging site (results 6 years post-dredging). *ICES Journal of Marine Science*, 62, 145-162.
- Brown, C. J., 2007. Seafloor imagery, remote sensing and bathymetry: Acoustic Ground Discrimination Systems (AGDS). In: *Mapping the Seafloor for Habitat*

- Characterization, ed. by Todd, B. J., Greene, H. G., Geological Association of Canada, 3-10.
- Brown, C.J., Blondel, P. 2009. Developments in the application of multibeam sonar backscatter for seafloor habitat mapping. *Applied Acoustics*, 70, 1242-1247.
- Brown, C. J., Collier, J. S. 2008. Mapping benthic habitat in regions of gradational substrata: An automated approach utilising geophysical, geological, and biological relationships. *Estuarine, Coastal and Shelf Science*, 78, 203-214.
- Brown, C. J., Cooper, K. M., Meadows, W. J., Limpenny, D. S., Rees, H. L. 2002. Small-scale Mapping of Sea-bed Assemblages in the Eastern English Channel Using Sidescan Sonar and Remote Sampling Techniques. *Estuarine, Coastal and Shelf Science*, 54, 263-278.
- Brown, C. J., Smith, S. J., Lawton, P., Anderson, J. T. 2011. Benthic habitat mapping: A review of progress towards improved understanding of the spatial ecology of the seafloor using acoustic techniques. *Estuarine, Coastal and Shelf Science*, 92 (3), 502-520.
- Campbell, J. B. 2002. Introduction to remote sensing, 3rd ed. New York, The Guilford Press, 621 pp.
- Capperucci, R., Bartholomä, A. 2012. Sediment vs. topographic roughness: anthropogenic effects on acoustic seabed classification. In: Leendert Dorst, L., van Dijk, T., van Ree, R., Boers, J., Brink, W., Kinneging, N., van Lancker, V., de Wulf, A., Nolte, H. (Eds), Conference Proceedings of Hydro12, Taking care of the sea, the Hydrographic Society Benelux (HSB), on behalf of the International Federation of Hydrographic Societies (IFHS), Rotterdam, the Netherlands, 12-15 November 2012, 23-28.
- Capperucci, R. M., Holler, P., Kubicki, A., Bartholomä, A. 2013a. Developing new concepts for environmental monitoring: the WIMO Project (Germany), Proceedings of GeoHab 2013, Rome, Italy, 6-10 May 2013, 10.
- Capperucci, R. M., Adolph, W., Hodapp, D., Jung, R., Schmidt, A., Holler, P., Bartholomä, A., Ehlers, M., Sörgel, U., Hillebrand, H., Farke, H. 2013b. From 630 km to the ground: a new multiscale approach to scientific habitat monitoring of intertidal and subtidal areas, Proceedings of GeoHab 2013, Rome, Italy, 6-10 May 2013, 79.
- Cochrane, G. R. 2008. Video Supervised Classification of Sonar Data for Mapping Seafloor Habitat. In: *Marine Habitat Mapping Technology for Alaska*, ed. by Reynolds, J. R., Greene, H. G., Alaska Sea Grant College Program, University of Alaska Fairbanks, 185-194.
- Cogan, C. B., Todd, B. J., Lawton, P., Noji, T. T. 2009. The role of marine habitat mapping in ecosystem-based management. *ICES Journal of Marine Science*, 66, 2033-2042.
- Coggan, R., Populus, J., White, J., Sheehan, K., Fitzpatrick, F., Piel, S. (Eds), 2007a. Review of Standards and Protocols for Seabed Habitat Mapping, MESH.
- Coggan, R., Mitchell, A., White, J., Golding, N. 2007b. Recommended operating guidelines (ROG) for underwater video and photographic imaging techniques. In: *MESH Guide to Habitat Mapping*, MESH Project, JNCC, Peterborough, 32 pp.
- Cohen, M. 1996. HABITAT II and the challenge of the urban environment: bringing together the two definitions of habitat. *International Social Science Journal*, 48, 95-101.
- Collier, J. S., Brown, C. J. 2005. Correlation of sidescan backscatter with grain size distribution of surficial seabed sediments. *Marine Geology*, 214 (4), 431-449.

-
- Copeland, A., Edinger, E., Devillers, R., Bell, T., LeBlanc, P., Wroblewski, J. 2013. Marine habitat mapping in support of Marine Protected Area management in a subarctic fjord: Gilbert Bay, Labrador, Canada. *Journal of Coastal Conservation*, 17, 225-237.
- Corsi, F., de Leeuw, J., Skidmore, A. 2000. Modeling species distribution with GIS. In: *Research techniques in animal ecology: controversies and consequences*, ed. By Boitani, L., Fuller, T. K., New York, Columbia University Press, 389–434.
- Council Directive (EEC) 92/43/EEC of 21 May 1992 on the conservation of natural habitats and of wild fauna and flora.
- Crowell, M., Edelman, S., Coulton, K., McAfee, S. 2007. How Many People Live in Coastal Areas? *Journal of Coastal Research*, 23 (5), iii–vi.
- Dauvin, J. C., Bellan, G., Bellan-Santini, D. 2008. The need for clear and comparable terminology in benthic ecology. Part II. Application of the European Directives. *Aquatic Conservation-Marine and Freshwater Ecosystems*, 18, 446-456.
- Davies, C. E., Moss, D., Hill, M. O. 2004. *EUNIS Habitat Classification Revised 2004*. Paris, European Topic Centre on Nature Protection and Biodiversity, 310 pp.
- Dekker, A., Mount, R., Jordan, A., 2007. Satellite and airborne imagery including aerial photography for benthic habitat mapping. In: *Mapping the Seafloor for Habitat Characterization*, ed. by Todd, B. J., Greene, H. G., Geological Association of Canada, 11-28.
- Diesing, M., Ware, S., Foster-Smith, R., Stewart, H., Long, D., Vanstaen, K., Forster, R., Morando, A. 2009. Understanding the marine environment – seabed habitat investigations of the Dogger Bank offshore draft SAC. Joint Nature Conservation Committee, Peterborough., JNCC Report No. 429, 89 pp., 5 Appendices.
- Elachi, C., van Zyl, J. J., 2006. *Introduction to the Physics and Techniques of Remote Sensing*. Hoboken, New Jersey, John Wiley & Sons, 584 pp.
- Eleftheriou, A. (Ed), 2013. *Methods for the Study of Marine Benthos*, 4th Edition. John Wiley & Sons, 496 pp.
- European Parliament and Council Directive (EC) 2000/60/EC of 23 October 2000 establishing a framework for Community action in the field of water policy.
- European Parliament and Council Directive (EC) 2008/56/EC of 17 June 2008 establishing a framework for community action in the field of marine environmental policy (Marine Strategy Framework Directive).
- Evans, D. 2006. The Habitats of the European Union Habitats Directive. *Biology & Environment: Proceedings of the Royal Irish Academy*, 106 (3), 167-173.
- Foster-Smith, R., Connor, D., Davies, J. 2007. What is habitat mapping? In: *MESH Guide to Habitat Mapping*, MESH Project, 2007, JNCC, Peterborough. Available online at: <<http://www.searchmesh.net/default.aspx?page=1900>>.
- Franklin, J., 2009. *Mapping Species Distributions. Spatial Inference and Prediction*. Cambridge, UK, Cambridge University Press, 320 pp.
- GESAMP (IMO/FAO/UNESCO-IOC/WMO/WHO/IAEA/ UN/UNEP Joint Group of Experts on the Scientific Aspects of Marine Environmental Protection) 2001. *Protecting the oceans from land-based activities. Land-based sources and activities affecting the quality and uses of the marine, coastal and associated freshwater environment*. Rep. Stud. GESAMP No. 71, UNEP: Nairobi, 168 pp.

- Gleason A. C. R., Preston, J. M., Bloomer, S. 2009. Reproducibility of Single-Beam acoustic seabed classification. Quester Tangent Corporation.
- Gordon, H. R. & McCluney, W. R. 1975. Estimation of the Depth of Sunlight Penetration in the Sea for Remote Sensing. *Applied Optics*, 14 (2), 413-416.
- Gottshall, Heckmann, 2013. Methods and applications of ocean remote sensing, In: *Recent Impulses to Marine Science and Engineering. From coast to deepsea: multiscale approaches to marine sciences*, Einsporn, M., Wiedling, J., Schöttener, S. (Eds), DGM publishing company.
- Grinnell, J. 1917. The niche relationship of the California Thrasher. *The Auk*, 34, 427-433.
- Hall, L. S., Krausman, P. R., Morrison, M. L. 1997. The Habitat Concept and a Plea for Standard Terminology. *Wildlife Society Bulletin*, 25, 173–182.
- Halpern, B. S., Walbridge, S., Selkoe, K. A., Kappel, C. V., Micheli, F., D'Agrosa, C., Bruno, J. F., Casey, K. S., Ebert, C., Fox, R. F., Heinemann, D., Lenihan, H. S., Madin, E. M. P., Perry, M. T., Selig, E., R., Spalding, M., Steneck, R., Watson, R. 2008, A Global Map of Human Impact on Marine Ecosystems. *Science*, 319 (5865), 948-952.
- Hamilton, L. J. 2005. A Bibliography of Acoustic Seabed Classification. Technical Report No. 27, Cooperative Research Center for Coastal Zone Estuary & Waterway Management, Australia, 131 pp.
- Harris, P. T. 2012. 4 - Biogeography, Benthic Ecology, and habitat Classification Schemes. In: *Seafloor Geomorphology as Benthic Habitat* ed. by Harris, P. T., Baker, E. K., London, Elsevier, 61-91.
- Harris, P. T., Baker, E. K. 2012. 1 - Why Map Benthic Habitats? In: *Seafloor Geomorphology as Benthic Habitat* ed. by Harris, P. T., Baker, E. K. (Eds), London, Elsevier, 3-22.
- Hass, H. C., Bartholomä, A., Bürk, D., Holler, P., Mielck, F., Reimers, H. C. 2012. Hydroacoustic seafloor classification in the SE North Sea. In: *Geophysical Research Abstracts*, Vol. 14, EGU2012-13612, EGU General Assembly 2012.
- Hinrichsen, D. 1999. The coastal population explosion. In: *Trends and Future Challenges for U.S. National Ocean and Coastal Policy*, Cicin-Sain, B., Knecht, R.W., Foster, H. (Eds), University of Delaware and NOAA, pp. 27-29.
- Holler, P., Bartholomä, A. 2010. Shallow Water Habitat Mapping of the Lower Saxony Wadden Sea Using Acoustic Classification Methods. In: *Hydro 2010. Rostock-Warnemünde, Germany 02-05 November 2010*.
- Hutchinson, G. E. 1957. Concluding Remarks. *Cold Spring Harbor Symposium 'Quantitative Biology'*, 22, 415-427.
- ICES, 2012. Report of the Working Group on Marine Habitat Mapping (WGMHM), 22–25 May 2012, Isle of Vilm, Germany. ICES CM 2012/SSGSUE:03, 32 pp.
- Ierodiaconou, D., Laurenson, L., Burq, S., Reston, M., 2007. Marine benthic habitat mapping using Multibeam data, georeferenced video and image classification techniques in Victoria, Australia. *Journal of Spatial Science*, 52 (1), 93-104.
- Jung, R., Ehlers, M., Klonus, S. 2013. High Resolution Remote Sensing Images for Tidal Lands Change Detection, In: *Recent Impulses to Marine Science and Engineering. From coast to deepsea: multiscale approaches to marine sciences*, Einsporn, M., Wiedling, J., Schöttener, S. (Eds), DGM publishing company.
- Kostylev, V. E. 2012. Benthic Habitat Mapping from Seabed Acoustic Surveys: Do Implicit Assumptions Hold?, In: *Sediments, Morphology and Sedimentary Processes on*

-
- Continental Shelves: Advances in Technologies, Research, and Applications, Li, M. Z., Sherwood, C. R., Hill P. R. (Eds), Chichester, West Sussex, UK, John Wiley & Sons Ltd.
- Kostylev, V. E., Todd, B. J., Fader, G. B. J., Courtney, R. C., Cameron, G. D. M., Pickrill, R. A. 2001. Benthic habitat mapping on the Scotian Shelf based on multibeam bathymetry, surficial geology and sea floor photographs. *Marine Ecology-Progress Series*, 219, 121-137.
- Kurland, J., Woodby, D. 2008. What Is Marine Habitat Mapping and Why Do Managers Need It? In: *Marine Habitat Mapping Technology for Alaska*, ed. by Reynolds, J. R., Greene, H. G., Alaska Sea Grant College Program, University of Alaska Fairbanks, 13-27.
- Laban, C. 1998. Seabed mapping. *Hydro International*, 2 (1), 4.
- Leaf, M., Pamuk, A. 1997. Habitat II and the Globalization of Ideas. *Journal of Planning Education and Research*, Fall 1997, 17 (1), 71-78.
- Lillesand, T. M., Kiefer, R. W. 1994. *Remote Sensing and Image Interpretation*, 3rd ed. Toronto, John Wiley & Sons, 750 pp.
- Livi-Bacci, M. 2012. *A concise history of world population*. Malden, MA, USA, Blackwell Publishing, 251 pp.
- Lurton, X. 2002. *An Introduction to Underwater Acoustics. Principles and Applications*. London, Springer, UK, Praxis Publ., 349 pp.
- MacMahon, J. A., Schimpf, D. J., Andersen, D. C., Smith, K. G., Bayn Jr., R. L. 1981. An organism-centered approach to some community and ecosystem concepts. *Journal of Theoretical Biology*, 88 (2), 287-307.
- McDermid, G. J., Franklin, S. E., LeDrew, E. F. 2005. Remote sensing for large-area habitat mapping. *Progress in Physical Geography*, 29 (4), 449-474.
- McGranahan, G., Balk, D., Anderson, B. 2007. The rising tide: assessing the risks of climate change and human settlements in low elevation coastal zones. *Environment & Urbanization*, 19 (1), 17-37.
- Mitchell, S. C. 2005. How useful is the concept of habitat? - A critique. *Oikos*, 110, 634-638.
- Purkis, S. J., Pasterkamp, R. 2004. Integrating in situ reef-top reflectance spectra with Landsat TM imagery to aid shallow-tropical benthic habitat mapping. *Coral Reefs* 23, 5-20.
- Schimel, A. C. G., Healy, T. R., Johnson, D., Immenga, D. 2010a. Quantitative experimental comparison of single-beam, sidescan, and multibeam benthic habitat maps. *ICES Journal of Marine Science*, 67, 1766-1779.
- Schimel, A. C. G., Healy, T. R., McComb, P., Immenga, D. 2010b. Comparison of a self-processed EM3000 Multibeam echosounder dataset with a QTC View habitat mapping and a sidescan sonar imagery, Tamaki Strait, New Zealand. *Journal of Coastal Research*, 26, 714-725.
- Schmidt, A., Rottensteiner, F., Soergel, U. 2013. Water-Land-Classification in Coastal Areas with Full Waveform Lidar Data. *Photogrammetrie, Fernerkundung, Geoinformation*, 2, 71-81.
- Schott, J. R. 2007. *Remote sensing: the image chain approach* (2nd ed.). New York, Oxford University Press, 688 pp.
- SEDAC 2010. Percentage of Total Population Living in Coastal Areas [pdf] Available at: http://sedac.ciesin.columbia.edu/es/papers/Coastal_Zone_Pop_Method.pdf

- Seto, K. C., Fragkias, M., Guneralp, B., Reilly, M. K. 2011. A Meta-Analysis of Global Urban Land Expansion. *PLoS ONE*, 6 (8), e23777, doi: 10.1371/journal.pone.0023777.
- SOBAP 2013. Working Group on Sonar Backscatter Data Acquisition and Processing. Establishment of the Working Group and Modality of Operation [pdf] Available at: <http://geohab.org/wp-content/uploads/2013/07/BackscatterWG-7Jul2013.pdf>
- Vanden Borre, J., Paelinckx, D., Mûcher, C. A., Kooistra, L., Haest, B., De Blust, G., Schmidt, A. M. 2011. Integrating remote sensing in Natura 2000 habitat monitoring: Prospects on the way forward. *Journal for Nature Conservation*, 19 (2), 116-125.
- Whitmire, C. E., Embley, R. W., Wakefield, W. W., Merle, S. G., Tissot, B. N. 2007. A quantitative approach for using multibeam sonar data to map benthic habitats. In: *Mapping the Seafloor for Habitat Characterization*, Todd, B. J., Greene, H. G. (Eds), Geological Association of Canada, 111-128.
- Whittaker, R. H., Levin, S. A., Root, R. B. 1973. Niche, Habitat, and Ecotope. *The American Naturalist*, 107 (955), 321-338.
- Wienberg, C., Bartholomä, A. 2005. Acoustic seabed classification in a coastal environment (outer Weser Estuary, German Bight)—a new approach to monitor dredging and dredge spoil disposal. *Continental Shelf Research*, 25, 1143-1156.
- Xie, Y., Sha, Z., Yu, M. 2008. Remote sensing imagery in vegetation mapping: a review. *Journal of Plant Ecology*, 1 (1), 9–23.

Page left intentionally blank

Chapter 3

Sediment vs. topographic roughness: anthropogenic effects on acoustic seabed classification

Ruggero Maria Capperucci^{1,2,3}, Alexander Bartholomä³

¹MARUM, Center for Marine Environmental Sciences, University of Bremen,
Leobener Str., D-28359 Bremen

²Department of Earth and Ocean Sciences, University of Waikato,
Private Bag 3105, Hamilton, New Zealand

³Marine Research Department, Senckenberg am Meer, Südstrand 40, 26382 Wilhelmshaven, Germany

3.1. Introduction

In recent years, environmental case studies of highly developed marine areas have become more relevant (Winter and Bartholomä 2006; van der Veen and Hulscher 2008): for monitoring both the short- and long-term human impact on bio- and geo-sphere; for modeling the effects of such increasing pressure on ecosystem; as a key tool for environmental and socio-economic policy and management.

Among the different marine domains, coastal areas are the most accessible ones and the most difficult to be studied in detail, due to the complexity of natural and anthropic processes in action (OSPAR 2008). As a consequence, there is an increased demand for reliable high-resolution mapping tools, less dependent on expertise interpretation, and therefore more objective (Cutter et al. 2003).

In this scenario, the combination of acoustic, sedimentological and biological data is becoming the main approach for seabed habitat mapping

Capperucci, R.M., Bartholomä, A. 2012. Sediment vs. topographic roughness: anthropogenic effects on acoustic seabed classification. In: Leendert Dorst, L., van Dijk, T., van Ree, R., Boers, J., Brink, W., Kinneging, N., van Lancker, V., de Wulf, A., Nolte, H. (Eds.), Conference Proceedings of Hydro12, Taking care of the sea, the Hydrographic Society Benelux (HSB), on behalf of the International Federation of Hydrographic Societies (IFHS), Rotterdam, the Netherlands, 12-15 November 2012, 23-28. Winner of the "Hydro 2012 Best Student Paper award".

studies (Brown et al. 2011). Nevertheless, some specific aspects need further investigations: firstly, the analysis of acoustic data is still largely dependent on human expertise (Cutter et al. 2003); secondly, repeated sampling technique is a standard procedure for biological studies but not a common practice for sedimentary research; and lastly, the ground-truthing process by means of sediment samples assumes that the point-based information can be consistently extended to the near vicinity of the sampling station. Besides, the positioning error/uncertainty is often not even mentioned as a key factor for assessing the reliability of the final seabed classification.

The latter assumptions have to be proved for extremely heterogeneous environments, where anthropogenic impact increases significantly the disturbance (and, hence, the variability) of ecosystems.

In our study site of the Jade channel in the German Bight (southern North Sea) hydrodynamic conditions, topography, sediments and bio-communities are tremendously influenced by multiple human activities. Fishing and mussel farms are present (Herlyn and Millat 2000); the navigation channel is constantly monitored and dredged by the local harbour authority (Wasser- und Schifffahrtsamt Wilhelmshaven – WSA); moreover, a new container terminal (Jade Weser Port, <http://www.jadeweserport.de/>) is under construction since 2008, with massive land reclamation, dredging and dumping operations. The Jade channel area represents, then, a unique site where to test the reliability of acoustic ground discrimination systems (AGDS) in a cumulative disturbed area.

The present study aims to address the following research questions:

1. What is the variability of repeated sediment samples in a highly heterogeneous environment?
2. How do the positioning error/uncertainty of sediment samples affect the ground-truthing process?
3. What drives the seabed classification in the different acoustic systems?

3.2. Study area and methods

The Jade channel connects the Jade Bay with the German Bight (southern North Sea), being part of a wide tidal flat system that includes the Weser estuary (Figure 3.1). The northern end (Outer Jade) is a mesotidal environment (*sensu* Hayes 1975), with semi-diurnal tides ranging between 2.3 and 2.8 m, whereas the southern part (Inner Jade) is a macrotidal environment, with the tidal gauge reaching 3.9 m in Wilhelmshaven.

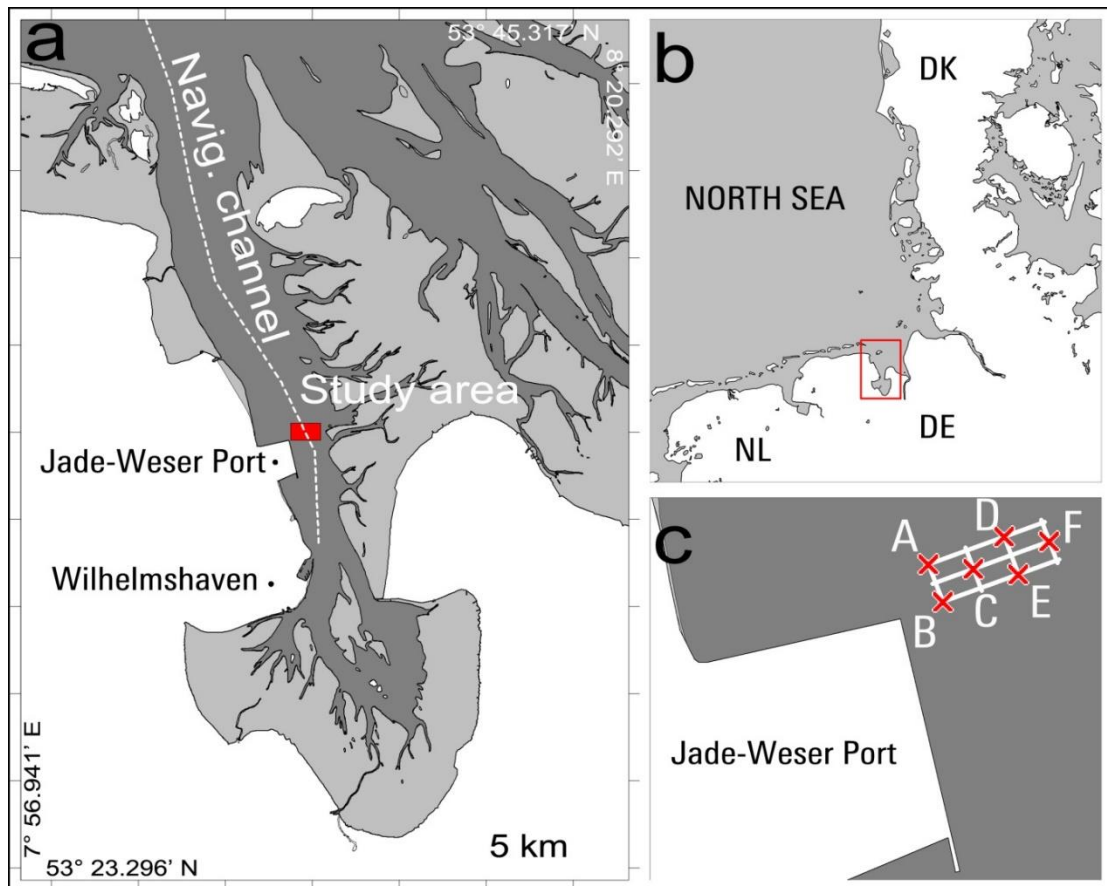


Figure 3.1. a) The Jade region, with the Jade Weser Port and, in red, the study area. b) Location map of the Jade system. c) close up on the research site; white lines: main acoustic transects, red crosses: sampling stations.

The sediment distribution shows a general decrease of the grain-size towards the high-tide line, with the finest sediments being located in the south-eastern part of the bay; the Inner Jade is characterized by the presence of fine sand; fine to medium sand occurs in the Outer Jade area (Kahlfeld and Schüttrumpf 2006). Bedforms are commonly observed along the tidal inlet. The research area covers approximately 0.8 km² in the Jade Channel, north-east of the Jade-Weser Port, partially within the old navigation channel. The water depth ranges between 14 and 26 m.

Acoustic data were collected aboard the R/V Senckenberg using a Reson Seabat 8125TM multibeam echosounder (MBES, 455 kHz), a dual-frequency Benthos 1624TM side-scan sonar (SSS, 110-390 kHz) and a QTC 5.5TM system mounted on a Furuno FCV 1000TM single-beam echosounder (SBES, 200 kHz). All devices were deployed simultaneously along 7 main transects (3 approximately east-west and 4 approximately north-south oriented). Additional lines were collected for a complete MBES coverage and a denser SBES grid. A DGPS system with LRK correction was used for positioning. 6 stations were sampled (4 replications each) using a Shipek grab.

3.2.1. *Data processing*

MBES bathymetric data were processed using QINSy™ and a final 0.5x0.5 m grid was computed. DTM generation and seabed features mapping was done under Global Mapper™ v13. A set of QTC™ software was used for acoustic seafloor classification: QTC IMPACT™ for SBES data, QTC SIDEVIEW™ for SSS data, QTC SWATHVIEW™ for MBES data, and QTC CLAMS™ for visualizing and editing classified data.

QTC IMPACT™ is based on a statistical analysis of the echo-trace shape, whereas QTC SIDEVIEW™ and QTC SWATHVIEW™ use statistical properties of backscatter images. The Automatic Clustering Engine function (QTC IMPACT User Manual, 2004), was used for splitting acoustic signals into a final number of classes that fits with the optimal split level suggested by the statistical parameters.

Sediment samples were analyzed following the procedure described by Wienberg and Bartholomä (2005) and classified using the GRADISTAT statistics package (Blott and Pye 2001). The PAST software (Hammer 2001) was used for statistical analysis (Non-metric MDS and Cluster analysis). All the data were finally loaded in ArcGIS v9.2 for interpretation.

3.3. Results

3.3.1. *Sedimentary data*

Due to the strong tidal currents acting in the area, sampling positions were shifted with respect to the planned locations, the average distance between replications being 20 m (Table 3.1a). Station C shows the highest positioning error (average distance between replications: 32 m).

Sediments grain sizes range from coarse silt to very fine gravel (Table 3.1, right), the main part (75%) falling into the sand fraction. Replications show significant difference in sediment composition: Station A presents the lowest variability, all the replications being dominated by sand. Station C, on the contrary, is characterized by the highest variability in composition, with the replication JSA04 muddy-based (47.6%), JSA09 totally sandy (91.8%) and JSA019 and JSA022 gravelly dominated (55.4% and 47.7%, respectively). Replications JSA02 and JSA14 (Station D) are the closest ones of the survey (distance = 2 m). Nevertheless, JSA02 presents a high content of mud (75.4%) and JSA14 is dominated by sand (60.1%). Similar results for Station E, where JSA10 is

characterized by a 75.7% of mud, while JSA15 composition is mainly given by the sand fraction (76.6%), albeit they are only 7 m far.

The results of statistical analysis confirm that there is no significant correlation between sediment similarity and sampling closeness. In particular, only replications from Station A tend to group, while the already mentioned replications from Station D and E show low similarity values, in spite of their closeness (Table 3.1, left).

Station	(av. dist=)	Sample	Gravel %	Sand %	Mud %
Station A	(15m)	JSA05	3.0	64.7	32.3
		JSA07	3.9	69.6	26.5
		JSA18	0.0	71.6	28.4
Station B	(20m)	JSA23	13.6	57.9	28.5
		JSA06	32.5	59.7	7.7
		JSA08	58.7	30.0	11.2
Station C	(32m)	JSA17	17.5	67.2	15.3
		JSA09	63.9	21.9	14.1
		JSA25	19.2	33.3	47.6
Station D	(21m)	JSA04	0.0	91.8	8.2
		JSA12	55.4	34.2	10.4
		JSA14	47.7	45.5	6.8
Station E	(13m)	JSA02	0.0	24.6	75.4
		JSA10	4.2	89.0	6.8
		JSA15	11.7	76.6	11.7
Station F	(16m)	JSA24	0.0	95.4	4.6
		JSA01	24.1	52.8	23.0
		JSA11	16.9	64.3	18.8
		JSA13	2.1	62.3	35.6
		JSA20	13.1	84.0	2.9

Table 3.1. Left: calculated (and average) distance among replications for each station. Right: sediment grain size analysis, expressed as dry weight percent on bulk sediment.

3.3.2. Acoustic data

The whole area is characterized by distinctive topographic features, mainly related to dredging operations. From West to East, 6 main morphological domains can be mapped (Figure 3.2):

- W: a wide area dominated by dredging marks related to the Jade-Weser Port construction phase;
- H: western high (min. depth: 14.4 m), without dredging scours;
- P: western pit (max. depth: 26.4 m), without dredging scours;
- N: old navigation channel, marked by regularly spaced and shaped dredging scours, elongated and parallels to the navigation channel;
- B: large bedform fields, mainly aside the old navigation channel;
- E: a wide domain characterized by the absence of dredging marks and by the presence of diffuse short-wave bedforms. It is the less disturbed area.

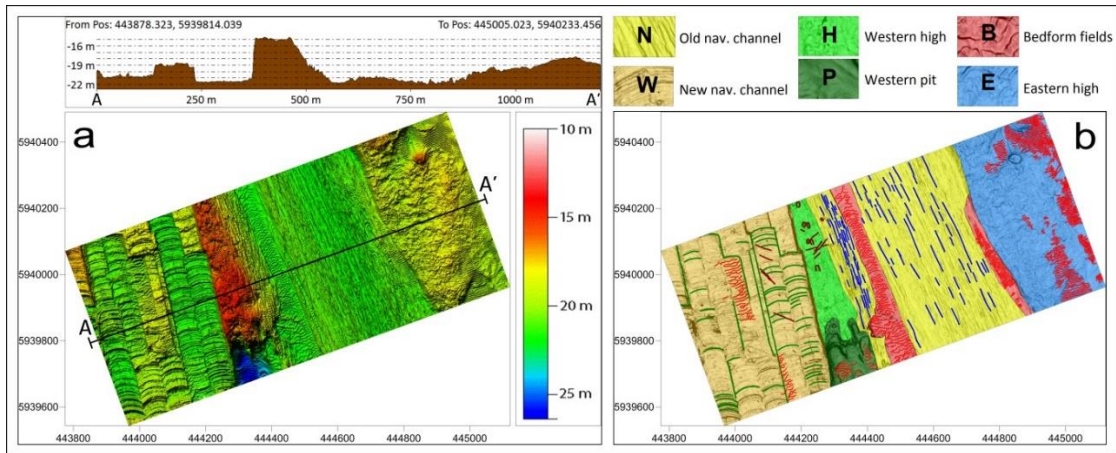


Figure 3.2. DTM of the research area (a) and main morphological domains (b).

The SBES final classification (optimal splitting level: 4) shows a patchy distribution of acoustic classes all over the area, with a dominance of the turquoise-colored class (42.2%) and brown-colored class (32.0%), which do not correspond to any morphological domain (Figure 3.3b). The pink-colored class (6.1%) is the only one focused around specific regions (H and P domains), while the blue-colored one (19.7%) is scattered all over the area, but scarcely represented in the same domains. All considering the extreme variability of sediment composition and distribution, the error in positioning and the patchiness of the acoustic classification, it is not possible to clearly correlate acoustic classes and sedimentary data.

The grey-colored class prevails (69,2%) in the MBES acoustic classification (optimal split level: 5. Figure 3.4a), marking both the western (W) and eastern (E) regions, including the B areas and with the exception of the H and P domains. 2 specific classes (light and dark blue-colored ones, 14.2% and 8.1%, respectively) cover the N morphological domain, where the green-colored class (2.8%) is also present. Thus, a correlation between main seabed features and acoustic classification is clear. The turquoise-colored class (5.7%) is spread all over the area. There is no correspondence between acoustic classes and sedimentary data: in fact, every acoustic class can be related to different sediment types and the same sedimentary group corresponds to more than one acoustic class.

The general pattern of the SSS classification (optimal split level: 4) follows the main morphological divisions (Figure 3.4b), with the green-colored class (36.3%) fitting the N area and the remaining classes distributed both in the western and eastern regions. The W domain seems to be equally represented by both the orange- (30.7%) and the violet-colored (24.0%) classes, while the E

topographic area is mainly covered by the orange-colored class. The blue-colored class characterizes the slope between the H-P and N regions.

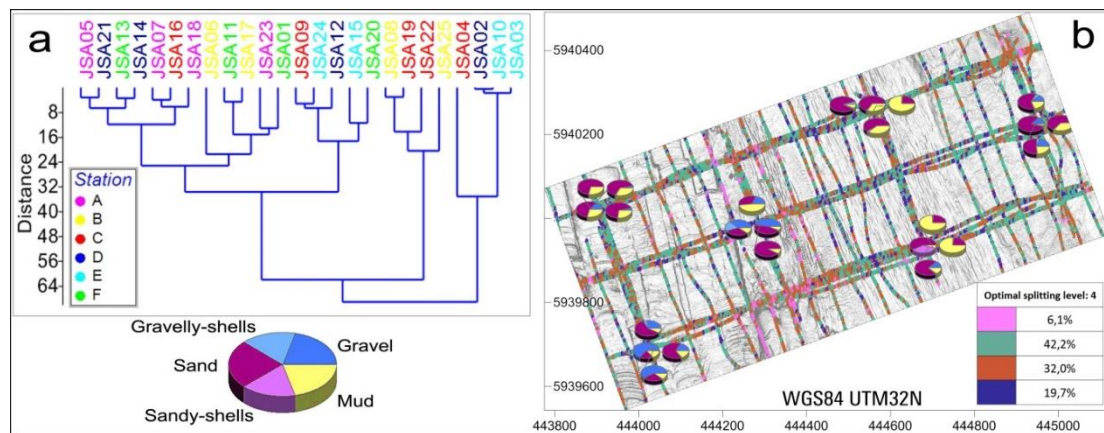


Figure 3.3. Clustering analysis, Euclidean similarity measure (a). SBES acoustic classification (b), overlaid by the sediment data.

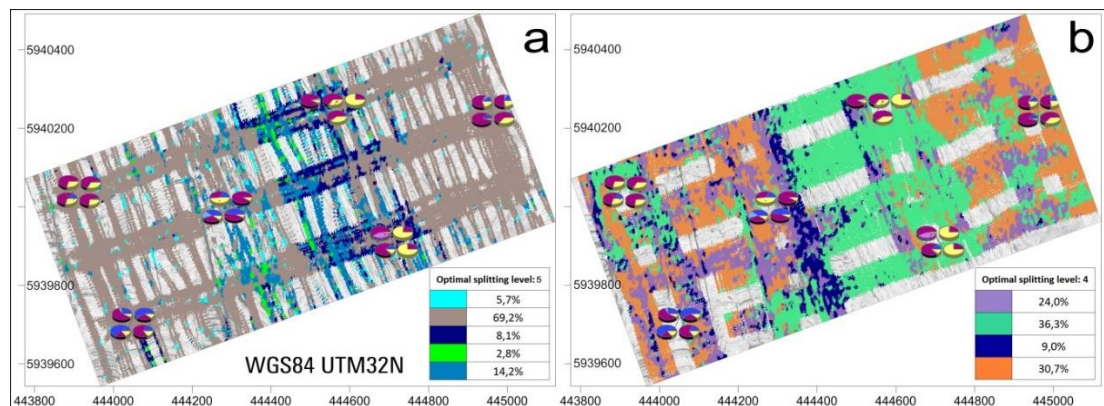


Figure 3.4. MBES acoustic classification (a) and SSS acoustic classification (b).

The same catalogue of 4 classes was used for classifying separately the 4 north-south and the 3 east-west SSS lines, showing significant differences. In particular, the area corresponding to the old navigation channel presents a homogeneous dominance of the turquoise-colored class in the east-west transects, whereas the same region shows a distinctive multi-class pattern parallel to the dredging marks in the north-south classification.

As for the MBES classification, the ground truthing process does not show any univocal correspondence between sediments and the SSS acoustic classes.

3.4. Discussion and conclusions

Errors are always associated with sampling positioning. The mismatch between the planned and the sampled location can be negligible in homogeneous

environment, giving a reliable classification. Punctual information can then be used for validating acoustic data even when the two sources does not perfectly overlap, assuming that the information inferred for a given position can be consistently extended to a certain neighborhood. This is not true for highly heterogeneous environments; in fact, repeated sampling clearly demonstrates that:

- Replications show significant differences in sediment composition;
- There is not clear relationship between positioning and similarity;
- Less disturbed areas (e.g. station F) present the same variability of directed multi-impacted ones (e.g., Station A), therefore there is no link between anthropic disturbance and heterogeneity.

The results show that repeated sampling is a must in such complex environments.

SBES classification reveals a highly heterogeneous seabed texture with no clear dominant pattern, thus being likely controlled by the distinctive patchiness in sediment distribution (=sediment roughness). Nevertheless, the extreme variability of sediment composition does not allow any interpolation: only the samples located exactly along the acoustic line could be theoretically used for ground-truthing, resulting in a scarcely sufficient amount of information. In conclusion, SBES classification is ruled by sediment patchiness, but the final classification can hardly be translated into sedimentological information.

On the contrary, swath-based systems (MBES and SSS) seem to be largely dependent on seabed topography for their classification, with acoustic classes that match the general division in morphological domains (= topographic roughness). MBES does not allow the distinction between W and E regions, although they represent end members of highly disturbed and less disturbed environments. SSS classification not only stresses the different topographic domains, but also distinguishes between W and E regions. The angle between the acoustic lines and the seabed features is crucial for the final acoustic classification. In fact, regularly shaped and spaced features, like dredging marks, could lead to significantly different results.

In conclusion, mapping highly heterogeneous and disturbed environments is a crucial challenge for monitoring and protecting these extremely sensitive areas. Hydro-acoustic systems coupled with repeated sampling allow running this process in high resolution, but the resulting classification is mainly ruled by the sediment roughness for SBES systems and by topographic micro-roughness for swath-based devices. In any case, the resulting classes can only partially be linked to a proper sedimentological meaning.

3.5. References

- Blott, S.J., Pye, K. 2001. GRADISTAT: a grain size distribution and statistics package for the analysis of unconsolidated sediments. *Earth Surface Processes and Landforms*, 26, 1237-1248.
- Brown, C.J., Smith, S.J., Lawton, P., Anderson, J.T. 2011. Benthic habitat mapping: a review of progress towards improved understanding of the spatial ecology of the seafloor using acoustic techniques. *Estuarine, Coastal and Shelf Science*, 92, 502-520.
- Cutter Jr., G.R., Rzhhanov, Y., Mayer, L.A. 2003. Automated segmentation of seafloor bathymetry from multibeam echosounder data using local Fourier histogram texture features. *Journal of Experimental Marine Biology and Ecology*, 285-286, 355-370.
- Hammer, Ø., Harper, D.A.T., Ryan, P.D. 2001. PAST: Paleontological Statistics Software Package for Education and Data Analysis. *Palaeontologia Electronica*, 4, 9 pp.
- Hayes, M.O. 1975. Morphology of sand accumulations in estuaries: an introduction to the symposium. In: Cronin, L.E. (Ed), *Estuarine Research*, vol. 2, Academic Press, New York, 3-22.
- Herlyn, M., Millat, G. 2000. Decline of the intertidal blue mussel (*Mytilus edulis*) stock at the coast of Lower Saxony (Wadden Sea) and influence of mussel fishery on the development of young mussel beds. *Hydrobiologia*, 426, 203-210.
- Kahlfeld, A., Schüttrumpf, H. 2006. Untrim modelling for investigating environmental impacts caused by a new container terminal within the Jade-Weser Estuary, German Bight. In: *Proceedings of the 7th International Conference on HydroScience and Engineering*, Philadelphia, USA, September 10-13, 2006, 13 pp.
- OSPAR 2004. Environmental Impacts to marine species and habitats of dredging for navigational purposes. OSPAR Commission, Biodiversity Series, 22 pp.
- OSPAR 2008. Assessment of the environmental impact of land reclamation, OSPAR Commission, Biodiversity Series, Publication number 368/2008, 37 pp.
- QTC IMPACT User Manual, 2004. QTC IMPACT Acoustic Seabed Classification. User Manual, Version 3.40. Quester Tangent Corporation, Marine Technology Centre, Sidney, B.C., Canada, 153 pp.
- van der Veen, H.H., Hulscher, S.J.M.H. 2008. Effect of large scale human activities on the North Sea seabed. In: Parsons, D., Garlan, T. and Best, J. (Eds), *Marine and River Dune Dynamics*, 307-314.
- Wienberg, C., Bartholomä, A. 2005. Acoustic seabed classification of a coastal environment (outer Weser Estuary, German Bight) - a new approach to monitor dredging and dredge spoil disposal. *Journal of Continental Shelf Research*, 25, 1143-1156.
- Winter, C., Bartholomä, A. 2006. Coastal dynamics and human impact: south-eastern North Sea, an overview. *Geo-Marine Letters*, 26, 121-124.

Page left intentionally blank

Chapter 4

Tools to evaluate seafloor integrity: comparison of multi-device acoustic seafloor classifications for benthic macrofauna-driven patterns in the German Bight, southern North Sea

Peter Holler^{a*}, Edith Markert^a, Alexander Bartholomä^a, Ruggero M. Capperucci^a, H. Christian Hass^b, Ingrid Kröncke^a, Finn Mielck^b, H. Christian Reimers^c

^aSenckenberg am Meer, Department for Marine Research, Südstrand 40, 26382 Wilhelmshaven, Germany

^bAlfred Wegener Institut, Helmholtz Zentrum für Polar- und Meeresforschung, Wattenmeer Station Sylt, Hafenstrasse 43, 25992 List, Germany

^cLandesamt für Landwirtschaft, Umwelt und ländliche Räume, Hamburger Chaussee 25, 24220 Flintbek, Germany

4.1. Abstract

To determine the spatial resolution of sediment properties and benthic macrofauna communities in acoustic backscatter, the suitability of four acoustic seafloor classification devices (single-beam echosounder with RoxAnn and QTC 5.5 seafloor classification system, sidescan sonar with QTC Swathview seafloor classification, and multi-beam echosounder with QTC Swathview seafloor classification) was compared in a study area of approx. 6 km² northwest of the island of Helgoland in the German Bight, southern North Sea. This was based on a simple similarity index between simultaneous sidescan sonar, single-beam echosounder and multi-beam echosounder profiling spanning the period 2011–2014. The results show a high similarity between seafloor classifications based on sidescan sonar and RoxAnn singlebeam systems, in turn associated with a lower

Holler, P., Markert, E., Bartholomä, A., Capperucci, R.M., Hass, H.C., Kröncke, I., Mielck, F., Reimers, H.C. 2016. Tools to evaluate seafloor integrity: comparison of multi-device acoustic seafloor classifications for benthic macrofauna-driven patterns in the German Bight, southern North Sea. *Geo-Marine Letters*, 37 (2), 1-17, doi: 10.1007/s00367-016-0488-9.

similarity for the multi-beam echosounder system. Analyses of surface sediment samples at 39 locations along four transects (0.1 m² Van Veen grab) revealed the presence of sandy mud (southern and western parts), coarse sand, gravel and cobbles. Rock outcrops were identified in the north-eastern and eastern parts. A typical *Nucula nitidosa*-*Abra alba* community was found in sandy muds to muddy sands in the northern part, whereas the southern part is characterised by widespread occurrence of the ophiuroid brittle star *Amphiura filiformis*. A transitional *N. nitidosa*-*A. filiformis* community was detected in the central part. Moreover, the southern part is characterised by a high abundance of *A. filiformis* and its commensal bivalve *Kurtiella bidentata*. The high number of *A. filiformis* feeding arms (up to ca. 6,800 per m²) can largely explain the gentle change of backscatter intensity along the tracks, because sediment composition and/or seafloor structures showed no significant variability.

4.2. Introduction

Over the last 30 years the human impact on the seafloor of the North Sea has strongly increased. This includes the exploration of oil and gas fields, sand mining for construction, the installation of underwater cables and pipelines, the construction of foundations for offshore wind farms, as well as fishing by bottom trawls and dredging activities. In order to mitigate adverse effects on the seafloor, the European Union released the Marine Strategy Framework Directive (MSFD) in 2008, including 11 descriptors of “good environmental status”. One of these is “seafloor integrity”, defined as “a level that ensures that the structure and functions of the ecosystems are safeguarded and benthic ecosystems, in particular, are not adversely affected” (European Union 2008). The European Commission selected six indicators of seafloor integrity (cf. Rice et al. 2012), including the type, abundance, biomass and areal extent of relevant biogenic substrates. To date, regular monitoring is based largely on grab sampling, associated with time-consuming biological analyses. Another major drawback is the point-type nature of such information, the full spatial coverage of habitats being mostly extrapolated.

Over the last decade, developments in hydroacoustic methods have enabled extensive seafloor mapping in a relatively short time period - for sidescan sonar, up to 67 km²/day (Kenny et al. 2003). The backscatter signal reflects several abiotic properties such as surface roughness and grain size (e.g. Collins and Galloway 1998; Bornhold et al. 1999; Preston et al. 2004; Ferrini and Flood 2006; Markert et al. 2013), as well as benthic faunal elements such as mussel beds

and shell debris (e.g. Quester Tangent Corporation 2003; Wienberg and Bartholomä 2005; van Overmeeren et al. 2009), coral reefs (e.g. Gleason et al. 2006; Gleason 2009), and macroalgae and seaweed (e.g. Preston 2006; Hass and Bartsch 2008; Mielck et al. 2014). In the Belgian sector of the southern North Sea, for example, Degraer et al. (2008) detected reefs of the polychaete *Lanice conchilega* by means of high-resolution sidescan sonar. This polychaete forms tubes composed of sand grains and shell fragments, which cause an increased reflectivity appearing as a patchy and grainy acoustic facies.

For the German Bight in the southern North Sea, the Marine Strategy Framework Directive-related project “WIMO” (“Scientific Monitoring Concepts for the German Bight”) aims to develop new concepts for the monitoring of marine habitats (for overviews, see Winter et al. 2014; Winter et al., Introduction article for this special issue). One topic focuses on the interactions of benthic macrofauna and hydroacoustic signals from single-beam echosounders, multi-beam echosounders and sidescan sonar. Based on an older sediment distribution map of Figge (1981) and survey results from earlier projects, the present study explores this aspect in the vicinity of the island of Helgoland, representing characteristic sediment types of the German Bight. Identifying surrogate hydroacoustic signatures would facilitate meaningful spatial extrapolation of point-type biological information, thereby reducing the time and costs of seafloor sampling from aboard ship. Within this context, the aims of this study are (1) to map the distribution of surficial sediments using different hydroacoustic devices in order to find the most appropriate system for this purpose, (2) to use automatic seafloor classification approaches for seafloor segmentation into distinct classes, (3) to provide ground-truthing for the results of the classification, and (4) to compare different sediment types and backscatter signals with the spatial distribution of macrofauna communities.

4.3. Study area

According to the sediment distribution map of Figge (1981), the seafloor in the vicinity of Helgoland is the only location in the German Bight with outcropping bedrock of Palaeozoic to Mesozoic age (Spaeth 1990), interspersed with Quaternary muddy sand to sandy mud. It is typified by the well-known benthic community dominated by the brittle star *Amphiura filiformis* (e.g. Salzwedel et al. 1985; Rachor and Nehmer 2003; Kröncke et al. 2004, 2011).

The eastern border of the study area is located about 2 km west of the island of Helgoland (Figure 4.1), extending approx. 17 km in a north–south

direction and approx. 6 km in a west– east direction (approx. 98 km²). Water depth varies between 17 and 54 m (Figure 4.2).

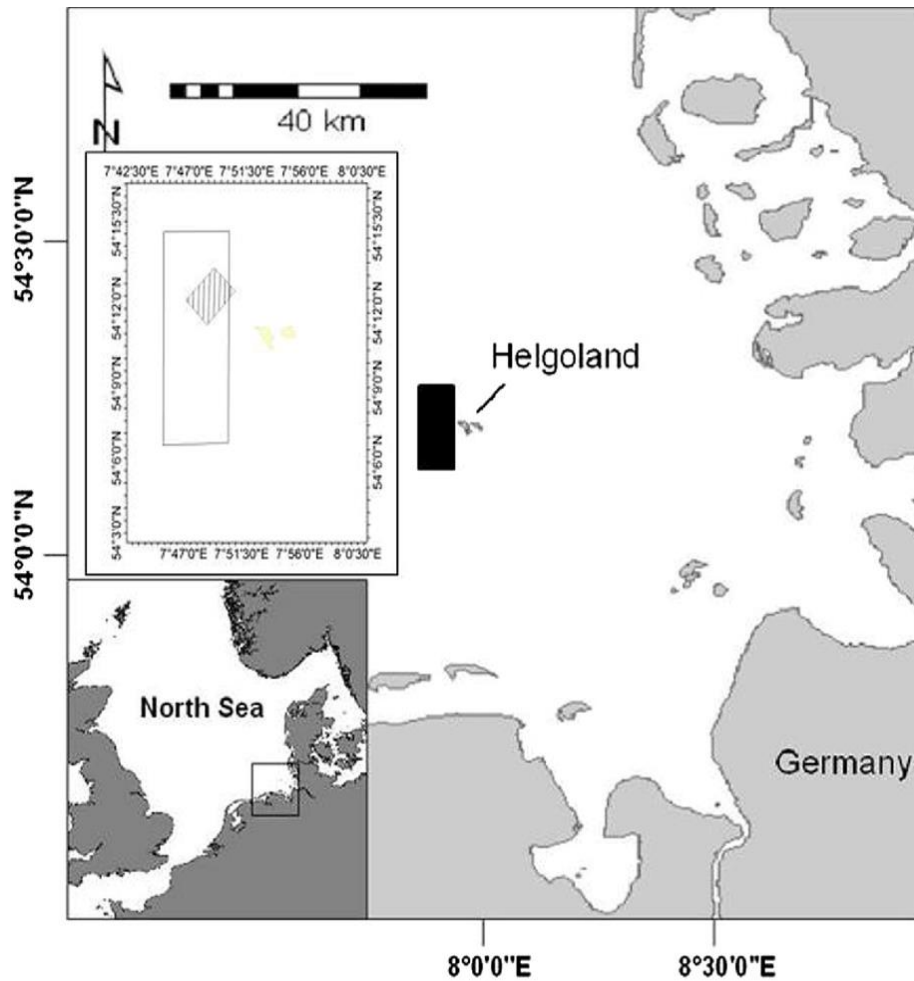


Figure 4.1. Location of the study area west of Helgoland, with the subarea (hatched box) selected for detailed surveying.

The easternmost part of the study area is located within the nature preservation area “Helgoland Felssockel”, where human impact is restricted to lobster-pot fishing. The study area was surveyed twice from aboard the RV Heinke in February and November 2014, using a RoxAnn seafloor classification system (Table 4.1; cf. Hass et al. 2016). A subarea in the north-eastern sector of the study area (approx. 3 km long and 2 km wide, depth range 19-35 m; Figure 4.3a) was selected for more detailed surveying because it includes many different habitats, some of them difficult to evaluate with hydroacoustic gear because of steep slopes and large boulders.

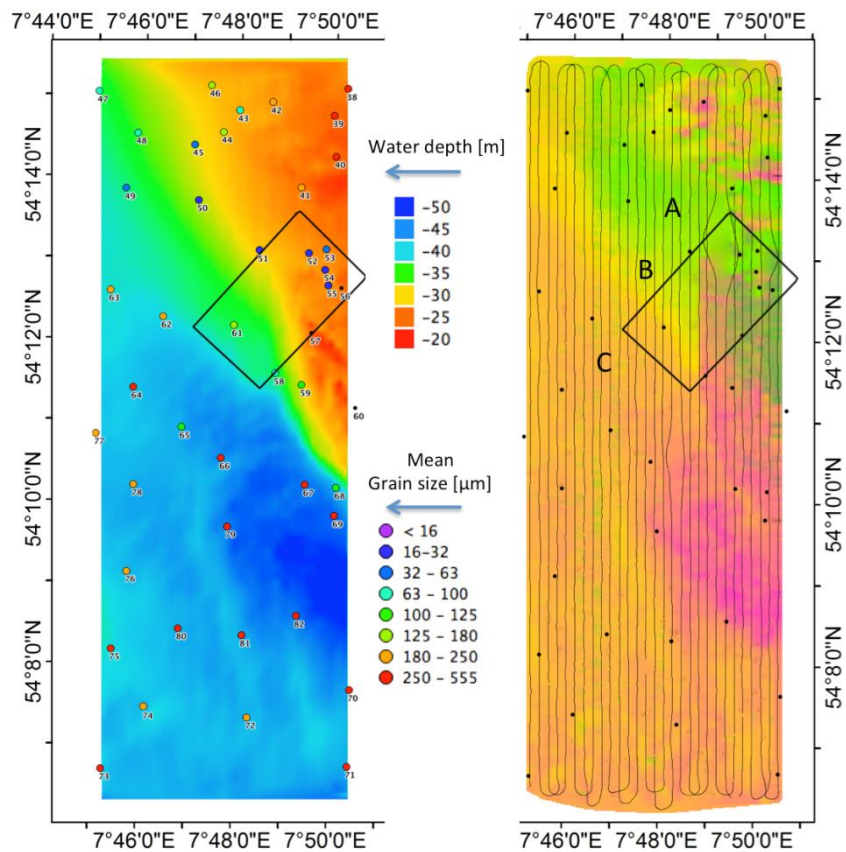


Figure 4.2. Study area. Left panel: Bathymetry (RoxAnn) and sample locations (with corresponding mean grain size). Right panel: Interpreted and interpolated results of RoxAnn data analysis: colour categories see Figure 4.5; A-C benthic communities (modified after Hass et al. 2016). Rectangle in both panels: subarea selected for detailed surveying.

Month/year	Vessel	Area	Sidescan sonar	Single-beam echosounder	Multi-beam echosounder	UW-TV	Grab sampling	Macro-benthos
07/2011	RV Senckenberg	Subarea	x	x	x		x	x
08/2011	RV Haitabu	Subarea		x		x		
09/2011	RV Heincke	Subarea		x	x			
07/2012	RV Senckenberg	Subarea	x	x	x			
07/2013	RV Senckenberg	Subarea	x	x		x	x	x
10/2013	RV Heincke	Subarea		x			x	
11/2013	RV Heincke	Subarea					x	
11/2013	RV Senckenberg	Subarea			x			
02/2014	RV Heincke	Total area		x	x			
07/2014	RV Senckenberg	Subarea	x	x	x	x	x	
11/2014	RV Heincke	Total area		x	x	x	x	

Table 4.1. Data acquisition in the working area between 2011 and 2014.

4.4. Materials and methods

4.4.1. *Acoustic data*

The subarea was surveyed 11 times between 2011 and 2014 by means of seven acoustic devices from aboard the RV Senckenberg, RV Heincke and RV Haitabu (Table 4.1). Simultaneous data collection was by means of a Furuno FCV 295™ or FCV 1000™ single-beam echosounder (SBS), a Reson SeaBat 8125™ multi-beam echosounder (MBES) and a Benthos 1624™ sidescan sonar (SSS) from aboard the RV Senckenberg, a RoxAnn™ system from aboard the RV Heincke, and an Echoplus system from aboard the RV Haitabu.

Onboard the RV Senckenberg, the FCV 295 single-beam echosounder was operated with a pole-mounted Furuno 200-8B transducer. The FCV 1000 single-beam echosounder was connected to a hull-mounted Furuno 200-8B transducer with a beam angle of 7.4° at 6 dB, an emission power of 1 kW, and a pulse length of 0.5 ms. A recording depth range of 0 to 40 m (FCV 295) or 0 to 50 m (FCV 1000) was selected. Data acquisition was carried out by QTCView 5.5™ from Quester Tangent Corporation (Victoria, BC, Canada).

The 455 kHz multi-beam echosounder Reson SeaBat 8125 was also pole-mounted on the portside of the RV Senckenberg. The system generated 240 beams by electronic beamforming, with a beam size of 1° along track and 0.5° across track. The opening angle of 120° enables a swath coverage of up to 3.5 times the water depth. A selected line spacing of 125 m achieved full areal coverage.

The data were acquired by means of QINSY version 7.1 software, the post-processing comprising a digital elevation model (DEM) with a grid size of 0.5 m. Further interpretation is based on the ArcGIS toolbox Bottom Terra in Modeller (Wright et al. 2005). For the subarea, this entailed calculations of bathymetric position indexes (BPIs), bottom slopes and terrain ruggedness from the bathymetric grid (Figure 4.3a).

According to Verfaillie et al. (2007), the BPI is a “measure which allows calculating where a certain location with a defined elevation is relative to the overall landscape”. The BPI algorithm compares each cell elevation to the mean elevation of the surrounding cells (Verfaillie et al. 2007). It can be calculated on a broad scale (B BPI) or on a fine scale (F BPI). Negative BPI values correspond to depressions, whereas positive BPI values correspond to crests. BPIs of zero are found for constant slopes and flat areas.

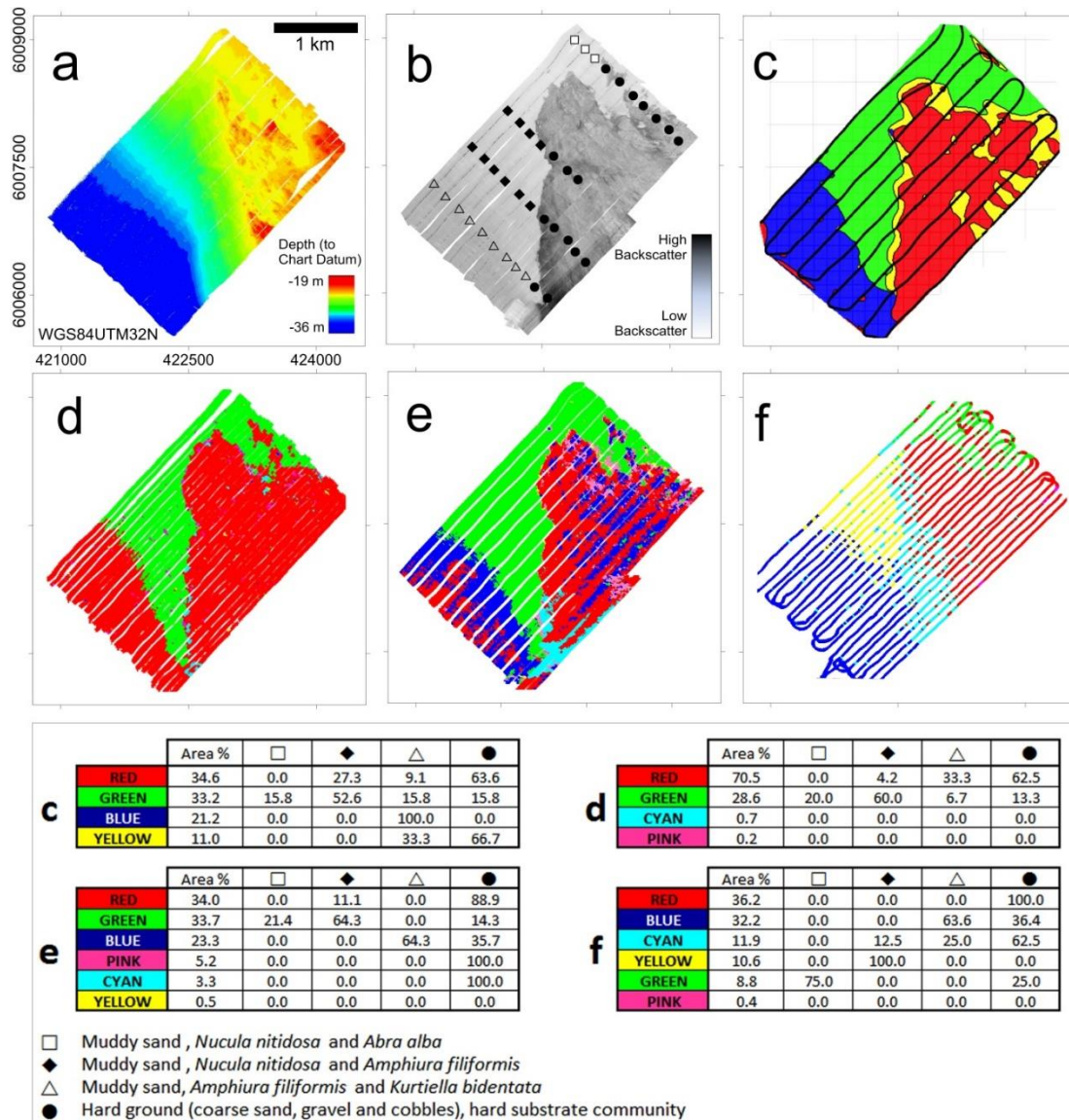


Figure 4.3. Subarea: bathymetry (2012) from multi-beam echosounder a) and backscatter (2011) from sidescan sonar b) with positions of 2011 grab samples and macrobenthos communities. c–f Sea floor classification: c) single-beam echosounder, RoxAnn GD-X (HE 364, 2011); d) multi-beam echosounder (2012), QTC swathview; e) sidescan sonar (2011), QTC swathview; f) single-beam echosounder (2012), QTC 5.5/QTC Impact. Lower tables: corresponding areal percentages of sea floor classes and percentages of macrobenthic communities.

The Benthos SIS 1624 sidescan sonar had a high frequency chirp signal of 370–390 kHz and a low frequency chirp signal of 110–130 kHz. The low frequency beam size was 0.5° (horizontal) and 55° (vertical), whereas the high-frequency beam size was 0.5° (horizontal) and 35° (vertical). The low-frequency data were used for automatic sea floor classification. A range of 100 m (200 m swath coverage) was selected for the 2011 and 2012 surveys, and of 150 m (300 m swath) for the 2013 and 2014 surveys. Sidescan sonar data were collected along all multi-beam echosounder lines (line spacing of 125 m) at a tow speed of 5 knots and a constant tow depth of ca. 7 m below the sea surface. Tow-fish

positioning was based on layback measurements. The horizontal range resolution of chirp systems is defined as $(\text{pulse length} \times \text{speed of sound})/2$ with pulse length = $1/\text{bandwidth}$. For the Benthos 1624 system (bandwidth 20 kHz, pulse length 0.00005 s) and a speed of sound of 1,500 m/s, a range resolution of 3.075 cm is calculated. The along-track resolution is defined by the vessel speed and ping rate of the sidescan sonar (BSH 2016). At a sidescan range of 100 m, 7–8 pings are emitted each second. This leads to an along-track resolution of ca. 0.35 m at a vessel speed of 5 knots (ca. 2.5 m/s). For the 150 m range setting, the maximum ping rate of five beams per second results in an along-track resolution of 0.5 m at a vessel speed of 5 knots (2.5 m/s). The backscatter data are displayed as a grey scale comprising 256 values, where 0 is assigned to black, corresponding to strong backscattering, and 255 to white, corresponding to low backscattering.

The RoxAnn (SONAVISION) system has a Furuno LS- 6100 fish-finder equipped with a 200 kHz FCV 1100 transducer (beam angle: 10°) mounted on a frame in the moon pool of the RV Heincke. The depth range was set to 80 m. All other settings were according to the manufacturer's recommendations. A calibration cycle was run prior to the measurements. The data were recorded using the RoxAnn acquisition software RoxMap 32 (SONAVISION, Aberdeen, UK) at a line spacing of 220 m.

The EchoPlus system is permanently installed onboard the RV Haitabu, connected to a Fahrenholz Lithograph XL echosounder. The working frequencies were 30 and 200 kHz. The data were recorded using JEDI software that is customer programmed for the Landesamt für Landwirtschaft, Umwelt und ländliche Räume, Flintbek, Germany. In contrast to the other single-beam echosounder classification systems (RoxAnn and QTC5.5), the classification of EchoPlus data was in the supervised mode with a line spacing of 250 m.

In order to compare the results of seafloor classification systems quantitatively, two approaches are commonly used. As outlined in Schimel et al. (2010a, 2010b), the conventional approach is to produce a case study map for each classification, followed by estimates and comparison of their accuracy based on ground-truthing data (see, for example, Brown et al. 2005; Lucieer 2008; Brown and Collier 2008). The other approach is a comparison of one map with another without referring to ground-truthing data. This approach is very valuable for the determination of similarities between the different classifications, but no information regarding map accuracy is gained. This kind of comparison of similarities is normally calculated using error matrices (Schimel et al. 2010a, 2010b).

The present ground-truthing datasets are based on sidescan sonar data from the subarea (ca. 6 km²), and the classification patterns for the different methods look very similar (cf. above). Therefore, similarity was not calculated by means of error matrices but rather by the Bray-Curtis similarity index of degree of areal coverage (Figure 4.3 c–f) using the PAST software package (Hammer et al. 2001). The software computes a number of similarities between all pairs of rows entered. The results are given as a symmetric similarity matrix.

4.4.2. *Grab sampling*

In 2011 surface samples were collected from aboard the RV Senckenberg by means of a 0.1 m² Van Veen grab at 39 sites along four transects in the subarea selected for more detailed exploration. At each site, three replicates were taken for macrofauna and sedimentological analyses (Figure 4.3b). Transect locations were chosen using a preliminary sidescan sonar mosaic in order to make sure that all different backscatter areas were sampled.

The 2013 survey concentrated on sampling sites characterised by fine-grained sediments (e.g. muddy sand), with an additional transect at the southern border of the subarea. Here, three additional samples were retrieved from aboard the RV Heincke (11/2013) using a spade-box corer (50×50×60 cm) at sites where high abundances of *A. filiformis* were determined in 2011.

During the 2014 survey of the RV Senckenberg, 40 grab samples for sedimentological analyses were retrieved by a Shipek grab. During the 2014 survey with the RV Heincke, samples from 44 sites were taken from the total study area using a HELCOM 0.1 m² Van Veen grab. Of these, 41 samples were retained for sediment analyses, three locations being characterised by stones.

4.4.3. *Macrofauna and sediments*

At all locations where samples for macrofauna analyses and sedimentological analyses were retrieved, three grabs were taken at each location. Two of the grabs were used for macrofauna analyses and one grab for sedimentological analyses. The average distance between replicates is estimated to range between 15 and 30 m (Capperucci and Bartholomä 2012).

For sediment analyses, a macroscopic description and photographic documentation of the sediment surface were conducted for each grab. Then, subsamples of surface sediments were taken for grain-size analyses. The upper 2 cm was chosen because this depth interval is close to the penetration of the high-frequency acoustic signal into sandy sediments (Huff 2008; 1.5 cm for 500 kHz). In the laboratory, the samples were desalted in semi-permeable hoses over 24 h.

Each desalted sample was washed through a 0.063 mm mesh screen to separate the mud fraction (<0.063 mm). The coarse fraction was then dried and dry-sieved through a 2 mm mesh. Shell debris and gravel were weighed in order to determine the gravel content (>2 mm) as well as the content of shell debris >2 mm. The coarse fraction (>2 mm) was not further analysed. The sand size fraction (0.063 to 2 mm) was weighed, treated with hydrochloric acid, and weighed again to determine the content of sand-sized shell debris. For the total amount of shell debris of the samples (see ESM Table 1, parts a and b, in the electronic supplementary material available online for this article), the shell debris of the gravel size fraction and the sand size fraction were summed up. The sand fraction was split into $1/4 \Phi$ units ($\Phi = -\log_2$ diameter of particle in mm) from -1 to 4Φ , using calculations from settling velocities measured by a MacroGranometer™ settling tube (Flemming and Thum 1978; Tucker 1988). The mud fraction was analysed using a Micromeritics SediGraph III 5120™ (Stein 1985).

Samples HE416-38 to 82 were photographed and macroscopically analysed. At every sampling location the underwater video set was deployed to produce high-definition videos of the seafloor at the sampling location. In the laboratory the samples were treated with acetic acid to remove carbonates and with hydrogen peroxide to remove organic compounds. After the chemical treatment the fraction >2,000 μm was separated and the fraction <2,000 μm was measured in 100 size fractions using the CILAS particle sizer. Then the data were processed and re-sampled in 10th phi steps.

For macrofauna analyses, each 0.1 m² Van Veen grab was sieved onboard ship at 1 mm mesh size and the retained material was fixed with 4% buffered formaldehyde. Samples of coarse-grained sediments were decanted 10 times while sieving. In the laboratory, organisms were stained with Rose Bengal and identified to species level.

4.5. Data analyses

4.5.1. *RoxAnn- and EchoPlus-based seafloor classification*

The RoxAnn and EchoPlus theory of operation is to release an initial sound pulse and to take the energy received in the electronically gated last third of the first echo return (E1) as a measure of seafloor roughness. The rougher the seafloor, the more energy is received back and the longer becomes the tail of the echo. All of the energy received with the second echo return (E2, after reflection

at the sea surface and again at the seafloor) is a measure of seafloor hardness. The amount of reflection is controlled by the difference in acoustic impedance between seawater and the seafloor (Chivers et al. 1990; Schlagintweit 1993; Dean et al. 2013). Adverse effects due to changing water depth, such as variations in the backscatter amplitude and the tail length of the return signals, are electronically compensated by a pulse-integration constant. This constant adjusts the total integral value of the E1 and E2 gate areas. RoxAnn uses TVG (time-varied gain) to compensate for spreading loss with increasing water depth (Chandu, SonaVision, pers. comm., 2014).

The E values are given in DC voltage, and measurements were taken every second. Each data line includes the geographic position, date and time, water depth, as well as E1 and E2 values. Whenever either one of the variables did not record or showed implausible data (outliers), the whole data line was removed from the dataset during data processing.

The resulting data were colour coded using 10,000 RGB bins in the E1/E2 space. Each colour band (R, G and B) was then separately interpolated using the “natural neighbor” method. After interpolation, the three colour bands were recombined, resulting in an RGB triplet for every data point on the interpolated grid. Since the colour values depend on the two variables E1 and E2, the legend for the map is also two dimensional. All data processing and graphics were produced using self-programmed MATLAB-based scripts and Quantum GIS 2.4.0-Chugiak. The JEDI software serving to record the Echoplus E1 and E2 data also allows a supervised classification, based on ground-truthing data entered into the system. However, in the context of this study, only the raw E1 and E2 data were used.

4.5.2. QTC-based acoustic seafloor classification

Based on promising findings of previous work in the southern North Sea (Wienberg and Bartholomä 2005; Bartholomä 2006; Bartholomä et al. 2011), Quester Tangent™ software was used for the acoustic seafloor classification. Full wave forms of single-beam echosounder data were collected and analysed with QTC 5.5™/QTC Impact™. Sidescan sonar and multi-beam echosounder backscatter data were classified using QTC Swathview, with processing steps including data cleaning, and compensation for depth, range and insonification angles. After compensation, the time-series data from the single-beam echosounder were aligned by their bottom picks and summed in stacks of five. The analyses of the echo shape using QTC proprietary algorithms generated 166 so-called full feature vectors (FFVs). With sidescan sonar and multi-beam

echosounder images, borders of rectangular patches were distributed over the unmasked regions of backscatter images. In order to shorten the processing time of the backscatter data, a reduced number of only 29 FFVs were extracted, comprising basic features (1–4), grey level co-occurrence matrix (GLCM) data (5–20), circular Fourier transformation data (21–28) and fractal dimension data (29): 1–4 mean, standard deviation, skewness, kurtosis; 5–8 GLCM correlation; 9–12 GLCM contrast; 13–16 GLCM entropy; 17–20 GLCM homogeneity; 21–28 circular Fourier transform; 29 fractal dimension (QTC, pers. comm.).

Further processing of the amplitude data for singlebeam echosounder records as well as for image data for sidescan sonar and multi-beam echosounder data was exactly the same for all systems. For all hydroacoustic datasets, PCA (principal component analysis) was used to reduce the FFVs (166 FFVs for single-beam data, 29 FFVs for multi-beam and sidescan sonar data) to three components, i.e. Q1, Q2 and Q3. These were plotted in three-dimensional space (Q space) and used for clustering (Preston et al. 2004).

Segmentation was done in the three-dimensional space of the Q values. Starting with all records in the same class, a variant of the k-means clustering method separated them into clusters, i.e. acoustic classes. The result of the k-means clustering is presented graphically as score against number of classes. The score is a statistical measure of cluster size and tightness (Quester Tangent Corporation 2011). The statistically optimal number of classes is characterised by the minimum score. Each record, originating from a stack of singlebeam echoes or from the amplitudes in a rectangle, was assigned to the closest class centre in the Q space in a process that was iterative and stable. According to QTC, each cluster represents an acoustically distinct area. The QTC seafloor classes files were gridded (nearest neighbour method) using a grid size of 1 m in QTC Clams™ software. This software also allows a categorical interpolation to extend point and line coverage to full coverage. The full coverage data was saved in the Geotif format for further analyses.

The final Geotif file was imported into a geographic information system (ArcGIS 10.3™) to generate maps of acoustic classes. In this GIS environment, the macrofauna clusters and sediment data were combined with the acoustic map for validation of the acoustic classes.

4.5.3. Macrofauna

The software PRIMER v6 (Plymouth Marine Laboratory; Clarke and Gorley 2006) was used for statistical analyses of macrobenthos data. Diversity was analysed according to Shannon and Weaver (1949) and the Pielou (1969)

evenness index. For multivariate analyses, the data were fourth root transformed and the Bray-Curtis similarity coefficient (Bray and Curtis 1957) was calculated. Cluster analyses were performed to detect similarities between communities. Significant differences between communities were evaluated by means of the ANOSIM randomisation test (Clarke and Green 1988). SIMPER was used to detect the characteristic species per community (Clarke and Warwick 2001).

4.6. Results

4.6.1. *Acoustic backscattering*

In the subarea, the sidescan sonar backscatter mosaic of 2011 (Figure 4.3b) shows two main zones of different seafloor backscatter. A zone of generally higher backscatter (darker grey tones) extends from the north-eastern boundary of the subarea and generally dominates the eastern sector, with grey values varying between ca. 47 and 200 (average of 160). The northern, northwestern and southern sectors display lower backscattering intensity with grey values of ca. 170–240 (mostly 200–210). Within the zone of weaker backscatter, a slight increase in grey tones is visible from the northeast to the southwest (Figure 4.3b). The grey values decrease from ca. 230 near the north-eastern boundary (A in Figure 4.3b) to ca. 210 in the centre (B in Figure 4.3b) and 170–180 near the south-western boundary (C in Figure 4.3b) of the subarea (Table 4.2). Although the absolute grey values for the years 2012 and 2014 are slightly different because of different environmental settings such as wave height and wave direction, the general increase of backscatter strength from the northeast to the southwest is confirmed for both surveys of 2012 and 2014 (Table 4.2).

	A	B	C
2011	230	210	170
2012	210	200	170
2013	235	225	200
2014	250	248	168

Table 4.2. Grey values (0=black, 255=white) for sidescan sonar mosaics from 2011 to 2014 in the subarea.

4.6.2. *Derivates from bathymetry*

In the subarea, the broad-scale BPI values (Figure 4.4, upper left) vary between –1 and 6. However, the strongest variation of BPIs is found in the north-eastern sector with a stronger backscattering of sidescan sonar data (Figure

4.3b). This sector is also characterised by stronger variations in bathymetry (Figure 4.3a). The remaining sectors show a BPI of zero, indicating a flat seafloor or a constant slope. The fine-scale BPI values (Figure 4.4, upper right) show variations between -1 and 4 , with most values being zero. Again, the strongest variations are visible in the north-eastern sector of the subarea.

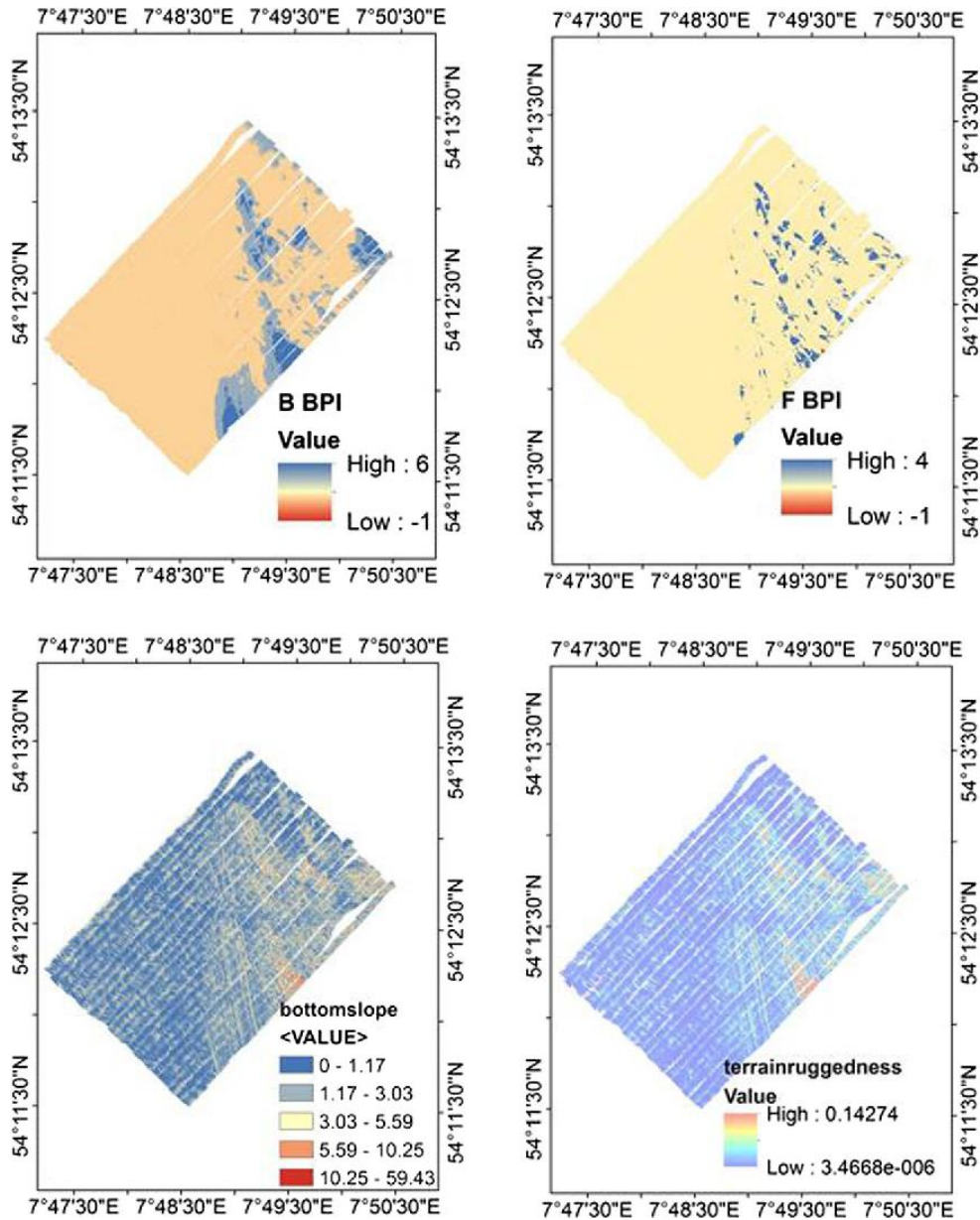


Figure 4.4. Subarea. Broad-scale bathymetric position index (BPI, upper left), fine-scale BPI (upper right), bottom slope (lower left) and terrain ruggedness (lower right).

The bottom slopes (Figure 4.4, lower left) vary between 0° and 59° . Again, the higher values are restricted to the northeast of the subarea, whereas gentler slopes ($0-1.1^\circ$) were recorded in the remaining sectors. The calculated terrain ruggedness (Figure 4.4, lower right) mirrors the results of the other bathymetry

derivates (BPI, bottom slopes), with higher values in the north-eastern sector of the subarea and lower values in the remaining sectors.

4.6.3. Acoustic seafloor classification

4.6.3.1. QTC Swathview™ sidescan sonar

In the subarea, segmentation of the acoustic backscatter data from sidescan sonar by QTC Swathview™ resulted in six seafloor classes (Figure 4.3e). The areal distribution of seafloor class green (coverage: 33.7% of the seafloor) coincides with the areas of light grey tones on the sidescan sonar mosaic (Figure 4.3b). Therefore, this class is related to low backscatter values (grey tones: 210–250) of the sidescan sonar signal. Seafloor class red (coverage: 34% of the seafloor, Figure 4.3e) correlates well with high backscatter values (grey tones: 168–200) of the sidescan sonar data in the central and southeastern sectors of the subarea, but occurs also in the southern and south-western sectors where low backscatter values are visible on the sidescan sonar mosaic (Figure 4.3b).

In the central and south-eastern sectors of the subarea, seafloor class blue (coverage: 23.3% of the seafloor) is visible near the nadir of the sidescan sonar data (Figure 4.3b). This suggests either that class blue is a classification artefact, due to the generally stronger backscatter signal close to the nadir, or that variations in seafloor cover (e.g. different types/amounts of epifauna) may have generated this class. However, in the southern and south-western sectors, the blue class (Figure 4.3e) correlates well with a slight increase in backscattering intensity seen in the sidescan sonar mosaics (Figure 4.3b). Seafloor class cyan (coverage: 3.3% of the seafloor) is predominantly visible in the south-eastern sector with high backscatter values. The remaining two classes yellow (coverage: 0.5% of the seafloor) and pink (coverage: 5.2% of the seafloor) occur in small patches mostly in and around the areas of high backscatter in the sidescan sonar signal (Figure 4.3b).

4.6.3.2. QTC Swathview™ multi-beam echosounder

In the subarea, backscatter data of the multi-beam echosounder were segmented into four acoustic seafloor classes using the QTC Swathview™ software. Most of the subarea is characterised by only two classes (Figure 4.3d): red and green. Class green covers 28.6% of the seafloor, coinciding with areas of low backscatter values in the sidescan sonar mosaic (Figure 4.3b). Seafloor class red covers 70.5% of the seafloor, coinciding with areas of strong seafloor backscattering in the central and south-eastern sectors of the subarea but also in the southern and south-western sectors where a gentle increase in

backscatter values is visible. The seafloor class cyan (coverage: 0.7% of the seafloor) is constrained within the area of high backscatter values, whereas the remaining class pink (coverage: 0.2%) is disseminated over the whole subarea and might be due to classification of noise.

4.6.3.3. RoxAnn

The E1/E2 data from the RoxAnn system were processed by means of two classification approaches. In the subarea, fuzzy seafloor classification (Figure 4.3c) reveals four classes. Class red covers 34.6% of the seafloor and coincides with the area of strong backscattering in the sidescan sonar data (Figure 4.3b). Class green (coverage 33.2%) corresponds to the area of weak backscattering, whereas class blue (coverage 21.2%) is associated with slightly increased backscattering in the southwestern sector of the subarea (Figure 4.3c). Class yellow covers 11.0% of the subarea, and mainly co-occurs with strong backscatter in the central sector (Figure 4.3 b, c).

For the second approach of processing (RoxProgs), the RoxAnn data are displayed in the E1/E2 space (“RoxAnn box”) in Figure 4.5 for the whole study area. Six acoustic classes can be distinguished. Since there are usually no sharp borders in nature, class borders were inserted neither in the RoxAnn box (Figure 4.5) nor in the map (Figure 4.5). If sharp borders occur, then they are clearly visible in both figures. Class I occurs exclusively above 30 m water depth. According to the RoxAnn box, the green colours suggest the softest and smoothest values of the entire dataset. Class I is largely congruent with QTC class green (single-beam echosounder as well as multi-beam and sidescan sonar) and with the areas of weakest backscatter of the sidescan sonar in the north-eastern part of the subarea. Class I demarcates a large curved sector in the upper northern part of the study area (Figure 4.2).

Class II (yellow) suggests a slightly harder and rougher seafloor. It is congruent with QTC class yellow but extends further into the southern part of QTC class cyan. Class III (orange) largely resembles QTC class blue; however, parts of the subarea in the south and southeast covered by QTC class blue belong more to RoxAnn class II (i.e. revealing lower roughness and hardness values than class III). Class III demarcates large sectors in the southern and western parts of the study area (Figure 4.2), associated with slightly increased backscatter in the sidescan sonar records. Class IV has hardness values similar to class III but associated with clearly higher roughness values. Class IV shows reddish colours and is congruent with QTC class cyan. It covers a large part of the eastern sector of the study area. Classes V and VI are congruent with QTC class red. They encompass the hardness values of classes I, II and partly III.

However, the roughness values are significantly higher and classes V and VI are clearly separated from classes I to III. They cover a distinct sector in the central eastern part of the study area.

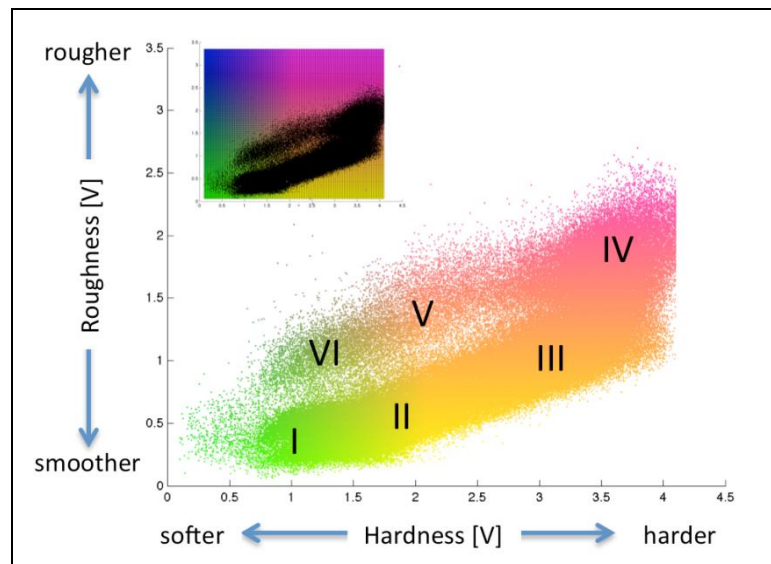


Figure 4.5. Study area. RoxAnn box of roughness (E1) vs. hardness (E2). I–V Classes mentioned in the text. Inset E1 vs. E2 plotted as black dots superimposed on the chosen colour scheme (modified after Hass et al. 2016).

4.6.3.4. QTC View 5.5TM/QTC ImpactTM single-beam echosounder

In the subarea, the single-beam echosounder data can be subdivided into six statistically significant different acoustic seafloor classes (Figure 4.3f). The sector characterised by low backscatter values of the sidescan sonar mosaic is covered by seafloor classes green (coverage: 8.8% of the seafloor) and yellow (coverage: 10.8%). Seafloor classes red (coverage: 36.2%) and cyan (coverage: 11.9%) are predominantly restricted to the central and south-eastern sectors of the subarea where high backscatter values are visible on the sidescan sonar mosaic (Figure 4.3b). The southern and south-western sectors, where the sidescan sonar mosaic shows slightly increased backscatter values, have seafloor class blue (coverage: 32.2%). Seafloor class pink covers only 0.4% of the seafloor and is mainly situated within seafloor class red in the central part of the subarea (Figure 4.3f).

4.6.4. Sediments

In the subarea, the locations of sediment samples in 2011 were determined on the sidescan sonar backscatter mosaic in order to ensure full coverage of backscatter signatures (Figure 4.3b). In assessing the whole study

area, sample locations of survey HE416 in 2014 were chosen on the basis of RoxAnn measurements (Figure 4.2).

According to the classification of Folk (1954), the seafloor samples range from gravel to sandy mud (ESM Table 1 in electronic supplementary material). In the subarea, most samples are classified as muddy sand (26 of 38 samples). For the whole study area, five samples are classified as gravel (samples 09, 45, 71, 72, 73), three as sandy mud (samples 10, 69, 70), two as muddy gravel (samples 46 and 47), one as gravelly muddy sand (sample 08) and one as muddy sandy gravel (sample 95). Grab samples characterised by high amounts of gravel contained not only granules (diameter 2–4 mm) but also pebbles (4–64 mm) and cobbles (64–256 mm; cf. Wentworth scale; Wentworth 1922; Krumbein and Aberdeen 1937).

Coarser-grained sediments were retrieved from the central and south-eastern sectors of the subarea, and finer-grained sediments from the northern, southern and south-western sectors (Figure 4.3b). In the latter, there are only small variations in grain size distributions from the northeast to the southwest (Figure 4.6). Using the Folk (1954) classification, all samples (2011_02, 2011_42, 2011_64, 2011_86) are muddy sand. However, using the phi mean of the sand size fraction of these samples (Figure 4.6) and the Wentworth (1922) scale, sample 2011_86 (phi mean 2.601) can be classified as muddy fine sand. According to this classification, the remaining samples are muddy very fine sand (phi mean 3.463–3.491). Samples from almost the same locations in the 2013 survey (from northeast to southwest: 2013_20, 2013_17, 2013_14, 2013_02) yielded the same results. The southernmost sample (2013_02) is classified as muddy fine sand, whereas the remaining samples are muddy very fine sand (Figure 4.7). Regarding the whole study area, there are similar spatial distribution patterns of hardness- and roughness-based classification (ESM Table 1, part c, in electronic supplementary material; Figure 4.2).

However, this dataset also highlights the patchy character of the area. The sediment becomes generally slightly coarser from north to south. The elevation highs in the NE of the study area reveal pebbles and boulders that inhibited the use of a grab sampler (HE416_56, 57, 60), as well as medium sands (HE416_38–40) and muddy sediments (HE416_47–55). The deeper southern third of the study area is characterised by sandy sediments throughout.

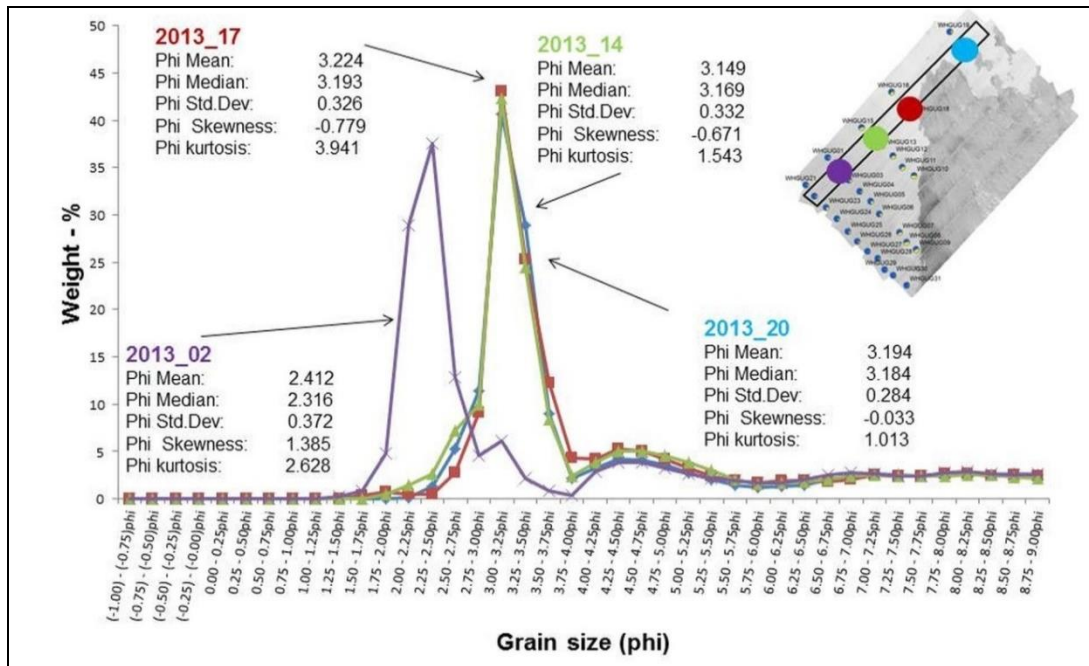


Figure 4.6. Subarea. Grain size distributions along the transect of 2013 from the northwest (sample 2013_20) to the southwest (sample 2013_02).

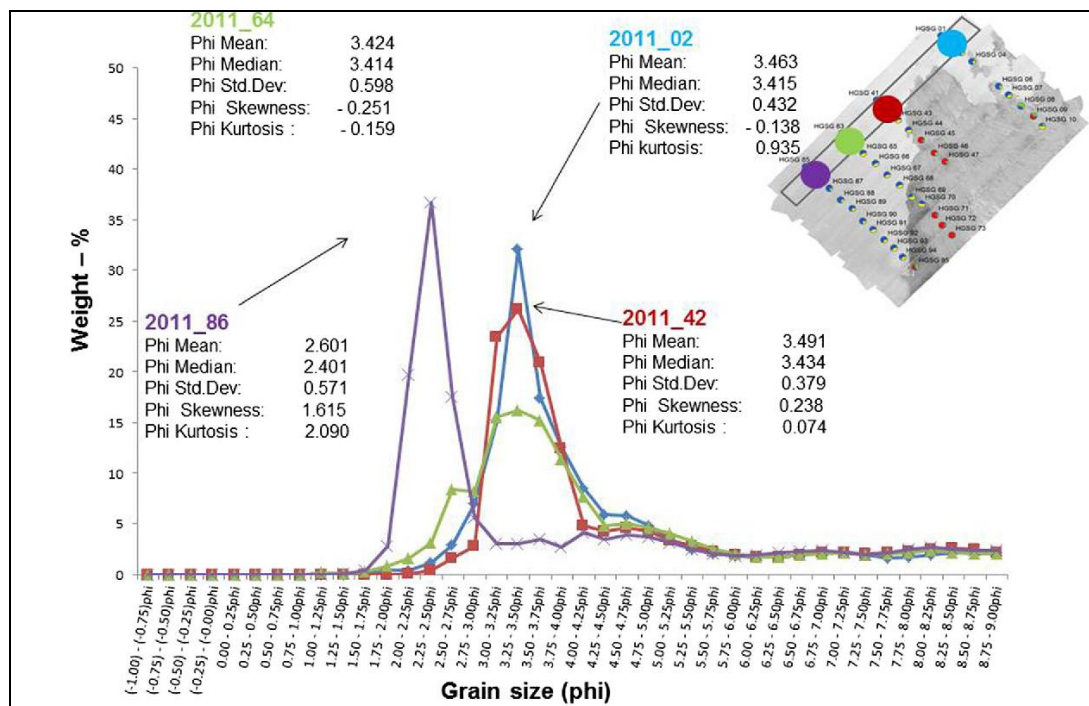


Figure 4.7. Subarea. Grain size distributions along the transect of 2011 from the northwest (sample 2011_02) to the southwest (sample 2011_86).

4.6.5. Macrofauna

In the samples from 39 stations taken in 2011 in the subarea, 189 macrofauna taxa were identified, comprising mostly molluscs (49%) followed by annelids (23.7%), echinoderms (18.6%) and crustaceans (7%). The four transects

T1 to T4 (Figure 4.3b) show a variation of the main macrofauna groups. The abundance of molluscs decreases from T1 to T4, whereas that of echinoderms increases (Figure 4.8). Despite the high sedimentary diversity, the cluster analyses provided only four significantly different macrofauna communities (Figure 4.9) based on the ANOSIM test (global R value of 0.92, significance level of 0.1%).

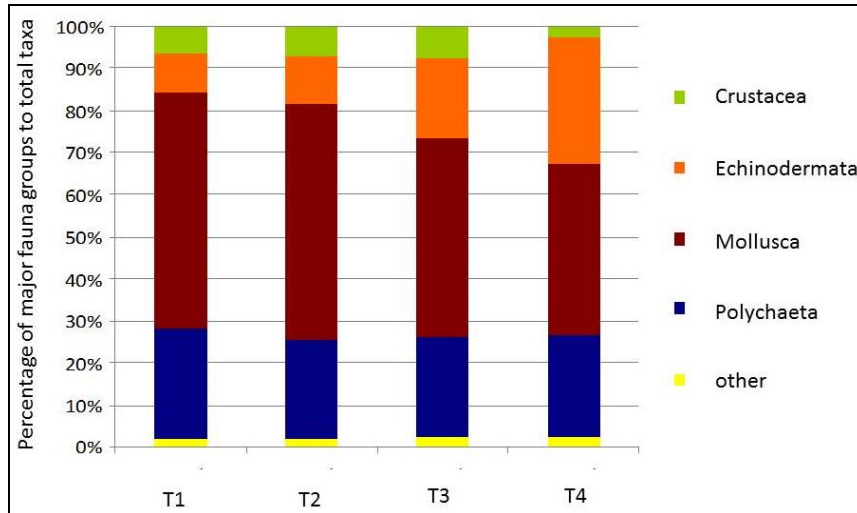


Figure 4.8. Subarea. Percentage of major fauna groups to total taxa along transects T1 to T4 (for location of T1-T4, see Figure 4.3b).

The three stations of community A (1-3) are in the northern part of the subarea (Figure 4.3b). According to the cluster analyses, this is a *Nucula nitidosa*-*Abra alba* community associated with polychaetes such as *Lagis koreni* and *Scalimbergma inflatum*. This community has a mean taxa number of 40/0.1 m², a mean Shannon index of 2.18, a high mean evenness (0.59), and the highest mean abundance (11,627 ind./m²). Community A is associated with the acoustic class green (sidescan sonar, multi-beam echosounder, single-beam echosounder QTC) or class I (single-beam echosounder RoxAnn; Figure 4.3 c–f, ESM Table 2 in the electronic supplementary material).

Stations belonging to community B are in the centre of the subarea (Figure 4.3b), earmarked by muddy sand to sandy mud. Dominant species are *N. nitidosa*, *A. filiformis* and *Hyala vitrea*. This community comprises species of both communities A and C, although in lower abundances—mean abundance of 5,160 ind./m², mean taxa number of 37/0.1 m², and highest mean Shannon index (2.48) and evenness (0.69; Figure 4.3c–f, ESM Table 2 in electronic supplementary material). Community B is associated with the acoustic class green (QTC sidescan sonar, QTC multi-beam echosounder), the class yellow (QTC single-beam) and the RoxAnn class I.

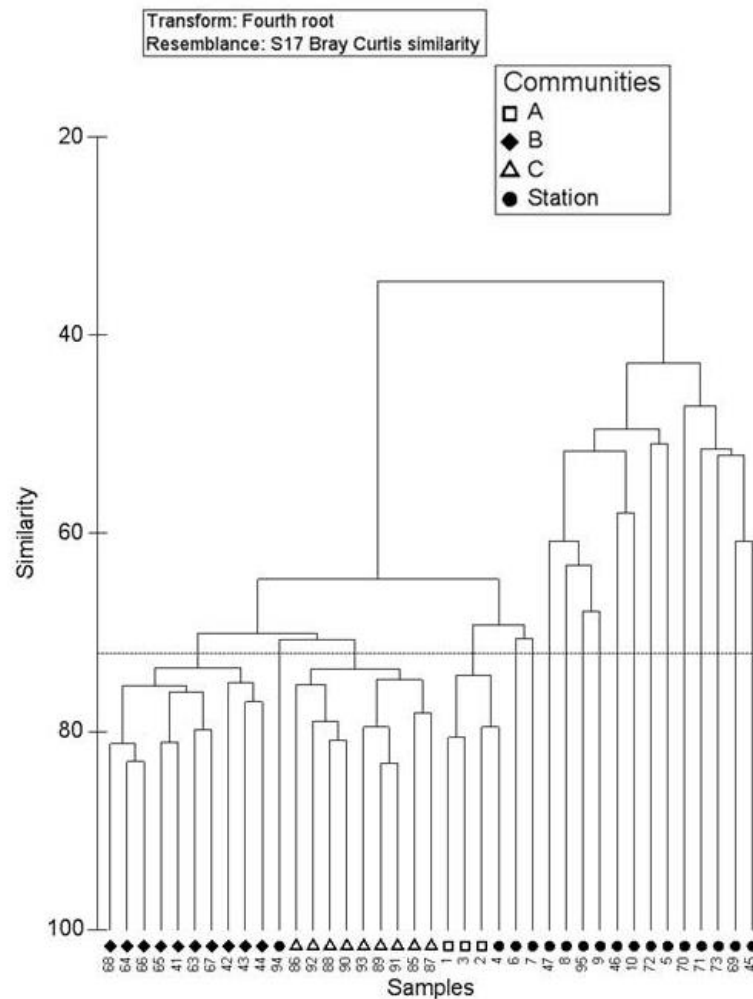


Figure 4.9. Subarea. Hierarchical clustering of macrofauna samples.

Community C is an *A. filiformis*-*Kurtiella bidentata* community dominated by the brittle star (1,711/m²) and commensal bivalve species. The highest mean taxa number of 42/0.1 m², mean abundance (5,702/m²), Shannon index (2.41) and evenness (0.64) were found. This community is associated with the acoustic class blue (QTC sidescan sonar), red (QTC multi-beam echosounder), QTC single-beam class blue and RoxAnn class III (Figure 4.3 c–f, ESM Table 2 in electronic supplementary material).

The fourth community included stations from an area of higher backscattering caused by coarser sediments with boulders and pebbles (Figure 4.3b). There, a quantitative sampling with the Van Veen grab was impossible. Qualitative samples revealed typical hard-substrate organisms such as the polychaetes *Pomatoceros triqueter* and *Sabellaria spinulosa* (Hartmann-Schröder 1996), a high abundance of anthozoans, but also soft-bottom species such as *Lagis koreni*, *Gattyana cirrhosa* and *Protodorvillea kefersteini*. A similar community was found by Kühne and Rachor (1996) at the “Steingrund” near Helgoland.

To confirm the results of 2011, the *A. filiformis* data of the 2013 samples were analysed. Again, high abundances of *A. filiformis* were detected in the southern part of the subarea (see ESM Table 3 in the online electronic supplementary material).

4.6.6. Brittle star abundance vs. side-scan sonar grey values

An increase in the abundance of the brittle star *A. filiformis* was found from the northern to southern parts of the subarea (Figure 4.8). The highest abundances were determined at stations with a water depth of about 30 m. In Figure 4.10 (cf. ESM Table 3 in electronic supplementary material), the abundance of *A. filiformis* is plotted against grey values (0=black, 255=white) from the 2011 sidescan sonar mosaic (Figure 4.3b). The Spearman rank order (Spearman 1904) shows a negative correlation between grey scale values and abundance of brittle stars. The variation increases from 2011 to 2013 (Figure 4.10).

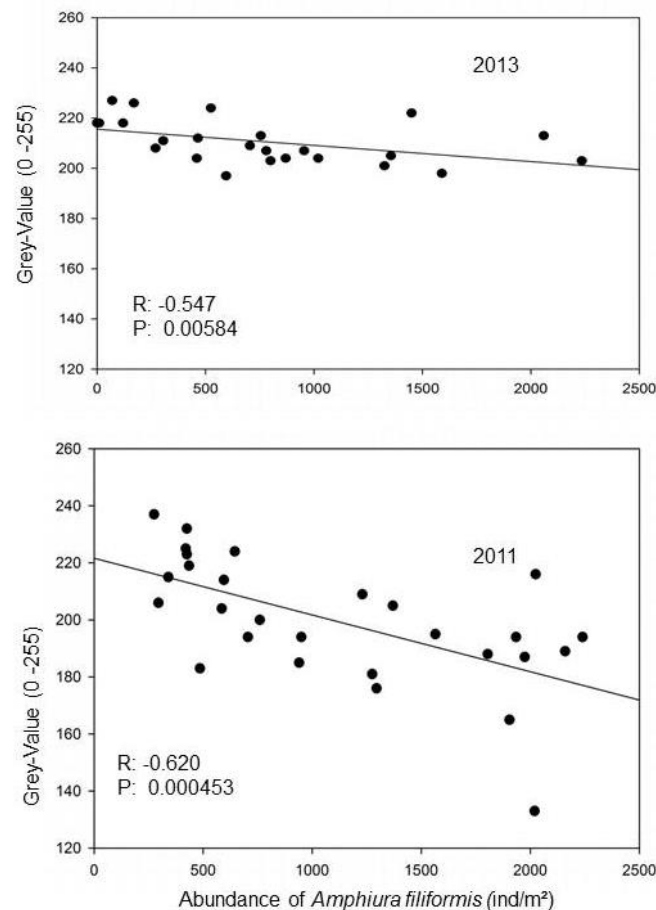


Figure 4.10. Subarea. Correlations (Spearman rank order) between grey values (0 = black, 255 = white) from sidescan sonar mosaic and total abundance of the brittle star *A. filiformis* in 2013 (upper panel) and 2011 (lower panel).

The 2013 samples again show similar high abundances of *A. filiformis* in the southern part of the subarea (ESM Table 3 in electronic supplementary material). The correlation between grey values and the abundance of the brittle star using the Spearman rank order reveals a correlation coefficient of -0.547 and P value of 0.00584. This confirms the results for the 2011 correlation. In contrast, the sample transect added near the southern border of the subarea in 2013 (samples WHGUG21–WHGUG31) shows average mean abundances of *A. filiformis* (ESM Table 3 in electronic supplementary material).

4.7. Discussion

4.7.1. Acoustic seafloor classification comparison

The physical configuration of swath-based and vertical down looking single-beam echosounders implies different types of return signals. Therefore, the classification of swath systems is based on statistical segmentation of images, whereas the classification of single-beam echosounder data is based on the statistical analysis of the wave shape (QTC 5.5) and multiple-echo envelope analysis (RoxAnn). For all systems, a very similar classification pattern was generated (Figure 4.3 c–f, Table 4.3). The seafloor classifications obtained by the RoxAnn system and from the sidescan sonar data (QTC Swathview) show the highest similarity of 0.89, whereas there is a similarity of 0.63 for the RoxAnn and multi-beam echosounder data (QTC Swathview). The similarity between the singlebeam echosounder classifications from RoxAnn and QTC 5.5 is 0.75.

	RoxAnn	Multi-beam	SSS	QTC
RoxAnn	1.00	0.63	0.89	0.75
Multi-beam	0.63	1.00	0.64	0.46
SSS	0.89	0.64	1.00	0.70
QTC	0.75	0.46	0.70	1.00

Table 4.3. Similarity index of seafloor classification based on Bray-Curtis.

The minimum similarity value was computed for the classifications of the multi-beam echosounder (QTC Swathview) and the QTC 5.5 single-beam data (0.46). The remaining similarities vary between 0.70 (QTC 5.5 and sidescan sonar) and 0.64 (sidescan sonar and multi-beam echosounder).

Generally lower similarities between classifications from single-beam echosounder data and swath systems have been noted earlier (Anderson et al.

2008; Schimel et al. 2010a, b; Bartholomä et al. 2011). Schimel et al. (2010b) pointed out that this can be at least partly explained by the differences of grazing angles between the systems. Single-beam echosounders operate at very high grazing angles only (85–90°), whereas sidescan sonar systems have low to medium grazing angles (1–45°) and most multi-beam echosounders operate from low to very high grazing angles (25–90°; Schimel et al. 2010b). Indeed, Lurton (2002) showed that the effects of surface roughness and volume backscattering vary strongly with grazing angle.

The generally lower similarity between the multi-beam echosounder classification and the classification from RoxAnn, QTC 5.5 and sidescan sonar was not expected. Preston et al. (2003), Bartholomä et al. (2011), Micallef et al. (2012), Markert et al. (2013) and Lurton and Lamarche (2015) showed that classifications obtained from multi-beam echosounder data are of superior quality. This is, among others, due to the fact that for every single beam of the multi-beam system, data on backscatter, depth and grazing angle are available for further processing (e.g. compensation). Classifications from multi-beam echosounders and sidescan sonar systems are normally very similar because they both are based on the backscatter image (Schimel et al. 2010a).

The low similarity between the multi-beam classification (Figure 4.3d) and all other classifications (Figure 4.3 c, e, f) is mainly caused by the areal coverage of classes green (28.6%, Figure 4.3d) and red (70.5%, Figure 4.3d). At the moment, it is not clear why the multi-beam echosounder classification is so different from the other classifications. The surveys were carried out in summer (July) 2011–2014, a season commonly earmarked by increased suspended particulate matter. Whether this partly impeded the acoustic energy of the high-frequency multi-beam echosounder (455 kHz) from reaching the seafloor is an aspect requiring further research. Mazel (1985) noted that suspended sediment scatters the signal on its way to the seafloor.

4.7.2. *Influence of macrobenthos*

All classification systems showed differences in acoustic results between the southern and northern parts of the subarea chosen for more detailed surveying (Figure 4.3), reflected also by the occurrence of community C (ESM Table 2 in electronic supplementary material). This can be explained neither by changes in sediment composition (e.g. Riegl et al. 2007; Freitas et al. 2011) nor by variations in bathymetry.

Both single-beam systems clearly reveal changing seafloor properties between the areas inhabited by communities B and C (Figure 4.2 and Figure 4.3

c, f). Slight differences between the results of the two systems might be due to different years and different months (seasons) in which the measurements were carried out. RoxAnn data suggest that community C also dominates large parts of the total study area (Figure 4.2, orange colours). Evidently, changes in backscatter signal strength can be explained by changes in seabed roughness induced by varying abundance of the ophiuroid *A. filiformis* in the southern part of the study area at about 30 m depth.

The brittle star is the dominant species of soft sediments in the North Sea—e.g. the Oyster Ground (Cadée 1984; Kröncke et al. 2004, 2011) and the German Bight (Salzwedel et al. 1985; Kröncke et al. 2004, 2011). Associated species of *A. filiformis* communities were *Harpinia antennaria* and the bivalves *K. bidentata* and *Corbula gibba* (e.g. Rachor and Nehmer 2003; Reiss et al. 2006). *A. filiformis* is found at depths of 5 m to more than 200 m (e.g. Buchanan 1964; Künitzer 1989; Künitzer et al. 1992; Sköld et al. 1994; Rosenberg et al. 1997; Josefson 1998; Southward and Campbell 2006).

The size of the disk of *A. filiformis* can reach a diameter of 10 mm, and the slender, flexible arms a length of up to 100 mm. The specimens (disks) have been found buried at sediment depths of 3–8 cm (e.g. Rosenberg et al. 1997, 4 cm depth; Josefson 1998, 3–6 cm depth), depending on the age and therefore on the size of the disk and the arm length of the specimen. The three box cores taken by the RV Heincke in November 2013 from the area with high abundances of *A. filiformis* showed a burial depth of 5 cm. The bioturbation caused by the brittle stars may change the physical properties of the sediments, as reported by Rowden et al. (1998). They found that the shear strength of the upper 5 cm of sediment was reduced by up to 45% due to bioturbation. This also may influence the acoustic properties of sediments, like firmness.

A. filiformis can switch between two different feeding types. For deposit feeding, the arm tips explore the sediment surface for particles. For suspension feeding, the arms are held vertically to 2–4 cm above the sediment surface to trap particulate suspended matter and phytoplankton (Buchanan 1964; Woodley 1975; Loo et al. 1996). The number of active feeding arms seems to vary. Ockelmann and Muus (1978) described 3–4 active arms per individual, whereas Loo et al. (1996) and Rosenberg et al. (1997) observed only 1–2. In the present study, the mean abundance of brittle stars/m² in community C would result in a minimum of 1,711 arms/m² (cf. one active arm per individual) and a maximum of 6,844 arms/m² (cf. four active arms). Since most of the specimens were adults, the mean length of the arms above the sediment surface probably reached 5–6 cm.

The high number of ophiuroid arms inferred for the subarea of the present study is expected to influence the surface roughness of the seafloor, causing a change in backscattering (cf. Lurton 2002). The roughness data (E1) from RoxAnn (Figure 4.4) show higher values in the southern part of the subarea. This indicates that the high number of ophiuroid arms increased the roughness of the seafloor. Such changes in surface micro-roughness can influence the backscattering signal and acoustic classification (Bartholomä et al. 2011). Capperucci and Bartholomä (2012) confirmed that, for high-frequency hydroacoustic systems (>100 kHz), such roughness changes may influence the acoustic signals more than actual changes of sediment composition. It is also important to note that the seafloor classes are based on the acoustic response of the footprint of the sonar system from both the seafloor itself and the arms of the ophiuroids. For a single-beam echosounder, the seafloor footprint size is based on water depth. At a water depth of 30 m, the QTC 5.5 system ensonifies an area of 11.8 m². Thus, the seafloor classification pattern of the southern part of the subarea of the present study would be influenced by changes in seafloor roughness and hardness caused by thousands of feeding arms of the brittle star *A. filiformis*.

4.8. Conclusions

Acoustic seafloor mapping and automatic classification is in general a valuable tool for the study of sediment distribution and also the EU MSFD descriptor “seafloor integrity”. In order to obtain reliable results, it is suggested to run at least two different systems simultaneously during a survey. One of these should be a swath system like a dual-frequency sidescan sonar or multi-beam echosounder. The other should be a single-beam echosounder-based acoustic seafloor classification system working in the 200 kHz range. The different grazing angles (high for single-beam systems and medium to low for sidescan sonar, and medium to high for multi-beam echosounder systems) reduce the effects of volume backscattering and surface roughness. A thorough ground-truthing program is required. Based on the similarities of classifications, the best choice for habitats like the northwest Helgoland area would be a sidescan sonar and the RoxAnn seafloor classification system.

Sidescan sonar data showed a slight increase of backscatter strength from the northeast to the southwest in the subarea chosen for more detailed surveying in the present study. Automatic seafloor classification methods segmented the area of increased backscatter intensity in the southern sector of the subarea as

separate class, although the sediment texture was not significantly different from that in the north-western sector (muddy fine sand to muddy very fine sand). The abundance of molluscs decreases from the north to the south of the subarea, whereas that of Echinodermata increases (especially *A. filiformis*). The correlation between the abundance of *A. filiformis* feeding arms and backscatter intensity in the southern sector revealed that most likely the feeding arms increased the sediment surface roughness and, thus, the backscatter intensity. It is suggested that the *A. filiformis* community C covers large parts of the subarea. The number of grab samples for macrofauna studies can be reduced significantly by the use of hydroacoustic data and automatic seafloor classification, saving time and money. The seafloor sediment distribution from acoustic backscatter and automatic seafloor classification shows a much higher resolution than from extrapolation of surface samples alone.

4.9. Acknowledgements

This study was part of the German framework project “Scientific monitoring concepts for the German Bight (WIMO)”, financed by the Lower Saxony Ministry for Environment and Climate Protection and the Lower Saxony Ministry for Science and Culture. We would like to thank the captains and crews of RV Senckenberg and RV Heincke for support during the cruises. U. Schückel provided additional data from the survey area. C. Schollenberger, A. Raschke as well as A. Steudle, J. Matschke and F. Gottschall are thanked for technical assistance. The article benefited from constructive assessments by P. Wintersteller and an anonymous reviewer.

4.10. References

- Anderson, J.T., Van Holliday, D., Kloser, R., Reid, D.C., Simard, Y. 2008. Acoustic seabed classification: current practice and future directions. *ICES J Mar Sci.* 65, 1004–1011.
- Bartholomä, A. 2006. Acoustic bottom detection and seabed classification in the German Bight, southern North Sea. *Geo-Mar Lett*, 26, 177–184.
- Bartholomä, A., Holler, P., Schrottke, K., Kubicki, A. 2011. Acoustic habitat mapping in the German Wadden Sea - Comparison of hydroacoustic devices. *J Coastal Res SI*, 64, 1–5.
- Bornhold, B.D., Collins, W.T., Yamanaka, L. 1999. Comparison of seabed characterization using sidescan sonar and acoustic classification techniques. In: *Proc Canadian Coastal Conf*, Victoria, Canada, 15 pp.
- Bray, J.R., Curtis, J.T. 1957. An ordination of the upland forest communities of southern Wisconsin. *Ecol Monogr*, 27, 325–349.

-
- Brown, C.J., Collier, J.S. 2008. Mapping benthic habitat in regions of gradational substrata: an automated approach utilising geophysical, geological, and biological relationships. *Estuar Coastal Shelf Sci.*, 78, 203-214.
- Brown, C.J., Mitchell, A., Limpenny, D.S., Robertson, M.R., Service, M., Golding, N. 2005. Mapping seabed habitats in the Firth of Lorn off the west coast of Scotland: evaluation and comparison of habitat maps produced using the acoustic ground-discrimination system. RoxAnn, and sidescan sonar. *ICES Journal of Marine Science*, 62, 790-802.
- BSH 2016. Guideline for Seafloor Mapping in German Marine Waters Using High Resolution Sonars. BSH-No 7201, 150 pp.
- Buchanan, J.B. 1964. A comparative study of some features of the biology of *Amphiura filiformis* and *Amphiura chiajei* (Ophiuroidea) considered in relation to their distribution. *J Mar Biol Assoc UK*, 44, 565–576.
- Cadée, C.C. 1984. Macrobenthos and macrobenthic remains in the Oyster Ground, North Sea. *Neth J Sea Res*, 18, 160-178.
- Capperucci, R., Bartholomä, A. 2012. Sediment vs. topographic roughness: anthropogenic effects on acoustic seabed classification. In: Leendert Dorst, L., van Dijk, T., van Ree, R., Boers, J., Brink, W., Kinneking, N., van Lancker, V., de Wulf, A., Nolte, H. (Eds), Conference Proceedings of Hydro12, Taking care of the sea, the Hydrographic Society Benelux (HSB), on behalf of the International Federation of Hydrographic Societies (IFHS), Rotterdam, the Netherlands, 12-15 November 2012, 23-28.
- Chivers, R.C., Emerson, N.C., Burns, D. 1990. New acoustic processing for underway surveying. *Hydrogr J*, 56, 9-17.
- Clarke, K.R., Green, R.H. 1988. Statistical design and analysis for a “biological effects” study. *Mar Ecol Prog Series*, 46, 213-226.
- Clarke, K.R., Warwick, R.M. 2001. Change in marine communities: an approach to statistical analysis and interpretation, 2nd ed. PRIMER-E, Plymouth.
- Clarke, K.R., Gorley, R.N. 2006. PRIMER v6: User Manual/Tutorial. PRIMER-E, Plymouth.
- Collins, W.T., Galloway, J.L. 1998. Seabed Classification and multibeam bathymetry: tool for multidisciplinary mapping. *Sea Technol*, 39, 45-49.
- Dean, B.J., Ellis, J.T., Irlandi E. 2013. Measuring nearshore variability in benthic environments: An acoustic approach. *Ocean Coastal Manage*, 86, 3-41.
- Degraer, S., Moerkerke, G., Rabaut, M., Van Hoey, G., Du Four, I., Vincx, M., Henriët, J.-P., Van Lancker, V. 2008. Very-high resolution side-scan sonar mapping of biogenic reefs of the tube-worm *Lanice conchilega*. *Remote Sensing Environ*, 112, 3323–3328.
- European Union. 2008. Directive 2008/56/EC of the European Parliament and of the Council of 17 June 2008 establishing a framework for community action in the field of marine environmental policy (Marine Framework Directive). In: Official Journal of the European Union, vol. L164, 19-40.
- Ferrini, V.L., Flood, R.D. 2006. The effects of fine-scale surface roughness and grain size on 300 kHz multibeam backscatter intensity in sandy marine sedimentary environments. *Marine Geology*, 228, 153-172.
- Figge, K. 1981. Karte zur Sedimentverteilung in der Deutschen Bucht, Nr. 2900. Hamburg, Germany, Bundesamt für Seeschifffahrt und Hydrographie, scale 1:250,000.
- Flemming BW, Thum A. 1978. The settling tube - a hydraulic method of grain size analysis of sands. *Kieler Meeresforschung, Special Issue*, 4, 82-95.

- Folk, R.L. 1954. The distinction between grain size and mineral composition in sedimentary rock nomenclature. *Journal of Geology*, 62 (4), 344-359.
- Freitas, R., Ricardo, F., Pereira, F., Sampaio, L., Carvalho, S., Gaspar, M., Quintino, V., Rodrigues, A.M. 2011. Benthic habitat mapping: Concerns using a combined approach (acoustic, sediment and biological data). - *Estuarine, Coastal and Shelf Science*, 92, 598-606.
- Gleason, A.C.R., Eklund, A.M., Reid, R.P., Koch, V. 2006. Acoustic seabed Classification, acoustic variability, and grouper abundance in a forereef environment. *NOAA Professional Papers NMFS*, 5, 38-47.
- Gleason, A.C.R. 2009. Single-beam acoustic seabed classification in coral reef environments with application to the assessment of grouper and snapper habitat in the upper Florida Keys, USA. PhD Thesis, University of Miami, Coral Gables, FL.
- Hammer, Ø., Harper, D.A.T., Ryan, P.D. 2001. PAST: Paleontological Statistics Software Package for Education and Data Analysis. *Palaeontologia Electronica*, 4 (1), 1-9.
- Hartmann-Schröder G. 1996. Teil 58. Annelida, Borstenwürmer, Polychaeta. 2. Neubearb. Auflage. In: Dahl F, Schuhmann H (eds) *Die Tierwelt Deutschlands und der angrenzenden Meeressteile nach ihren Merkmalen und nach ihrer Lebensweise*. Zoologisches Museum Berlin, Jena.
- Hass, H.C., Bartsch, I. 2008. Acoustic kelp bed mapping in shallow rocky coasts - case study Helgoland. In: Doerffer, R., Colijn, F., van Beusekom J. (Eds) *Observing the Coastal Sea - an Atlas of Advanced Monitoring Techniques*. LOICS Reports & Studies 33. Geesthacht, Germany: GKSS Research Centre, 50-53.
- Hass, H.C., Mielk, F., Fiorentino, D., Papenmeier, S., Holler, P., Bartholomä, A. 2016. Seafloor monitoring west of Helgoland (German Bight, North Sea) using the acoustic ground discrimination system RoxAnn. *Geo Mar. Lett.* Doi: 10.1007/s00367-016-0483-1
- Huff, L.C. 2008. Acoustic remote sensing as a tool for habitat mapping in Alaska waters. In: Reynolds, J.R., Greene, H.G. (Eds) *Marine Habitat Mapping Technology for Alaska*. Alaska Sea Grant College Program, University of Alaska Fairbanks. doi:10.4027/mhmta.2008.03
- Josefson, A.B. 1998. Resource limitation in marine soft sediments- differential effects of food and space in the association between the brittle-star *Amphiura filiformis* and the bivalve *Mysella bidentata*. *Hydrobiologia*, 375/376, 297-305.
- Kenny, A.J., Cato, I., Desprez, M., Fader, G., Schüttenhelm, R.T.E., Side, J. 2003. An overview of seabed-mapping technologies in the context of marine habitat classification. *ICES Journal of Marine Science*, 60, 411-418.
- Kröncke, I., Stoeck, T., Wieking, G., Palojarvi, A. 2004. Relationship between structural and functional aspects of microbial and macrofaunal communities in different areas of the North Sea. *Mar Ecol Prog Ser*, 282, 13-21.
- Kröncke, I., Reiss, H., Eggleton, J.D., Aldridge, J., Bergman, M.J.N., Cochrane, S., Craeymeersch, J., Degraer, S., Desroy, N., Dewaromez, J.-M., Duineveld, G., Essink, K., Hillewaert, H., Lavaleye, M.S.S., Moll, A., Nehring, S., Newell, J., Oug, E., Pohlmann, T., Rachor, E., Robertson, M., Rumohr, H., Schratzberger, M., Smith, R., Vanden Berghe, E., van Dalen, J., van Hoey, G., Vincx, M., Willems, W., Rees, H.L. 2011. Changes in North Sea macrofauna communities and species distribution between 1986 and 2000. *Estuarine, Coastal and Shelf Science*, 94, 1-15.

-
- Krumbein, W.C., Aberdeen, E. 1937. The sediments of Barataria Bay. *Journal of Sedimentary Petrology*, 7, 3-17.
- Kühne, S., Rachor, E. 1996. The macrofauna of a stony sand area in the German Bight (North Sea). *Helgol Meeresunters*, 50, 433-452.
- Künitzer, A. 1989. Factors affecting the population dynamics of *Amphiura filiformis* (Echinodermata: Ophiuroidea) and *Mysella bidentata* (Bivalvia: Galeommatacea) in the North Sea. Reproduction, genetics and distributions of marine organisms Proc 23rd Europ Mar Biol Symp (J S Ryland, P A Tyler, eds) Olsen & Olsen, Fredensborg, Denmark, 395-406.
- Künitzer, A., Basford, D., Craeymeersch, J.A., Dewarumez, J.M., Dörjes, J., Duinveld, G.C.A., Eleftheriou, A., Heip, C., Herman, P., Kingston, P., Niermann, U., Rachor, E., Ruhmor, H., de Wilde, P.A.J. 1992. The benthic infauna of the North Sea: species distribution and assemblages. *ICES J Mar Sci*, 49, 127-143.
- Loo, L.-O., Jonsson, P.R., Sköld, M., Karlsson, Ö. 1996. Passive suspension feeding in *Amphiura filiformis* (Echinodermata: Ophiuroidea): feeding behaviour in flume flow and potential feeding rate of field populations. *Mar Ecol Prog Ser*, 139, 143-155.
- Lucieer, V. 2008. Object-oriented classification of sidescan sonar data for mapping benthic marine habitats. *Int J Mar Sensing*, 29, 905-921.
- Lurton, X. 2002. An introduction to underwater acoustics: principles and applications. Springer, London.
- Lurton, X., Lamarche, G. (Eds) 2015. Backscatter measurements by seafloor-mapping sonars. Guidelines and recommendations. <http://geohab.org/wp-content/uploads/2014/05/BSWG-REPORT-MAY2015.pdf>
- Markert, E., Holler, P., Kröncke, I., Bartholomä, A. 2013. Benthic habitat mapping of sorted bedforms using hydroacoustic and ground-truthing methods in a coastal area of the German Bight/ North Sea. *Estuarine, Coastal and Shelf Science*, 129, 94-104.
- Mazel, C. 1985. Side Scan Sonar Record Interpretation. Klein Associates Inc. Report 11230001 Rev 01.
- Micallef, A., Le Bas, T.P., Huvenne, V.A.I., Blondel, P., Hühnerbach, V. 2012. A multi-method approach for benthic habitat mapping of shallow coastal areas with high-resolution multibeam data. *Cont Shelf Res* 39/40, 14-26, doi:10.1016/j.csr.2012.03.008
- Mielck, F., Bartsch, I., Hass, H.C., Wöfl, A.-C., Bürk, D., Betzler, C. 2014. Predicting spatial kelp abundance in shallow coastal waters using the acoustic ground discrimination system RoxAnn. *Estuarine, Coastal and Shelf Science*, 143, 1-11.
- Ockelmann, K.W., Muus, K. 1978. The biology, ecology and behaviour of the bivalve *Mysella bidentata* (MONTAGU). *Ophelia*, 17, 1-93.
- Pielou, E. 1969. An introduction to mathematical ecology. Wiley, New York.
- Preston, J.M., Christney, A.C., Beran, L.S., Collins, W.T. 2004. Statistical seabed segmentation - From images and echoes to objective clustering. In: Proc 7th European Conf Underwater Acoustics, Delft, The Netherlands, 813-813.
- Preston, J.M., Parrott, D.R., Collins, W.T. 2003. Sediment Classification Based on Repetitive Multibeam Bathymetry Surveys of an Offshore Disposal Site. Proc. IEEE Oceans '03 Conf., 69-75.
- Preston, J.M. 2006. Acoustic classification of seaweed and sediment with depth-compensated vertical echoes. Proceedings of MTS/IEEE Oceans 2006, Boston, USA, 1-5.

- Quester Tangent Corporation 2003. Mapping intertidal oysters with QTC View, North Inlet-Winyah Bay, South Carolina. QTC Technical Report SR41-03.
- Quester Tangent Corporation 2011. QTC Swathview 11.1. User Manual and Reference: DMN-SWVW-0000-R02.
- Rachor, E., Nehmer, P. 2003. Erfassung und Bewertung ökologisch wertvoller Lebensräume in der Nordsee. Abschlussbericht fuer das F+E –Vorhaben FKZ 89985310 (Bundesamt fuer Naturschutz).
- Reiss, H., Meybohm, K., Kröncke, I. 2006. Cold winter effects on benthic macrofauna communities in near-and offshore regions of the North Sea. *Helgol Mar Res*, 60, 224-238.
- Rice, J., Arvanitidis, C., Borja, A., Frid, C., Hiddink, J.G., Krause, J., Lorange, P., Ragnarsson, S.A., Sköld, M., Trabucco, B., Enserink, L., Norkko, A. 2012. Indicators for Sea-floor Integrity under the European Marine Strategy Framework Directive. *Ecological Indicators*, 12, 174-184.
- Riegl, B.M., Halfar, J., Purkis, S.J., Godinez-Orta, L. 2007. Sedimentary facies of the eastern Pacific's northernmost reef-like setting (Cabo Pulmo, Mexico). *Marine Geology*, 236, 61-77.
- Rosenberg, R., Nilsson, H.C., Hollertz, K., Hellman, B. 1997. Density-dependent migration in an *Amphiura filiformis* (Amphiuridae, Echinodermata) infaunal population. *Mar Ecol Prog Ser*, 159, 121-131.
- Rowden, A.A., Jago, C.F., Jones, S.E. 1998. Influence of benthic macrofauna on the geotechnical and geophysical properties of surficial sediments, North Sea. *Continental Shelf Research*, 18, 1347-1362.
- Salzwedel, H., Rachor, E., Gerdes, D. 1985. Benthic macrofauna communities in the German Bight. *Veröff. Inst. Meeresforsch. Bremerh.*, 20, 199-267.
- Schimmel, A.C.G., Healy, T.R., McComb, P., Immenga, D. 2010. Comparison of a Self-Processed EM3000 Multibeam Echosounder Dataset with a QTC View Habitat Mapping and a Sidescan Sonar Imagery, Tamaki Strait, New Zealand. *Journal of Coastal Research*, 26 (4), 714-725.
- Schimmel, A.C.G., Healy, T.R., Johnson, D., Immenga, D. 2010. Quantitative experimental comparison of single-beam, sidescan, and multibeam benthic habitat maps. *ICES Journal of Marine Science*, 67, 1766-1779.
- Schlagintweit, G.E.O. 1993. Real-time acoustic bottom classification for hydrography: A field evaluation of RoxAnn. Canadian Hydrographic Services, Department of Fisheries and Oceans, Canada.
- Shannon, C.E., Weaver, W. 1949. The mathematical theory of communication. University of Illinois Press, Urbana.
- Sköld, M., Loo, L.-O., Rosenberg, R. 1994. Production, dynamics and demography of an *Amphiura filiformis* population. *Mar Ecol Prog Ser*, 103, 81-90.
- Southward, E.C., Campbell, A.C. 2006. Echinoderms: Keys and Notes for the Identification of British Species. Synopses of the British fauna (New Series), 56. Field Studies Council, Shrewsbury.
- Spaeth, C. 1990. Zur Geologie der Insel Helgoland. *Die Küste*, 49, 1-32.
- Spearman, C.E. 1904. The proof and measurement of association between two things. *Am J Psychol*, 15, 72-101

-
- Stein, R. 1985. Rapid grain-size analyses of clay and silt fractions by SediGraph 5000d: comparison with Coulter Counter and Atterberg methods. *J Sed Petrol*, 55 (4), 590-593.
- Tucker, M. 1988. *Techniques in sedimentology*. Blackwell, Oxford.
- Van Hoey, G., Degraer, S., Vincx, M. 2004. Macrobenthic community structure of soft-bottom sediments at the Belgian Continental Shelf. *Estuarine, Coastal and Shelf Science*, 59, 599-613.
- Van Overmeeren, R., Craeymeersch, J., van Dalssen, J., Fey, F., van Heteren, S.M., van Meesters, E. 2009. Acoustic habitat and shellfish mapping and monitoring in shallow coastal water – Sidescan sonar experiences in the Netherlands. *Estuar Coastal Shelf Sci*, 85(3), 437-448.
- Verfaillie, E., Doornebal, P., Mitchell, A.J., White, J., Van Lancker, V. 2007. The bathymetric position index (BPI) as a support tool for habitat mapping. Worked example for the MESH Final Guidance. www.searchmesh.net
- Wentworth, C.K. 1922. A scale of grade and class terms for clastic sediments. *Journal of Geology*, 30, 377-392.
- Wienberg, C., Bartholomä, A. 2005. Acoustic seabed classification of a coastal environment (outer Weser Estuary – German Bight) - a new approach to monitor dredging and dredge spoil disposal. *Cont Shelf Res*, 25, 1143-1156.
- Winter, C., Herrling, G., Bartholomä, A., Capperucci, R., Callies, U., Heipke, C., Schmidt, A., Hillebrand, H., Reimers, C., Bremer, P., Weiler, R. 2014. Scientific concepts for monitoring the ecological state of German coastal seas (in German). *Wasser und Abfall* 07-08/2014, 21-26, doi:10.1365/s35152-014-0685-7
- Woodley, J.D. 1975. The behaviour of some amphiuroid Brittle-Stars. *Journal of Experimental Marine Biology and Ecology*, 18, 29-46.
- Wright, D.J., Lundblad, E.R., Larkin, E.M., Rinehart, R.W., Murphy, J., Cary-Cothra, L., Draganov, K. 2005. *ArcGIS Benthic Terrain Modeler*. Oregon State University, Corvallis, Davy Jones Locker Seafloor Mapping/Marine GIS Laboratory and NOAA Coastal Services Center. <http://www.csc.noaa.gov/digitalcoast/tools/btm>

Chapter 5

Sidescan sonar meets airborne and satellite remote sensing: challenges of a multi-device seafloor classification in extreme shallow water intertidal environments.

Ruggero Maria Capperucci¹, Adam Kubicki^{1,2}, Peter Holler¹,
Alexander Bartholomä¹

¹ Senckenberg Institute, Südstrand 40, D-26382 Wilhelmshaven, Germany

² Geo Ingenieurservice Nord-West GmbH & Co. KG, Kutterstr. 3, 26386 Wilhelmshaven

Key words sidescan sonar, tidal flats, seafloor classification, Lidar, sediments, shellfish beds

5.1. Abstract

Tidal ecosystems like the Wadden Sea are particularly valuable for their ecological and economic importance. Here, the natural dynamics of the abiotic and biotic processes is threatened by the human pressure, and great efforts are made on mapping and monitoring programs. Remote sensing techniques (e.g. satellite and airborne sources) are commonly used on land and intertidal areas, whereas hydroacoustic devices are deployed in the subtidal zones. The overlap of hydroacoustics (sidescan sonar) and airborne Lidar data in such sensitive transitional zone (inter- to subtidal) is rather uncommon. In order to test the limitations of both techniques in extremely shallow waters (0.7 m min. water depth) and to find the most efficient methods for the spatial classification of intertidal areas, a portion of the backbarrier tidal flat of Norderney was investigated. Lidar bathymetric data were used for extracting high resolution

Capperucci, R.M., Kubicki, A., Holler, P., Bartholomä, A., 2020. Sidescan sonar meets airborne and satellite remote sensing: challenges of a multi-device seafloor classification in extreme shallow water intertidal environments. Geo-Marine Letters, <https://doi.org/10.1007/s00367-020-00639-7>

morphological information. Sidescan sonar mosaics were collected in two following years under contrasting weather conditions. An expert classification based on sidescan sonar backscatter intensity, seafloor texture, morphology, and surface sediment data subdivided the research area into 10 classes. The outcomes were compared with an existing RapidEye-based classification. The tested methods showed both advantages and limitations, which were discussed based on statistical analyses. Satellite and Lidar approaches were most suitable for mapping biogenic features (e.g. shellfish beds) over large areas, whereas sidescan sonar was superior for detail detection and discrimination of morpho-sedimentary regions. As an outlook, it is postulated to perform ground-truthed hydroacoustic mapping on small testing areas, and to use the obtained classification for training satellite-based classification algorithms.

5.2. Introduction

Coastal environments represent the interface between land and sea (Carter 1988), each of these characterized by specific morpho-dynamic processes (Hinrichsen 1998). The coast is the place where some of these processes interact, increasing the complexity of such ecosystem and the parameters to be taken into account in order to describe it. Despite being accounted among the most diverse natural habitats on earth (Gopal et al. 2000), coastal ecosystems are undermined by multiple factors, mostly related to the human presence (e.g. Mc Lachlan and Brown 2006), due to their strategic economic value. The increased general awareness about concepts like habitat loss, biodiversity, and human impact, led in the last 30 years to political actions in order to guarantee the protection of the most endangered ecosystems, specifically with national and international mapping and monitoring programs (e.g. ICES 2014). Any activity aiming to preserve a habitat has to face one fundamental task: the definition of specific sets of measurable parameters, which are able to simplify the natural complexity and, still, to realistically and reliably describe the habitat. Once the status quo of a habitat has been proved, a monitoring program can account for modifications in the sets of parameters.

Many tools are available to approach such tasks. Among them, the correct application of remote sensing techniques in long-term programs of habitat mapping and monitoring, particularly for vulnerable ecosystems, assumed a central role in supporting land-use decision making.

Tidal driven coasts clearly express such a dynamic equilibrium of a transition zone between land and sea, being characterized by long-term stable

geomorphologies and short-term transport processes. The world nature heritage “Wadden Sea”, in the southern North Sea, is one of such dynamic and diverse ecosystems, with a high economic and ecological value (Park et al. 2010; van der Wal & Herman 2007). Tides, waves, human activities (such as fisheries, land reclamation works, tourism, etc.), and extreme weather events shape the tidal flat environment constantly. Therefore, a selection of time- and cost-efficient methods for large-scale coastal mapping and monitoring is required (van Beijma et al. 2014).

Because of their ecological relevance, specific programs have been undertaken for detecting changes in the biotic and abiotic characteristics of the tidal flats in the Wadden Sea (e.g. shifts in sediment composition and/or in the biocommunities), and in order to point out potential loss of the natural or semi-natural habitats. Such a diversity of issues requires a variety of in-situ measurements, which are in turn strongly affected by the limited accessibility of tidal flats (Park et al. 2010). In this context, the implementation of remote sensing techniques represents a great advantage.

Since decades, multispectral remote sensing by means of satellite and airborne imaging systems represents a cost-efficient method for spatial mapping and monitoring on land. However, its use in mapping intertidal habitats presents still strong limitations. Satellite data (TerraSAR, SAR) have been used in the Wadden Sea – alone or in combination with other remote sensing sources – for detecting morphological changes (e.g. bedform shift, Adolph et al. 2017a, 2017b; tidal channel movements, Adolph et al. 2018) and for the definition and contouring of shellfish beds (Adolph et al. 2018). Most of the studies focussed on the discrimination of the three main components of a backbarrier tidal system: the water surface, the shellfish beds, and the tidal flat deposits, without any closer look into the sediment composition and distribution. Müller et al. (2016) investigated the presence of seagrass by means of optical and radar sources, while Gade et al. (2008) used the presence of ripples on SAR data as a surrogate for mapping sandy sediments. Jung et al. (2015) tried to differentiate the tidal deposits, using a combination of SAR and RapidEye (RE) multispectral data. Excluding the water surface and the unclassified area, he successfully distinguished four sediment classes: mud, mixed sediments, wet sand, and dry sand.

The most modern Lidar technique (Light detection and ranging) has also been implemented to intertidal monitoring (Shan and Toth 2018). Lidar devices are airborne remote sensing tools, which provide high-precision bathymetry and backscatter intensity data of extensive areas in a short time and at a reasonable

cost. The Lidar technology presents the advantage to be largely independent from the weather (e.g. cloud coverage) and sea conditions (as the flight takes place during low tide), although its main limitation is given by the water level, which in case of adverse weather can high-stand on the tidal flat even during low tides. The application of dual frequency systems (red and green laser) to increase the light penetration in the water column is strongly limited in the Wadden Sea area, where the high amount of fine sediments in suspension in the water column (up to 120 mg/l, e.g. Badewien et al. 2009, Bartholomä et al. 2009) limit the light penetration to < 0.5 m (Staneva et al. 2009). Nevertheless, Lidar data have been used for the automatic detection of water surfaces and for extracting the land-water boundaries in the Wadden Sea region (Schmidt et al 2013). The attempt to resolve more elements was limited to the identification of the intertidal areas, namely mudflats (Schmidt et al. 2012, Schmidt et al. 2019).

Among other remote sensing systems, hydroacoustic devices are standard underwater tools for seafloor classification and habitat mapping. In particular, sidescan sonars (SSS) are versatile systems, which can be deployed in different water ranges, as their lateral ability to investigate the seafloor (swath) is independent from the water depth.

They have been used successfully on various substrates (e.g. Collier and Brown 2005, Bartholomä 2006, Holler et al 2017, Heinrich et al. 2016). However, SSS have been poorly used in extreme shallow water tidal ecosystems, where other remote sensing sources offered a faster and broader coverage. Existing application of SSS to intertidal environments were usually limited to the lower intertidal-subtidal interface. Degraer et al. (2008) explored the ability of SSS to detect biogenic reefs along the Belgian coast, while Rahnemoonfar et al. (2018) focused on the automatic identification of seagrass. In the Wadden Sea region, van Overmeeren et al. (2009) used the SSS for mapping mussel banks in the tidal flat.

Effectiveness can be defined as the ability to accomplish a task, achieving the intended results (Cambridge University Press 2014). Efficiency is the most convenient way to do that. Systems can be effective, but not efficient, depending on the task. The same applies also to remote sensing techniques, with the effectiveness and efficiency strictly depending on the goal. The detection of a shellfish bed, for example, can be efficiently achieved by applying suitable automatic algorithms on very large datasets of remote sensing records (e.g. Schill et al. 2006; NOAA 2003 for an overview of automatic and expert based classification methods). However, if the goal is to find out the seasonal growing rate of such shellfish beds, that approach will probably not be effective, because

of the filtering-coarsening-interpolating steps connected to the automatic classification. On the other hand, the manual contouring of shellfish beds on SSS data could give an unpaired effectiveness, but with a scarce efficiency if the goal is the mapping of the entire Wadden Sea.

The combination of SSS and Lidar data is rather uncommon, although recommended by some authors (e.g. Schmidt et al. 2019), as the main limiting factor for the Lidar is the presence of water, which is the mean for collecting SSS data. On the other hand, SSS can be operated only during specific time windows (high tide) and using limited swath (a few hundred meters, maximum), and therefore only small areas can be surveyed within a single high tide. The transition intertidal-subtidal, hence, represents the zone where both the technologies show some limitations.

For the present research, a SSS was deployed in the intertidal flat of Norderney (German Wadden Sea) in extremely shallow water conditions (up to 0.7 m water depth) in order to check the feasibility of using acoustic data for seafloor characterization on tidal flats. The data were combined with bathy/topographic information from Lidar data, and compared with an existing sediment classification performed by means of RE data (Jung et al. 2015).

5.3. Physical settings

The Island of Norderney is part of the East Frisian barrier islands, in the German Bight (southern North Sea). The Wadden Sea barrier lagoon system spans for over 480 km from the Netherlands (West Frisian) through the German coast (East- and North Frisian) to Denmark (North Frisian), and includes the most extensive meso-tidal environment in the world. The East Frisian back barrier depositional system is slightly ebb-dominant, with maximum flow velocity of 1.2 to 1.5 m/s in the tidal inlets, and 0.4 to 0.5 m/s on the tidal flats (e.g. Joerdel et al. 2002, Stanev et al. 2007, Bartholomä et al. 2009, Staneva et al. 2009). The water mass movement also acts as the main source of nutrients for suspension feeders, which are an important source for fine-grain deposits (e.g. Bartholomä et al. 2000, Delafontaine et al. 2000).

The recent position and shape of Norderney is the result of the deposition of mobile sediments on a Pleistocene palaeo-relief (Saalian and Weichselian glacial/periglacial deposits) following the sea level rise over the last 6500 years (Streif 1990). The early deposits acted as a sediment trap, leading to the development of large eolian dunes, which are still the signature landscape of the islands (Oost et al. 2012).

The island of Norderney extends eastward for 14 km. The Riffgat channel (Figure 5.1) separates Norderney from the island of Juist on the western side, whereas the Ostbalje tidal inlet divides it from the island of Baltrum on the eastern side. Both inlets cut through the tidal flat, parallel to the coastline of the island, and merge in the Norderney Wattfahrwasser (watershed), which, depending on the tidal conditions, is a navigable waterway for small boats. The tidal inlet connects the catchment area with the open North Sea, and the tidal prism controls its size (Walter 1972). The mean tidal range in the Riffgat channel is of 2.4 m (Dörjes et al. 1986), with maximum amplitudes up to 3.2 m during spring tides. The channel is ebb-dominated, as the westward ebb current reaches slightly higher speeds than the eastward flood current. During both tidal phases the current velocity typically exceeds 1 m/s (Stanev et al. 2003).

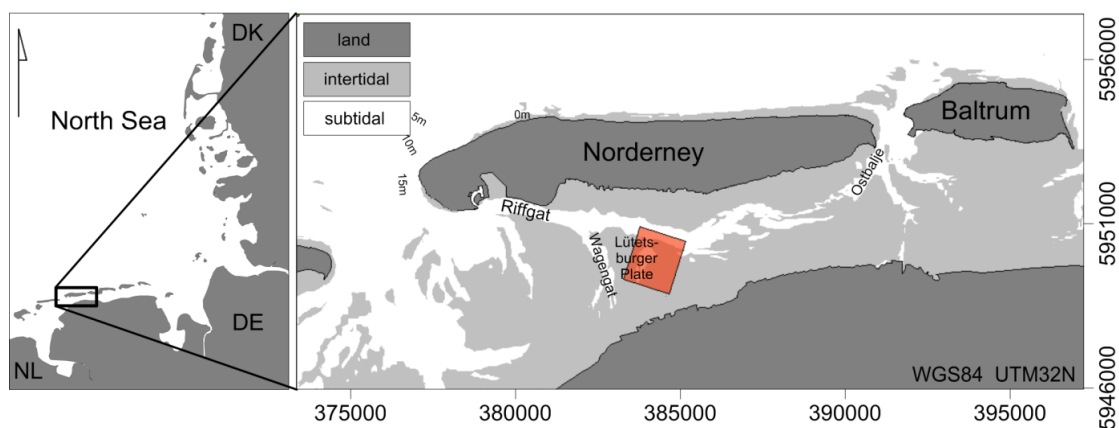


Figure 5.1. Location map of the study site (in orange) with the names of the main geographical and morphological units used in the text.

The Riffgat channel branches into several secondary channels; one of them (named Wagengat, Figure 5.1) borders from west a large sandbank called Lütetsburger Plate, which is the research area of the present study. This Lütetsburger Plate region is extremely shallow, with depths from -6.5 m (depth referred to Chart Datum = LAT, Lowest Astronomical Tide) close to the Riffgat channel to the +2.2 m in the shallowest regions.

Altogether, the backbarrier tidal area between the island of Norderney and the mainland covers over 72 km², with a typical sequence of subtidal to supratidal deposits: salt marshes, mud flat, mixed flat, sand flat, and subtidal gullies and channels (Reineck and Singh, 1980; Flemming 2012). The sediment composition covers the whole spectrum of mud, sand, and gravel mixture, with the fine fractions (clay, silt, and sand) particularly dominant. Changes in the sediment composition are gradual (e.g. Bartholomä and Flemming 2007) and therefore challenging for any kind of investigation aiming to segment, to classify, or to

delineate sediment patches. The subdivision among mud-, mixed-, and sand flats takes also into account the structures and geometries of the deposits (beddings, hummocky, etc., Flemming 2012). In general, the sediments show a parallel to the coastline oriented zonation, which fines up towards the dike line (e.g. Flemming and Ziegler 1995). Such spatial distribution is controlled by tidal currents and by local wind-induced waves.

The most evident biocommunities are represented by shellfish banks of pacific oysters, which replaced the blue mussel banks starting in the late 90s of last century. Meanwhile the blue mussels have been reestablished on top of the oyster reefs, which can be considered as a new “local” hardground for the Wadden Sea area (Markert et al. 2010, 2013).

5.4. Methods

Sidescan sonar (SSS) data and surface sediment samples were collected during two surveys in June 2013 and September 2014. Since most of the area falls dry during low water, high tide windows (3 hours before and after the predicted high tide) were used for the acoustic data collection; low tide windows (predicted low tide ± 3 hours) were used for sediment sampling and in-situ observations (in-field description, photos, etc.). Weather and tide conditions were logged.

5.4.1. *Sidescan sonar data collection and processing*

A Starfish 452F was pole mounted on the small work boat “Scanner” for SSS data acquisition. The tracks were designed parallels to the main morphologies (coastline and Riffgat channel), with 240 m swath and 100 m line-spacing (Table 5.1). In total, 17 and 13 lines were recorded in 2013 and 2014, respectively (the lower amount of 2014 lines was due to the adverse tidal/weather conditions). A RTK-GPS Trimble SPS 852 system (base rover configuration) was deployed for RTK positioning. The data were collected starting from the lines corresponding to the deepest areas (near the Riffgat) and following the rise of the tide, till the most internal regions to the south, where the mean water depth recorded underneath the SSS was about 0.7 m.

Data processing included geometric (offset, bottom pick, slant range), and radiometric (Time Variable Gain, Empirical Gain Normalization table, nadir filter) corrections and was performed with the SonarWiz 7 software. A 0.5 m pixel-resolution mosaic was exported for the two datasets (2013 and 2014, Figure 5.2 and Figure 5.4). Low and high backscatter values were displayed in a 256 greyscale palette (high backscatter = low greyscale values = darker greyscale

tones; low backscatter = high greyscale values = lighter greyscale tones). Due to the difference in data quality, only the 2013 mosaic was further used for the acoustic classification. The comparison between the 2013 and 2014 data was based on a reduced set of seafloor features, which could be recognized and mapped in both datasets. Additional mosaics (at 0.25 m and 0.125 m pixel-resolution) were generated for individual sub-regions, in order to check the ability of the system in resolving specific targets (i.e. shellfish patches, tidal gullies), and compare the results with the outcomes from different remote sensing systems.

Starfish 452f SSS		
Frequency	450 kHz	
Beam angle along track	0.8°	
Beam angle across track	60°	
Max. horizontal resolution (nominal)	2.5 cm	
Pulse length	400 ms	
Ping rate	14 Hz	
Survey data	June 2013	September 2014
Number of lines	17	13
Swath (m)	120	120
Total coverage (sqm)	2200000	1877000
Av. wind speed (km/h)	10.5	28.0
Av. wind direction	NNE	NNW
Max. wind gusts (km/h)	34.9	55.2
Max. wave height (m)	0.7	1.2
Av. wave direction	N	NNW

Table 5.1. Technical specifications of the Starfish 452f and overview about SSS data collection and weather/sea conditions recorded during the two surveys in 2013 and 2014.

5.4.2. Sediment samples data collection and processing

Surface sediment sampling and in-field observations took place along 5 transects (transect 1, T1: from station T11 to T17; transect 2, T2: from station T21 to T25, etc.), NS oriented, for a total amount of 32 stations (12 in 2013, 20 in 2014, Figure 5.2). For each station, a volume of sediments between 300 and 500 ml was scooped from the surficial layer (~ 1-2 cm), labeled, described, and stored for grain size analysis. The seabottom along the Riffgat channel was not sampled during the 2013 and 2014 campaigns. However, sediment data for the western part of the Riffgat channel were available from a previous survey (September 2011).

In-situ observations and sample description included a short report about the sampling location (i.e. water coverage, presence and characteristics of bedforms and biota) and a macroscopic description of the sediments (color, grain size, sorting, stratification, presence of shells and organisms). Where possible,

photos of the sample site were taken. The positioning of the sampling locations was recorded by means of a GPS Garmin GPA72 system.

Sediment samples were processed in the Lab for grain size analysis. The preparation of the samples included: osmotic desalinization of the samples, wet sieving through a $63\ \mu$ mesh size for separating the mud fraction, dry sieving through a 2 mm mesh size for splitting the sand and gravel fractions. The sand fraction was analyzed using a MacroGranometer™ settling tube (Brezina 1979) and divided into five 1ϕ intervals following the nomenclature of Wentworth (1922, based on Udden 1914; the Udden-Wentworth scale), from very coarse sand ($-1 \leq \phi < 1$) to very fine sand ($3 \leq \phi < 4$). The $\frac{1}{4}\ \phi$ sediment distribution was then used for classifying the sediments into textural classes (Folk, 1954), using the Gradistat Excel working sheet (Blott and Pye 2001).

The in-situ macroscopic description of the sediments and of the sampling locations, together with the grain-size results were used for improving the definition and refining the description of the acoustic-based classes.

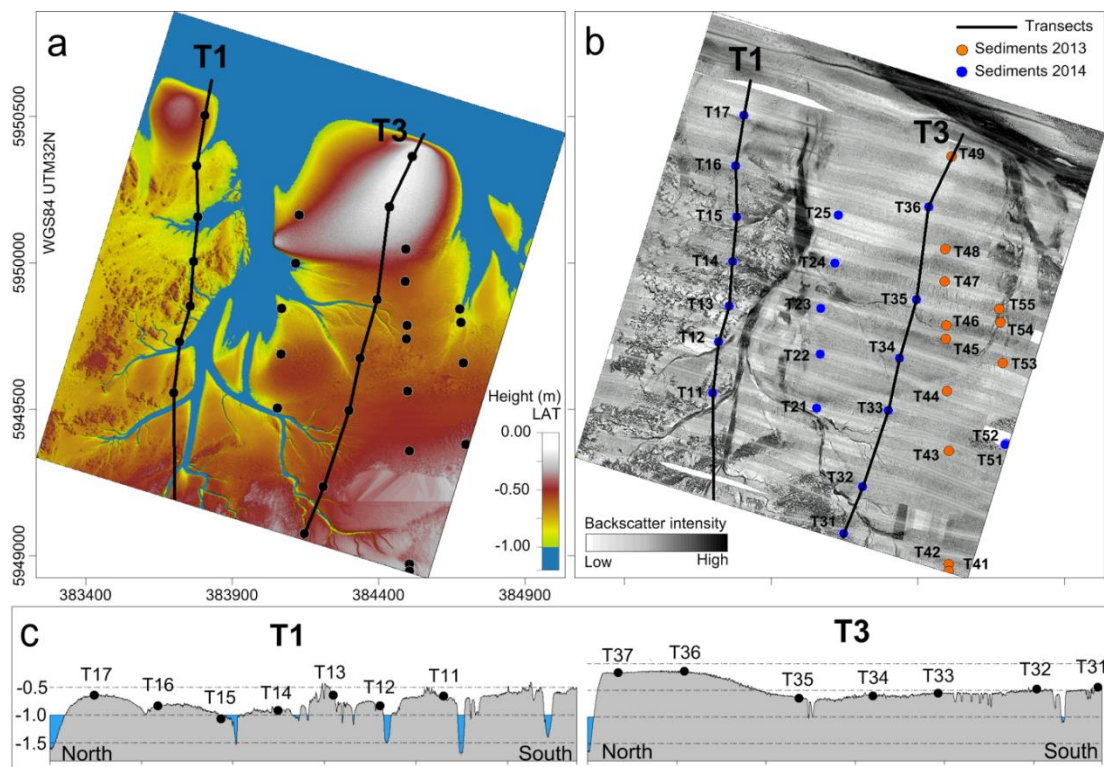


Figure 5.2. Digital Terrain Model - DTM (a) and SSS mosaic (b) of the study area. The DTM was based on Lidar data collected in 2013; the blue color corresponds to the areas covered by water during the Lidar flight. 32 sediment samples (black dots, in a) were collected along 5 north-south transects (T1 to T5, from west to east) in 2013 (orange dots, in b) and 2014 (blue dots, in b). Two transects (T1 and T3) are highlighted (black lines) and presented in details within the text.

5.4.3. Lidar data

Lidar (Light detection and ranging) data were collected in 2013 by the MILAN Geo Service Company, on behalf of the Lower Saxony Water Management, Coastal Defence and Nature Conservation Agency (Niedersächsischer Landesbetrieb für Wasserwirtschaft, Küsten und Naturschutz, NLWKN) over two regions of the Norderney tidal flat, one of them matching the study area of this research. 8 routes with 320 m spacing were designed east-west oriented. 2 extra lines for calibration were collected orthogonally to the main grid. The system (a RIEGL VQ 820-G red LiDAR) was deployed from an altitude of 600 m and achieved a horizontal/vertical accuracy of 0.40/0.15 m, respectively. The NLWKN kindly provided the dataset in 1 m grid size. The points were gridded in Global Mapper v15 and a DTM in 1 m grid size) was used for extracting the bathymetric information for defining the main morphological features. The areas corresponding to the water surface were blanked and therefore not further considered for the analysis. Within the framework of the WIMO project (Winter 2017) a second Lidar dataset was collected by the MILAN Geo Service in October 2014 (using the same Lidar system and setups), covering an area of approximately 30 km² between the mainland and the island of Norderney. The acquisition included both bathymetric and intensity (backscatter) data. However, these datasets were only partially included in the present study, specifically for a small sector, which was used for the comparison of the shellfish beds detection between the SSS and the Lidar system (Figure 5.6). All the depths reported in the present study are referred to Chart Datum (Lowest Astronomical Tide, BSH 2019).

5.4.4. Seafloor classification

An attempt to use a semi-automatic classification approach (“SonarWiz7 Seabed Characterization” tool, Chesapeake Technology, 2017) was made on the 2013 SSS records, varying both the geometric settings (e.g. window size, window step) and the classification options (number of classes, Grey Level Co-occurrence Matrix algorithms). The final outcome, however, resulted in a “salt-and-pepper” pixelized image, with any clear correlation between the acoustic classes and the physical characteristics of the seafloor (sediments and morphologies). Therefore, a combined expert-based classification approach was preferred. The 0.5 m SSS mosaic from the survey in 2013 was segmented into different regions (acoustic classes, manually contoured). Where present, the sharp changes in SSS backscatter intensity were used for the segmentation of the mosaic. However, most of the area presented gradual transitions in the backscatter greyscale values.

In these cases, the SSS mosaic was firstly used for a coarse definition of the main backscatter region. The exact contouring process, instead, made use of a combination of different grey level values (backscatter intensity), seafloor texture (e.g., bedforms, seafloor marks, shellfish beds, etc.), morphologies (from the Lidar bathymetric data), and sediment grain size characteristics.

5.4.5. *Comparison with RapidEye-TerraSAR-X seafloor classification*

Jung et al. (2015) performed a seafloor classification of the Norderney tidal flats, based on RapidEye (RE) and TerraSAR-X (TSX, multispectral satellite and synthetic aperture radar) data. The TSX data were used for outlining the water surface extension and the shellfish beds, which were then excluded from the sediment classification based on RE data (for details, Jung et al. 2015). Four RE images collected between 2010 and 2011 were classified, and the tidal flat area was segmented into sediment classes. One of the maps (June 2011) was used in this study for comparing the SSS vs. RE system ability of resolving the composition and the spatial distribution of the tidal flat sediments. In their research Jung et al. (2015) were able to distinguish the shellfish beds and four sediment classes (mud, mixed sediments, wet sand, and dry sand). In order to be able to compare the SSS-sediment classes with the ones defined by Jung et al. (2015), the amount of classes based on SSS-sediments were reduced accordingly. All the areas classified by Jung et al. (2015) as “water” were blanked in the SSS-sediment classification and not taken into account for the final comparison.

5.4.6. *Geographic Information System (GIS)*

All the data were loaded on GIS software (QGIS 2.7 and Global Mapper 15) for data visualization, analysis, bordering, and for the computation of the spatial statistics.

5.5. Results

5.5.1. *Morphology (Lidar data)*

Based on the areas marked as “water” in the Lidar data, the subtidal system covered about 25% of the entire study site (Figure 5.2).

The Wagengat channel (Figure 5.1) divided the area in two domains:

- A western region (transect T1 in Figure 5.2), cut by four main- and several secondary gullies. The extensive presence of shellfish beds (identified by their patchy-like topographic roughness on the Lidar data) was the

distinctive feature of this region. The northwest sandbank bordering the Riffgat channel (northern end of transect T1, Figure 5.2) was the only area not covered by shellfish beds.

- An eastern region characterised by a smoother and less articulated morphology. The topography gently sloped northward (0.03%, transect T3 Figure 5.2c) till the creek near to the station T35 (Figure 5.2b; elevation difference: -0.25 cm). In the central part, a depression marked the watershed between two drainage sub-systems (which streamed to the Wagengat and to the eastern secondary channel) and showed a rougher texture (irregular bedforms) than the surrounding areas. A slightly steeper slope (0.09%) reached the max height of -0.14 m, where a sand flat (average slope: 0.02%) bordered the Riffgat channel edge. This highest sector (average height: -0.23 m) presented a sub-elliptical shape and a steeply slope into the Riffgat channel (average slope angle of 3.95%). The only shellfish bed present in the eastern region was located on its southeastern margin.

5.5.2. *Sediment grain size distribution*

Fine to very fine sediments characterized the research area (Figure 5.3, Table 5.2), ranging from sandy mud (mud content up to 80 weight% = w%) to well sorted fine sand (fine sand > 94 w%), with a content of coarser fractions generally negligible (only one sample with medium sand > 1 w%). Sediments coarser than medium sand were not found. For the computation of the pie charts showed in Figure 5.3 and Figure 5.4, only three grain size fractions were used (mud, very fine sand, fine sand), as the coarser fraction was largely absent or sub-represented (sediments \geq medium sand = 0.1-1.4 w%).

The western region (transect T1) showed the highest amount of mud (average mud content >55 w%) in correspondence to the presence of the large shellfish beds. A succession of muddy sand and sandy mud characterized the eastern region (transects T2 to T5), where a higher amount of fine fraction (muddy sediments) corresponded to the morphologically depressed areas (Figure 5.3 and Figure 5.4). Although a proper direct sampling was not possible inside the gullies (as they were mostly covered by water even during low tide), in-field observations allowed to characterize those sediments as a mixture of sand and shell debris, typically covered by a layer of soft muddy sediments. A sampling campaign carried out in the Riffgat channel in 2011 showed a sediment composition from sand (fine to very coarse) to gravel, with an average content of 6 w% of gravel and 14 w% of shell debris.

N_UTM	E_UTM	Name	Gravel		Sand			Mud		Folk (1954)
			G	VcS	CS	MS	FS	VfS	M	
			$\phi < -1$	$-1 \leq \phi < 0$	$0 \leq \phi < 1$	$1 \leq \phi < 2$	$2 \leq \phi < 3$	$3 \leq \phi < 4$	$4 \leq \phi$	
			%	%	%	%	%	%	%	
5949558	383700.4	T11	0	0	0	0	2.6	30.5	66.8	sM
5949731	383721	T12	0	0	0	0	3.1	30.7	66.2	sM
5949852	383756.4	T13	0	0	0	0	1.2	17.2	81.6	sM
5950004	383767.8	T14	0	0	0	0	8.3	25.3	66.4	sM
5950157	383782.6	T15	0	0	0	0	9.7	28.1	62.2	sM
5950331	383779.1	T16	0	0	0	1.1	16.6	39.2	43.2	mS
5950503	383807.8	T17	0	0	0	1.1	94	4.5	0.3	S
5949506	384054.5	T21	0	0	0	0	38.1	36.8	25.1	mS
5949688	384067.7	T22	0	0	0	0.1	68.6	25.7	5.6	S
5949845	384068.8	T23	0	0	0	0	74.5	21.8	3.8	S
5949999	384116.5	T24	0	0	0	0	39	40.3	20.7	mS
5950163	384128.6	T25	0	0	0	0.1	77.2	20.9	1.8	S
5949077	384147.7	T31	0	0	0	0.1	8.9	22.6	68.4	sM
5949237	384211.7	T32	0	0	0	0.3	47.9	14.8	36.9	mS
5949496	384299	T33	0	0	0	0.1	34.5	29.8	35.6	mS
5949676	384337.4	T34	0	0	0	0	66.8	26.7	6.5	S
5949875	384393.8	T35	0	0	0	0	13.7	38.9	47.4	mS
5950192	384436.2	T36	0	0	0	0.1	81.3	18.1	0.6	S
5948948	384505.1	T41	0	0	0	0.2	58.9	21.5	19.5	mS
5948972	384505.7	T42	0	0	0	0.6	51.3	41.2	6.9	S
5949358	384504.2	T43	0	0	0.1	0.8	34.9	23.1	41.1	mS
5949562	384499.3	T44	0	0	0	0.1	30.7	33.9	35.3	mS
5949740	384493.8	T45	0	0	0.5	0.9	84.1	12.3	2.2	S
5949787	384497.1	T46	0	0	0	0	27.7	32.5	39.8	mS
5949937	384489.8	T47	0	0	0.1	0.2	15.6	41.2	42.9	mS
5950047	384492.5	T48	0	0	0	0	87	12	1.1	S
5950363	384515.7	T49	0	0	0	0.1	92.2	7.2	0.5	S
5949385	384699.6	T51	0	0	0	1	37.3	28	33.7	mS
5949382	384696.2	T51	0	0	0	0	25.1	20.5	54.4	sM
5949660	384687.8	T53	0	0	0	0	32.6	28.3	39.1	mS
5949797	384681.3	T54	0	0	0	0.6	87.5	10.7	1.2	S
5949844	384675.8	T55	0	0	0	0.1	16.1	33.4	50.4	sM

Table 5.2. Sediment grain size distribution (in ϕ intervals, Wentworth scale) and relative sediment classes (after Folk, 1954).

5.5.3. Sidescan sonar 2013

Compared to its larger spatial extent (~78% of the entire study site) the area presented gradual backscatter changes across a very limited amount of greyscale values (177-210: min-max of mean greyscale values, cf. greyscale histogram in Table 5.3), which could be further segmented in subclasses only at very large scale and by implementing Lidar and sediment information (see next paragraph). Sharp backscatter changes (boundaries) in the SSS mosaic, instead, were produced by a very few specific seafloor features (shellfish beds and tidal drainage system i.e. channels and gullies), easy to be identified and delineated (Figure 5.3a). Based on the backscatter data, the study site was therefore subdivided into three *main morphological elements*:

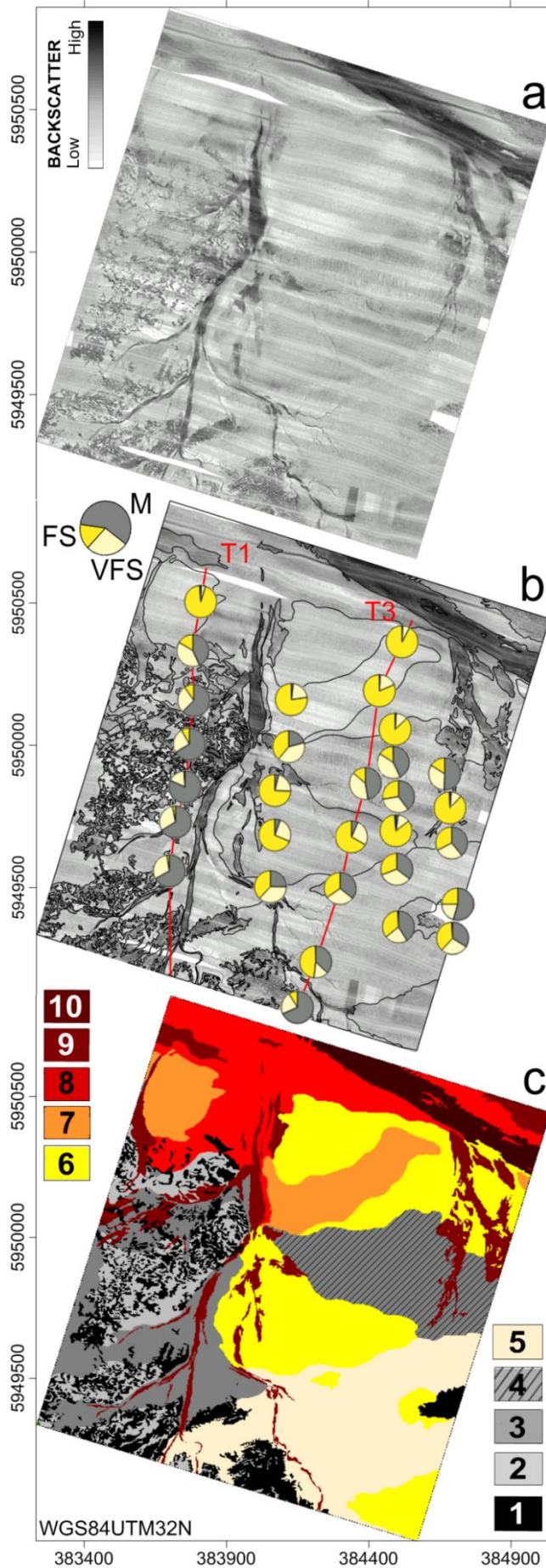


Figure 5.3. Mosaic of the SSS backscatter data of 2013 (a), overlaid by the sediment composition pie charts (b). Seafloor classification of the Lütetsburgerplate, based on SSS, Lidar, and sediment data (c). The pie charts were built using the three main sediment fractions (M: mud, VFS: very fine sand, FS: fine sand). Transects T1 and T3 are highlighted in red. The area was segmented into 10 classes, corresponding to different backscatter regions, seafloor textures, morphologies (bedforms, channels, etc.), and sediment characteristics. For the description of the classes, see the text.

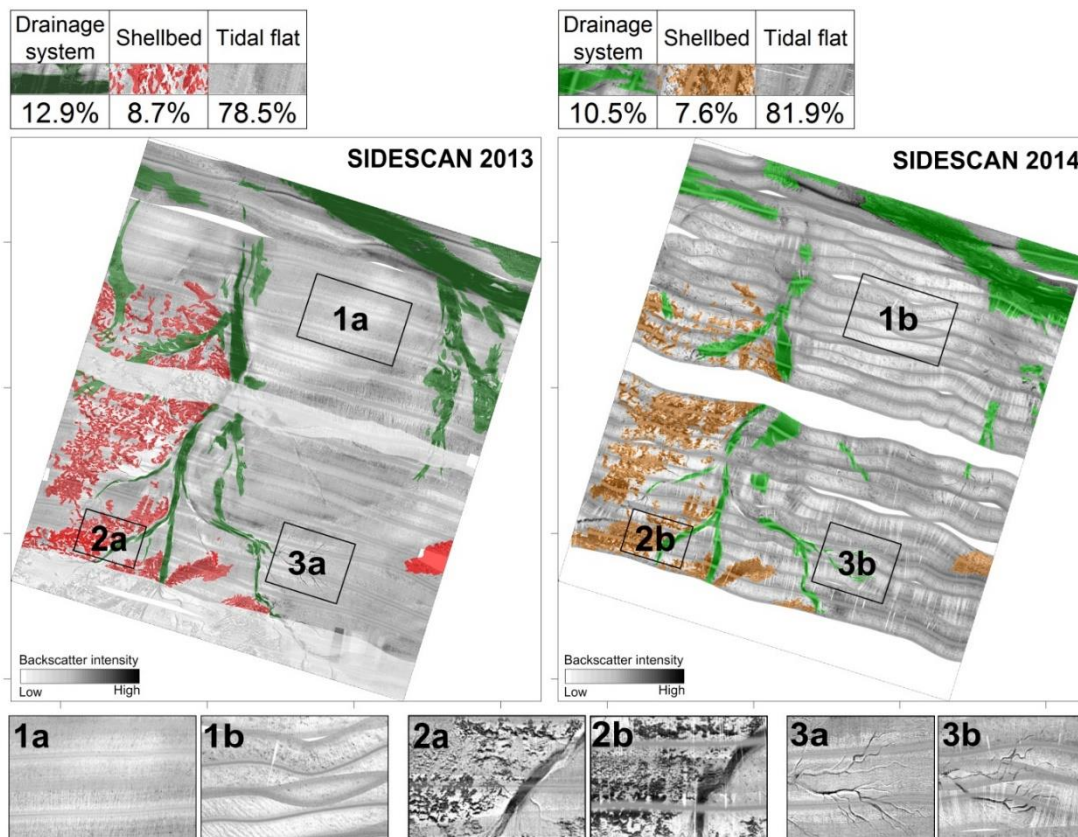


Figure 5.4. Sidescan sonar mosaics of 2013 (left) and 2014 (right) in 1 m resolution. Red (2013) and Orange (2014) lines correspond to the shellfish beds extension; green colors (dark green: 2013, bright green: 2014) correspond to the tidal drainage system (Riffgat channel and secondary channels). The regions corresponding to these classes were used for comparison. The adverse weather conditions (see Table 5.1) during the 2014 data collection severely influenced the data quality of the related SSS records, and the acoustic signal is disturbed by acoustic noise and artifacts. While the sharp changes in backscatter intensity are still visible (shellfish beds and drainage system), the gradual transitions among the intertidal flat deposits are overridden by the noise, making impossible a further subdivision of such region into classes. The small boxed areas zoom into the three main tidal system components: intertidal deposits (1a and 1b); shellfish beds (2a and 2b); drainage system (3a and 3b).

- *shellfish beds* (Figure 5.4: red polylines in SSS 2013), dominant in the western region and only present in one bank in the eastern region. It corresponds to class 1 of the seafloor classification (see next paragraph). The greyscale histogram showed a bimodal distribution and a mean greyscale value lower than the average tidal flat deposit histograms (Table 5.3);
- *tidal drainage system*, (Figure 5.4: dark green polylines in SSS 2013) corresponding to the Riffgat channel, the Wagengat secondary channel and its equivalent on the eastern side; the Wagengat extended southward across the entire area and did not show a clear connection with the Riffgat. It includes class 9 and class 10 of the seafloor classification. The

drainage system was characterized by the highest average backscatter values (= lowest mean greyscale values, classes 9 and 10, Table 5.3);

- *tidal flat deposits*, (Figure 5.4), which covered most of the area and were characterized by greyscale backscatter values gradually fading into each other and within a very narrow average range (177-210, classes 2 to 8, Table 5.3). It corresponds to class 2 to 8 in the seafloor classification

Bedforms (Figure 5.3a, north-east corner) were observed at the margin of the area, in a dune field (average wavelength 6 m) near the Riffgat channel. The dunes were not visible in the Lidar-based DTM, as the sector was covered by water during the data acquisition. The depressed area in the center of the western region (already identified in the Lidar data) presented a specific seafloor texture, with bedforms (mostly north-northeast/south-southwest oriented, not regularly spaced) and seafloor marks.

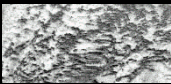
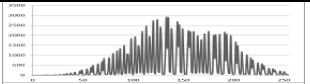
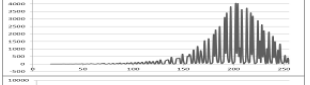
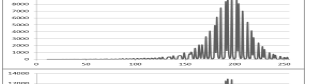
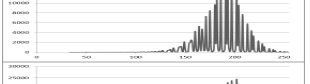
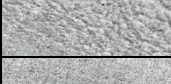
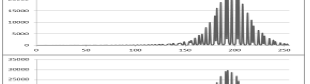
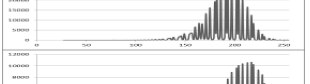
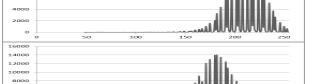
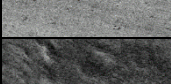
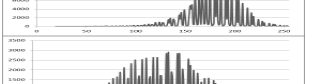
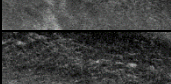
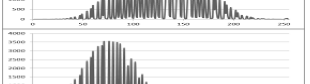
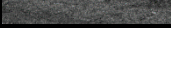
<i>Class n.</i>	<i>Mean mud content</i>	<i>Class description</i>	<i>Class code</i>	<i>Coverage</i>	<i>Mean greyscale value</i>	<i>SSS backscatter (detail)</i>	<i>Greyscale histogram</i>
Class 1	no data	<i>Shellfish beds</i>	SB	10.1%	146		
Class 2	71.6%	<i>Mud</i>	M	6.7%	199		
Class 3	65.7%	<i>Mud to Very fine Sand</i>	M-VFS	9.2%	191		
Class 4	27.6%	<i>Mud to Very fine Sand with bedforms</i>	M-VFS (bd)	9.0%	186		
Class 5	37.6%	<i>Mud to Fine Sand</i>	M-FS	15%	194		
Class 6	8.5%	<i>Very fine Sand to Fine Sand</i>	VFS-FS	19.5%	189		
Class 7	0.8%	<i>Fine Sand</i>	FS	7.2%	210		
Class 8	43.2%	<i>Fine Sand to Medium Sand</i>	FS-MS	11.4%	177		
Class 9	25.8%	<i>Sand with shells</i>	S (sh)	8.8%	130		
Class 10	71.6%	<i>Sand with shells and gravel</i>	S (sh G)	3.2%	81		

Table 5.3. Summary of the sediment and backscatter characteristics for the 10 seafloor classes. Greyscale histograms (on the right): X axis = 8-bit greyscale values, from 0 (black) to 255 (white), corresponding to high and low backscatter intensities, respectively. Y axis: number of counts per class (not the same scale for all the classes).

5.5.4. *Seafloor classification*

The intertidal area presented gradational changes in the SSS backscatter intensity around a very narrow range of greyscale values. Nevertheless, differences in the backscatter intensity and in the seafloor texture were observed, especially at a large scale, where it was possible to distinguish sub-metric sized bedforms and seafloor patterns. The integration of the morphological information derived by the Lidar data was useful in setting up boundaries among the classes. The surface sediment results confirmed the definition of the classes and helped in the description of their characteristics. Based on the SSS backscatter intensity, on the seafloor texture and morphologies (SSS and Lidar data), and on the sediment composition and distribution, *10 classes* were identified (Table 5.3, Figure 5.3):

- ***Class 1, Shellfish bed:*** large banks of shellfish (mainly blue mussels and oysters), with size from ~ 10 to 38000 m². The class showed a greyscale histogram (with a bimodal envelope, Table 5.3) and a mean greyscale value (146), which differed significantly from all the other classes. Class 1 was dominant in the western region, while in the eastern region only a single shellfish bank was described and mapped. The presence of shellfish beds on the SSS data was consistent with the Lidar information, where the shellfish beds produced a specific topographic texture, more elevated (0.4-0.5 m) and rougher than the surrounding muddy and sandy areas.
- ***Class 2, Mud:*** mean mud content >71 w%. Class 2 occurred mainly in the western region, associated with the shellfish beds. If compared with the other intertidal flat classes (classes 3 to 8), class 2 showed a greyscale histogram shifted toward higher greyscale values (lower backscatter intensity).
- ***Class 3, Mud to Very fine Sand:*** mean mud content = 65.7 w%. It showed a higher amount of sand, a smoother seafloor surface (SSS data) and higher backscatter intensity, if compared with class 2. It was present mostly in the western region in association with classes 1 and 2. In general, classes 3 to 7 showed comparable greyscale histograms and mean values, all within a very small range (177-210).
- ***Class 4, Mud to Very fine Sand with bedforms:*** average mud content lower than in class 3 (27.6 w% and 65.7 w%, respectively). Class 4 corresponded with the depressed area in the center of the eastern region, and presented a specific seafloor texture characterized by bedforms of different size and orientation.

-
- ***Class 5, Mud to Fine Sand:*** class 5 covered an area which constantly and gently sloped northward (average 0.04 w%). The three grain size fractions were almost equally distributed (mud: 37.6 w%, very fine sand: 26.8 w%, fine sand: 36.6 w%). The classes 5 and 6 showed similar greyscale values and seafloor texture in the SSS data, although sporadic bedforms and seafloor marks were present in class 5.
 - ***Class 6, Very fine Sand to Fine Sand:*** the most significant differences respect to class 5 were represented by the mud content (which dropped from the 37.6 w% of class 5 to the 8.5 w% of class 6) and by the presence of fine sand (64.1 w%) as dominant fraction. The surface showed generally a smooth aspect on the SSS mosaic, only sporadically characterized by seafloor marks.
 - ***Class 7, Fine Sand:*** corresponding to the most elevated areas of the study site (sand banks), which bordered the Riffgat from the south. The sediment composition was sand for > 99 w%, with fine sand > 85 w%. The seafloor within class 7 presented a smooth surface both in the Lidar and in the SSS data, with the highest mean greyscale value (210) among the intertidal-sediment classes.
 - ***Class 8, Fine Sand to Medium Sand:*** characterized by the presence of medium sand (1.1 w%) and a backscatter intensity significantly higher than class 7. The class bordered the Riffgat channel and the north-western sandbanks and presented a few sporadic bedforms and seafloor marks. It showed the lowest mean greyscale value (177).
 - ***Class 9, Sand with shells:*** together with class 10, it characterized the tidal drainage system (channels and gullies) and presented the highest backscatter intensity recorded in the area. Specifically, Class 9 referred to the secondary channels. The sediment analysis was based on only 2 samples (T54 and T55) with a high variance in composition. The sand content is >74 w%, with medium sand > 50 w% for T55. In-field observations showed a high amount of shell debris mixed with sandy sediments on the bottom of the secondary channels.
 - ***Class 10, Sand with shells and gravel:*** it corresponded to the Riffgat channel and it showed a sharp change in backscatter intensity values respect to the surrounding regions. On the bottom of the Riffgat channel it was possible to recognize both regular bedforms and different morphological structures. Class 10 showed the lowest mean greyscale value (81, corresponding to the highest mean backscatter).

5.5.5. *Comparison sidescan sonar 2013 and 2014*

The SSS mosaics of 2014 showed a great difference in quality respect to the 2013 data (Figure 5.4). The acoustic record - especially in the intertidal region - was significantly affected by the noise, due to the adverse weather conditions. Attempts to filter or minimize the noise (enhancing the seafloor signature) did not succeed. Nevertheless, the three main morphological elements (shellfish beds, drainage system, and tidal flat deposits) could be recognized and mapped in SSS image of 2014. In its total amount, the area covered by each of these three components did not vary significantly in one-year time (Figure 5.4).

The surface classified as drainage system showed limited variation in spatial coverage (from 12.0 % to 10.5 %) and the main morphological changes were observed in the connection between the eastern secondary channel and the Riffgat, which was clearly visible in the 2013 and blurred one year later. Minor modifications occurred also in the geometry of some of the gullies (Figure 5.4, 3a and Figure 5.3b), which presented meter-sized shifts and differences in shape.

The shellfish bed extension in the two mosaics did not change significantly from 2013 to 2014 (8.7% and 7.6%), and even isolated and meter-size shellfish patches could be detected in the 2014 dataset (Figure 5.4, 2a and 2Figure 5.2b).

The main difference between the 2013 and 2014 mosaics was represented by the impossibility of subdividing the intertidal flat deposits into classes: the acoustic artifacts, in fact, strongly masked the information coming from the seafloor (Figure 5.4, 1a and 1b). As a consequence, a unique class was assigned for the intertidal region, where 7 classes were defined in the 2013 mosaic.

5.6. Discussion

5.6.1. *Seafloor classification*

The three main morphological components of the Lütetsburger tidal flat system (drainage network, intertidal deposits, and shellfish beds) were identified and mapped in both the SSS and in the Lidar datasets (Figure 5.2). Although the SSS has a very limited ability in reconstructing the morpho-bathymetry of the seabed, in the study area it allowed the definition and delineation of the same morphological seafloor features recognized in the Lidar-DTM dataset and, in some cases, at a higher detail.

5.6.2. *Tidal drainage system*

The high backscatter mean values (Table 5.3) and the sharp contrast with the surroundings served as acoustic signature for contouring the tidal drainage system. Such high backscatter intensity was due to the presence of shell debris and gravel on the channels' bottom. The missing connection between the Wagengat and the Riffgat in the SSS 2013 mosaic (Figure 5.3a and 5.3b) was likely due to a lack of coarse material. In fact the hydraulic section of the Wagengat channel was much broader in the connection to the Riffgat than in its southern part, where it cuts sharply through the intertidal flat sediments. As a result, the energy of the tidal flow is much lower at the Riffgat-Wagengat branching, and likely not enough to either remove the finer fractions (selecting the coarser material), or to transport and deposit coarser material and shell debris in that area. On the other hand, this result could be also related to the mobility of the sandy sediments, which – depending on energetic events – can temporarily cover and smooth the coarser fraction. The same effect can be observed where the Riffgat branches in its secondary channel (eastern region), by comparing the SSS mosaics of 2013 and 2014 (Figure 5.4). The clear connection showed in 2013 disappeared in the 2014 dataset, where a lower backscatter area is still recognizable, without any distinctive border.

5.6.3. *Shellfish beds*

Shellfish beds (Class1, Figure 5.3c) were clearly recognizable in the SSS datasets, representing the second most prominent acoustic features in both records. Similarly to the drainage system, the shellfish beds generated a unique acoustic signature on SSS data, with high backscatter intensity and a bimodal envelope of its greyscale histogram (Table 5.3). The bimodal distribution could be either due to the twofold nature of the seabed (shellfish patches and fine sediments trapped in between) resolved by the SSS in two slightly overlapping peaks (the second peak resembles the histograms of the other intertidal classes), or it could be the result of the scatter-shadow succession (high and low backscatter). The latter, in fact, depends on the specific geometry of the SSS system (side looking beams), the elevated reliefs of the shellfish beds, the operation conditions (water depth shallower than 1 m), and the angle between the shellfish beds and the travel direction of the SSS, which produce streams of extremely high backscattering reefs (dark greyscale tones), followed by their related shadows (with low backscatter values, light greyscale tones).

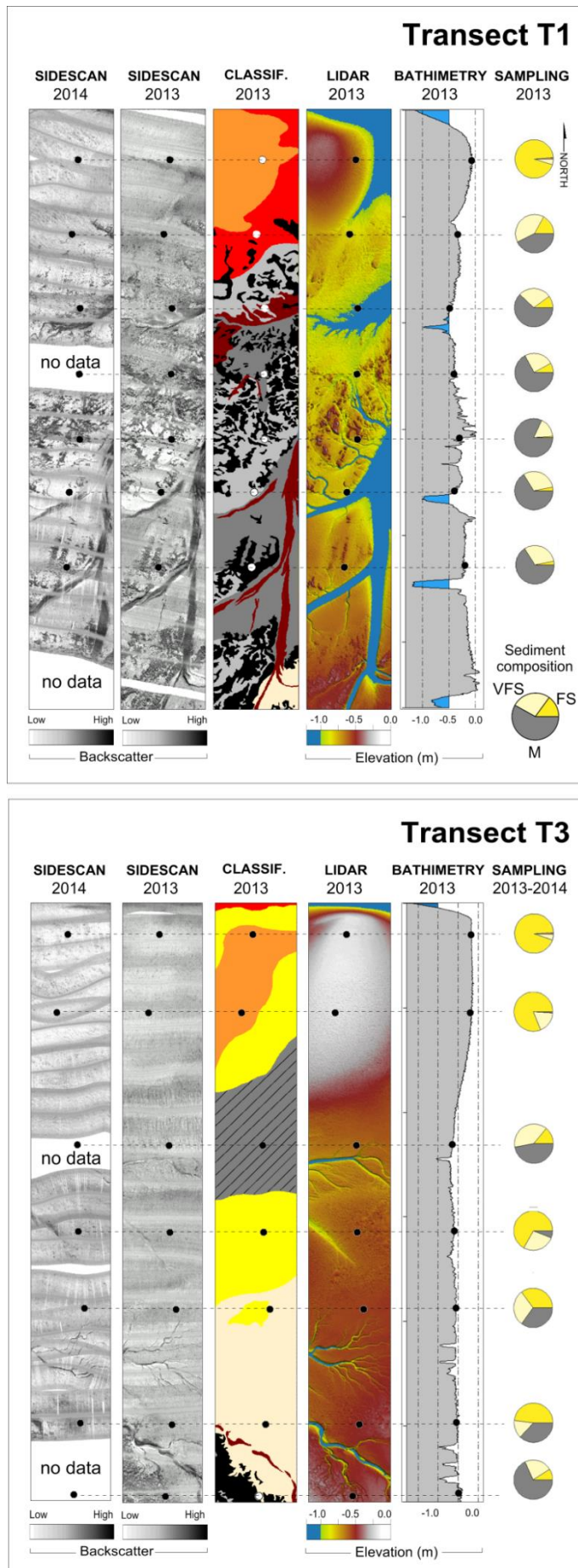


Figure 5.5. Comparison of SSS backscatter data (2013 and 2014), seafloor classification, Lidar-based bathymetry, and sediment fractions (mud, very fine sand, sand) along transects T1 and T3 (for the location of the transects, cf. Figure 5.2). These two transects were chosen to best represent the high variability of sediments, backscatter, and topographic features in the western and eastern regions of the study site, dominated by the association shellfish-mud (T1, west of the Wagengat) and by the typical intertidal mixed flat-sand flat sequence (T3, east of the Wagengat). For the details about the seafloor classification, see Figure 5.3 and the body text.

Shellfish beds were also recognized as patchy-like topographic features in the Lidar bathymetry, more elevated (0.4-0.5 m) than the surrounding areas (Figure 5.2). However, their spatial extension was different in the SSS and Lidar records (Figure 5.6). In fact, the SSS backscatter was mainly influenced by the roughness associated with such communities, independently on the age and/or development stage of the shellfish beds. On the contrary, the topography (which plays the major role in generating the shellfish beds fingerprints on the bathymetric data) is strongly influenced by the development stage of these communities. The Lidar intensity data for the 2014 dataset were also tested, in regard to a small site (20x15 m, Figure 5.6e), in order to check the sensitivity of the different remote sensing system in detecting and mapping the shellfish beds. The size of the reefs in the intensity data matched the one in the SSS image. On the other hand, the intensity pattern (which corresponds to the shellfish beds) occurred also in areas where those beds were not present (Figure 5.6e, red dotted line). Segawa et al. (2008) deployed a sidescan sonar for characterizing the seagrass distribution in near-to-shore areas, and used such classification for performing a supervised classification of satellite images. Similarly, as a future development, the possibility of performing high resolution seafloor classification on small testing areas by means of ground-truthed SSS, and to use the outcomes for training Lidar intensity and satellite classification algorithm should be proved.

5.6.4. Tidal flat deposits

The combination of shellfish beds (Class 1) and the related fine sediment deposits (Class 2 – Mud, and Class 3 – Mud to very fine sand) outlined a specific region (the western one), with distinctive biological, sedimentological, morphological, and geographical characteristics, which were summed up in transect T1 (Figure 5.5). In this region, the shellfish beds acted as sediment traps for the finest fractions, slowing down the currents and allowing the sedimentation of muddy sediments, which are not removed by tidal currents. The primary production of fine organic material (fecal pellets) from the shellfish beds must be taken into account.

The remaining five classes (Class 4 to Class 8) represented a typical tidal flat succession, the sedimentological composition of which included a continuous mixture of three grain size fractions: clay, silt, and sand. The spatial distribution of these classes and their relationship with the morphology are summed up in transect T3, which crossed all of them (Figure 5.5). The general decrease in mud content from Class 4 to Class 8 marked the transition from mixed flat (Class 4 to Class 6) to sand flat (Class 7 and Class 8). The mud content in Class 4 (27.6 w%, lower

than in Class 5, Table 5.3) was explained as a result of the two sediment samples(outliers) collected at the transition with Class 6 (T45, T48, cf Figure 5.2b

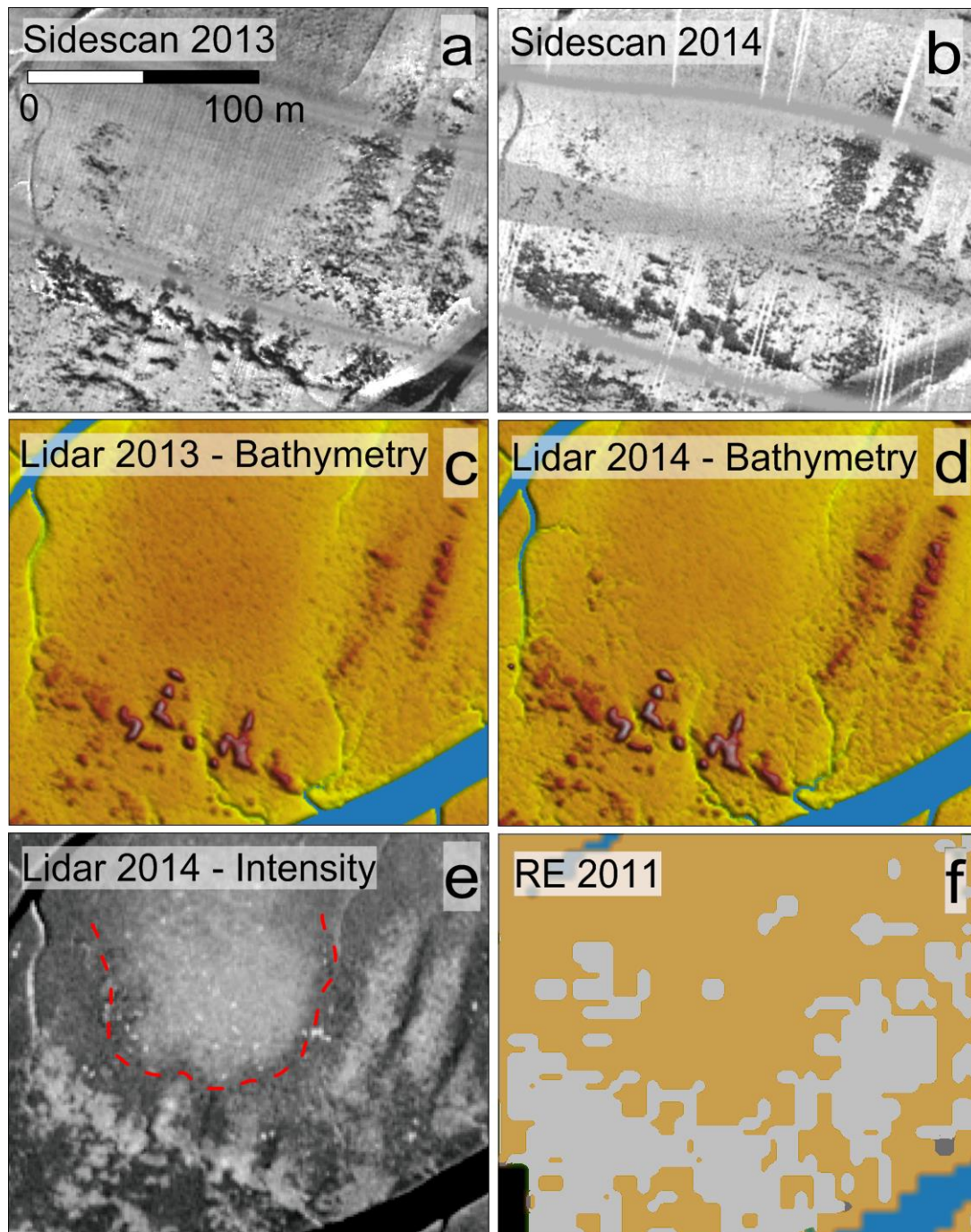


Figure 5.6. Detection of shellfish beds and patches by means of different remote sensing devices. SSS and Lidar data were exported at 0.5 m grid. Shellfish beds can be easily recognized and mapped both in the SSS and in the Lidar topographic data, although the extension of the banks is much more clear in the SSS datasets (even in the 2014, despite of the poor quality of the dataset). Similarly to the SSS backscatter, Lidar intensity could be used for the detection and mapping of shellfish beds, although similar intensity values and pattern are not univocally generated by the presence of such features: the area contoured with a dashed line present intensity values similar to the shellfish beds ones.

and Figure 5.3b). If excluded, the average mud content for Class 4 would have been of 38.0 w%. Class 4 (Mud to very fine sand with bedforms) corresponded to the morphologically depressed area in the center of the eastern region. Despite its mud content (>40 w%) exceeded the threshold defined by Reineck and Wunderlich (1968, modified by Flemming 2003) for a sand flat (mud <5%), Class 8 (fine sand to medium sand) was included in sand flat deposits. In fact, only one sediment sample was collected in the area.

The subdivision into five classes (Classes 4 to 8) was possible only integrating the sediment grain size analyses, the morphological information, and the backscatter texture. The interpretation had to take into account the time difference between the acoustic and the sediment data collection. The seafloor conditions recorded in the SSS data, in fact, could potentially not agree with the information provided by the grain size analysis, as the seafloor was reworked during the ebb or flood flow between two slack water intervals.

5.6.5. Comparison sidescan sonar 2013 and 2014

The weather seems to be the most impacting factor for the quality of the SSS data (Figure 5.4). The sea conditions recorded in 2014 differed significantly from 2013 (Table 5.1): the maximum wave height (1.2 m) adversely affected the sonar movements (which could not be completely compensated in post-processing) and the seawater characteristics (more air bubbles and sediments in the water column). The effects were amplified in such extreme shallow conditions. The decreased signal-to-noise ratio and the presence of acoustic artifacts distorted the seafloor information. As a result, it was not possible to define any sub-class within the intertidal deposits. Nevertheless, the SSS sonar can be still considered a suitable and reliable tool for investigating the seafloor, if the main focus is to resolve the tidal system into its three main components (drainage network, shellfish beds, and tidal flat deposits, as expression of morphology, biology, and sediments).

5.6.6. Comparison with RapidEye-TerraSAR-X seabed classification

For the comparison with the classification performed by Jung et al. (2015) in 4 classes, the original number of 10 classes was decreased accordingly. Excluding the shellfish beds, in fact, Jung and coauthors (2015) divided the tidal flat deposits into four classes: Mud, Mixed sediments, Wet sand, and Dry sand, with reference to the EU Habitat Directive (Council Directive 92/43/EEC) for the sediment definition. The definition of littoral and sublittoral mixed sediments according to the European Environmental Agency (EUNIS) includes any kind of

poorly sorted mixture of non-consolidated sediments, with grain size ranging from clay to gravel. Pebbles, cobbles, and boulder are also included among the mixed sediments, mainly depending on their relationship with other grain size fractions and on the observation scale. Within this frame, any kind of grouping or clustering of the seafloor classification classes was necessarily subjective, to some extent. In this comparison, Class 1 (SB) and Class 2 (M) found direct correspondence to the Shellfish bed and Mud classes in Jung et al. (2015; Figure 5.7). The “muddy-sediment” classes (Class 3, M-VFS; Class 4, M-VFS (bd); Class 5, M-FS) were grouped and compared with the “mixed sediment” class of Jung and coauthors (2015), whereas the “sandy-sediment” classes (Class 6, VFS-FS; Class 7, FS; Class 8, FS-MS) were grouped and compared with the “Sand” class

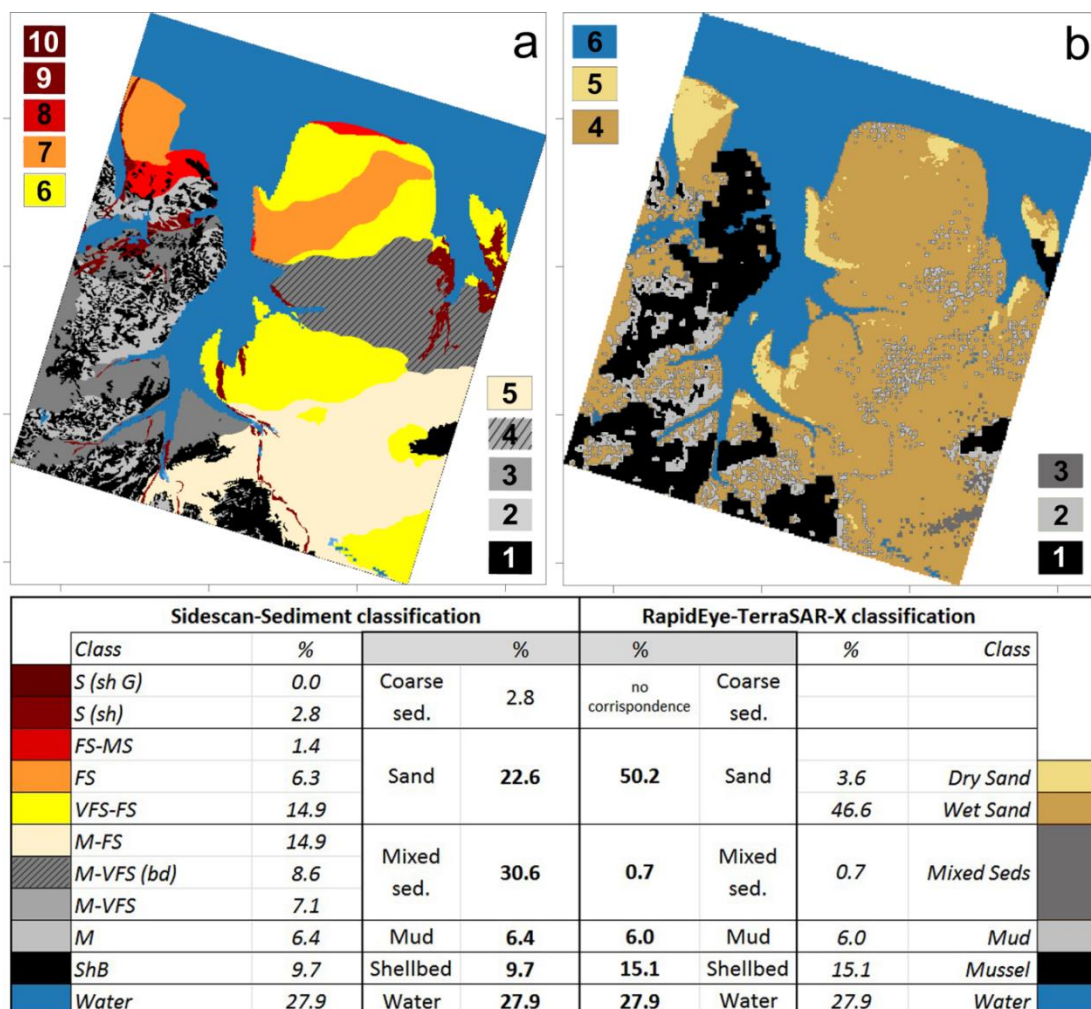


Figure 5.7. Seafloor classification of the Lütetsburger area by means of a) SSS, Lidar and sediment data and b) satellite data (RapidEYE - RE and TerraSAR-X, Jung et al. 2015). The area covered with water in the RE classification was excluded from further computation. The 10 seafloor classes were grouped and reduced to four, in order to match the RE classification, and the corresponding coverage (in %) was given for comparison.

in Jung et al. (2015). The remaining two coarse sediment classes (Class 9 and Class 10) had no correspondence in the RE classification, as they mainly occurred in the subtidal area (drainage network), which was excluded from the RE classification. The surface coverage was calculated for each of the new classes and the comparison was summarized in Figure 5.7.

Whereas the shellfish bed class looked overestimated in the RE data, the area covered by mixed sediments approximated to zero. Based on these results, almost the entire study site should have been considered as sand flat, which was hard to explain considering its position in the backbarrier system and the sediment grain size results. The mixed sediment class covered the largest area in the seafloor classification (>30% spatial coverage), immediately followed by the Sand class (>22%; > 25%, if the values corresponding to Class 9 and 10 were added), which was instead the most relevant sediment class (>50% spatial coverage) in the RE classification. In contrast, the mud class showed similar spatial extension in both classifications, with a spatial coverage, which varied of 0.4%.

In the comparison with the RE classification, the difference in resolution had to be taken into account: in fact, a single RE multispectral record is delivered in 25x25 km tiles, with a 5.0 m pixel size and a 6.5 m resolution (ground sampling distance) at nadir, whereas the maximum resolution of the Starfish record was < 0.2 m (minimum size of a recognizable object). The semiautomatic process of picking up and interpolate the shellfish bed borders on TSX data, and to apply suck masks on the RE dataset produced a coarsening effect, which was likely responsible for the overestimation of the shellfish beds.

5.7. Conclusions

This very unique comparison of hydroacoustic SSS data, LIDAR and satellite data of TerraSAR X and Rapid Eye in this study could be summarize as follows:

- The transition zone between intertidal and subtidal can be investigated by means of both multispectral (RapidEye, Lidar) and hydro-acoustic (sidescan sonar) techniques. Rather than being an advantage, this may result in an increased uncertainty, because both approaches are limited by specific processes occurring in such transition zone (presence of water for the satellite and airborne systems; extreme shallow bathymetry and sensitivity to adverse weather conditions for the SSS).

- SSS showed to be a successful tool for classifying sediments and biological components (shellfish beds), with a resolution hardly achievable by most of the other sources, resulting to be a high performing system, in terms of effectiveness. The ability of detecting the lateral variability of sediments in gradational environments was proved. In this perspective, sidescan sonars can be used for mapping and monitoring the evolution of biotic and abiotic components of a tidal system (e.g. the modifications in shellfish bed coverage) as long as weather/sea conditions allow collecting undisturbed data.
- The use of the SSS has the potential to be extended even further to the upper intertidal with a high effectiveness, although the efficiency would be much lower.
- SSS allows also the reconstruction of the main tidal morphological structures (channels, gullies, bedforms etc.). If coupled with Lidar data, the classification can be improved and extended to the upper intertidal and in areas where boats would have no access. In this frame, it can be used for monitoring the morphological changes (sediment supply, sediment balance etc.).
- The limited SSS swath allows the system to cover areas of 2-3.5 km² per tide, which makes the system not very efficient, if compared with satellite or airborne remote sensing techniques.
- Satellite and airborne based classification present the advantage of an extremely large coverage (high efficiency), if compared with sidescan. They have been used quite successfully for mapping and monitoring biogenic features (reefs, mussel beds etc.), whereas the detection of sedimentary regions is still impaired (lower effectiveness).
- As a future perspective, it is recommended to test the possibility to perform the sediment classification on small areas, based on sidescan sonar and sediment dataset. The outcomes could be used for training satellite. The SSS-sampling technique could be performed on small areas, and the relative classification being used for training airborne-satellite remote sensing based algorithm and classification processes.

5.8. Acknowledgments

This study was partly founded by the German Research Foundation (DFG) within the INTERCOAST Project (an international research training group led by the University of Bremen, the Senckenberg Institute in

Wilhelmshaven, and the University of Waikato), and partly financed by the Lower Saxony Ministry of Environment (MU Niedersachsen), Energy and Climate Protection and by the Ministry of Science and Culture (MWK Niedersachsen), within the frame of the WIMO Project (Scientific monitoring concepts for the German Bight).

The authors would like to thank the crew of the RV Senckenberg, the colleagues from the Wadden Sea National Park, University of Hannover, University of Oldenburg, University of Osnabrück, who took part in the fieldwork activities, and, in particular, Jasmin Osterloh for her sampling efforts in the tidal flat. Many thanks to Astrid Raschke for the grain-size analysis, and to Maik Wilsenack for his technical support.

We are particularly thankful to the Lower Saxony Water Management, Coastal Defence and Nature Conservation Agency (NLWKN Niedersachsen) for the access to the 2013 Lidar dataset. We also want to express our thanks to the anonymous reviewers, who contributed to improve the paper.

The data reported in this paper will be archived in Pangaea (www.pangaea.de).

5.9. References

- Adolph W, Farke H, Lehner S, Ehlers M (2018) Remote Sensing Intertidal Flats with TerraSAR-X. A SAR Perspective of the structural elements of the tidal basin for Monitoring the Wadden Sea. *Remote Sensing*, 10, 10.3390/rs10071085.
- Adolph W, Jung R, Schmidt A, Ehlers M, Heipke C, Bartholomä A, Farke H (2017a) Integration of TerraSAR-X, RapidEye and airborne lidar for remote sensing of intertidal bedforms on the upper flats of Norderney (German Wadden Sea). *Geo-Marine Letters*, 37, 193-205, 10.1007/s00367-016-0485-z.
- Adolph W, Schückel U, Chang S S, Jung R, Bartholomä A, Ehlers M, Kröncke I, Lehner S, Farke H (2017b) Monitoring spatiotemporal trends in intertidal bedforms of the German Wadden Sea in 2009-2015 with TerraSAR-X, including links with sediments and benthic macrofauna. *Geo-Marine Letters*, 37, 79-91, 10.1007/s00367-016-0478-y.
- Badewien T H, Zimmer E, Bartholomä A, Reuter R (2009) Towards continuous long-term measurements of suspended particulate matter (SPM) in turbid coastal waters. *Ocean Dynamics*, 59 (2), 227-238.
- Bartholomä A (2006) Acoustics bottom detection and seabed classification in the German Bight, southern North Sea. *Geo-Marine Letters*, 26, 177-184.
- Bartholomä A, Flemming B W (2007) Progressive grain-size sorting along an intertidal energy gradient.- In: Flemming BW, Hartmann D. (eds): From particle size to sediment dynamics. Proceeding of a Workshop, 15-18 April 2004, Hanse Institute for Advanced Study, Delmenhorst (Germany). *Sedimentary Geology (Spec. Issue)*, 202, 464-472, 10.1016/j.sedgeo.2007.03.010

- Bartholomä A, Flemming B W, Delafontaine M T (2000) Mass balancing the turnover of mud and sand in the vicinity of an intertidal mussel bank in the German Wadden Sea (southern North Sea).- In: Flemming BW, Delafontaine M T, Liebezeit G (eds), *Muddy Coast Dynamics and Resource Management*. Elsevier Science, Amsterdam, pp. 85-106.
- Bartholomä A, Kubicki A, Badewien Th H, Flemming B W (2009) Suspended sediment transport in the German Wadden Sea - seasonal variations and extreme events. *Ocean Dynamics*, Spec. Issue, 59, 213-225, DOI 10.1007/s10236-009—0193-6.
- Brezina J (1979) Particle size and settling rate distributions of sand-sized materials. PARTEC - 2nd European Symposium on Particle Characterization. Nürnberg, 1-47.
- Cambridge University Press (2014) Cambridge online dictionary. <https://dictionary.cambridge.org/dictionary/english>
- Carter RWG (1988) Coastal environments. An introduction to the physical, ecological and cultural systems of the coastlines. Academic Press, New York, 617 pp.
- Collier J S, Brown C J (2005) Correlation of sidescan backscatter with grain size distribution of surficial sediment. *Marine Geology*, 214, 431-449.
- Degraer S, Moerkerke G, Rabaut M, Van Hoey G, Du Four I, Vincx M, Henriët J P, Van Lancker V (2008) Very-high resolution side-scan sonar mapping of biogenic reefs of the tube-worm *Lanice conchilega*. *Remote Sensing of Environment*, 112, 3323-3328, 10.1016/j.rse.2007.12.012.
- Delafontaine M T, Flemming B W, Bartholomä A (2000) Mass balancing the turnover of POC in mud and sand on a back-barrier tidal flat (southern North Sea). In: Flemming BW, Delafontaine M T, Liebezeit G (eds), *Muddy Coast Dynamics and Resource Management*. Elsevier Science, Amsterdam, pp. 107-124.
- Dörjes J, Michaelis H, Rhode B (1986) Long-term studies of macrozoobenthos in intertidal and shallow subtidal habitats near the island of Norderney (East Frisian coast, Germany). *Hydrobiologia* 142:217–232
- Flemming B W (2012) Siliciclastic Back-Barrier Tidal Flats. In: Davis R A Jr, Dalrymple R W (eds), *Principles of Tidal Sedimentology*, 231-267, DOI: 10.1007/978-94-007-0123-6_10.
- Flemming B W, Ziegler K (1995) High-resolution grain size distribution patterns and textural trends in the backbarrier tidal flats of Spiekeroog Island (southern North Sea). *Senckenbergiana maritima*. 26. 1-24.
- Gade M, Alpers W, Melsheimer C, Tanck G (2008) Classification of sediments on exposed tidal flats in the German Bight using multi-frequency radar data. *Remote Sensing of Environment*, 112, 1603-1613, 10.1016/j.rse.2007.08.015.
- Gopal B, Junk W J, Davis JA (2000) Biodiversity in wetlands: assessment, function and conservation. Volume 1. Backhuys Publishers, Leiden, The Netherlands, 353 pp.
- Heinrich C, Feldens P, Schwarzer K (2016) Highly dynamic biological seabed alterations revealed by side scan sonar tracking of *Lanice conchilega* beds offshore the island of Sylt (German Bight). *Geo-Marine Letters*. 37 (3), 289-303, 10.1007/s00367-016-0477-z.
- Hinrichsen D (1998) Coastal waters of the world: trends, threats and strategies. Washington DC, Island press, 275 pp.
- Holler P, Markert E, Bartholomä A, Capperucci R, Hass C H, Kröncke I, Mielk F, Reimers C H (2017) Tools to evaluate seafloor integrity: comparison of multi-device acoustic seafloor

-
- classifications for benthic macrofauna-driven patterns in the German Bight, southern North Sea. *Geo-Marine Letters*, 37 (2), 93-109.
- ICES (2014) Report of the Working Group on Marine Habitat Mapping (WGMHM), 19–23 May 2014, San Sebastian, Spain. ICES CM 2014/SSGSUE:07, 59.
- Joerdel O, Bartholomä A, Flemming B W (2002) Wave measurements using an ADCP?- The method and first results from the East Frisian Wadden Sea.- In Turla, T. (Eds.) (2002): Hydro 2002- Papers of the 17th Hydrographic Days 2002; The Hydrographic Special Publication, 46, 340-346.
- Jung R, Adolph W, Ehlers M, Farke H (2015) A multi-sensor approach for detecting the different land covers of tidal flats in the German Wadden Sea — A case study at Norderney. *Remote Sensing of Environment*, 170: 188-202.
- Markert A, Esser W, Frank D, Wehrmann A, Exo K M (2013) Habitat change by the formation of alien *Crassostrea*-reefs in the Wadden Sea and its role as feeding sites for waterbirds. – *Estuarine Coastal Shelf Science*, 131, 41-51.
- Markert A, Wehrmann A, Kröncke I (2010) Recently established *Crassostrea*-reefs versus native *Mytilus*-beds: differences in ecosystem engineering affects the macrofaunal communities (Wadden Sea of Lower Saxony, southern German Bight). *Biological Invasions*, 12 (1): 15-32.
- McLachlan A, Brown A C (2006) *The Ecology of Sandy Shores* (Second Edition), 14 - Human Impacts, 273-301.
- Müller G, Stelzer K, Smollich S, Gade M, Adolph W, Melchionna S, Kemme L, Geissler J, Millat G, Reimers H C, Kohlus J, Eskildsen K (2016) Remotely sensing the German Wadden Sea-a new approach to address national and international environmental legislation. *Environmental monitoring and assessment*, 188, 595, 10.1007/s10661-016-5591-x.
- NOAA Coastal Services Center (2003) Pilot investigation of remote sensing for intertidal oyster mapping in coastal South Carolina: a methods comparison. NOAA/CSC/20514-PUB, 32 pp.
- Oost A P, Hoekstra P, Wiersma A, Flemming B W, Lammerts E J, Pejrup M, Hofstede J, van der Valk B, Kiden P, Bartholdy J, van der Berg M W, Vos P C, de Vries S, Wang Z B (2012) Barrier island management: Lessons from the past and directions for the future. *Ocean & Coastal Management*, 68, 18-38.
- Park S E, Kim D H, Lee H S, Moon W, Wagner W (2010) Tidal wetland monitoring using polarimetric synthetic aperture radar. *International Archives of the Photogrammetry, Remote Sensing and Spatial Information Sciences - ISPRS Archives*, 38.
- Rahnemoonfar M, Rahman F, Kline R, Greene A (2018) Automatic Seagrass Disturbance Pattern Identification on Sonar Images. *IEEE Journal of Oceanic Engineering*, 1-10, 10.1109/JOE.2017.2780707.
- Reineck H E, Singh I B (1980) *Depositional Sedimentary Environments*. Springer-Verlag Berlin Heidelberg, 551.
- Sagawa T, Mikami A, Komatsu T, Kosaka N, Kosako A, Miyazaki S, Takahashi M (2008) Mapping seagrass beds using IKONOS satellite image and side scan sonar measurements: A Japanese case study, (June 2013). *International Journal of Remote Sensing*, 29, 281-291.

- Schmidt A, Adolph W, Klonus S, Ehlers M, Farke H, Soergel U (2019) Potential of Airborne Laser Scanning Data for Classification of Wadden Sea Areas. *Advances in Geosciences*.
- Schmidt A, Niemeyer J, Rottensteiner F, Soergel U (2012) Contextual Classification of Full Waveform Lidar Data in the Wadden Sea. *Geoscience and Remote Sensing Letters, IEEE*, 11, 1614-1618, 10.1109/LGRS.2014.2302317.
- Schmidt A, Rottensteiner F, Soergel U (2013) Water-Land-Classification in Coastal Areas with Full Waveform Lidar Data. *PFG 2* (2013), 71-81.
- Shan J, Toth C K (2018) *Topographic laser ranging and scanning: principles and processing*. “nd Edition. CRC Press, 638 pp.
- Schill S R, Porter D E, Coen L D, Bushek D, Vincent J (2006) Development of an Automated Mapping Technique for Monitoring and Managing Shellfish Distributions: A Final Report. The NOAA/UNH Cooperative Institute for Coastal and Estuarine Environmental Technology (CICEET), 91 pp.
- Stanev E V, Flemming B W, Bartholomä A, Staneva J V, Wolff J O (2007) Vertical circulation in shallow tidal inlets and back-barrier basins. *Continental Shelf Research*, 27, 798-831.
- Stanev E V, Wolff J-O, Burchard H, Bolding K, Flöser G (2003) On the circulation in the East Frisian Wadden Sea: numerical modeling and data analysis. *Ocean Dyn*, 53, 27–51, 10.1007/s10236-002-0022-7.
- Staneva J, Stanev E, Wolff J-O, Badewien T, Reuter R, Flemming B W, Bartholomä A, Bolding K (2009) Hydrodynamics and sediment dynamics in the German Bight: A focus on observations and numerical modelling. *Continental Shelf Research*, 29 (1), 302-319.
- Streif H (1990) *Das ostfriesische Küstengebiet: Nordsee, Inseln, Watten und Marschen*. Reihe: Sammlung geologischer Führer, Bd. 57. Berlin Stuttgart, 1990.
- Udden J A (1914) Mechanical composition of clastic sediments. *Geological Society of America Bulletin*. 25 (1), 655–744.
- Van Beijma S, Comber A, Lamb A (2014) Random forest classification of salt marsh vegetation habitats using quad-polarimetric airborne SAR, elevation and optical RS data. *Remote Sensing of Environment*, 149, 118-129.
- Van der Wal D, Herman P M J (2007) Regression-based synergy of optical, shortwave infrared and microwave remote sensing for monitoring the grain-size of intertidal sediments. *Remote Sensing of Environment*, 111, 89–106.
- van Overmeeren R, Craeymeersch J, Van Dalssen J, Fey F, Heteren S, Meesters Erik (2009) Acoustic habitat and shellfish mapping and monitoring in shallow coastal waters - Sidescan sonar experiences in The Netherlands. *Estuarine Coastal and Shelf Science*, 85, 437-448, 10.1016/j.ecss.2009.07.016.
- Walter F (1972) Zusammenhänge zwischen der Größe der ostfriesischen Seegaten mit ihren Wattgebieten sowie den Gezeiten und Strömungen. *Jber. Forschungsstelle Küste*, 23, 7-32.
- Wentworth C K (1922) A Scale of grade and class terms for Clastic sediments. *Jour. Geol.*, 30, 377-392.
- Winter C (2017) Monitoring concepts for an evaluation of marine environmental states in the German Bight. *Geo Marine Letters*, 37 (2), 75-78.

Page left intentionally blank

Chapter 6

Hydrodynamics and hydroacoustic mapping of a benthic seafloor in a coarse grain habitat of the German Bight

Alexander Bartholomä², Ruggero Maria Capperucci^{1,2}, Lydia Becker²,
Susanne I.I. Coers^{1,2}, Chris N. Battershill³

¹ University of Bremen, Department of Geosciences, P.O. Box 330440, D-28359 Bremen, Germany

² Senckenberg am Meer, Südstrand 40, D-26382 Wilhelmshaven, Germany

³ School of Science and Engineering, University of Waikato, Hillcrest Road, Hamilton 3040, New Zealand

Key words *Hydroacoustics, Sediment, Habitat mapping, Macro benthos, ADCP, Currents, Marine hard substrate*

6.1. Abstract

Coarse-grained hard substrate areas with grain sizes up to very coarse boulder (>2 m) are very rare in the German North Sea. The “Helgoländer Steingrund” is one of such highly biodiverse areas: it is characterized by a half-moon-shaped hard substrate ridge, which subdivides the site into a more exposed (westerly) and a less exposed (easterly) flank, characterized by a mixture of sand and gravel deposits. Sonar systems, underwater videos, and bottom samples were used for mapping and classifying the abiotic and biotic components in such very patchy and coarse grained habitat. Three main seabed types (sand, gravel and hard substrate) were identified, based on acoustic backscatter data. The additional information coming from underwater videos and sediment bottom samples analysis allowed the description of six different seabed types, which included

Bartholomä, A., Capperucci, R., Becker, L., Coers, S.I.I., Battershill, C.N. 2019. Hydrodynamics and hydroacoustic mapping of a benthic seafloor in a coarse grain habitat of the German Bight, Geo-Marine Letters, in press.

both the abiotic (sediments, morphology, etc.) and biotic components. The flanks of the ridge and their transition to the surrounding soft-ground areas were characterized by a distinct dominance of the bryozoa *F. foliacea* and *A. diaphanum* on the western and on the eastern side, respectively. Morphology and hydrodynamics are likely responsible for such zonation. This is proved by the outcomes of the Acoustic Doppler Current Profiler data, which showed the general flow pattern across the ridge and even resolved the local variability of current pattern, dependent on the tidal stage and on the bottom relief.

6.2. Introduction

Most parts of the seafloor in the German Bight consist of reworked Holocene and Pleistocene sand, with a small amount of silt and clay (Schwarzer et al. 2008, Zeiler et al. 2008). In contrast, coarse-grained hard substrate areas with grain sizes up to very coarse boulder (following the extended nomenclature of Terry and Goff 2014) are very rare in the German North Sea. Hard substrates with strong geomorphological gradients have been described in the closer vicinity of the Helgoland Island (Mielck et al. 2014, Hass et al. 2017, Holler et al. 2017). A different kind of hard ground, with grain size up to boulders and a smoother topographic relief occurs in the “Sylter Aussenriff” area (Papenmeier and Hass 2018, Feldens et al. 2018). An even smoother relief characterizes the “Helgoländer Steingrund” (HSG), which is known as one of the rare hard substrates made by cobble-size to small boulders deposits. In contrast to the wide-spread and spatially distributed deposits of the “Sylter Aussenriff”, the HSG is shaped as a half-moon hard substrate ridge, with different hydrodynamic regimes characterizing the westerly and the easterly flanks. The HSG is part of the Nature Conservation Areas (BFN 2018) due to its high biodiversity, whose preservation requires a detailed mapping and a monitoring.

As highlighted by Dyrinda 1994, the colonization pattern of benthic communities largely depends on the substrate type. Rachor and Nehmer (2003) pointed out the relevance of hard substrates for the biodiversity and for the lateral variability of such patterns.

The HSG ridge was firstly surveyed and described in 1908 (Stocks, 1955). A former study of the abiotic ensemble characterizing the HSG site was carried out by Schulz (1983), who analyzed Sidescan sonar (SSS) images and classified the seafloor in five different sediment types. Several studies focused on the epibenthic communities living on the hard ground (Kluijver 1991, Kühne and Rachor 1996), while a more comprehensive overview of the organisms living in

and on the HSG hard substrate was given by Dederer et al. (2015). They showed that the cobble and boulder deposits are mainly colonized by different bryozoan species. Moreover, they pointed out the importance of understanding the colonization mechanism of the bryozoans, in order to be able to preserve such a rare environment. However, the study did not provide a detailed geographical distribution of the different taxa, and did not take into account the abiotic and the hydrodynamic characteristics of the area.

In-situ investigations, like seafloor sampling and scuba diving observations, can offer detailed information about single spots, while a different approach is required for the areal characterization (i.e. composition and lateral distribution) of both the abiotic and the biotic components of an ecosystem. On the other hand, backscatter from hydroacoustic devices (e.g. SSS, echo-sounder systems, etc.) allows to spatially cover large areas in a short time, but lack of a direct investigation of the seafloor nature. The backscatter summarizes information about e.g. grain size, suspended sediments, morphological elements, fauna and flora. A combination of acoustic sources and seafloor ground-truthing is therefore helpful in resolving the habitat distribution pattern on different scales, depending of the acoustic configuration (frequency, swath angle, etc.). In addition, the knowledge of the local current hydrodynamic conditions can provide useful information for understanding the colonization pattern and mechanisms of the hard-ground related biocommunities (Michaelis et al. 2019). Acoustic current measurements (e.g. by means of Acoustic Doppler Current Profiler) can be used for such purpose.

Many studies investigated the hydroacoustic response of sonar systems to different habitat types (e.g. Freitas et al. 2003, Quintino et al. 2010, Bartholomä et al. 2011, Freitas et al. 2011, Arendartchuk et al. 2017, Greene et al. 2018). At the North Sea, Mielck et al. (2014) investigated the spatial abundance of kelp around the Helgoland Island, by means of a single-beam echo sounder (SBES) system. A combination of SBES data and underwater videos was used by Hass et al. (2017) for distinguishing seafloor substrate types in the southern North Sea. Holler et al. (2017) used different acoustic sources for differentiating between hard- and soft-grounds, and for studying the modification of the acoustic signal due to soft-sediments related communities (brittle stars). However, there are still significant gaps in mapping the hard substrate biotic and abiotic components in the North Sea region (specifically regarding the areal composition and distribution on a small scale), and in understanding the factors, which are driving the colonization mechanisms.

The general current regime in the North Sea is well known (e.g. Staneva et al. 2009, Callies et al. 2017). Under regular conditions, westerly winds cause a counterclockwise circulation in the North Sea (Sündermann and Pohlmann 2011), which results in mainly northwards currents in the HSG area. Occasionally, the main wind direction changes, which causes in a reversion or stagnation of the currents.

The present study aims to offer a new glimpse about the small scale distribution pattern of both abiotic and biotic components of a highly-protected and rare hard-ground environment, particularly regarding the different communities living on the hard substrates. For this purpose, a new high-resolution morphobathymetry of the area was produced, together with a new classification of the seafloor in sediment types (based on SSS, SBES, underwater videos and bottom samples data), which made use of the acoustic data for spatially extend the point-based information coming from the *in-situ* investigations. In addition, the local dynamic conditions were estimated by means of repeated SSS surveys (for the mobility of the sandy soft-ground) and by means of ADCP measurements for the influence of the currents in the development of different bryozoan association along the two flanks of the HSG ridge.

6.3. Physical settings

The “Helgoländer Steingrund” (HSG) is located in the German Bight (southern North Sea), 11 km east-north-east of the Helgoland Island, and covers an area of nearly 1.6 km² (Figure 6.1A).

The area consists of patches of very coarse grain deposits, the size of which ranges from pebbles to boulders, and surrounded by sand (Schulz 1983). The very coarse-grained sediments were transported during the Warthe Stage (140 kyr BP, Lambeck et al. 2006) of the Saalian Ice Age, as a result of an end moraine deposit (Pratje 1951, Schulz 1983). Due to its broad spectrum of grainsizes, the HSG area offers a set of physical substrates, potentially suitable to many different biocommunities. The HSG is listed in the Flora-Fauna-Habitat guidelines and it is part of the German natural conservation areas (BFN Report 477 2018). Kühne and Rachor (1996) counted 289 different species, while Dederer et al. (2015) pointed out the heterogeneous spatial distribution of the very densely- and very sparsely-colonized areas. Visual ground-truthing by scuba diving showed significant distribution patterns of benthic coverage, which represent an ecosystem with high biodiversity (Dederer et al. 2015).

The water depth ranges between 9 and 20 m, with the minimum depth in the shallow part of the central ridge. Semi-diurnal tide occurs with a range of ~ 1.5 m, the flood flow enters from the southwest. Westerly winds are dominant, with the largest fetch length from the northwest. The tidal current model of the Federal Maritime and Hydrographic Agency (Bundesamt für Seeschifffahrt und Hydrographie, BSH) shows surface currents velocities between decimeters and more than 1 m/s. During the field work the weather conditions included periods of strong wind (up to 8 Bft.) with wave height > 2 m, which affected the quality of some dataset.

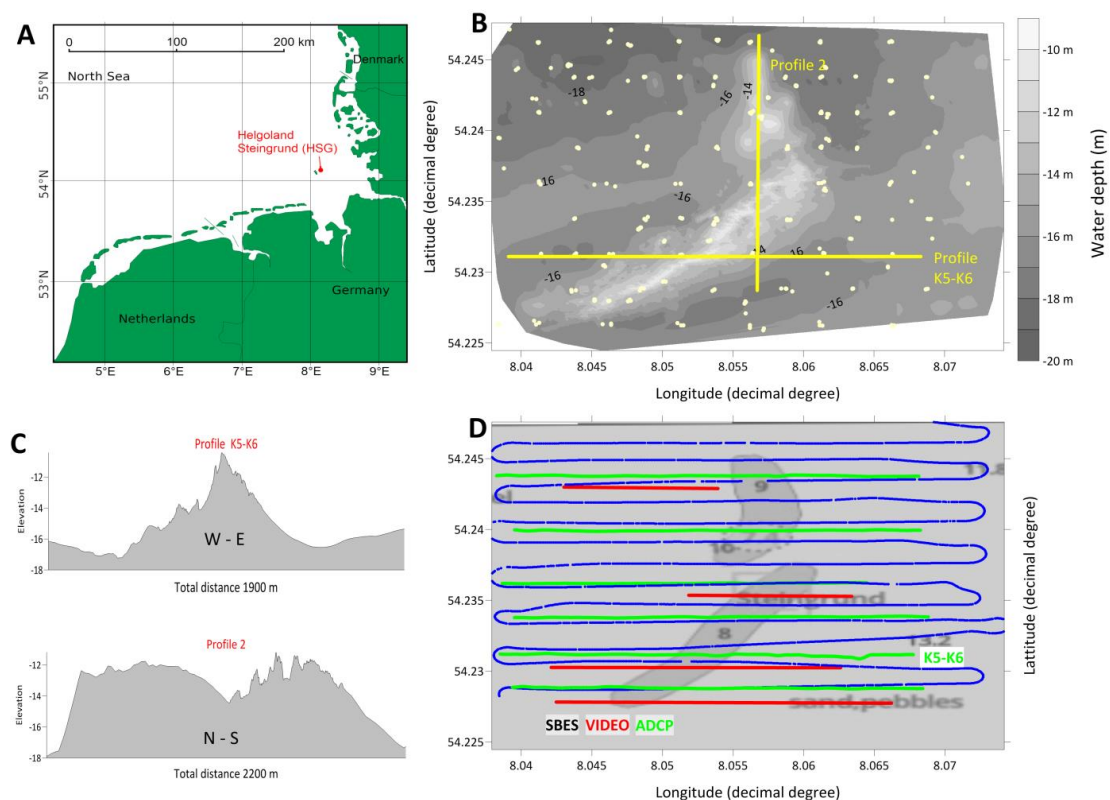


Figure 6.1. A) Location map of the study site "Helgoländer Steingrund", east of the Helgoland Island, in the southern North Sea. B) Bathymetry map from Multibeam echo-sounder and Subbottom profiler data (SBP). Sampling stations are showed as yellow dots; the yellow lines (Profile 1 and Profile K5-K6) correspond to the transect showed in C. C) Elevation profiles in west-east (K5-K6 = Acoustic Doppler Current Profiler (ADCP) time series transect) and north-south directions. D) nautical chart with the survey lines for the Singlebeam echo-sounder (SBES, blue), underwater video (red), and ADCP (green). SBP survey lines correspond to the SBES ones.

6.4. Data collection and processing

The field measurements have been carried out aboard the RV Senckenberg and RV Heincke during three cruises in Sep. 2016, Nov. 2016, and Nov. 2018. The survey site encloses an area of 6.1 km² east of the Helgoland

Island, in the German Bight (Figure 6.1A). Hydroacoustic data were recorded with an average vessel speed of 5 knots.

6.4.1. Bathymetry and Acoustic Seafloor Mapping - Singlebeam echosounder (SBES), Subbottom profiler (SBP), and Multibeam echosounder (MBES)

Individual acoustic sources have been used for the seafloor acoustic classification because vertical and oblique angle operating hydroacoustic devices differ in their acoustic backscatter characteristics (e.g. Lurton 2002). During the surveys a combination of Single Beam Echo Sounder (SBES, 50/200 kHz Furuno FCV 1000) and Subbottom profiler (SBP, SES-Innomar 2000 standard plus) was used for collecting bathymetric and seafloor backscatter data (Figure 6.1D). The SBP was coupled with a motion sensor (IXblue Octans) for ship movement compensation and corrections. Positioning was achieved by means of a Trimble D-GPS system (Helgoland Beacon). Tide corrections were calculated using tide gauge values recorded at the Helgoland port station (“Helgoland Binnenhafen”, seven nautical miles away from the study site). The tide- and motion-corrected high frequency signal (100 kHz) of the SBP was used for extracting the bottom depth information and, together with the Multibeam echosounder (MBES) data, for producing the bathymetric map.

In order to dense the coarse bathymetric grid based on SBP data, a MBES dataset (from 2016, with 0.5m grid size, kindly provided by the BSH) was further processed, in particular for the central region of the study site. Bathymetry data of SES and MBES has been contoured by means of the triangulation algorithm of Golden Software Surfer™ 15. The 200 kHz signal of the SBES system was used for the waveform analysis. In a water depth of 15 m, the footprint has a beam radius of almost 1m and a beam area of nearly 3 m², given a beam angle of 7.4° (Bartholomä 2006). The SBES signal was processed with the QTC IMPACT software, which analyzes the full waveform of the received acoustic wave by means of a principal component analysis (PCA). The PCA finds the three most significant descriptors (so called Q-values), which describe the best statistical similarity of the echoes (e.g. Preston et al. 2000, Bartholomä 2006, Freitas et al. 2011). These values identify a vector in a 3D Q-space. The cloud of points can be subdivided into different classes (splitting process), which ends up with a number of classes depending on the optimal splitting level (based on statistical function, e.g. Cluster Performance Index and the Chi²).

6.4.2. Acoustic Seafloor Mapping - Sidescan Sonar (SSS)

SSS data were collected in Nov. 2016 by means of a Benthos SIS-1624 dual frequency system (110 kHz and 390 kHz). Nine north-south profiles were recorded, with a length of 2500 m and a spacing of 250 m. A swath range of 300 m was set, with 50 m overlap between the lines. For this study, only the low frequency data were processed, as the high frequency dataset resulted to be adversely affected by the severe weather conditions. In Nov. 2018 a second SSS dataset was collected by means of a Klein 4000 (100 and 400 kHz), along 11 transects west-east oriented, 200 m spaced and with a swath range of 300 m (i.e. 100 m overlap between the lines). The low frequency was used for the seafloor classification.

The SonarWiz software (v7.04) was used for producing the final mosaics (after applying geometric and radiometric corrections), and for segmenting the dataset in acoustic classes (only for the Nov. 2018 dataset). SonarWiz allows choosing among different algorithm and classification functions (Seabed Characterization Tool, SonarWiz UserGuide 2017). For this study, a combination of Gray-Level Co-occurrence Matrix (GLCM) functions was used (Contrast, Homogeneity, Energy, and Entropy, Haralick et al. 1973). Due to its larger coverage, the SSS mosaic of Nov. 2016 (in 1 m resolution, Figure 6.3 B, C) was used as a base for the interpretation of the bottom samples and video results (Figure 6.3 A, B) and, therefore, for spatially extending these point information on an areal scale. This process was performed on ArcGIS (v10.2). The Nov. 2018 dataset (Figure 6.3D), instead, resulted to be more suitable for the classification, due to the larger overlap between the lines and to its west-east orientation, which better fits to the main morphological structures of the area.

6.4.3. Groundtruthing – Bottom samples

Seafloor samples were collected for grain size analysis from 128 stations, in series of 3 replicates, by means of a 0.2m² Shipek grab sampler. A total amount of 353 samples were recovered (Figure 6.1B), as many attempts to sample the hard-ground locations failed (empty grabs). Due to the vessel drifting and to the positioning error connected to the vessel-sampling device offsets, the replicates from the same sampling station presented a distance up to 50 m from the planned position. The sediment samples were macroscopically described on board, a photo was taken for each sample and, for soft sediments, a subsample was collected for grain size analysis.

The sediments were desalinated in the lab, wet-sieved on a 63 µm mesh, and the shell content for the fraction coarser than 2mm were removed. The sand

fraction (2000 – 63 μm) was analyzed by means of a settling tube (Brezina 1979) and the mud fraction (< 63 μm) by means of a Sedigraph particle analyzer. The sediment classes were named after Folk (1954).

6.4.4. Groundtruthing – Underwater videos

The underwater videos were recorded along five west-east tracks (total length: ~5500 m, Figure 6.1D). The tracks were designed to fit with the sampling positions. A drop camera (Kongsberg 1366 MKII- 0321) was deployed, frame-mounted, slowly towed behind the vessel at the average speed of 0.8 knots. The videos were replayed on the Adobe Premiere Pro CC software, in order to visually identify the main seabed types (e.g. seafloor sediments, structures, and biota). The videos were therefore split accordingly, and the position of each class reported as a vector line on ArcGIS. In regard to the hard ground, a semi-quantitative estimation of the spatial coverage of the bryozoa was given.

6.4.5. Hydrography – Acoustic Doppler Current Profiler (ADCP)

A vessel mounted Teledyne Rio Grande ADCP with 1200 kHz frequency was deployed in Nov. 2017 and Nov. 2018, in order to measure the current velocity and direction over tidal cycles. The system was coupled with a D-GPS positioning (also for heading); the compass calibration achieved a good fit in direction between bottom track and D-GPS track (<5° variation). The high frequency mode (Water Mode 12) with a bin-size of 25 cm was set, in order to cover the entire water column (max. depth: ~20 m). The raw data were then smoothed using an average of 10 ensembles, in order to reduce the noise and to increase the signal/noise ratio.

Nine ADCP transects parallel and perpendicular to the ridge were recorded over more than one tidal cycle and in both directions. For the time series analysis, only the east-west tracks of Nov. 2018 were considered (Figure 6.1D). One of these east-west transects (named K5-K6 in Figure 6.1B and Figure 6.1D) was used for comparison with the overlaying underwater video. Tidal data recorded at the Helgoland port gauge (Helgoland Binnenhafen” in Figure 6.4, approximately 7 nautical miles south-west of the study site) were used for relating the ADCP measurements to the tidal phase. The tidal curve was provided by the German Federal Institute of Hydrology (Bundesanstalt für Gewässerkunde BfG), in one minute interval (Figure 6.4). The ADCP data were processed by means of the USGS Velocity Mapping Toolbox (Parson et al 2013).

The vessel movements produced an interference with the ADCP records, in regard to the close-to-surface bins (the first 1-1.5 m from the water surface).

As a result, the uppermost bins showed often a higher current velocity, randomly changing in values and direction, depending on the orientation of the transects respect to the ship movement, the currents, and the wave action.

6.5. Results

6.5.1. *Bathymetry and Morphology*

The morphobathymetric map (Figure 6.1B and Figure 6.2) confirms the presence of a half-moon shaped structure, which in this new high-resolution version shows a morphological complexity particularly in the south-western end. Three morphological sections can be recognized, separated by the ridge, which in its central region is ~450 m wide and 6 m higher than its margins (Figure 6.1B). The cross section shows the asymmetric profile of the ridge, with the steeper side on the western flank (Figure 6.1C). The shallowest part of the ridge reaches a water depth of ~9 m. The complex topographic pattern (surface roughness), which distinguishes the central and south-western part of the ridge, decreases along the flanks, where they gradually merge with the smooth and softground-covered regions (Figure 6.1B and Figure 6.1C).

6.5.2. *Bottom samples*

Based on the first macroscopic description of the grab samples, on the photos taken on board, and on the grain sizes analysis results, the sediments were grouped into 3 classes (Figure 6.2):

- Sandy sediments (yellow dots, Figure 6.2),
- Gravelly sediments (orange dots),
- Hard substrate (purple dots).

The sandy sediments (125 samples) are composed by sand (90-100 wt%), small amounts of gravel (0-10 wt%) and of shell fragments (0-10 wt%). Mud content is negligible. The gravelly sediments (92 samples) show higher amount of gravel (> 10 wt%) and a sand content < 90 wt%. The hard substrate class (136 samples) includes the coarser material, which could be characterized, based on the bottom samples, only in its gravel- to cobble-size fraction, due to the limitation of the sampler (occasionally, cobbles were recovered in the Shipek grab). The softground regions (west and east of the central ridge) differ in their main sedimentological components: the western one is dominated by sandy sediments, while the eastern area is mainly composed by a mixture of both sand

and gravel. The hard substrate class overlaps the central ridge and extends to the north-west area.

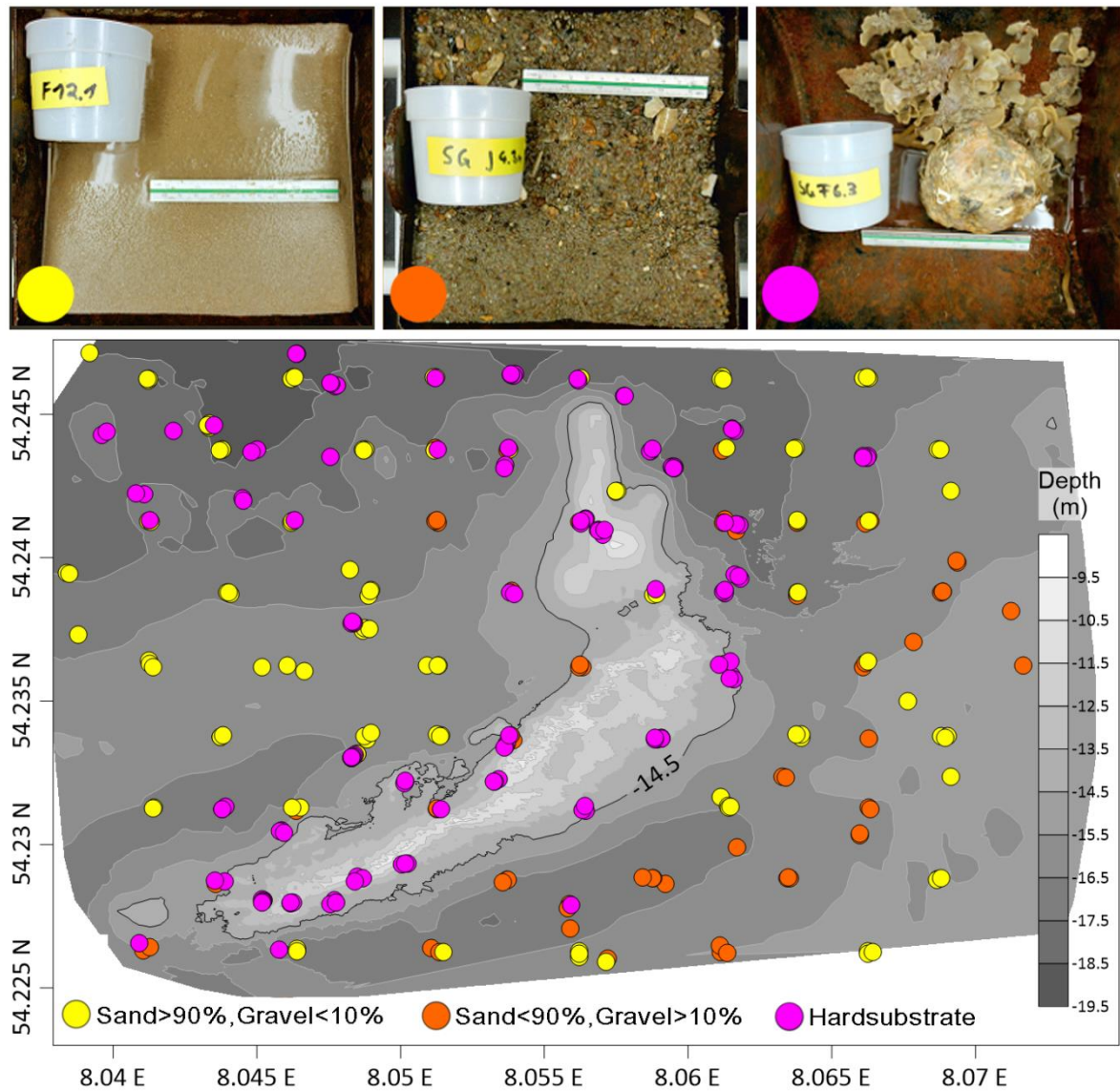


Figure 6.2. The three main sediment types and the sediment distribution map in the Helgoländer Steingrund area. The colored dots (and the related photos) correspond to sandy sediments (yellow), gravelly sediments (orange), and hard substrate (purple). The high-resolution morpho-bathymetric map in the background shows in detail the complex topography characterizing the half-moon shaped ridge, especially in its central and south-western parts.

6.5.3. Underwater video analysis

The analysis and segmentation of the underwater videos revealed the presence of seafloor structures (e.g. bedforms, hardground, etc.) and of different benthic assemblages (Figure 6.3A). Six seabed types (Figure 6.3A and Figure 6.3B) were distinguished, based on such characteristics:

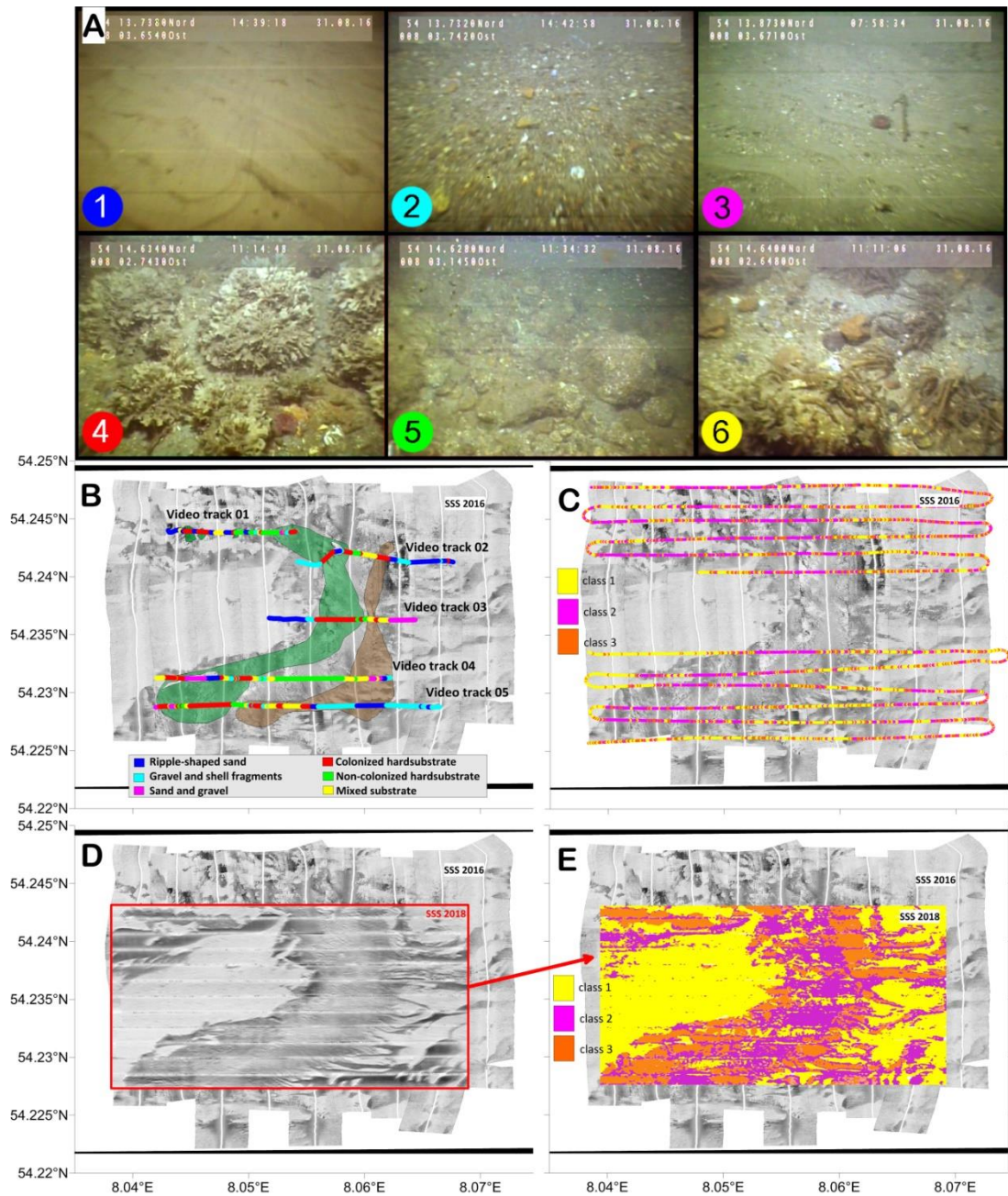


Figure 6.3. Seafloor classification based on underwater videos and acoustic data – A) Video classification: (1) Ripple-shaped sand, (2) Gravel and shell fragments, (3) Sand and gravel, (4) Colonized hard substrate, (5) Non-colonized hard substrate, (6) Mixed substrate – B) Segmentation of the video tracks into the six seabed types (see above), the zones of high abundance of the two bryozoan species have been highlighted with polygons: green = *F. foliacea* and brown = *A. diaphanum*. C) Singlebeam (SBES) acoustic classification (three classes); on the background: Sidescan sonar (SSS) backscatter mosaic (2016 dataset). D) SSS backscatter mosaic (2018 dataset), on top of the 2016 one. E) Acoustic seafloor classification of the 2018 SSS data. The color code of the three classes corresponds to the colors of the SBES ones.

- Seabed type 1, Ripple-shaped sand: sand with bedforms, with rare epifaunal organisms and small shell debris.

-
- Seabed type 2, Gravel and shell fragments: gravelly and sandy sediments (without bedforms), with a higher content of shell debris.
 - Seabed type 3, Sand and gravel: sand with bedforms, the troughs of which are filled by fine gravelly sediments and shell fragments.
 - Seabed type 4, Colonized hard substrate: hard substrate mainly made by cobbles and boulders, totally covered by epifaunal communities, with a dominance of the two bryozoa species *Flustra foliacea* (Figure 6.3B, green-colored area) and *Alcyonidium diaphanum* (Figure 6.3B brown-colored area), each of them dominating a specific region of the ridge.
 - Seabed type 5, Non-colonized hard substrate: hard substrate mainly made by cobbles and boulders, poorly covered or not covered by epifauna.
 - Seabed type 6, Mixed substrate: a very heterogeneous mix of small sand patches with individual coarse-grained particles (from gravel to boulder size).

The hard substrate seabed types (4, 5, and 6) can mainly be found in the ridge area, while the sandy and gravelly seabed types (1, 2, and 3) occur in the western and eastern regions (Figure 6.3A). Spatial distribution and coverage density of the bryozoa shows a geographic zonation of the two main species: the western and central parts are characterized by the bryozoa *F. foliacea*, while the *A. diaphanum* become dominant along the transition zone of the eastern flank, till the beginning of the large eastern sand field (with a spatial density of > 70%) (Figure 6.3B)

6.5.4. Hydroacoustics - Sidescan sonar (SSS)

SSS data shows a clear distinction between hard substrate (darker grayscale tones, Figure 6.3C and Figure 6.3D) and softground regions (light grayscale tones). The comparison of the two SSS mosaics (Nov. 2016, Fig 3C, and Nov. 2018, Figure 6.3D) shows no significant difference in the backscatter distribution pattern: minor changes occur only along the outer rim of the ridge.

The Nov. 2018 was used for the acoustic classification. The spatial backscatter pattern was split into 3 classes (Figure 6.3E): Class 1 (~50% of the total area) occurs mostly on the western region (softground) and, associated with both Class 2 and Class 3, in the eastern one. Class 2 and Class 3 correspond to the ridge and its flanks, with Class 3 (~30%), which covers the ridge crest and its surroundings and Class 2 (~20%), which appears in the transition zones between Class 1 and Class 3.

6.5.5. Hydroacoustics – Singlebeam (SBES)

At the beginning of the statistical analysis, the SBES data were split into five acoustic classes, according to the optimal splitting level suggested by the software statistics. Two classes stood out among the others, both for the statistic relevance (Class 1: 37%, Class 3 28%, yellow and purple in Figure 6.3E, respectively) and, in regard to Class 1, for the distinctive area of occurrence (it appeared mostly in the western region, characterized by sandy sediments). The remaining three classes, instead, were sub-represented (e.g. Class 3: 3%) and, moreover, they occurred always in association and were not distinguishable as separated classes. Therefore, these three classes were merged into a new one (named Class 2: 35%, orange dots in Figure 6.3E), which still occurred in association with Class 3, but with a distinctive presence along the ridge flanks and rim.

6.5.6. Hydrography – Acoustic Doppler Current Profiler (ADCP)

A selection of the 73 original ADCP records, chosen among the most representative and of better quality datasets, was used for giving a picture of the current velocity and direction over the entire area (6 east-west transect, Figure 6.1D) and, more specifically, along the southern K5-K6 profile (Figure 6.1D). The time stamp for each transect is given in the water level curve of the Helgoland port (Figure 6.4).

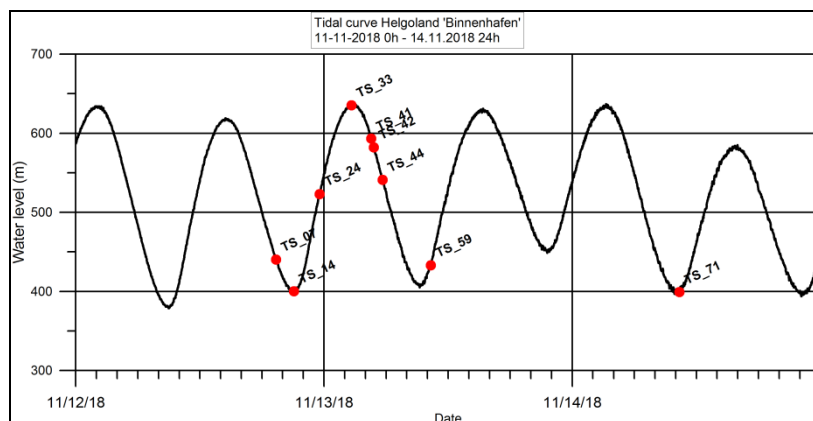


Figure 6.4. Tidal curve recorded at the Helgoland harbour gauge during the Acoustic Doppler Current Profiler survey (transect K5-K6). The red dots correspond to the current velocity/direction measurements showed in Figure 6.5.

During slack water time, the recorded current velocity over the entire water column was $<0.1\text{m/s}$, while at maximum flow the average velocity was $\sim 0.8\text{m/s}$, with peaks up to 1.2m/s . For the near-to-seafloor region, the current data of the first two meters above sea bottom (8 bin cells) were integrated.

During maximum ebb flow, near-to-seafloor current velocities ≥ 0.5 - 0.6 m/s were recorded (Figure 6.5). During maximum flood flow, the near-to-seafloor velocity rose up to ~ 0.7 m/s (Figure 6.5). The flow direction followed the general current pattern of the German Bight (westerly/easterly for ebb/flood flows). According to the complex seafloor morphology, the local flow pattern showed strong variations across the water column.

The times series of transect K5-K6 (corresponding to video track 4) pointed out such complex flow pattern (Figure 6.6). The flow direction rotated from 250° (K5-K6_TS07 in Figure 6.6) to 300° from flood to maximum ebb flow (K5-K6_TS41 and K5-K6_TS44, Figure 6.6). The flow direction moved westward and further to south-east during the ebb flow.

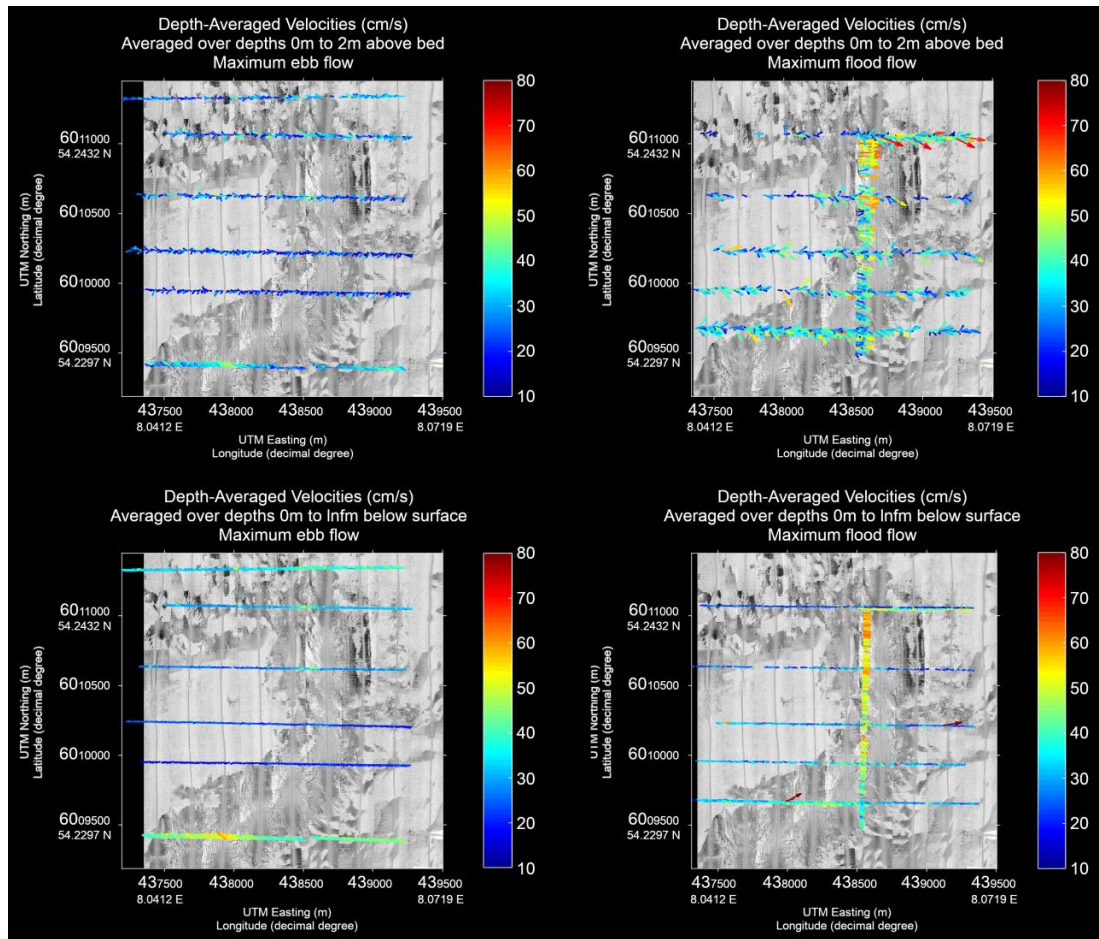


Figure 6.5. Averaged velocity vectors of the six Acoustic Doppler Current Profiler transects of November 2018 (positions in Figure 6.1D). Ebb flow 2 m above sea bottom (upper left) and over the entire water column (lower left). Flood flow 2 m above sea bottom (upper right) and over the entire water column (lower right).

The averaged maximum velocity increased from to 0.5 to 0.8 m/s at maximum ebb flow and decreased again to less than 0.5 m/s. The east-west transect across the central ridge clearly showed the influence of the HSG ridge on

the flow pattern. In fact, during the higher flow phases (both ebb and flood) the ridge altered the flow, as showed by the scattering of the current values (velocity and direction) in Figure 6.6 and in Figure 6.7. At flood flow the eastern part of the transect show a south running current in the deeper part of the water column, meanwhile the upper part shows into the opposite direction (Figure 6.7). Around slack water the pattern is heterogeneous, only at the western flank a weak flow zonation can be observed (Figure 6.6). During ebb flow, on top of the ridge a stronger north-directed current separates the current regime into three spatial sections following the morphology (Figure 6.7)

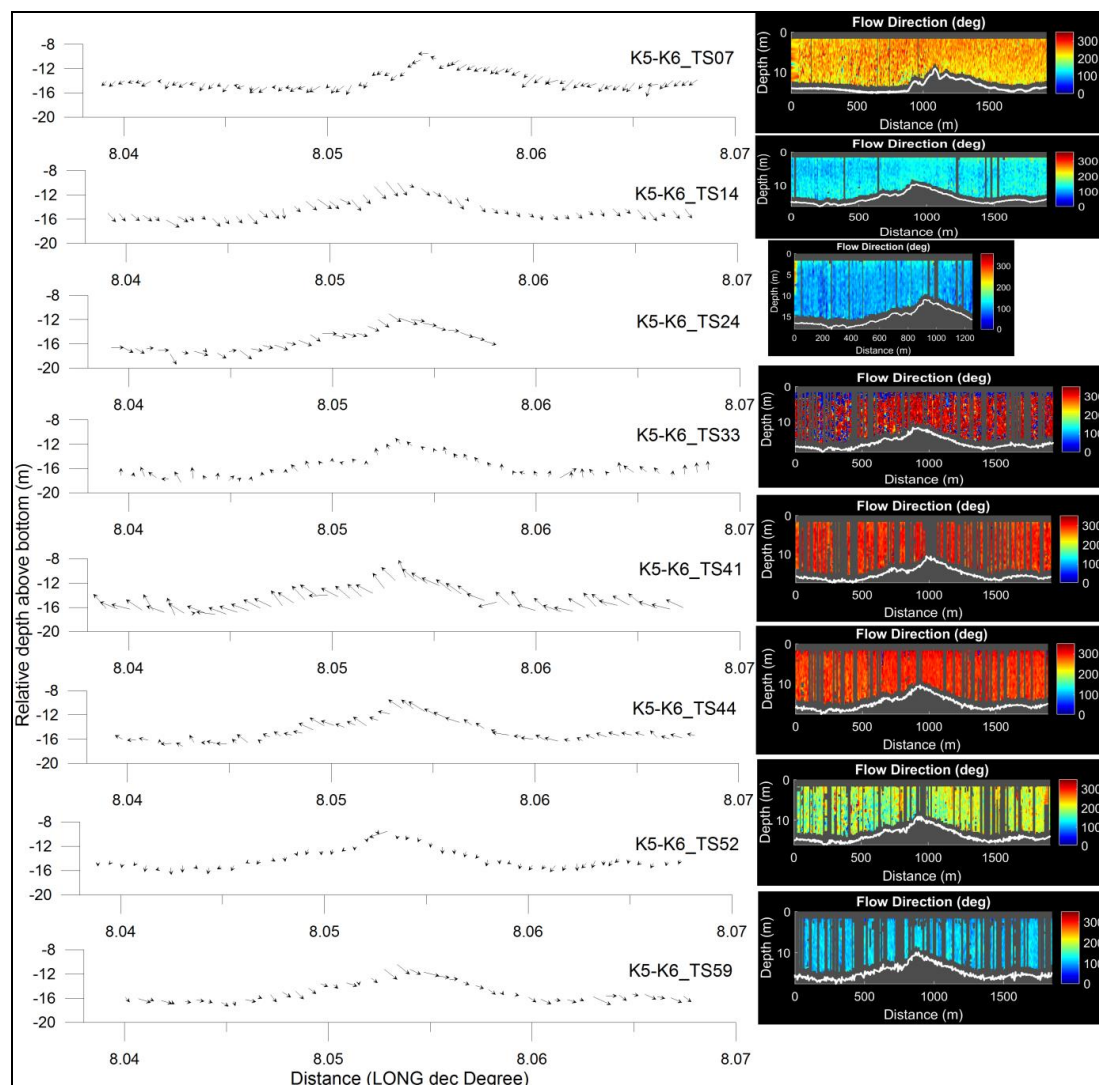


Figure 6.6. Time series of the transect K5-K6 (position in Figure 6.1D) during different tidal stages (shown in Figure 6.4). The left column shows the averaged velocity vector for the first 2 meters above sea bottom, the right column gives the velocity direction (in geographic orientation) over the entire water column.

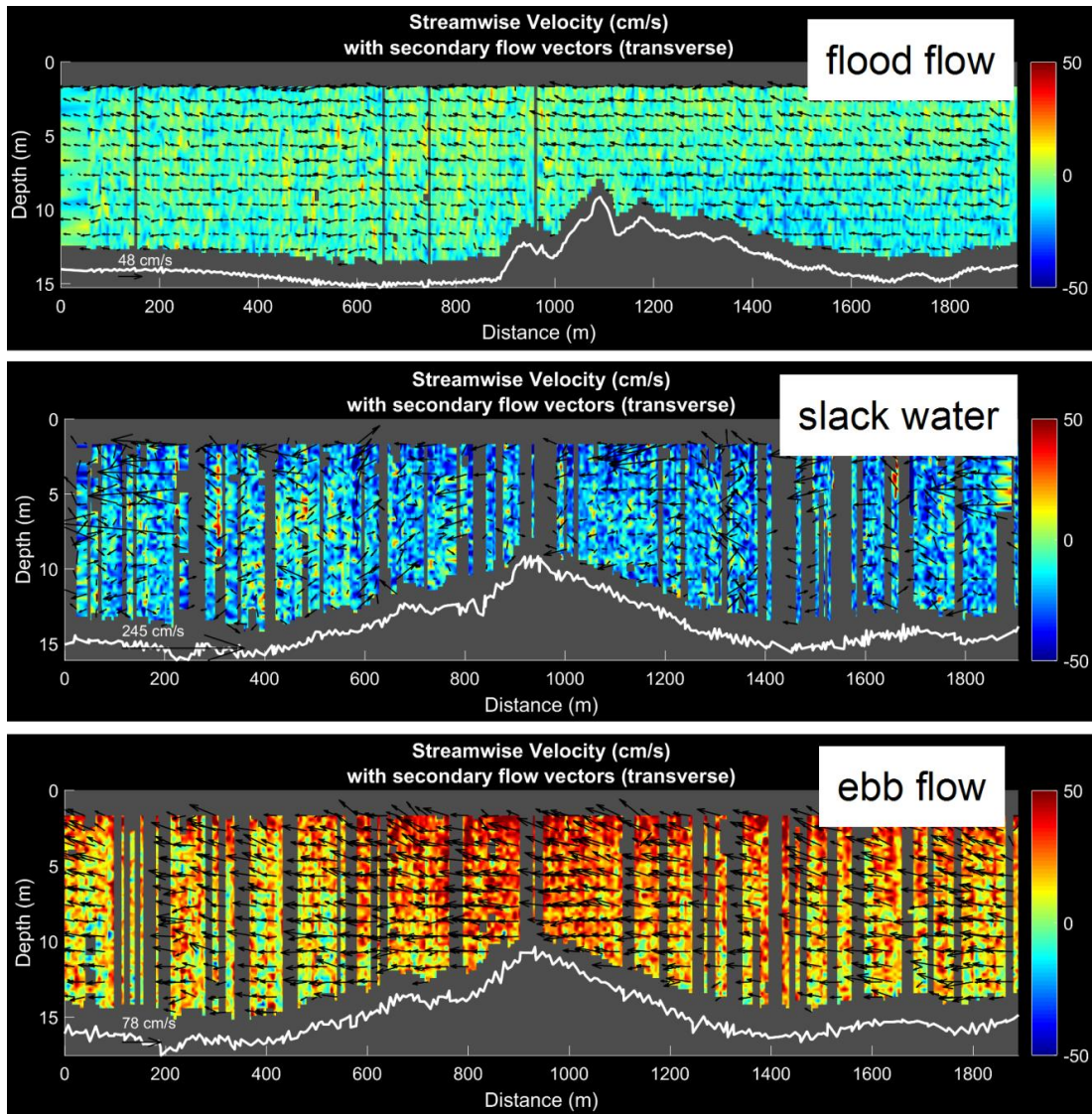


Figure 6.7. Time slots of the different tidal stages of Transect K5-K6 during ebb-flow, slack water and flood flow. The colored pattern shows the two flow direction perpendicular to the transect direction. In such a west-east-oriented transect, positive values indicate the north-directed component and negative values the south-directed component.

6.6. Discussion

The “Helgoländer Steingrund” area belongs to a small number of hard substrate sites in the German Bight, which are highly regarded due to their ecological value. It includes a very broad spectrum of sediment grain sizes, ranging from sand to large boulders, with a high spatial patchiness, which offers a potential suitable substratum for benthic communities. Such a high complexity of the substrate and its related hydrodynamic conditions influences the patchy distribution pattern of colonized and non-colonized areas. The outcomes from underwater video analysis confirmed the high biodiversity showed by Dederer et

al. (2015). In comparison to former works, the hydroacoustic mapping of the present study provided a small scale description of such complex patchiness. As similarly showed by e.g. Freitas et al. (2011), the wave analysis of the SBES signal allowed discriminating the different seabed types, which fit the grain size classes present in the area (sand, gravel and coarser deposits). Ellingsen, Gray et al. (2002) stated that “seabed homogeneity is important if each acoustic class should represent on single seabed type”. An attempt to use a higher amount of classes (respect to the ones indicated as optimal splitting level by the QTC statistics) failed to reveal a connection to the benthic coverage. While the SBES-QTC approach was successfully used in previous studies (e.g. Holler et al. 2017) to detect the presence of biogenic assemblages over soft-ground substrates, in the HSG area the SBES classification was mainly driven by the sediments and the related seafloor roughness. The main reason can be found in the relationship between the density and size of the epibenthic fauna at our study site, and the size of the area investigated by a single echo (foot print size). In fact, while the beams collected from homogeneous areas (both hard- or soft-grounds) reflect the interaction of the acoustic wave with one sediment type, the echoes covering patchy areas average the influence of different components, and their spatial relationship. This effect is even more significant due to the wave form processing, which stacks up to 5 echoes in one signal before performing the PCA. In contrast to this study, Anderson et al. (2002) analyzed SBES-QTC data along the coast of Newfoundland and distinguished “rocks” and “rocks with macrofauna”, but on a steeper depth gradient of more than 200m water depth. Their successful discrimination of macrofauna implies a much broader depth range, and in fact the same approach was successfully followed by Mielck et al. (2014), which used the hardness/roughness values of a SBES RoxAnn system in order to map the dense kelp forests around the western underwater outcrops of the Helgoland Island.

In several studies the SSS was used as a successful tool for habitat mapping (e.g. Collier and Brown 2005). Besides, the recent trend moved from the manual segmentation to semi-automatic detection tools for classifying the SSS signal, especially in coarse grain habitats (Papenmeier et al. 2018, Michaelis et al. 2019). The results of our GLCM-based semi-automatic classification showed a similar distribution pattern as Schulz (1983). The comparison of the two SSS datasets (Nov. 2016 and Nov. 2018) showed only minor changes around the ridge rim, which can be interpreted as mobile sediment layers, the mobility of which is likely controlled by storm events. The movement of these sand layers and the interaction with the rocks can act as a driving factor in preventing the

colonization of such transitional areas (Michaelis et al. 2019). The strong contrast change of sandy sediments, gravelly sediments, and hard substrates is consistently showed in the spatial distribution pattern of the SBES classification (Figure 6.3C).

However, our study points out the importance of using an integrated approach (hydroacoustic mapping and *in-situ* seafloor ground-truthing) in order to be able to spatially resolve the lateral variability of extremely patchy environments, characterized by a combination of seafloor substrates and communities, which varies on a meter-size scale. In fact, the combination of acoustic and ground truth data made possible to work out the spatial separation of the bryozoa *Flustra foliacea* and *Alcyonidium diaphanum*. While *F. foliacea* dominates the western flank and the ridge, *A. diaphanum* is most abundant in the more patchy gravel-to-boulders area (eastern flank of the ridge). Such region forms a transition zone, where the relict moraine deposits (cobbles, boulders, etc.) gradually fade into the easternmost sandy soft-ground, forming individual and isolated stones amongst gravel and sandy sediments. Such a strong zonation of the bryozoan communities could be likely linked to the local micro- and macro-hydrodynamic conditions: the former could be related to the surface roughness, as the relict moraine deposits are denser and steeper on the western flank than on the eastern one; the latter could reflect the general hydrodynamic conditions of the water column (e.g. exposure, nutrients, etc.), as a result of the interaction between the general circulation and the local morphology of the seafloor (ridge) (Dyrynda 1994).

The ADCP data shows a general flow pattern with current velocities of almost 1 m/s during flood flow, in accordance with the major current regime of the tidal driven circulation in the North Sea (Sündermann and Pohlmann 2011, Staneva et al 2009). However, the presence of the half-moon shaped ridge had a strong influence in modifying the temporal and spatial current flow pattern. In fact, during the different tidal stages the ridge divides the current flow in opposite directions. The maximum flow velocities show a slightly stronger impact of the flood current, which helps explaining the dominance of *F. foliacea* in this region. A closer look into the current profiles shows a stronger variation in direction and velocity in the near-to-seafloor region of the ridge and in the transition zone to the east (Figure 6.6 and Figure 6.7). Such a flow pattern shows a similar behavior to the one occurring over bedforms (e.g. ripples or dunes). Kwohl et al. (2014) analyzed the relationship between mobile bedforms and tides. Dunes with height of up to 8 m (similar in size to the HSG hard substrate topography) show that the flow velocity strongly increases when the flood flow hits the steep site of the

dune, and then decreases on the less steep lee side. On the contrary, during ebb flow the water hits the less steep site first and decelerates significantly at the steep lee side of the ridge. This can explain the general difference of both sides of the ridge but the patchiness along the transition zone needs to be downscaled. This locally sheltered area is the preferred place of *A. diaphanum*, which avoids stronger currents (Porter et al. 2001). Migné and Davoult (2002) that species like *A. diaphanum* generally prefer strong tidal currents exposed areas. That contradicts with our observation of currents, with estimated velocity of 0.3 m/s close to the seabottom. It has to be considered, that the resolution of our ADCP is limited (due to a 0.25 m bin size), but still the data represents a phase of higher hydrodynamic conditions of the fall period in the North Sea.

6.7. Conclusion

At the hard substrate area “Helgoländer Steingrund” (HSG) hydroacoustic devices, underwater videos, and bottom samples were used for mapping and classifying such very patchy and coarse grained habitat. The SBES and SSS data allowed a clear distinction of the morphological units, including the rocky ridge, its flanks and the transition zones toward the gravelly-sandy surrounding areas. The major challenge in the hydroacoustic data was the identification of colonized and non-colonized hard substrates in the small-scale patchy areas composed of the full range of grain sizes, from gravel to boulder.

Three classes of sediment types were identified. While the acoustic-based approach could not resolve the biotic components (colonized vs non-colonized substrates) or their specific fingerprints (the difference between bryozoan species), the use of underwater videos allowed a more detailed classification into six different seabed types, which took into account both the abiotic (sediments, morphology, etc.) and biotic components. The two flanks of the ridge and the transition to the surrounding softground areas resulted to be differentiated into two regions, with a distinct dominance of the bryozoa *F. foliacea* and *A. diaphanum* on the western and on the eastern side, respectively.

The comparison between SBES and SSS dataset showed a similar distribution of the main three acoustic classes (corresponding to sand, gravel, and hard substrate); however, the SSS overrated the sand and the SBES the hard substrate areas. Although the presence of distinct benthic communities was not detected in the hydroacoustic data, SSS images can be successfully applied for a high resolution mapping of hard substrates, which can be used as surrogates for the presence of bryozoan assemblages. The occurrence of bedforms in the

northeastern part of the study site and the strong heterogeneity in colonization of the hard substrate reflect complex hydrodynamic conditions. This is proved by the outcomes of the ADCP data, which could show the general flow pattern at this side but even resolved the local variability of current pattern dependent on the tidal stage and on the bottom relief. At this stage the influence of waves was not considered, which is in addition an important driver for local hydrodynamics. More small-scaled hydrodynamic data and the use of habitat models will help in resolving the complexity of the patchy habitat in future.

6.8. Acknowledgments

This study is financed by the German Research Foundation (DFG) and is part of the INTERCOAST project, which is a collaboration of the University of Bremen, the Senckenberg Institute in Wilhelmshaven and the University of Waikato. The authors would like to thank the crew of the RV Senckenberg for the support on the vessel.

Many thanks go to the Federal Maritime and Hydrographic Agency (BSH) Hamburg which provided the (MBES) multibeam data for the bathymetry. The authors are grateful to Astrid Raschke for the grain-size analysis, to Maik Wilsenack for the technical support and to our student assistant Vanessa Köhler.

The data reported in this paper will be archived in Pangaea (www.pangaea.de)

6.9. References

- Anderson J T, Gregory R S, Collins W T (2002) Acoustic classification of marine habitats in coastal Newfoundland. *ICES Journal of marine Science*, 59, 156-167.
- Arendartchuk F, Prado M F V, Bonetti J (2017) Classification of geomorphological in Pântano do Sul Bay (SC) from side-scan sonar images. 2017 IEEE/OES Acoustics in Underwater Geosciences Symposium (RIO Acoustics).
- Bartholomä A. (2006) Acoustic bottom detection and seabed classification in the German Bight. *Geo Mar. Lett.*, 26, (3), 177-184, doi: 10.1007/s00367-006-0030-6.
- Bartholomä A Holler P, Schrottke K, Kubicki A (2011) Acoustic habitat mapping in the German Wadden Sea - Comparison of hydro-acoustic devices. *Journal of Coastal Research*, Spec Issue, 64, 1-5.
- Brezina, J. (1979). Particle size and settling rate distributions of sand-sized materials. PARTEC - 2nd European Symposium on Particle Characterization. Nürnberg, 1-47.
- Callies U, Gaslikova L, Kapitza H, Scharfe M (2017) German Bight residual current variability on a daily basis: principal components of multi-decadal barotropic simulations. *Geo-Marine Letters*, 37(2), 151-162, doi: 10.1007/s00367-016-0466-2.

- Collier J S & Brown C J (2005) Correlation of sidescan backscatter with grain size distribution of seabed sediments. *Marine Geology*, 214, 431-449.
- Dederer G, Boos K, Kanstinger P, Krone R, Schneider C, Beher J, Kuhlenkamp R, Kind B (2015) Tauchuntersuchung des „Steingrund“ bei Helgoland (FFH DE 1714 - 391) und Konzeptentwicklung eines Tauch Monitorings für den FFH Lebensraumtyp Riff. Final report, 74 p.
- Dyrynda, P. (1994), Hydrodynamic gradients and bryozoan distributions within an estuarine basin (Poole Harbour, UK), Olsen & Olsen, Fredensborg.
- Ellingsen K E, Gray J S, Bjørnbom E (2002) Acoustic classification of seabed habitats using the QTC VIEW system. *Jour. Marine Science*, 59, 4: 825-835.
- BfN (Federal Agency for Nature Conservation) (2018) Die Meeresschutzgebiete in der deutschen ausschließlichen Wirtschaftszone der Nordsee - Beschreibung und Zustandsbewertung, (2. überarb. Auflage). BfN-Report, 477, 486 p.
- Feldens P, Schulze I, Papenmeier S, Schönke M, Schneider von Deimling J. (2018) Improved Interpretation of Marine Sedimentary Environments using Multi-Frequency Multibeam Backscatter Data. *Geosciences*.
- Freitas R F, Ricardo F, Pereira L, Sampaio S, Carvalho M, Gaspar V, Quintino V, Rodrigues A M (2011) Benthic habitat mapping: Concerns using a combined approach (acoustic, sediment and biological data). *Estuarine, Coastal and Shelf Science*, 92, 598-606.
- Folk, R L (1954) The distinction between grain size and mineral composition in sedimentary-rock nomenclature. *Journal of Geology*, 62, 4, 344-359.
- Freitas R, Silva S, Quintino V, Rodrigues A M, Rhynas K P, Collins W T (2003) Acoustic seabed classification of marine habitats: studies in the western coastal-shelf area of Portugal. *Jour. Marine Science*, 60, 599-608.
- Greene A, Rahman A F, Kline R, Rahman M S (2018) Side scan sonar: A cost-efficient alternative method for measuring seagrass cover in shallow environments. *Estuarine, Coastal and Shelf Science*, 207, 250-258.
- Haralick R M, Shanmugam S, Dinstein S (1973) Textural Features for Image Classification. *IEEE Transactions on Systems, Man and Cybernetics*, 3 (6), 610-620.
- Hass Ch, Mielck F, Fiorentino D, Papenmeier S, Holler P, Bartholomä A (2017) Seafloor monitoring west of Helgoland (German Bight, North Sea) using the acoustic ground discrimination system RoxAnn. *Geo-Mar Lett*, 37, 125–136, doi 10.1007/s00367-016-0483-1.
- Holler P, Markert E, Bartholomä A, Capperucci R, Hass C H, Kröncke I, Mielck F, Reimers C H (2017) Tools to evaluate seafloor integrity: comparison of multi-device acoustic seafloor classifications for benthic macrofauna-driven patterns in the German Bight, southern North Sea. *Geo-Mar Lett*, 37 (2), 93-109.
- Kluijver M J de (1991) Sublittoral hard substrate communities off Helgoland. *Helgoländer Meeresuntersuchungen*, 45, 317-344.
- Kühne S & Rachor S (1996) The macrofauna of a stony sand area in the German Bight (North Sea). *Helgoländer Meeresuntersuchungen* 50 (4), 433-452.
- Kwoll E, Becker M, Winter Ch (2014) With or against the tide: The influence of bed form asymmetry on the formation of macroturbulence and suspended sediment patterns. *Water Resources Research*, 50 (10), 7800-7815, doi: 10.1002/2013WR014292.

-
- Lambeck K, Purcell A, Funder S, Kjær K H, Larsen E, Møller P E R (2006) Constraints on the Late Saalian to early Middle Weichselian ice sheet of Eurasia from field data and rebound modelling. *Boreas* 35 (3), 539-575.
- Michaelis R, Hass CH, Mielck F, Papenmeier S, Sander L, Ebbe B, Gutow L, Wiltshire KH (2019) Hard-substrate habitats in the German Bight (South-Eastern North Sea) observed using drift videos. *Journal of Sea Research*, 144, 78-84. <https://doi.org/10.1016/j.seares.2018.11.009>
- Mielck F; Bartsch I; Hass H C, Wölfl A C; Bürk D, Betzler C (2014) Predicting spatial kelp abundance in shallow coastal waters using the acoustic ground discrimination system *RoxAnn*. *Estuar. Coast. Shelf Sci.*, 143, 1–11.
- Migné A & Davoult D (2002) Experimental nutrition in the soft coral *Alcyonium digitatum* (Cnidaria: Octocorallia): removal rate of phytoplankton and zooplankton. *Cahiers de Biologie Marine*, 43 (1), 9-16.
- Papermeier S, Hass C H (2018) Detection of Stones in Marine Habitats Combining Simultaneous Hydroacoustic Surveys, *Geosciences* 2018, 8 (8), 279; doi:10.3390/geosciences8080279.
- Parsons D R, Jackson P R, Czuba J A, Engel F L, Rhoads B L, Oberg K A, Best J L, Mueller D S, Johnson K K, Riley J D (2013) Velocity Mapping Toolbox (VMT): a processing and visualization suite for moving-vessel ADCP measurements. *Earth Surf. Process. Landforms*, 38, 1244-1260.
- Porter J S, Hayward P J, Spencer Jones M E (2001) The identity of *Alcyonidium diaphanum* (Bryozoa: Ctenostomatida), *Journal of the Marine Biological Association*, 81 (6), 1001-1008, doi: <https://doi.org/10.1017/S0025315401004970>.
- Pratje O (1951) Die Deutung der Steingründe in der Nordsee als Endmoränen, *Deutsche Hydrographische Zeitschrift*, 4 (3), 106-114, doi: 10.1007/bf02027271.
- Preston J M, Collins W T (2000) Bottom classification in very shallow water by high-speed data acquisition. *Oceans Conference Record (IEEE)*, 2, 1277, doi: 1282 vol.2. 10.1109/OCEANS.2000.881778.
- Quester Tangent (2004). "QTC IMPACT User Manual."
- Quintino V, Freitas R, Mamede R, Ricardo F, Rodrigues A M, Mota J, Perez-Ruzafa A, Marcos C (2010) Remote sensing of underwater vegetation using single-beam acoustics. *ICES Journal of Marine Science*, 67, 594-605, doi: 10.1093/icesjms/fsp251.
- Rachor E & Nehmer P (2003) Erfassung und Bewertung ökologisch wertvoller Lebensräume in der Nordsee-Abschlussbericht für das F+E-Vorhaben FKZ 899 85 310. Report, Bundesamt für Naturschutz, 175 pp.
- Schulz H (1983) Der Steingrund bei Helgoland - Restsedimente einer saaleiszeitlichen Endmoräne. *MEYNIANA*, 35, 43-53.
- Schwarzer K, Ricklefs K, Bartholomä A, Zeiler, M (2008) Geological development of the North Sea and the Baltic Sea. *Die Küste*, 74, 1-17.
- Staneva J, Stanev E, Wolff J-O, Badewien T, Reuter R, Flemming BW, Bartholomä A, Bolding K (2009) Hydrodynamics and sediment dynamics in the German Bight: A focus on observations and numerical modelling. *Continental Shelf Research*, 29 (1), 302-319.
- Teff J P, Goff J (2014) Megaclasts: Proposed revised nomenclature at the coarse end of the Udden-Wentworth grain-size scale for sedimentary particle. *Jour. Sed. Res.*, 84, 192-197.

- Zeiler M, Schwarzer K, Bartholomä A, Ricklefs K (2008) Seabed Morphology and Sediment Dynamics. - *Die Küste*, 74, 31-44.
- Sündermann J & Pohlmann T (2011) A brief analysis of North Sea physics, *Oceanologia*, 53 (3), 663-689.
- Stocks T (1955) *Deutsche-Hydrographische Zeitschrift* 8: 112.
<https://doi.org/10.1007/BF02019797>.

Page left intentionally blank

Chapter 7

Benthic biodiversity changes in response to dredging activities during the construction of a deep-water port

Ruth Gutperlet*, Ruggero Maria Capperucci*, Alexander Bartholomä*,
Ingrid Kröncke*

*Marine Research Division, Senckenberg am Meer, Südstrand 40, 26382 Wilhelmshaven

7.1. Abstract

During the construction of a deep-water port (JadeWeserPort), bathymetry, sediment distribution and macrofauna community structure were studied in the Inner Jade, a highly anthropogenically impacted tidal channel located in the southern North Sea. In order to assess the effects of additional disturbance by dredging activities, macrofaunal community compositions between 2002 (before the construction work had begun) and 2010 (during the final construction phase) were compared. The sand extraction for land reclamation and the redirection of the fairway changed the bathymetry markedly. While the old fairway in the centre of the study area remained mud dominated, a general increase in coarser sediments was detected in 2010. The dynamic nature of the study area in combination with the direct and indirect effects of dredging increased bathymetric heterogeneity (measured by singlebeam (2002) and multibeam (2010) echo-sounder). In 2010, the macrofauna community structure roughly resembled the different categories of dredging activities. The most recently dredged northwestern area was inhabited by a community, which was different from the community in the regularly dredged old fairway. Both were different from the community in the northeastern non-dredged area. In the

Gutperlet, R., Capperucci, R.M., Bartholomä, A., Kröncke, I. 2015. Benthic biodiversity changes in response to dredging activities during the construction of a deep-water port. Marine Biodiversity, 45 (4), 819-839, doi: 10.1007/s12526-014-0298-0.

southern area and in the transition areas between the other three communities a fourth community was found. A general increase of macrofaunal abundance and taxa number was observed in 2010, with the exception of the recently dredged area. The structure of the macrofauna community during the port construction phase seemed to be determined by secondary dispersal of the dominant taxa and recolonisation by highly mobile and opportunistic species.

Keywords: *JadeWeserPort, Sediment extraction, Benthos, Physical disturbance, Recolonisation*

7.2. Introduction

Human use of coastal regions has a long history and various anthropogenic effects on the marine ecosystems have been documented (Halpern et al. 2008). In particular, the North Sea is highly frequented as a provider of food, energy and other resources and is used as a waterway for freight transport from all over the world (Lozán et al. 2003). The sustainable use of marine resources requires research of natural and anthropogenically induced changes in this already highly impacted ecosystem.

Macrofauna communities seem to be primarily determined by the substrate type (Green et al. 1995; Auster and Langton 1999), but hydrodynamically mediated food availability also plays a major role in their distribution, structure, and diversity (Rosenberg 1995; Pearson 2001; Wieking and Kröncke 2005; Kröncke 2006). Thus, the substrate in relation to the food availability determines to a large extent the occurrence of benthic species and may modify the recovery from disturbance. Many species living in hydrodynamically exposed sandy habitats, exhibit behaviors and feeding modes that enable them to survive daily tidal scouring events (Gorzelay and Nelson 1987; Reiss and Kröncke 2001; Nehmer and Kröncke 2003). Conversely, species found in low-energy muddy habitats are adapted to low oxygen, hydrogen sulphide enriched environments (Forbes et al. 1994; Reiss and Kröncke 2001; Kröncke et al. 2004). Thus, soft bottom macrofauna community structure is strongly related to both hydrodynamic force and sediment composition (Warwick and Uncles 1980; Rhoads and Boyer 1982; Yates et al. 1993). Therefore, macrofauna communities are often used as an indicator of physical disturbance such as dredging and dumping activities (Muxika et al. 2005; Taupp and Wetzel 2013; Whomersly et al. 2008), which affects the hydrodynamic regime as well as the sediment composition.

The impact of sediment extraction (e.g. dredging activities) on macrofauna has been well documented in European waters (e.g. Newell et al. 1998; Sardá et al. 2000; vanDalfsen et al. 2000; Simonini et al. 2007). Direct effects of sediment extraction can include an initial reduction in species diversity, abundance, and biomass (Sutton and Boyd 2009). Even the areas around the dredging site can be indirectly affected by sediment resuspension, the release of nutrients and chemicals, and changes in food resources by shifts of plankton bloom seasons (Boyd et al. 2005; Newell et al. 1998; Simonini et al. 2007; vanDalfsen et al. 2000). Thus, the key question is not whether dredging activities have an impact, but to which extent the affected macrofauna communities can recover MESL (Marine Ecological Survey Limited 2007). Although the recovery rates are highly site-specific (Boyd et al. 2004; Cooper et al. 2005; Kenny and Rees 1994; 1996; Kenny et al. 1998), some general principals are well known.

Based on the adaptive strategies of different assemblages and environmental conditions, there is evidence that communities found in hydrodynamically active sandy habitats will recover more quickly following physical disturbance than those found in less energetic muddy environments (Hall 1994; Kaiser 1998; Ferns et al. 2000). The recovery process of a disturbed habitat follows a succession of species composition over time (Pearson and Rosenberg 1978; Zajac et al. 1998). This sequence of colonization and extinction depends on the severity of the disturbance e.g. total or partial biota removal (Pearson and Rosenberg 1978; Gutt and Starmans 2001; Sousa 2001; Valdivia et al. 2005) and the coupling with additional disturbance events (e.g. Cifuentes et al. 2007; Sugden et al. 2007). The size of the patch to be colonized (e.g. Petraitis and Latham 1999; Petraitis and Dudgeon 2004; Norkko et al. 2006) and the seasonal variation in the supply of colonizers (e.g. Morgan 2001) determines the recolonisation time. Moreover, succession is mediated by biological interactions (e.g. inhibition, facilitation, and tolerance) among early and late colonizing species (Connell and Slatyer 1977). Any of these factors can complicate the community response to disturbance. In particular, when dredging activities remove the surface layers of sediments, the remaining substratum may comprise a totally different sediment type than the original one and might be unsuitable for recolonization by the species that previously inhabited the area (Kenny and Rees 1996; Boyd et al. 2005).

However, the generated mosaic of different macrofaunal succession stages integrates spatial and temporal changes in the marine ecosystem (Johnson 1972). Thus, in environmental impact assessments, the macrofauna community composition is used as an essential tool for the evaluation of the status quo of the

ecosystem (Warwick 1993, Borja et al. 2013). Knowledge about benthic macrofaunal succession patterns can help to understand the dynamics of community structure and the responses to human induced disturbances (Berlow and Navarrete 1997). For the improvement of such succession models, an understanding of processes that occur throughout an ongoing disturbance is crucial (Vöge et al. 2008), but the intermediate state is often missing in the standard before/after disturbance analyses.

During the land reclamation for the construction of a deep-water port in the southern North Sea (JadeWeserPort - JWP, Germany), sediments were extracted from the Inner Jade, changing the physical conditions of the local marine environment. The Inner Jade is a naturally dynamic system (Dörjes et al. 1969, Schuchardt et al. 2007). As early as the 1960s, macrofauna community structure and sediment distribution in the Jade were influenced by the local fishery and dredging and dumping activities (Dörjes 1992). Based on differences in macrofauna and sediments between the 1960s and 2002, the western part of the Inner Jade was classified as a “heavily modified water body” (Schuchardt et al. 2007). In qualitative comparison, one third of the formerly present polychaetes did not appear in 2002 and one third of the polychaetes was not found by Dörjes et al. in the 1960s. Additionally, fewer bivalves and more mobile crustaceans were detected by Schuchardt et al. in 2002. This altered macrofauna community structure was most likely caused by changes in hydromorphology due to land reclamations, construction of pile founded jetties, and deepening of the old fairway (Schuchardt et al. 2007).

Thus, the overarching aim of the present study was to assess the impact of the dredging and dumping activities for the JWP as additional stressors in the already anthropogenically disturbed Inner Jade. In order to evaluate the status quo of an ecosystem, it is recommended to use historical data of the formerly undisturbed state as a reference condition, if there is no pristine area nearby (Borja et al. 2012). Because of the natural and anthropogenically induced heterogeneity in the Inner Jade, the areas adjacent to dredged parts of the study area were not suitable to represent an undisturbed condition and probably also were (indirectly) affected by the dredging activities for the JWP. Thus, changes in bathymetry, sediment distribution, biodiversity, taxa number, abundance, and macrofauna community structure were compared between the period before the port construction (2002) and during the final construction phase (2010). An earlier comparison between the 2002 dataset and the historic references study from the 1960s by Dörjes et al. (1969) was carried out by Schuchardt et al. (2007). The specific objectives of the present study were i) to document the physical

disturbance caused by the dredging and dumping activities for the JWP and ii) to study the direct and indirect effects of these activities on the spatial distribution of sediments and macrofauna communities.

7.3. Material and methods

7.3.1. Study area

The Inner Jade is a tidal channel in the German Bight of the southern North Sea, which is bordered by the Outer Jade to the north and the Jade Bay to the south. It is classified as an upper mesotidal regime with semi-diurnal tides ranging from 2.8 m at the entrance of the channel in the north to 3.8 m at the Jade Bay in the south (Kubicki and Bartholomä 2011). The eastern channel margin of the Inner Jade is separated from the Weser estuary by a broad tidal flat area. In March 2008, land reclamation started for the JWP, a deep-water port in the western Inner Jade. For completion in 2012, around 46 million m³ sand was required to create the 360 ha terminal area (Kluth and Ehmen 2010). The study area comprised the subtidal areas around the JWP with the redirected fairway in the Inner Jade between km 14.5 and km 7.1 of the old fairway (Figure 7.1a).

The old fairway in the centre of the Inner Jade connects the harbours of Wilhelmshaven with the North Sea. Its width of 300 m and a minimum guaranteed depth of 20.1 m (referred to the local chart datum, Normalhöhennull (NHN)) are maintained by regular dredging with a hopper suction dredger (Kubicki and Bartholomä 2011). The local harbour “Neuer Vorhafen” at the southern Inner Jade is also periodically dredged (Figure 7.1a).

Several dumping sites are located in the Outer and Inner Jade (BfG and WSA 2003; Figure 7.1a). The closest site is located 4.7 km south of the southern border of the study area. Dumping of fine, mobile sediments (e.g. extracted from the old fairway or the harbour “Neuer Vorhafen”) has potential effects on the sediment distribution in the study area.

In the 1960s, the seafloor of the study area was mainly dominated by medium to fine sand, while finer sediments (silt to silty fine sand) were present on the shallowest slopes of the channel (Dörjes et al. 1969). The Jade channel itself was characterised by medium sand, locally by fine or coarse sand (Dörjes et al. 1969; Irion 1994). At that time, the spatial distribution of the different macrofauna communities in the Jade largely corresponded to the sediment types in the study area (Dörjes et al. 1969). The *Petricolaria pholadiformis* community occurred, where finer sediments prevailed on the shallow slopes of the Jade

channel. The *Magelona papillicornis* community appeared in medium sand on the current slopes, whereas the *Ophelia limacina* community was found on the coarser sediments of the Jade channel. Quantitative abundance data from the 1960s were not available.

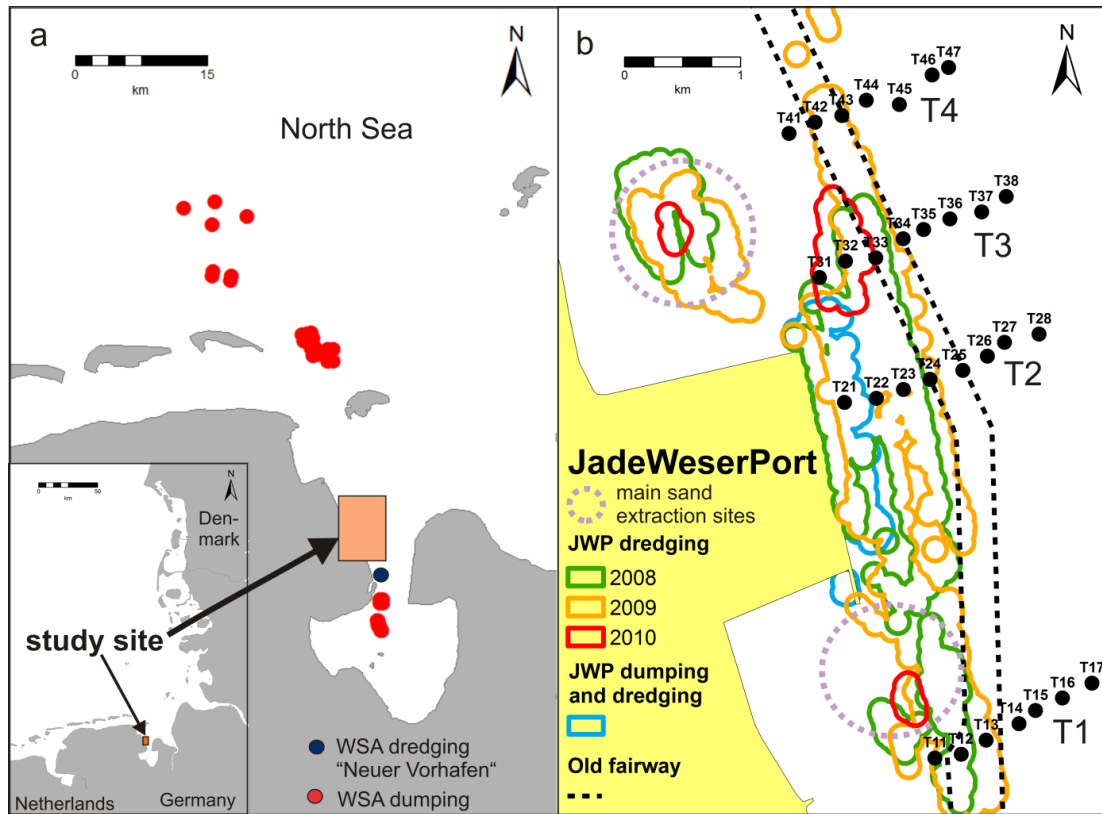


Figure 7.1. Location of a) the study area in the German Bight of the southern North Sea and b) the main features related to the modified coastline (yellow: land), the construction activities for the “JadeWeserPort” (JWP), and the regularly dredged old fairway (pointed lines). Along the transects (T1-T4) the location of the sampling stations (black dots) are shown in relation to the dredging and dumping activities for the JWP.

7.3.2. Dredging and dumping data

For land reclamation sand was mainly taken from two extraction sites, north and south of the new port area (Figure 7.1b). In order to enable access to the JWP, a new fairway was dredged (Figure 7.2). Suction and suction cutter dredgers were mainly employed for sand removal. Backhoe dredgers were used for mining compact clay deposits underneath, the “Lauenburger Ton” formation. Since this clay was not suitable for land reclamation, the extracted “Lauenburger Ton” was dumped into the formerly exploited southern sand extraction site (Kluth and Ehmen 2010). Before piling, fine soft material had to be replaced by coarser sediments. Therefore, sand was dumped not only directly in the land reclamation zone, but also in front of the new bulkhead (Figure 7.1b).

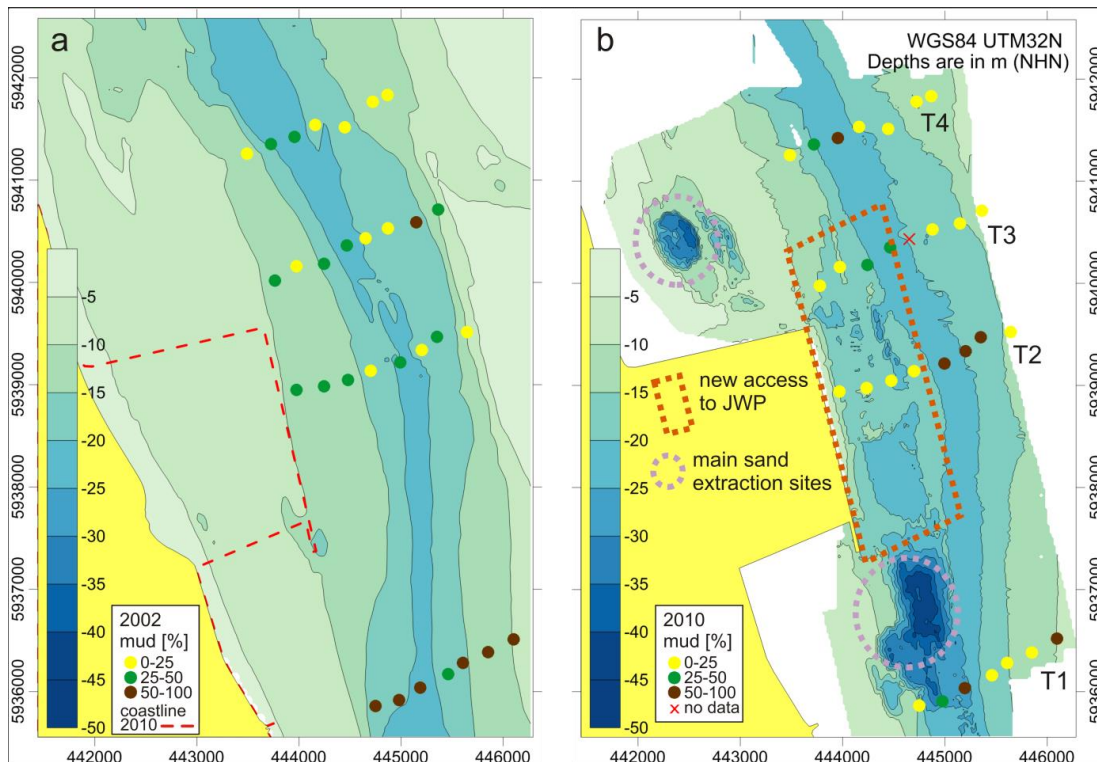


Figure 7.2. Bathymetry of the study area (depths in m referred to Normalhöbennull (NHN)) and mud content (percentage by weight) at the sampling stations in a) 2002 and b) 2010.

The JadeWeserPort Realization Company provided data on their dredging and dumping activities: position, date, time, and dredging volume (no data for the dumping of “Lauenburger Ton” into the southern pit). Since only midpoint coordinates were given, a buffer of 100 m was created around each dredging and dumping position. These data were merged according to four categories (Figure 7.1b): dredging and dumping (2008-2010), dredging 2008 (March-December), dredging 2009 (January-December), dredging 2010 (January-May). Within the 100 m radius around each sampling station, all dredging and dumping activities before and during the sampling were summed up. All stations with dredging or dumping activities within the 100 m radius were classified as directly affected by these activities (Table 7.1).

The local harbour authority WSA (Wasser- und Schifffahrtsamt Wilhelmshaven) provided data on the yearly total sediment volumes, that were dredged in the old fairway (between km 8 and km 12) in the years 2000-2002 and 2008-2010.

categories of disturbance	stations
construction works for JWP	(n = 11)
dumping + dredging (2008-2010)	T21
dredged in 2010	T31, T32
dredged in 2009	T12, T13, T21-T24, T32, T33, T42, T43
dredged in 2008	T12, T21-T23, T32, T33
maintenance of the old fairway	(n = 8)
regularly dredged (also before 2002)	T12, T13, T24, T25, T33, T34, T42, T43
non-dredged areas	(n = 17)
	T11, T14-T17, T26-T28, T35-T38, T41, T44-T47

Table 7.1. Areas of interest according to the categories of disturbance in the study area with the involved sampling stations.

7.3.3. Bathymetric data

In order to study the changes in seafloor topography between 2002 and 2010, two Digital Terrain Models (DTM) were generated based on bathymetric measurements.

For 2002, data was provided by the federal maritime and hydrographic agency BSH (Bundesamt für Seeschifffahrt und Hydrographie) and the WSA, measured by singlebeam echosounder (SBES). In May 2010, bathymetric data was recorded on board the RV “Senckenberg” by means of a Reson 8125 multibeam 455 kHz echosounder (MBES) along 14 main transects parallel to the old fairway (north-south oriented). In order to obtain better coverage, the resulting dataset was combined with MBES data collected on behalf of the JadeWeserPort Realization Company in April 2010.

Both the 2002 and 2010 data were processed by means of Global Mapper 13™ for data cleaning, quality checking and interpolation. Two grid files were generated (25 m grid cell size). Depths were referred to the local chart datum (Normalhöhennull, NHN). The final maps (with 5 m interval contour lines) were generated by means of Surfer 10 Golden Software™.

7.3.4. Sampling and sample procedure

The company BIOCONSULT (Bremen) provided data of the sediment and macrofauna distributions in the Inner Jade for April 2002 (Schuchardt et al. 2003). In total, they sampled 30 stations along four west-east oriented transects. One sample per station was collected using a 0.1 m² van Veen grab.

From each sample a subsample (approx. 200 ml) was removed for grain size analysis. The remaining sample was washed over a 1 mm mesh and macrofauna was fixed with 70% ethanol. At three stations (T17, T33, T41) no macrofauna was found by BIOCONSULT.

The sediment grain size composition for the 2002 sediments was determined by the company BÖL (Bremen) according to DIN 18123 (1983). For this procedure, wet and dry sieving with six mesh sizes according to DIN 4022 (1987) were used, after shells > 5 mm were discarded.

In May 2010, a survey was carried out with the RV “Senckenberg”. Sediment and biological samples were collected along four transects (T1-T4), matching the previously investigated stations (Figure 7.1b). A total of 30 stations were sampled twice with a 0.1 m² van Veen grab.

One sample was used to take a subsample (approx. 150 ml) for laboratory grain size analysis. In the laboratories of Senckenberg am Meer the sediment samples were separated into mud fraction (<63 µm) and sand/gravel fraction by wet sieving over 63 µm mesh size. The sand fraction was analysed by means of settling velocity measurements in the MacroGranometer™ settling tube (Brezina 1979). The gravel content (>2,000 µm) was determined by dry sieving over a 2,000 µm mesh. At one station (T35) no sediment sample was collected for May 2010.

Because of the different methods of analyses used by Senckenberg am Meer and BÖL, sediment data was presented as mud content (<63 µm) and sand content (>63 µm and <2,000 µm). Only for 2010, gravel content (>2,000 µm) was added.

The other sample was sieved over a 1 mm mesh and the retained macrofauna samples were fixed in a 4% buffered seawater formalin solution. Organisms were identified to the lowest taxonomic level possible. After counting, the sorted animals were preserved in 70% ethanol and their biomass (wet weight) was determined to an accuracy of ±0.0001g. Although the lack of replicates has the potential for misinterpretation, only one sample per station could be used to compare the macrofauna abundance with the 2002 dataset (also only one sample per station).

The biological data was taxonomically adjusted to allow for comparison between 2002 and 2010. For some taxa, the taxonomic resolution differed between BIOCONSULT and Senckenberg. As a consequence, taxa belonging to the genera *Ampharete*, *Autolytus*, *Caprella*, *Cheirocratus*, *Ensis* or the families *Anoplodactylidae*, *Mytilidae* sp. juv. or the order *Anthozoa* were all lumped at the genus/family/order level respectively. *Hydrozoa*, *Bryozoa*, *Balanidae* and single large, mobile epifauna were not sampled quantitatively by using the van Veen grab and were excluded from analysis.

7.3.5. *Statistical data analyses*

The effective number of taxa was chosen as the measure of community diversity, because it provides the true diversity (not the entropy) in units of the number of taxa (Jost 2006). Other diversity indices can easily be converted into this linear number of equally-common taxa, e.g. the exponent of the Shannon-Wiener index gives the effective number of taxa (Jost 2006). The significance of changes in taxa number, abundance and effective number of taxa was tested with one way ANOVA using PAST version 2.17.

Changes in the macrofauna community structure were determined by cluster analyses performed with abundance data from 2002 and 2010 after fourth root transformation using the PRIMERTM v6 program package. Similarities between sampling sites were calculated with the Bray-Curtis coefficient and interpreted by means of the similarity profile permutation test SIMPROF, which tests the null hypothesis that a specific set of samples, which are not a priori divided into groups, do not differ from each other (Clarke and Gorley 2006). The similarity percentage routine, SIMPER, compares the taxa abundance between the clusters and identified which taxa characterised the different macrofauna communities (Clarke and Warwick 2001). Regarding the most common feeding type of species, they were characterised as omnivores/predators, deposit feeders, and suspension feeders. BIOENV tested for significant Spearman rank correlations (Clarke and Ainsworth 1993) between the community structure in 2010 and the dredging activities for the JWP (number of dredging days), depth or the sediment composition (gravel, sand, and mud content). Therefore the resemblance matrix of macrofauna abundance/biomass was compared with the resemblance matrix of the normalized abiotic variables. The significance of the correlation was determined using a permutation procedure. Results indicated which abiotic variable explained the highest percentage of the variability within the macrofauna dataset in 2010.

The routine RELATE was used to match the resemblance matrices of 2002 and 2010 in order to compare the similarity of patterns in the macrofauna abundances (Clarke and Gorley 2006). The significance of differences between clusters was tested with one-way PERMANOVA (Anderson et al. 2008) using fourth root transformed abundance data. The routine PERMDISP was used for testing the homogeneity of multivariate dispersions from group centroids on basis of the resemblance measure.

In addition, both datasets were combined in one cluster analysis. Following the approach of Kröncke et al. (2011), the similarity of the two corresponding stations was categorised into high (same sub-cluster), medium

(same main cluster, but different sub-cluster) and low (different main cluster). Using ArcMap10TM, GIS (Geographic Information System) maps were generated to visualize the changes in the patterns of macrofauna communities (clusters), taxa number, abundance, biomass, and selected species in relation to the dredging and dumping activities.

7.4. Results

7.4.1. *Dredging and dumping*

From the start of the construction work for the JWP (March 2008) until the sampling date for this study (May 2010), the dredging activities in the western Inner Jade overlapped (Figure 7.1b, Table 7.1). Only one station (T21) in front of the bulkhead was affected by dredging and dumping. Two stations (T31, T32) were situated in the recently dredged area. In total, 11 stations were directly affected by dredging for the JWP (Table 7.1). 6 of these 11 stations were located in the regularly dredged old fairway. In 2009, the JadeWeserPort Realization Company extracted about 1.11 million m³ sediment at these 6 stations (according to the dredging data provided by the JadeWeserPort Realization Company).

In total, 8 stations were positioned in the regularly dredged old fairway. In the years 2000, 2001, 2002, and 2008 the volumes of sediment dredged by the WSA were similar with an annual mean of about 2.52 million m³. In 2009 and 2010 less dredging activities by the WSA were necessary for the maintenance of the old fairway (2009: 0.75 million m³ and 2010: 1.23 million m³). Thus, the total annual volume of removed material (1.86 million m³ in 2009) from the old fairway was lower in 2010 before the sampling campaign than in 2002.

All stations east of the old fairway represented the area which was not directly disturbed by the dredging and dumping activities.

7.4.2. *Changes in seabed morphology*

Despite the different data sources (SBES and MBES), specific morphologies were recognised in both the 2002 and 2010 contour maps (Figure 7.2). However, as expected, the MBES data displayed a greater amount of detail. In particular, the area close to the JWP showed geometries that matched the different dredging phases and corresponded to the new fairway under construction.

The main changes occurred close to the bulkhead and at the two extraction sites. While in 2002 the old fairway was the deepest part of the study

area (approximately 20 m; Figure 7.2a), the sand extraction resulted in two almost 50 m deep pits north and south of the JWP (Figure 7.2b). The least disturbed environment was the area east of the old fairway, where no significant morphological changes were observed.

7.4.3. Changes in sediment composition and distribution

In 2002, sediments with medium and high mud content were dominant: 12 of 30 stations with 25-50% mud (percentage by weight) and seven stations with more than 50% mud (Figure 7.2a). The highest mud content was observed at the southernmost transect (T1), where six out of seven stations had a mud content of more than 50%.

In 2010, no sediment sample was collected at one station (T35; Figure 7.2b). In comparison to 2002, 15 of 29 stations showed a change in sediment composition in 2010. Generally coarser sediments were found in 2010, 19 of 29 stations were classified as sand with low mud content (less than 25% by weight). Higher mud contents were still a specific signature of the old fairway (6 of 8 stations with 25-50% mud and 1 station with more than 50% mud).

In qualitative comparison, transects T1 and T2 were most affected by changes in sediment composition (Figure 7.2). A reduction in mud content was found at five of seven stations of transect T1 (T11, T12, T14-T16). Along transect T2, coarser sediments were found close to the JWP bulkhead (T21-T23) while mud contents increased further away from the construction site (T25-T27). An increase of coarse material was also observed at transect T3, where three of seven stations showed a reduction of mud content; T31 was also close to the JWP, but T37 and T38 were the easternmost stations of transect T3. The northernmost transect T4 revealed the least changes, with a slight increase in mud content at the station within the fairway (T43). In 2010, gravel with more than 10% by weight was present at six stations (T36-T38, T45-T47) in the northeastern area (no data of the gravel content in 2002).

7.4.4. Changes in macrofauna diversity and abundance

In 2002, 428 individuals were collected and 31 taxa in total were identified. The samples from 2010 contained 1535 individuals, representing 57 taxa in total (Figure 7.3).

At the 11 stations which were dredged for the JWP, the mean effective number of taxa decreased, the mean taxa number was similar to 2002, but the mean abundance increased (Table 7.2).

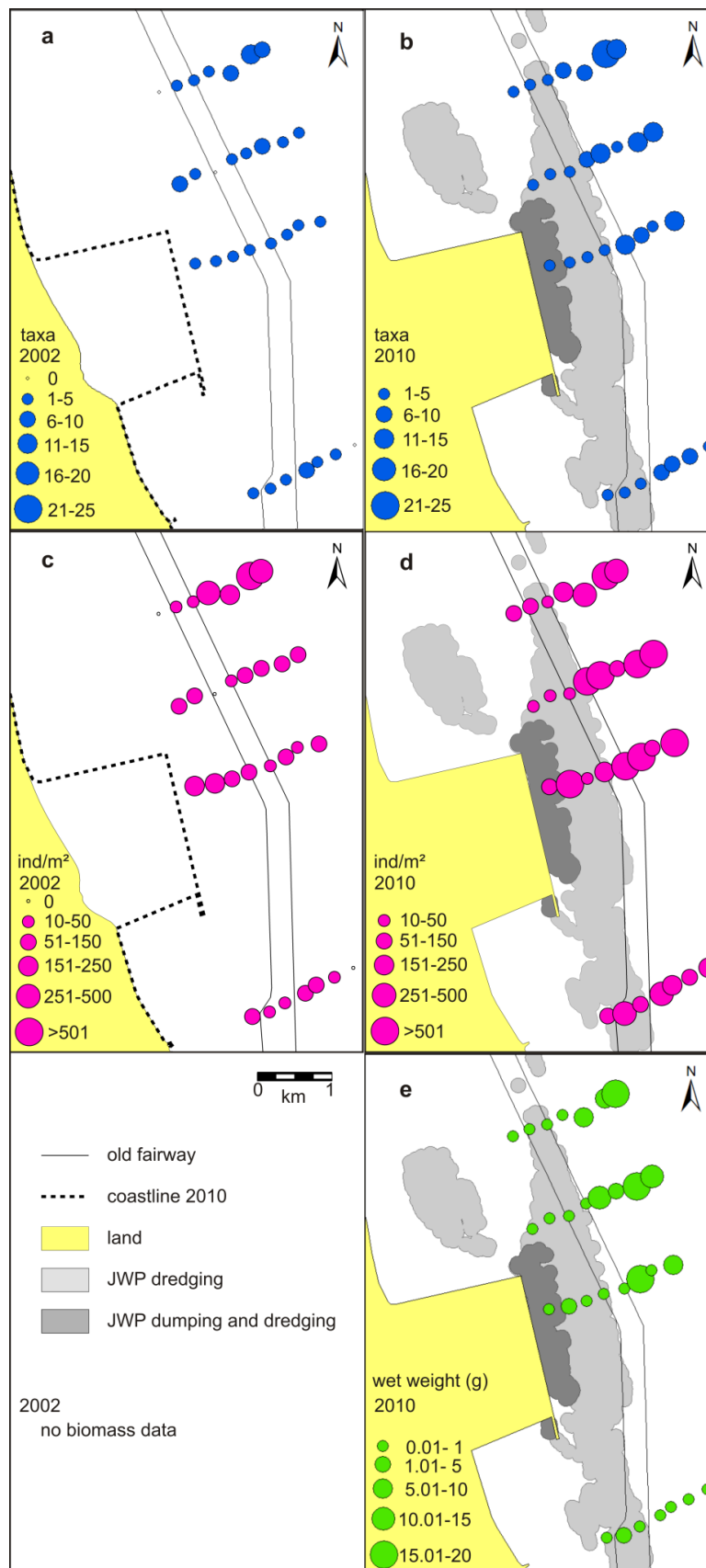


Figure 7.3. Macrofauna taxa number per sampling station (0.1m^2) in a) 2002 and b) 2010, abundance of macrofauna (individuals/ m^2) per sampling station in c) 2002 and d) 2010, and biomass (wet weight in g) per sampling station in e) 2010 (no biomass data for 2002).

areas of interest (see Table 1)		taxa number				abundance [ind./m ²]				effective number of taxa			
		mean	(sd)	df	ANOVA F p	mean	(sd)	df	ANOVA F p	mean	(sd)	df	ANOVA F p
JWP	dumping + dredging 2008-2010 n = 1	2002	5.0			170.0				4.1			
		2010	5.0			130.0				2.8			
JWP	dredged in 2010 n = 2	2002	6.0 (2.8)			135.0 (7.1)				4.8 (3.1)			
		2010	2.5 (0.7)			40.0 (0.0)				2.3 (0.8)			
JWP	dredged 2008-2010 n = 10 (without T33)	2002	3.8 (2.1)	1,18	0.257 0.618	95.0 (62.2)	1,18	1.048 0.320		3.1 (1.8)	1,18	0.512 0.483	
		2010	3.4 (1.3)			208.0 (343.5)				2.6 (0.9)			
	n = 9 (without T33, T22)	2002	3.7 (2.2)	1,16	0.000 1.000	84.4 (55.7)	1,16	0.286 0.600		3.0 (1.8)	1,16	0.076 0.786	
		2010	3.7 (1.1)			102.2 (82.7)				2.8 (0.7)			
old fairway	regularly dredged n = 7 (without T33)	2002	2.4 (1.3)	1,12	5.454 0.038	44.3 (31.5)	1,12	5.242 0.041		2.2 (1.0)	1,12	5.645 0.035	
		2010	5.7 (3.5)			302.9 (297.1)				3.5 (1.4)			
	non-dredged n = 15 (without T17, T41)	2002	4.9 (2.6)	1,28	10.800 0.003	217.3 (317.2)	1,28	4.370 0.046		3.4 (1.2)	1,28	8.770 0.006	
		2010	9.5 (4.8)			768.0 (969.8)				5.1 (1.9)			

Table 7.2. Comparison of the defined areas of interest (see Table 7.1) in 2002 and 2010 referring to the taxa number, macrofauna abundance (individuals/m²), and effective number of taxa given as mean with standard deviation (sd), and the results of the performed ANOVAs; T17, T33, T41 were excluded, because at these stations no macrofauna was found in 2002; at T22 a high number of *Gastrosaccus spinifer* was found in 2010.

These differences were not significant. At only one of the dredged stations (T22) 1160 ind./m² of the mysidacea *Gastrosaccus spinifer* were found in 2010. Even when this station is excluded, the mean abundance of the western dredged area was higher in 2010 than in 2002. At the station directly in front of the bulkhead (T21), which was affected by dredging and dumping activities, the same taxa number and a slight decrease in abundance were found in 2010. Only in the most recently dredged area (T31, T32) both, mean taxa number and mean abundance, were lower in 2010 than in 2002.

In the old fairway, mean effective number of taxa, mean taxa number and mean abundance were lowest in 2002, but increased significantly in 2010. In areas that were not dredged the mean effective number of taxa increased in 2010, mean taxa number nearly doubled and a threefold increase in mean abundance was recorded. These differences were significant.

7.4.5. Changes in distribution and abundance of taxa between 2002 and 2010

In Table 7.3 only those taxa are listed, which were present at least at three stations less or more in 2010 than in 2002, in order to shorten the taxa list of Table 7.3 and to stress the major changes in taxa presence. According to this arbitrary threshold (in total more than 10% change), the presence of only five taxa decreased at the 30 stations, the presence of 12 taxa increased in the old fairway, and the presence of 13 taxa increased in the JWP dredged area.

In 2002, a total of 14 taxa were found at the 11 stations that were directly affected by dredging activities for the JWP in 2008-2010. 11 of these 14 taxa were

not listed in Table 7.3, because *Bathyporeia elegans*, *Diastylis bradyi*, *Eteone longa*, *Lagis koreni*, *Macoma balthica*, *Retusa obtusa*, *Retusa trunculata*, *Schistomysis spiritus*, *Scoloplos (Scoloplos) armiger*, *Spiophanes bombyx*, and *Tubificoides benedii* showed less than 10% change of their absence/presence in the study area. These results would not differ much, if a slightly lower/higher threshold was chosen.

Taxa found in 2010 at a minimum of 3 stations with lower (↓) or higher (↑) presence than in 2002 (30 stations in total)	2002 presence (x) in the:			2010 presence (x) in the:		
	area later dredged for the JWP	regularly dredged old fairway	remaining non-dredged areas	area dredged for the JWP	regularly dredged old fairway	non-dredged areas
<i>Abra alba</i>	↓		x			
<i>Bivalvia</i> spp. juv.	↑				x	x
<i>Caprella</i> spp.	↑		x	x	x	x
<i>Corophium volutator</i>	↑			x	x	x
<i>Dyopodos monacantha</i>	↑			x	x	x
<i>Eunereis longissima</i>	↓		x			
<i>Gastrosaccus spinifer</i>	↑		x	x	x	x
<i>Gattyana</i> cf. <i>cirrhosa</i>	↑					x
<i>Heteromastus filiformis</i>	↓	x	x			x
<i>Mesopodopsis slabberi</i>	↑			x		x
<i>Monocorophium acherusicum</i>	↑					x
<i>Mytilidae</i> sp. juv.	↑		x	x	x	x
<i>Nephtys caeca</i>	↑		x	x	x	x
<i>Nephtys hombergii</i>	↓	x	x	x		x
<i>Nephtys</i> spp. juv.	↓	x	x			x
<i>Peringia ulvae</i>	↑			x	x	x
<i>Petricolaria pholadiformis</i>	↑			x	x	x
<i>Photis reinhardi</i>	↑					x
<i>Polydora cornuta</i>	↑			x	x	x
<i>Pontocrates altamarinus</i>	↑			x	x	x
<i>Pygospio elegans</i>	↑			x	x	x

Table 7.3. Changes in the presence of all macrofauna taxa, which were found in 2010 at a minimum of 3 stations (10%) less (↓) or more (↑) than in 2002 (30 stations in total). Presence at the stations, which were affected by the dredging activities for the JWP (2008-2010) and in the old fairway, was listed in comparison to the presence at the not dredged stations.

7.4.6. Macrofauna community structure in 2002

By 2002, the taxa spectrum and the spatial distribution of the characteristic taxa changed markedly since the 1960s (Schuchardt et al. 2007). In particular, the formerly dominant species *Petricolaria pholadiformis*, *Magelona papillicornis*, and *Ophelia limacina* were absent at the 30 stations of the BIOCONSULT study used for this comparison. However, they were present in low abundance at some additionally sampled stations in 2002. The cluster analysis with integrated SIMPROF routine identified only two significant clusters ($p < 0.05$), which indicated two communities (“A” and “B”) among sampling stations in 2002 (Figure 7.4a). These communities coincided less with the altered sediment distribution than in the 1960s (Table 7.4).

macrofauna community	n	mud content			gravel >10%	taxa in total	taxa per station (0.1m ²)	abundance [ind./m ²]	effective number of taxa	
		0-25%	25-50%	50-100%			mean (sd)	mean (sd)	mean (sd)	(sd)
A (2002)	6	6	0	0	no data	22	6.0 (3.0)	37.0 (47.0)	3.7	(1.5)
B (2002)	21	4	11	6	no data	19	4.0 (2.0)	10.0 (8.0)	2.7	(1.5)
C (2010)	6	5	0	1	0	10	3.0 (1.0)	25.0 (45.0)	2.2	(1.5)
D (2010)	10	7	0	2	5	45	11.0 (5.0)	107.0 (108.0)	4.9	(1.5)
E (2010)	4	0	1	3	0	16	7.0 (4.0)	45.0 (32.0)	4.0	(1.2)
F (2010)	10	7	3	0	1	18	5.0 (2.0)	14.0 (10.0)	3.0	(1.8)

Table 7.4. Macrofauna communities of 2002 and 2010 with sediment categories at the concerning stations, total macrofauna taxa number per community, and macrofauna taxa number per station (0.1 m²), abundance (individuals/m²), and the diversity index: effective number of taxa given as mean with standard deviation (sd).

a) 2002		mean abundance	mean similarity	contribution %
community "A"				
	<i>Scoloplos (Scoloplos) armiger</i>	5.2	14.88	46.49
	Anthozoa spp.	16.0	10.54	32.92
	Mytilidae sp. juv.	2.3	3.13	9.78
	<i>Gastrosaccus spinifer</i>	0.3	1.23	3.85
community "B"				
	<i>Nephtys hombergii</i>	1.7	12.85	35.54
	<i>Nephtys</i> spp. juv.	2.1	9.78	27.04
	<i>Macoma balthica</i>	1.5	8.39	23.22
	<i>Scoloplos (Scoloplos) armiger</i>	2.3	3.30	9.13
b) 2010		mean abundance	mean similarity	contribution %
community "C"				
	<i>Gastrosaccus spinifer</i>	22.5	14.86	65.55
	<i>Pontocrates altamarinus</i>	0.5	5.39	23.76
	<i>Macoma balthica</i>	0.5	2.42	10.69
community "D"				
	Anthozoa spp.	19.3	8.25	21.78
	Mytilidae sp. juv.	26.2	7.89	20.83
	<i>Pygospio elegans</i>	15.4	6.78	17.90
	<i>Scoloplos (Scoloplos) armiger</i>	4.4	5.43	14.34
	<i>Gattyana cf. cirrhosa</i>	4.3	2.11	5.56
	<i>Caprella</i> spp.	21.5	1.78	4.70
	<i>Monocorophium acherusicum</i>	0.7	1.30	3.43
	<i>Nephtys caeca</i>	0.8	1.26	3.32
community "E"				
	<i>Corophium volutator</i>	19.0	18.74	40.37
	<i>Pygospio elegans</i>	7.0	7.33	15.79
	<i>Petricolaria pholadiformis</i>	1.0	6.80	14.66
	Mytilidae sp. juv.	2.5	5.06	10.91
	<i>Caprella</i> spp.	1.0	4.57	9.85
community "F"				
	<i>Scoloplos (Scoloplos) armiger</i>	3.7	14.89	39.18
	<i>Macoma balthica</i>	3.0	10.39	27.34

Table 7.5. Characteristic macrofauna taxa in a) 2002 and b) 2010 with mean abundance of not transformed data and mean similarity and percentage of their contribution to the community, based on Bray-Curtis similarity, using fourth-root transformed taxa abundance data.

Figure 7.4. Cluster analyses of macrofauna data in a) 2002 and b) 2010, based on Bray-Curtis similarity, using fourth-root transformed taxa abundance data, black lines indicate the significantly different cluster according to the SIMPROF test ($p < 0.05$), and the concerning spatial alignment of the macrofauna communities in c) 2002 and d) 2010 in the study area.

In the northeastern part, six stations with sand and low mud content were clustered within community “A” (2002), which was characterized by Anthozoa, *Scoloplos (Scoloplos) armiger*, juvenile Mytilidae, and *Gastrosaccus spinifer* (Figure 7.4 a, c; Table 7.4, Table 7.5). While community “A” (2002) was dominated by omnivores, in community “B” (2002) deposit feeders were the most abundant feeding type (Figure 7.5). Community “B” (2002) represented the remaining 21 stations and was found on various sediments with low to high mud content (Figure 7.4a, c; Table 7.4). The characteristic taxa were the polychaetes *Nephtys hombergii*, juvenile *Nephtys* spp., *Scoloplos (Scoloplos) armiger* and the bivalve *Macoma balthica* (Table 7.5). The mean abundance of this community was lower than in all communities in 2010 (Table 7.4).

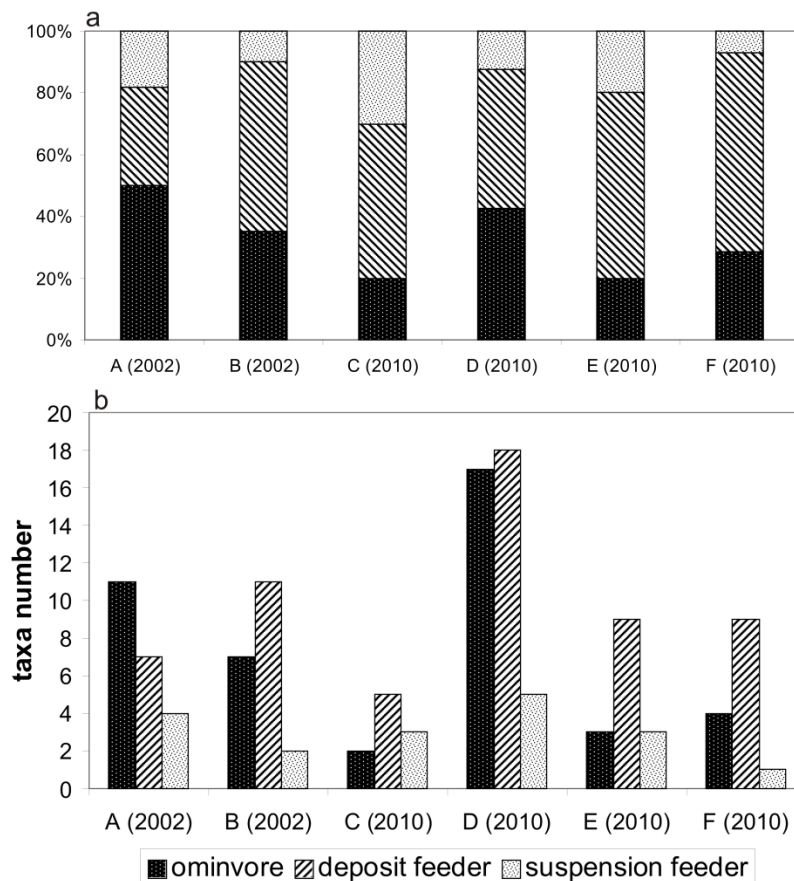


Figure 7.5. Relative and absolute dominance of the different feeding types in the macrofauna communities A-F.

7.4.7. Macrofauna community structure in 2010

The macrofauna community structure in 2010 was clearly different from the macrofauna spatial distribution maps generated in the 1960s by Dörjes et al. (1969). The cluster analysis with integrated SIMPROF routine revealed four significant communities in 2010 (“C”, “D”, “E”, “F”; $p < 0.05$; Figure 7.4b). This

community structure provided a different pattern in the Inner Jade than in the 1960s and were dominated by different taxa (except for *Petricolaria pholadiformis* in community E"). In general, deposit feeders dominated the macrofauna communities in 2010 and only few suspension feeders were found (Figure 7.5).

In the western dredged area, including the two recently dredged stations, community "C" (2010) exhibited a low taxa number (Table 7.4) at mainly sandy sediments. Characteristic species were *Macoma balthica*, *Gastrosaccus spinifer*, and *Pontocratus altamarinus* (Table 7.5).

Community "D" (2010) was situated in the northeastern part, which was not dredged for the construction works (Figure 7.4d). Mainly sandy sediments, partly with relatively high gravel content (Table 7.4), and the highest mean biomass of the study area (10.1 ± 6.8 g; Figure 7.3) were found in this area. Like community "A" (2002), community "D" (2010) was dominated by Anthozoa (Table 7.5). A relatively high number of accompanying species such as juvenile Mytilidae, *Pygospio elegans*, *Scoloplos (Scoloplos) armiger*, *Gattyana cf. cirrhosa*, *Caprella* sp., *Monocorophium acherusicum*, and *Nephtys caeca* led to the highest diversity of the study area in community "D" (2010) (Table 7.4). In community "D" (2010) omnivores occurred in similar numbers as deposit feeders.

Community "E" (2010) was mainly located within the old fairway (Figure 7.4d) and characterised by medium to high mud content (Table 7.4). The amphipod *Corophium volutator* dominated this community and *Caprella* sp., juvenile Mytilidae, the spionids *Pygospio elegans* and *Polydora cornuta*, and the bivalve *Petricolaria pholadiformis* were discriminating species (Table 7.5).

Community "F" (2010) was spread over the non-dredged eastern as well as in the dredged western areas (Figure 7.4d), mainly at sandy sediments (Table 7.4). Characteristic species were *Scoloplos (Scoloplos) armiger*, *Macoma balthica*, *Peringia ulvae*, and juvenile Mytilidae (Table 7.5).

The community structure in 2010 was best explained by the dredging intensity of the JadeWeserPort Realization Company, although the correlation factors calculated by BIOENV ($p = 0.01$) revealed only a weak correlation between the macrofauna abundance data from 2010 and the number of JWP dredging days. Only about 36% of the variability within the resemblance matrix of the macrofauna abundance was explained by the number of JWP dredging days (Table 7.6). However, depth, gravel content, sand content, mud content, and the different combinations of these parameters correlated even less with the community structure in 2010. In contrast, macrofauna biomass correlated best with gravel content (Table 7.6).

variables used for BIOENV analysis with macrofauna data 2010	df	abundance		biomass	
		%	p	%	p
number of JWP dredging days	11, 348	36.2	0.001	2.8	0.314
sand content (%)	29, 870	17.8	0.013	7.8	0.109
depth (m)	29, 870	10.4	0.116	0.2	0.428
mud content (%)	29, 870	9.3	0.144	10.7	0.053
gravel content (%)	29, 870	3.9	0.309	28.9	0.003

Table 7.6. Results of the BIOENV analysis with fourth-root transformed macrofauna abundance and biomass data of 2010 and normalized abiotic variables.

7.4.8. Changes in macrofauna community structure between 2002 and 2010

The RELATE routine determined no significant similarities between the patterns of the macrofauna communities in 2002 and 2010 ($R^2=0.0056$; $p=0.18$). The SIMPROF test for the cluster analysis of the samples from 2002 revealed only two significantly separated clusters on a low similarity level: communities “A” and “B” (Figure 7.4 a, c). Despite equally low similarity levels, four significantly different clusters were found in 2010: communities “C”, “D”, “E”, and “F” (Figure 7.4 b, d). The PERMANOVA revealed significant differences between all the clusters (PERMANOVA main test, $df=5$, mean squares= 16108, $F=7.2684$, $p=0.001$, $p(\text{Monte Carlo}) = 0.001$; Table 7.7). Sample dispersion was only not homogeneous between the groups (C,E). For all other groups PERMDISP generated p -values >0.05 (Table 7.7).

macrofauna communities	df	PERMANOVA		PERMDISP	
		t	p	t	p
B (2002), A (2002)	25	2.8068	0.001	0.0611	0.960
B (2002), F (2010)	29	2.5975	0.001	0.6239	0.573
B (2002), C (2010)	25	2.5940	0.001	1.0524	0.381
B (2002), D (2010)	29	3.7460	0.001	0.6045	0.560
B (2002), E (2010)	23	3.1856	0.001	1.7883	0.172
A (2002), F (2010)	14	2.0893	0.003	0.4748	0.693
A (2002), C (2010)	10	2.0753	0.004	1.1937	0.350
A (2002), D (2010)	14	1.6856	0.007	0.5613	0.648
A (2002), E (2010)	8	2.5131	0.005	2.2511	0.096
F (2010), C (2010)	14	2.3407	0.001	1.4899	0.197
F (2010), D (2010)	18	2.6083	0.001	0.0746	0.951
F (2010), E (2010)	12	2.6997	0.004	1.3094	0.290
C (2010), D (2010)	14	2.6811	0.001	1.8520	0.130
C (2010), E (2010)	8	2.3058	0.004	2.8722	0.032
D (2010), E (2010)	12	2.1959	0.001	1.8986	0.137

Table 7.7. Results of the PERMANOVA and PERMDISP pairwise test of all macrofauna communities in 2002 and 2010, statistically significant differences ($p < 0.05$) are marked in bold.

characteristic taxa (see Fig. 7)	2002		2010		ANOVA		
	mean	(sd)	mean	(sd)	df	F	p
1 Anthozoa spp.	32.7	(144.2)	64.3	(164.2)	1,58	0.630	0.431
2 <i>Corophium volutator</i>	0.0	(0.0)	26.7	(80.0)	0	0 <i>C. volutator</i> in 2002	
3 <i>Gastrosaccus spinifer</i>	0.7	(2.5)	46.0	(212.3)	1,58	1.368	0.247
4 <i>Macoma balthica</i>	10.7	(16.4)	12.0	(26.7)	1,58	0.054	0.817
5 Mytilidae sp. juv.	5.0	(14.6)	97.0	(295.8)	1,58	2.895	0.094
6 <i>Nephtys hombergii</i>	12.0	(15.8)	2.0	(4.8)	1,58	10.930	0.002
7 <i>Nephtys</i> spp. juv.	15.3	(23.0)	1.0	(4.0)	1,58	11.300	0.001
8 <i>Peringia ulvae</i>	0.0	(0.0)	8.7	(20.3)	0	0 <i>P. ulvae</i> in 2002	
9 <i>Petricolaria pholadiformis</i>	0.0	(0.0)	2.3	(5.0)	0	0 <i>P. pholadiformis</i> in 2002	
10 <i>Pygospio elegans</i>	0.0	(0.0)	61.7	(169.4)	0	0 <i>P. elegans</i> in 2002	
11 <i>Scoloplos (Scoloplos) armiger</i>	26.7	(59.7)	27.3	(38.9)	1,58	0.003	0.959

Table 7.8. Comparison of mean abundances (individuals/m²) of 11 characteristic taxa at the 30 sampling stations in 2002 and 2010 with standard deviation (sd) and results of the performed ANOVAs.

The combined cluster analysis revealed that the similarity between community “A” (2002) and community “D” (2010) was high (Figure 7.6). In contrast, the majority of stations from community “B” (2002) aligned in a separate cluster, which showed little overlap with the communities “C”, “E”, and “F” (2010). Even the splitting of community “B” (2002) into sub-clusters did not reveal any relationships between macrofauna patterns and regular dredging activities in the old fairway or the differences in sediment composition. It also did not improve the similarities with the macrofauna community structure in 2010.

Table 7.8 provides the abundance of 11 characteristic macrofauna taxa in 2002 and 2010. While the mean abundance of the polychaete *Nephtys hombergii* and juvenile *Nephtys* spp. decreased, the abundance of the bivalve *Macoma balthica* and the polychaete *Scoloplos (Scoloplos) armiger* remained almost stable. In contrast, the abundance of Anthozoa, *Corophium volutator*, *Gastrosaccus spinifer*, juvenile Mytilidae, *Peringia ulvae*, *Petricolaria pholadiformis*, and *Pygospio elegans* increased. Only the abundance of *Nephtys hombergii* and juvenile *Nephtys* spp. differed significantly in 2010 from 2002 (Table 7.8). The changes in abundances of *Corophium volutator*, *Peringia ulvae*, *Petricolaria pholadiformis*, and *Pygospio elegans* could not be tested with ANOVA, because these species were not present in 2002.

In 2010, *Gastrosaccus spinifer* was found mainly within or close to the areas dredged for the JWP (Figure 7.7). *Nephtys hombergii* and juvenile Mytilidae occurred in the dredged areas as well as in the non-dredged eastern region. *Macoma balthica* and *Scoloplos (Scoloplos) armiger* were widely distributed over the entire study area. In contrast, the occurrence of *Peringia ulvae* was almost limited to the southern transect (T1). The distribution of *Corophium volutator* and

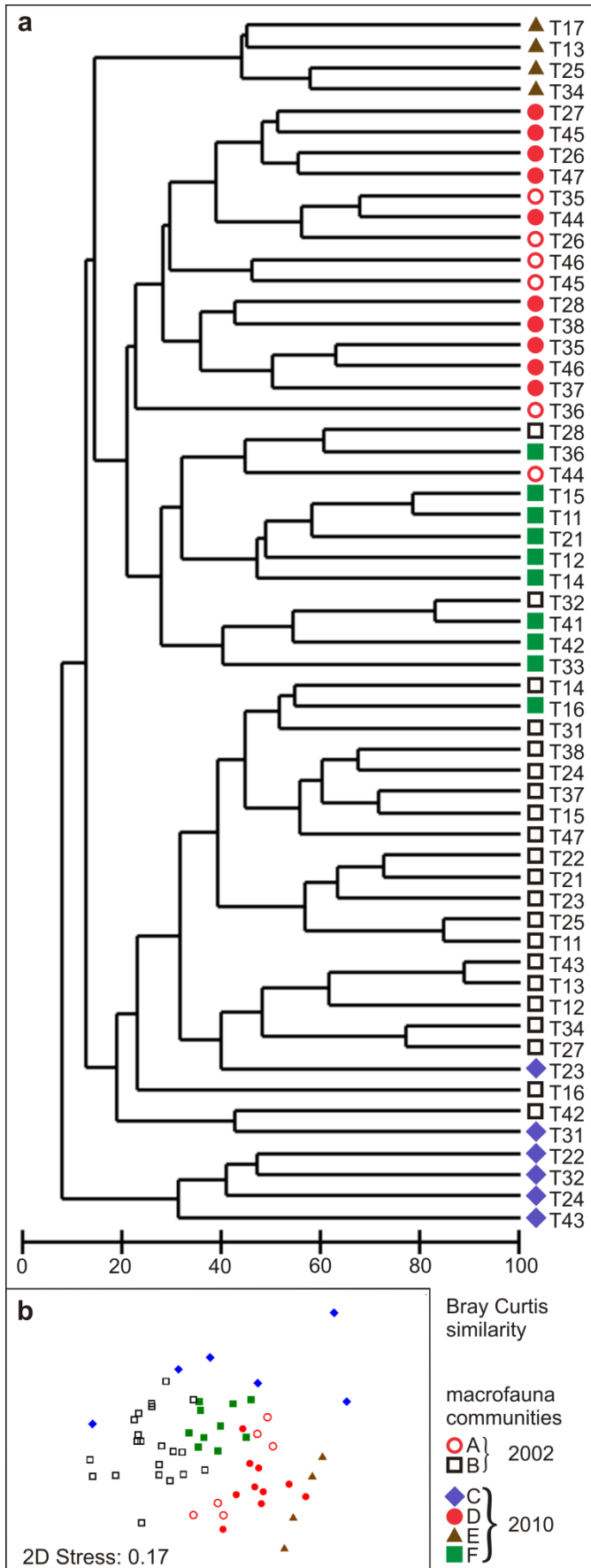


Figure 7.6. Combined cluster analyses (a) and MDS (b) of macrofauna data in 2002 and 2010, based on Bray-Curtis similarity, using fourth-root transformed taxa abundance data.

Petricolaria pholadiformis coincided with medium or high mud contents, within the old fairway and in the eastern part. Anthozoa, juvenile *Nephtys* spp., and *Pygospio elegans* occurred in the areas which were not dredged.

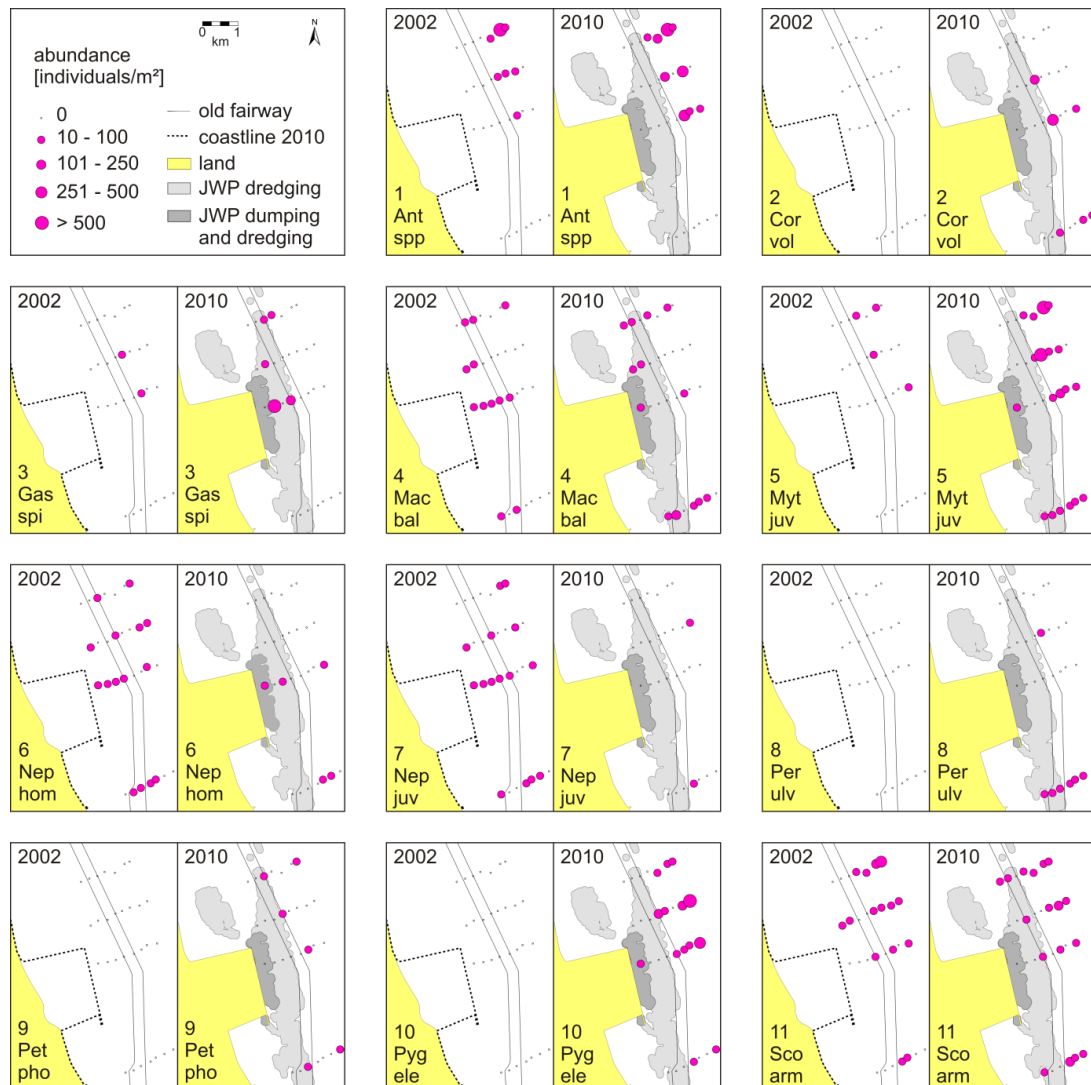


Figure 7.7. Abundance of characteristic macrofauna taxa (individuals/m²) in 2002 and 2010, 1 *Anthozoa* spp.; 2 *Corophium volutator*; 3 *Gastrosaccus spinifer*; 4 *Macoma balthica*; 5 juvenile *Mytilidae* sp.; 6 *Nephtys hombergii*; 7 juvenile *Nephtys* spp.; 8 *Peringia ulvae*; 9 *Petricolaria pholadiformis*; 10 *Pygospio elegans*; 11 *Scoloplos (Scoloplos) armiger*.

7.5. Discussion

7.5.1. Physical effects of the construction work

The highly heterogeneous seafloor of Inner Jade was described by Capperucci and Bartholomä (2012). In 2010, this region was characterized by patchy small scale variations in composition and distribution of sediments, both

in the dredged and in the non-dredged areas. The construction of the JWP, in particular, the dredging activities, transport and dumping of fine sediments (sand and mud) increased the complexity of the system. These effects were difficult to quantify, and the impact of the JWP construction work was hardly distinguishable from the natural variance.

Most of the dredged sediments consisted of sand, which explained the observed coarsening trend in the study

area, especially the increase of the sand fraction at the southern transect T1, close to the southern extraction site (Figure 7.2). In fact, the region is dominated by a dynamic sediment transport regime, confirmed by the existence of large, very mobile bedform fields (Kubicki and Bartholomä 2011). The presence of a mobile sand layer, nourished by the dredging activities, could temporarily cover the previously existing fine deposits and/or replace them.

The coarsening of sediments observed along the western part of transect T2 (T21-T23), the closest to the construction site, could be attributed to the direct dumping of sand in the bulkhead area, or to the exposure of the Pleistocene sand deposits beneath the removed sea bottom.

In contrast, the eastern part of transect T2 showed an increase in mud fraction (T25-T27). This transect was the one closest to the “Lauenburger Ton” mining location. The intense reworking of the clay deposit and some unavoidable dispersion of the same material could potentially explain the increase of mud content recorded at stations T25-T27. On the other hand, different sources (e.g. Neuer Vorhafen dredging spoils; natural presence of fine sediments in the Jade Bay tidal flat areas) could not be excluded.

In contrast to earlier studies (Dörjes et al. 1969; Irion 1994), the old fairway was characterized by fine sediments in 2002 and 2010. Thus, this area was the most stable region of the system. The slight increase in mud content measured in 2010 could be linked to the “Lauenburger Ton” dredging and dumping operations (although different sources could not be excluded). In fact, besides the two sand extraction sites, the old fairway was the deepest part of the study area and seemed to act as a trap for soft sediments (ICES 1992).

For the land reclamation of the JWP terminal area, the original seafloor surface was removed, and the Pleistocene sand deposits below were exposed and exploited, especially from the two extraction sites in the Jade Channel (north and south of the new bulkhead). Underneath the sand cover, a thick deposit of consolidated clay (“Lauenburger Ton” formation) was dug, mainly in the area between the bulkhead and the old fairway. The removed material was dumped into the southern extraction site (Kluth and Ehmen 2010). Dredging and

dumping operations are commonly associated with sediment resuspension (mainly the fine sand and mud fractions of the suspended load near the bottom), as well as leaks and spills (Newell et al. 1998; Winterwerp 2002). This material can be easily remobilized and spread, especially at periods of maximum flow intensity.

There is no evidence that the observed sediment changes were controlled by a variation in the hydrodynamic conditions. Kahlfeld and Schüttrumpf (2006) modelled the impact of deepening and narrowing the Inner Jade on the morphodynamics of the area. They predicted that only local changes in flow velocity of the Inner Jade would occur in the immediate proximity of the JWP. However, the predicted values (mean ebb flow velocity increased up to +0.1 m/s) were too low for inducing sediment changes, in comparison with the maximum average flow velocities (generally larger than 1.5 m/s, Grabemann et al. 2004).

7.5.2. Changes in macrofauna community structure

In 2002, the patchy distribution of the few characteristic taxa in low abundances reflected the study area as a more homogeneous habitat than in 2010. Only community “A” (2002) in the northeastern area was distinguishable from the predominating community “B” (2002) in the remaining area (Figure 7.4 a, c). Community “B” (2002) showed the characteristics of an early succession stage: low taxa number, low abundance, and dominance of opportunistic or stress tolerant species.

The spatial distribution of the macrofauna communities in 2010 matched roughly with the division of the study area according to the different categories of disturbance: the most recently dredged northwestern area (community “C”), the regularly dredged old fairway (community “E”), and the northeastern non-dredged area (community “D”). The southern area (T1) was mainly inhabited by community “F”, which also occurred in the transition areas between the other communities (Figure 7.4 b, d).

7.5.3. Direct dredging effects on the macrofauna community structure in 2010

The BIOENV analysis proved the dredging activities for the JWP as the most important structuring parameter in 2010 (Table 7.6). According to known effects of dredging activities on macrofauna (e.g. Kenny et al. 1998; Sardá et al. 2000; van Dalssen et al. 2000; van Dalssen and Essink 2001; Newell et al. 2002; Sutton and Boyd 2009), a decrease in diversity, taxa number, and abundance was expected in the area that was directly affected by the dredging activities for the JWP. Thus, the very low taxa number in the northwestern area (community “C”,

2010) was probably a direct effect of the recently conducted dredging activities (Kenny and Rees 1994; 1996). In community “C” (2010) the high number of the mysidacea *Gastrosaccus spinifer*, which actually belongs to the hyperbenthos, and the occurrence of the amphipod *Pontocrates altamarinus* (Table 7.5), which is also a very mobile species, hinted at an early stage of recolonisation in the newly available substrate.

For the old fairway the date of the last dredging activity by the WSA is not exactly known, but the increased taxa number and abundance in community “E” (2010) indicate recolonisation in the regularly disturbed area with relatively stable sediment composition. This recolonisation by opportunistic (r-selected) species such as *Corophium volutator* and *Pygospio elegans* is a typical response after dredging (e.g. Newell et al. 1998).

This study confirmed that quick recolonisation is possible after physical disturbance in highly dynamic areas (Borja et al. 2010). Post-settlement dispersal may have resulted in dispersal of juvenile and adult *Macoma balthica* over the wide range of different habitats in the entire study area (Figure 7.7). Juvenile Mytilidae can disperse by byssus drifting (Armonies 1996), probably originating from the mussel farms and banks in the Inner Jade (Herlyn and Millat 2000). The appearance of the mud snail *Peringia ulvae* in the southern transect (T1) could also be explained by drifting. This species occurred in very high abundance in the adjacent Jade Bay (Schückel et al. 2013) and disperses by floating at the water surface (Armonies and Hartke 1995).

Thus, recolonisation by opportunistic and highly mobile species as well as secondary dispersal of several dominant species seemed to follow the construction phase of the JWP. Despite the high recolonisation potential of the study area, it is unlikely that full recovery to the state of the 1960s is attainable.

7.5.4. Indirect dredging effects on the macrofauna community structure in 2010

The combination of naturally very mobile bedforms (Kubicki and Bartholomä 2011) and the different dredging activities in the Inner Jade formed a dynamic mosaic of microhabitats. In 2002 and 2010, the presence of some dominant species (e.g. *Macoma balthica*, *Scoloplos (Scoloplos) armiger*) in different communities (Table 7.5) indicated the high tolerance of these species to variable environmental conditions (Schückel et al. 2013).

Overall, the macrofauna pattern in 2002 was obviously less influenced by the sediment distribution than in the 1960s. Nevertheless, despite the lack of information about the gravel content of the study area in 2002, the dominance of

Anthozoa in community “A” (2002) indicated the presence of hard substrate in the northeastern area. Indeed, the expanded dominance of Anthozoa in the northeastern area (community “D”, 2010) coincided with the presence of gravel in 2010. Within 8 years between the two sampling campaigns, the spatial extension of the Anthozoa dominated community “A” (2002) shifted slightly towards the shallower eastern Jade slope (community “D”, 2010). The hard ground characteristics of the coarse gravel bed supported the settlement of Anthozoa and their presence explained the high biomass in the north eastern area (Table 7.6). For the other characteristic taxa in 2002 no strict sediment preferences are known.

In 2010, a more heterogeneous seabed morphology and sediment distribution (Capperucci and Bartholomä 2012) coincided with the more complex macrofauna community structure in comparison to 2002. Community “E” (2010) was restricted to areas with medium or high mud content (Table 7.4), because the characteristic species *Corophium volutator* and *Petricolaria pholadiformis* prefer fine sediments (Fenchel et al. 1975; Tebble 1976). The majority of stations belonging to the communities “C” and “F” (2010) coincided with sandy areas, but (according to the BIOENV analysis, Table 7.6) a significant relationship between the macrofaunal community structure in 2010 and the altered sediment distribution was not determined.

The increased taxa number and abundance in the old fairway and the not dredged areas (Table 7.2) could not be explained by the presence of invasive species. All taxa from the 2010 samples are typical inhabitants of the southern North Sea, which were found in the study area prior to the JWP construction (Dörjes et al. 1969; Schuchardt et al. 2003). In the Australian Moreton Bay Poiner and Kennedy (1984) observed a fast increase of biodiversity and population density outside dredged areas. They suggested that the macrofauna expanded because of the increase in suspended organic material due to the sediment plume of fine particles generated by the dredging activities. Transferred to the study area in the Inner Jade, the old fairway and even the non-dredged areas were indirectly affected by the JWP construction. In 2010, resuspension and spilling of the dredged sediments could explain the increased abundance of some macrofauna taxa, which probably profited from the enhanced food availability. In the non-dredged areas, the number of omnivores and deposit feeders increased markedly (Figure 7.5).

In contrast, the abundance and spatial distribution of the polychaete *Nephtys hombergii* declined significantly in 2010, even in the non-dredged areas (Figure 7.7, Table 7.8). Brooks et al. (2006) assumed that the predator *Nephtys*

hombergii benefits from organisms that were injured or died during the dredging process. Its main prey, the polychaete *Scoloplos (Scoloplos) armiger* (Beukema et al. 2000), was still abundant in 2010, suggesting that food shortage could not explain the decrease in *Nephtys hombergii*. Instead, its sensitivity to low winter temperatures (Beukema et al. 2000) has to be taken into account, because the mean temperatures of January (0.6°C) and February (6.0°C) 2010 were lower than in January (-0.2°C) and February (0.9°C) 2002. Monthly CTD time series data, measured by the RV “Senckenberg”, revealed up to 5°C difference in February at ton 48 (geographic position according to WGS84 UTM32N: Easting 445722.91099; Northing 5937336.36463) in the study area between 2002 and 2010. This suggests a temperature dependent decrease of the predator *Nephtys hombergii*, which may have contributed to the relatively high abundance of its prey *Scoloplos (Scoloplos) armiger* in 2010. This example highlights the importance of interannual variability, which can have a strong influence on the abundance of several species (Kröncke et al. 2013) and may have masked the impact of the dredging activities for the JWP in the Inner Jade.

7.6. Conclusion

For decades, the Inner Jade has been classified as a dynamic ecosystem characterised by both natural and anthropogenic factors. In comparison to the local hydrodynamic regime, the predicted increase in current velocity due to the harbour construction was negligible. The dredging and dumping activities for the JWP changed the bathymetry and contributed to the permanent redistribution of sediments within the study area. Opportunistic and mobile macrofauna species, without strict sediment preferences, had colonized the area from the 1960s to 2002. Nevertheless, the community structure in 2010 was clearly different. Although interannual variability has to be taken into account, the distribution pattern of the recolonising species in 2010 was best explained by the dredging activities for the JWP.

7.7. Acknowledgements

The international research training group INTERCOAST (“Integrated Coastal Zone and Shelf-Sea Research”) facilitated this study and the study was funded by the Deutsche Forschungsgemeinschaft (DFG). We thank Captain Karl Baumann and the crew of RV “Senckenberg” for their help with sampling in 2010 and Corinna Schollenberger, Astrid Raschke, and Kerstin Thaler for their

technical assistance. The local harbour authority (Wasser- und Schifffahrtsamt Wilhelmshaven (WSA)) provided data for dredging activities in the old fairway and, the WSA and the Bundesamt für Seeschifffahrt und Hydrographie (BSH) provided SBES data for 2002. The JadeWeserPort Realization Company provided data for dredging and dumping activities for the JWP, MBES data for 2010, and provided access to sediment and macrofauna data of 2002 elaborated by BÖL (Bremen) and BIOCONSULT (Bremen), which are all kindly acknowledged. Many thanks also to Dr. Henning Reiss for helpful comments on the manuscript and to Rachel Harris for English corrections.

7.8. References

- Anderson, M.J., Gorley, R.N., Clarke, K.R. 2008. PERMANOVA+ for PRIMER: Guide to Software and Statistical Methods. PRIMER-E, Plymouth.
- Armonies, W. 1996. Changes in distribution patterns of 0-group bivalves in the Wadden Sea: byssus-drifting releases juveniles from the constraints of hydrography. *Journal of Sea Research*, 35 (4), 323-334.
- Armonies, W., Hartke, D. 1995. Floating of mud snails *Hydrobia ulvae* in tidal waters of the Wadden Sea, and its implications in distribution patterns. *Helgoländer Meeresuntersuchungen*, 49, 529-538.
- Auster, P.J., Langton, R.W. 1998. The effects of fishing on fish habitat. Paper presented at the Sea Grant Symposium on Fish Habitat - Essential Fish Habitat and Rehabilitation at the 1998 Annual Meeting, Hartford, Connecticut, 26-27 August 1998.
- Berlow, E.L., Navarrete, S.A. 1997. Spatial and temporal variation in rocky intertidal community organization: Lessons from repeating field experiments. *Journal of Experimental Marine Biology and Ecology*, 214 (1-2), 195-229.
- Beukema, J.J., Essink, K., Dekker, R. 2000. Long-term observations on the dynamics of three species of polychaetes living on tidal flats of the Wadden Sea: the role of weather and predator-prey interactions. *Journal of Animal Ecology*, 69, 31-44.
- BfG, WSA 2003. Bundesanstalt für Gewässerkunde and Wasser- und Schifffahrtsamt Wilhelmshaven. Bagger- und Klapptellenuntersuchungen in der Jade. BfG Bericht, 1349, 104 pp.
- Borja, À., Chust, G., del Campo, A., González, M., Hernández, C. 2013. Setting the maximum ecological potential of benthic communities, to assess ecological status, in heavily morphologically-modified estuarine water bodies. *Marine Pollution Bulletin*, 71, 199-208.
- Borja, À., Dauer, D.M., Elliott, M., Simenstad, C.A. 2010. Medium- and long-term recovery of estuarine and coastal ecosystems: patterns, rates and restoration effectiveness. *Estuaries and Coasts*, 33, 1249-1260.
- Borja, À., Dauer, D.M., Grémare, A. 2012. The importance of setting targets and reference conditions in assessing marine ecosystem quality. *Ecological Indicators*, 12, 1-7.
- Boyd, S.E., Cooper, K.M., Limpenny, D.S., Kilbridge, R., Rees, H.L., Dearnaley, M.P., Stevenson, J., Meadows, W.J., Morris, C.D. 2004. Assessment of the rehabilitation of

-
- the seabed following marine aggregate dredging. Science Series Technical Report, 154 pp.
- Boyd, S.E., Limpenny, D.S., Rees, H.L., Cooper, K.M. 2005. The effects of marine sand and gravel extraction on the macrobenthos at a commercial dredging site (results 6 years post-dredging). *ICES Journal of Marine Science*, 62, 145-162.
- Brezina, J. 1979. Particle size and settling rate distributions of sandsized materials. Paper presented at the 2nd European Symposium on Particle Characterisation, Nürnberg.
- Brooks, R.A., Purdy, C.N., Bell, S.S., Sulak, K.J. 2006. The benthic community of the eastern US continental shelf: A literature synopsis of benthic faunal resources. *Continental Shelf Research*, 26, 804-818.
- Capperucci, R., Bartholomä, A. 2012. Sediment vs. topographic roughness: anthropogenic effects on acoustic seabed classification. In: Leendert Dorst, L., van Dijk, T., van Ree, R., Boers, J., Brink, W., Kinneking, N., van Lancker, V., de Wulf, A., Nolte, H. (Eds), *Conference Proceedings of Hydro12, Taking care of the sea*, the Hydrographic Society Benelux (HSB), on behalf of the International Federation of Hydrographic Societies (IFHS), Rotterdam, the Netherlands, 12-15 November 2012, 23-28.
- Cifuentes, M., Kamlah, C., Thiel, M., Lenz, M., Wahl, M. 2007. Effects of temporal variability of disturbance on the succession in marine fouling communities in northern-central Chile. *Journal of Experimental Marine Biology and Ecology*, 352 (2), 280-294, doi:10.1016/j.jembe.2007.08.004
- Clarke, K.R., Ainsworth, M. 1993. A method of linking multivariate community structure to environmental variables. *Marine Ecology Progress Series*, 92, 205-219.
- Clarke, K.R., Gorley, R.N. 2006. *PRIMER v6: User Manual/Tutorial*. PRIMER-E, Plymouth.
- Clarke, K.R., Warwick, R.M. 2001. *Change in Marine Communities: An Approach to Statistical Analysis and Interpretation.*, Second ed., PRIMER-E, Plymouth.
- Connell, J.H., Slatyer, R.O. 1977. Mechanisms of succession in natural communities and their role in community stability and organization *American Naturalist*, 111, 982, 1119-1144, doi:10.1086/283241
- Cooper, K.M., Eggleton, J.D., Vize, K., Vanstaen, K., Boyd, S.E., Ware, S., Morris, C.D., Curtis, M., Limpenny, D.S., Meadows, W.J. 2005. Assessment of the rehabilitation of the seabed following marine aggregate dredging - Part II. Science Series Technical Report, 81 pp.
- DIN4022 1987. Baugrund und Grundwasser - Benennung und Beschreibung von Boden und Fels. Schichtenverzeichnis für Bohrungen ohne durchgehende Gewinnung von gekernten Proben im Boden und Fels. In: e.V.V. NBNiDDIfN (Ed) *Erkundung und Untersuchung des Baugrunds Teil 1*, DIN-Taschenbuch 113. Beuth-Verlag, Köln.
- DIN18123 1983. Baugrund; Untersuchung von Bodenproben; Bestimmung der Korngrößenverteilung. In: e.V.V. NBNiDDIfN (Ed) *Erkundung und Untersuchung des Baugrunds*, DIN-Taschenbuch 113. Beuth-Verlag, Köln.
- Dörjes, J. 1992. Langzeitentwicklung makrobenthischer Tierarten im Jadebusen (Nordsee) während der Jahre 1974 bis 1987. *Senckenbergiana Maritima*, 22 (1/2), 37-57.
- Dörjes, J., Gadow, S., Reineck, H.E., Bir Singh, I. 1969. Die Rinnen der Jade (südliche Nordsee). Sedimente und Makrobenthos. *Senckenbergiana maritima*, 50 (1), 5-62.

- Fenchel, T., Kofoed, L.H., Lappalainen, A. 1975. Particle size-selection of two deposit feeders: the Amphipod *Corophium volutator* and the Prosobranch *Hydrobia ulvae*. *Marine Biology*, 30, 119-128.
- Ferns, P.N., Rostron, D.M., Siman, H.Y. 2000. Effects of mechanical cockle harvesting on intertidal communities. *Journal of Applied Ecology*, 37, 464-474.
- Forbes, T.L., Forbes, V.E., Depledge, M.H. 1994. Individual physiological responses to environmental hypoxia and organic enrichment: Implications for early soft-bottom community succession. *Journal of Marine Research*, 52 (6), 1081-1100, doi:10.1357/0022240943076849
- Gorzelay, J.F., Nelson, W.G. 1987. The effects of beach replenishment on the benthos of a sub-tropical Florida beach. *Marine Environmental Research*, 21, (2), 75-94, doi:10.1016/0141-1136(87)90043-2
- Grabemann, H.-J., Grabemann, I., Eppel, D.P. 2004. Climate change and hydrodynamic impact in the Jade-Weser area: a case study. In: Schernewski, G., Dolch, T. (Eds), *Geographie der Meere und Küsten*, vol 1. Coastline Reports, 83-91.
- Green, H.G., Yoklavich, M.M., Sullivan, D., Cailliet, G.M. 1995. A geophysical approach to classifying marine benthic habitats: Monterey Bay as a model. Applications of side-scan sonar and laser-line systems in fisheries research. Alaska Fish and Game Special Publication, 9, 15-30.
- Gutt, J., Starmans, A. 2001. Quantification of iceberg impact and benthic recolonisation patterns in the Weddell Sea (Antarctica). *Polar Biology*, 24 (8), 615-619.
- Hall, S.J. 1994. Physical disturbance and marine benthic communities: life in unconsolidated sediments. *Oceanography and Marine Biology: An Annual Review*, 32, 179-239.
- Halpern, B.S., Walbridge, S., Selkoe, K.A., Kappel, C.V., Micheli, C.C.F., Bruno, J.F., Casey, K.S., Ebert, C., Fox, H.E., Fujita, R., Heinemann, D., Lenihan, H.S., Madin, E.M.P., Perry, M.T., Selig, E.R., Spalding, M., Steneck, R., Watson, R. 2008. A global map of human impact on marine ecosystems *Science*, 319, 948-952.
- Herlyn, M., Millat, G. 2000. Decline of the intertidal blue mussel (*Mytilus edulis*) stock at the coast of Lower Saxony (Wadden Sea) and influence of mussel fishery on the development of young mussel beds. *Hydrobiologia*, 426, 203-210.
- ICES 1992. Report of the ICES working group on the effects of extraction of marine sediments on fisheries. ICES Cooperative Research Report, 182, 78 pp.
- Irion, G. 1994. Morphological, sedimentological and historical evolution of the Jade Bay, Southern North Sea. *Senckenbergiana maritima*, 24, (1/6), 171-186.
- Johnson, R.G. 1972. Conceptual models of marine benthic communities. In: Schopf, T.J.M. (Ed), *Models in paleobiology*. Freeman Cooper and Co., San Francisco, 148-159.
- Jost, L. 2006. Entropy and diversity. *Oikos*, 113, 363-375.
- Kahlfeld, A., Schüttrumpf, H. 2006. UnTRIM modelling for investigating environmental impacts caused by a new container terminal within the Jade-Weser-Estuary, German Bight. Paper presented at the 7th International Conference on HydroScience and Engineering, Philadelphia, USA, 10-13 September 2006.
- Kaiser, M.J. 1998. Significance of bottom-fishing disturbance. *Conservation Biology*, 12 (6), 1230-1235.
- Kenny, A.J., Rees, H.L. 1994. The effects of marine gravel extraction on the macrobenthos - early post-dredging recolonization. *Marine Pollution Bulletin*, 28 (7), 442-447.

-
- Kenny, A.J., Rees, H.L. 1996. The effects of marine gravel extraction on the macrobenthos: Results 2 years post-dredging. *Marine Pollution Bulletin*, 32 (8-9), 615-622.
- Kenny, A.J., Rees, H.L., Greening, J., Campell, S. 1998. The effects of marine gravel extraction on the macrobenthos at an experimental dredge site off North Norfolk, UK (results 3 years post-dredging). *ICES Document CM*, 14, 7 pp.
- Kluth, A., Ehmen, J. 2010. JadeWeserPort Wilhelmshaven - port construction and logistics. In: van Schel, L. (Ed), *PIANC Yearbook 2010*. PIANC - The world association for waterborne transport infrastructure, Brussels.
- Kröncke, I. 2006. Structure and function of macrofaunal communities influenced by hydrodynamically controlled food availability in the Wadden Sea, the open North Sea and the Deep-sea. A synopsis. *Senckenbergiana Maritima*, 36 (2), 123-164.
- Kröncke, I., Reiss, H., Dippner, J.W. 2013. Effects of cold winters and regime shifts on macrofauna communities in shallow coastal regions. *Estuarine, Coastal and Shelf Science*, 119, 79-90.
- Kröncke, I., Reiss, H., Eggleton, J.D., Aldridge, J., Bergman, M.J.N., Cochrane, S., Craeymeersch, J.A., Degraer, S., Desroy, N., Dewarumez, J.M., Duineveld, G.C.A., Essink, K., Hillewaert, H., Lavaleye, M.S.S., Moll, A., Nehring, S., Newell, R., Oug, E., Pohlmann, T., Rachor, E., Robertson, M., Rumohr, H., Schratzberger, M., Smith, R., Berghe, E.V., van Dalfsen, J., van Hoey, G., Vincx, M., Willems, W., Rees, H.L. 2011. Changes in North Sea macrofauna communities and species distribution between 1986 and 2000. *Estuarine Coastal and Shelf Science*, 94 (1), 1-15, doi:10.1016/j.ecss.2011.04.008
- Kröncke, I., Stoeck, T., Wiekling, G., Palojarvi, A. 2004. Relationship between structural and trophic aspects of microbial and macrofaunal communities in different areas of the North Sea. *Marine Ecology Progress Series*, 282, 13-31.
- Kubicki, A., Bartholomä, A. 2011. Sediment dynamics in the Jade tidal channel prior to port construction, southeastern North Sea. *Journal of Coastal Research (Proceedings of the 11th International Coastal Symposium, Szczecin, Poland)* SI, 64, 771-775.
- Lozán, J.L., Rachor, E., Reise, K., Sündermann, J., Westernhagen, H. 2003. *Warnsignale aus Nordsee & Wattenmeer: Eine aktuelle Umweltbilanz*. Wissenschaftliche Auswertungen, Hamburg.
- MESL (Marine Ecological Surveys Limited) 2007. Predictive framework for assessment of recoverability of marine benthic communities following cessation of aggregate dredging. Technical Report to the Centre for Environment, Fisheries and Aquaculture Science (CEFAS) and the Department for Environment, Food and Rural Affairs (Defra) MEPPF 04/02, 466 pp.
- Morgan, S.G. 2001. The larval ecology of marine communities. In: Bertness, M.D., Gaines, S.D., Hay, M.E. (Eds), *Marine Community Ecology*. Sinauer Associates Inc, Sunderland, Massachusetts, 159-182.
- Muxika, I., Borja, Á., Bonne, W. 2005. The suitability of the marine biotic index (AMBI) to new impact sources along European coasts. *Ecological Indicators*, 5, 19-31.
- Nehmer, P., Kröncke, I. 2003. Macrofauna communities in the Wichter Ee, a channel system in the East Frisian Wadden Sea. *Senckenbergiana Maritima*, 32, 1-10.
- Newell, R.C., Seiderer, L.J., Hitchcock, D.R. 1998. The impact of dredging works in coastal waters: a review of the sensitivity to disturbance and subsequent recovery of biological

- resources on the sea bed. *Oceanography and Marine Biology: An Annual Review*, 36, 127-178.
- Newell, R.C., Seiderer, L.J., Simpson, N.M., Robinson, J.E. 2002. Impact of marine aggregate dredging and overboard screening on benthic biological resources in the central North Sea: production licence area 408. Coal Pit Marine Ecological Surveys Limited Technical Report No 1/4/02 to the British Marine Aggregate Producers Association (BMAPA), 72 pp.
- Norkko, A., Rosenberg, R., Thrush, S.F., Whitlatch, R.B. 2006. Scale- and intensity-dependent disturbance determines the magnitude of opportunistic response. *Journal of Experimental Marine Biology and Ecology*, 330, 196-207.
- Pearson, T.H. 2001. Functional group ecology in soft-sediment marine benthos: The role of bioturbation. *Oceanography and Marine Biology*, 39, 233-267.
- Pearson, T.H., Rosenberg, R. 1978. Macrobenthic succession in relation to organic enrichment and pollution of the marine environment. *Oceanography and Marine Biology: An Annual Review*, 16, 229-311.
- Petratits, P.S., Dudgeon, S.R. 2004. Detection of alternative stable states in marine communities. *Journal of Experimental Marine Biology and Ecology*, 300, (1-2), 343-371.
- Petratits, P.S., Latham, R.E. 1999. The importance of scale in testing the origins of alternative community states. *Ecology*, 80 (2), 429-442.
- Poiner, I.R., Kennedy, R. 1984. Complex patterns of change in the macrobenthos of a large sandbank following dredging. *Marine Biology*, 78, 335-352.
- Reiss, H., Kröncke, I. 2001. Spatial and temporal distribution of macrofauna in the Otzumer Balje (East Frisian Wadden Sea, Germany). *Senckenbergiana Maritima*, 31 (2), 283-298.
- Rhoads, D.C., Boyer, L.F. 1982. The effects of marine benthos on physical properties of sediments - A successional perspective. In: McCall, P.L., Tevesz, M.J.S. (Eds), *Animal-sediment relations - The biogenic alteration of sediments*. Plenum Press, New York, London, 3-52.
- Rosenberg, R. 1995. Benthic marine fauna structured by hydrodynamic processes and food availability. *Netherlands Journal of Sea Research*, 34 (4), 303-317.
- Sardá, R., Pinedo, S., Gremare, A., Taboada, S. 2000. Changes in the dynamics of shallow sandy-bottom assemblages due to sand extraction in the Catalan Western Mediterranean Sea. *ICES Journal of Marine Science*, 57, 1446-1453.
- Schuchardt, B., Scholle, J., Bildstein, T., Günther, C.P., Henning, D., 2007. Ist die Jade ein erheblich verändertes Gewässer? Eine Analyse im Rahmen der WRRL, 119 pp.
- Schuchardt, B., Scholle, J., Henning, D., Dau, K., Brandt, T., Bildstein, T., Bröder, N., Günther, C.P., Hildebrandt, J., Dittmann, S. 2003. JadeWeserPort Los d) - Kartierung der aquatischen Lebensgemeinschaften, 221 pp.
- Schückel, U., Beck, M., Kröncke, I. 2013. Spatial variability in structural and functional aspects of macrofauna communities and their environmental parameters in the Jade Bay (Wadden Sea Lower Saxony, southern North Sea). *Helgoland Marine Research*, 67, 121-136.
- Simonini, R., Ansaloni, I., Bonini, P., Grandi, V., Graziosi, F., Iotti, M., Massamba-N'Siala, G., Mauri, M., Montanari, G., Preti, M., De Nigris, N., Prevedelli, D. 2007. Recolonization and recovery dynamics of the macrozoobenthos after sand extraction in relict sand bottoms of the Northern Adriatic Sea. *Marine Environmental Research*, 64, 574-589.

-
- Sousa, W.P. 2001. Natural disturbance and the dynamics of marine benthic communities. In: Bertness, M.D., Gaines, S.D., Hay, M.E. (Eds), *Marine Community Ecology*. Sinauer Associates Inc, Sunderland, Massachusetts, 5-130.
- Sugden, H., Panusch, R., Lenz, M., Wahl, M., Thomason, J. 2007. Temporal variability of disturbances: is this important for diversity and structure of marine fouling assemblages? *Marine Ecology*, 28, 368-376.
- Sutton, G., Boyd, S. 2009. Effects of extraction of marine sediments on the marine environment 1998-2004. ICES Cooperative Research Report, 297, 180 pp.
- Taupp, T., Wetzel, M.A. 2013. Relocation of dredged material in estuaries under the aspect of the Water Framework Directive - A comparison of benthic quality indicators at dumping areas in the Elbe estuary. *Ecological Indicators*, 34, 323-331.
- Tebble, N. 1976. *British bivalve seashells - a handbook for identification*. Second edn. Royal Scottish Museum, Edinburgh.
- Valdivia, N., Heidemann, A., Thiel, M., Molis, M., Wahl, M. 2005. Effects of disturbance on the diversity of hard-bottom macrobenthic communities on the coast of Chile. *Marine Ecology Progress Series*, 299, 45-54.
- vanDalfsen, J.A., Essink, K. 2001. Benthic community response to sand dredging and shoreface nourishment in Dutch coastal waters. *Senckenbergiana Maritima*, 31 (2), 329-332.
- vanDalfsen, J.A., Essink, K., Madsen, H.T., Birklund, J., Romero, J., Manzanera, M. 2000. Differential response on macrozoobenthos to marine sand extraction in the North Sea and the Western Mediterranean. *ICES Journal of Marine Science*, 57, 1439-1445.
- Vöge, S., Reiss, H., Kröncke, I. 2008. Macrofauna succession in an infilling salt marsh clay pit. *Senckenbergiana maritima*, 38, 93-106.
- Warwick, R.M. 1993. Environmental impact studies on marine communities: pragmatical considerations. *Australian Journal of Ecology*, 18, 63-80.
- Warwick, R.M., Uncles, R.J. 1980. Distribution of benthic macrofauna associations in the Bristol Channel in relation to tidal stress. *Marine Ecology Progress Series*, 3 (2), 97-103.
- Whomersly, P., Ware, S., Rees, H.L., Mason, C., Bolam, T., Huxham, M., Bates, H. 2008. Biological indicators of disturbance at a dredged-material disposal site in Liverpool Bay, UK: an assessment using time-series data. *ICES Journal of Marine Science*, 65, 1414-1420.
- Wieking, G., Kröncke, I. 2005. Is benthic trophic structure affected by food quality? The Dogger Bank example. *Marine Biology*, 146 (2), 387-400.
- Winterwerp, J. 2002. Near-field behavior of dredging spill in shallow water. *Journal of Waterway, Port, Coastal, and Ocean Engineering*, 128 (2), 96-98.
- Yates, M.G., Gosscustard, J.D., McGroarty, S., Lakhani, K.H., Durell, S., Clarke, R.T., Rispin, W.E., Moy, I., Yates, T., Plant, R.A., Frost, A.J. 1993. Sediment characteristics, invertebrates densities and shorebird densities on the inner banks of the Wash. *Journal of Applied Ecology*, 30 (4), 599-614.
- Zajac, R.N., Whitlatch, R.B., Thrush, S.F. 1998. Recolonization and succession in soft-sediment infaunal communities: the spatial scale of controlling factors. *Hydrobiologia*, 375/376, 227-240.

Chapter 8

Relationships between spatial patterns of macrofauna communities, sediments and hydroacoustic backscatter data in a highly heterogeneous and anthropogenic altered environment

Ruth Gutperlet*, Ruggero Maria Capperucci*, Alexander Bartholomä*,
Ingrid Kröncke*

*Marine Research Division, Senckenberg am Meer, Südstrand 40, 26382 Wilhelmshaven

8.1. Abstract

A survey was conducted in the Inner Jade tidal channel, the connection between the Jade Bay and the southern North Sea, to investigate the relationships between macrofauna community structure and environmental variables in a highly heterogeneous human disturbed environment. A manual expertise based classification of sidescan sonar records was successful in confirming the general relationship between backscatter intensity and sediment grain size in weakly disturbed environments. In highly disturbed environments, instead, the classification showed the influence of the topographic roughness over the sediment roughness in backscatter intensity. Low, but significant relationships between hydroacoustic classification and macrofauna community structure, as well as sediment distribution and the macrofaunal communities were identified. The most important impact on spatial community structure was the number of days after dredging/dumping activity for the JadeWeserPort, followed by

Gutperlet, R., Capperucci, R., Bartholomä, A., Kröncke, I. 2017. Relationships between spatial patterns of macrofauna communities, sediments and hydroacoustic backscatter data in a highly heterogeneous and anthropogenic altered environment. *Journal of Sea Research*, 121, 33-46, doi: 10.1016/j.seares.2017.01.005.

sediment characteristics. Sand dominated western stations that were dredged for the JWP exhibited a characteristic macrofaunal community. Another distinct community occurred in stations with elevated mud content within the regularly dredged old navigation channel and in the undisturbed south eastern area. The macrofaunal communities in the north eastern undisturbed area coincided with elevated gravel and shell contents. This study stresses the problems of benthic habitat mapping in such a heterogeneous area.

Key words *JadeWeserPort, Macrofauna, Spatial variability, Sediment heterogeneity, Hydroacoustics, Dredging activities*

8.2. Introduction

Patterns in macrofaunal community structure integrate temporal and spatial changes in marine habitats (Johnson 1972) and are often used to evaluate the status of ecosystems for environmental impact assessments (Warwick 1993; Borja et al. 2013). Biodiversity in a benthic habitat is influenced by biological and physical oceanographic factors such as oxygen, temperature, salinity and load of organic material (Robert et al 2014). Furthermore, benthic community structure depends on hydrodynamically mediated food resources (Wieking and Kröncke 2005; Kröncke 2006) and, at least to some degree, on substrate type (Gray 1974; Rhoads 1974; Snelgrove and Butman 1994). Anthropogenic physical disturbance, e.g. fishing (Auster and Langton 1998) and dredging (Newell et al. 1998; van Dalfsen et al. 2000; Simonini et al. 2007) can also have a strong impact on the composition and abundance of taxa.

The influences of dredging and dumping on the seabed and the associated macrofauna have been widely reviewed (Boyd et al. 2003; ICES 1992, 2001; Newell et al. 1998). Initial effects of dredging include a 30-70% reduction of species diversity and a 40-90% reduction in population density within the boundaries of dredged areas (Newell et al. 1998). Adjacent areas can also be affected by the redeposition of material mobilised during dredging and transported outside the boundaries of the dredge site (Newell et al. 2002; Hitchcock and Bell 2004). Macrofaunal community recovery rates are highly site specific (Boyd et al. 2004; Cooper et al. 2005; Kenny and Rees 1994, 1996; Kenny et al. 1998) and vary between 2 and 10 years (Newell et al. 1998). When dredging activities remove the surface layers of sediments, the remaining substrate may be altered and become unsuitable for re-colonisation by the species that previously inhabited that particular area (Kenny and Rees 1996; Boyd et al. 2005).

Specific tools are needed to catch and document such rapid changes (and the related processes), both spatially and temporally. Many studies have shown the effectiveness of hydroacoustic systems (i.e. singlebeam echo sounder SBES, sidescan sonar SSS, multi-beam echo sounder MBES) in benthic habitat mapping (e.g. Brown et al. 2002; Brown et al. 2004b; Freitas et al. 2003a, 2003b; Freitas et al. 2005). Recent studies focus on spatially continuous sampling, since this low cost, efficient method allows 100% coverage of the seafloor (Brown et al. 2004b). In heterogeneous areas with a patchy distribution of sediments and/or biological communities full coverage is extremely useful for mapping the diversity of habitats. Acoustic backscatter reflects abiotic surficial seabed characteristics (Collier and Brown 2005, Markert et al. 2013), such as seafloor topography, sediment grain size and bed roughness. In addition, biological assemblies, such as seaweed meadows (Preston 2006), blue mussel beds (Van Overmeeren et al 2009), coral reefs (Gleason et al 2006; Gleason 2009), oyster beds (Quester Tangent Corporation 2003) or aggregations of tube building worms (e.g., *Lanice conchilega*: Degraer et al 2008) or brittle star arms (e.g., *Amphiura filiformis*: Markert 2015) can also be successfully detected and mapped using acoustic backscatter. Although high-resolution SSS images can show decimetre-size features (Kenny et al. 2003), individual macrofaunal organisms are difficult to detect and ground-truthing of the backscatter data is needed to acquire a comprehensive dataset (Kenny et al. 2003). Many field studies first map the seabed with hydroacoustic tools, segmenting the images in regions, and then take only a few samples for each of them (Eastwood et al. 2006). This leads to interpolations, which may neglect habitat complexity (Diaz et al. 2004). Even with a dense ground-truth sampling grid, uncertainties are often detected in many study areas. For example, Markert et al. (2013) noted sharp boundaries between habitats of sorted bedforms, yet the hydroacoustic classification failed to detect a transition in the macrofaunal community. Similarly, Freitas et al. (2006) described three acoustic classes, yet four biological affinity groups were found along the acoustic gradient. In contrast, distinct communities occurring in multiple habitats have been reported using acoustic techniques (Kostylev et al. 2001, Freitas et al. 2003a, 2003b). Often, soft-sediment environments show gradational habitat changes, which are difficult to contour (Holler et al 2016). Moreover, the coexistence of different communities on the same substrate and/or the presence of the same community in different substrates make the habitat classification of such environments not straightforward (Shumchenia and King 2010).

Heterogeneous habitats are even more difficult to map than homogenous environments with clearly definable boundaries (Brown et al 2004a), or substrates

with a distinct gradient. One example of a heterogeneous sea bottom is the Jade channel in the German Bight, a tidal inlet which connects the Jade Bay with the open southern North Sea. Naturally mobile bedforms (Kubicki and Bartholomä 2011) coupled with dredging activities and construction works have resulted in a dynamic mosaic pattern of substrates in the Inner Jade channel (Capperucci and Bartholomä 2012). Moreover, the maintenance dredging of a navigational channel and the construction works for a deep-water port have introduced new sources of different sediments, e.g. the old Pleistocene basin clay “Lauenburger Ton” formation.

An initial study carried out in the Inner Jade channel compared sediment characteristics and macrofaunal communities before and during the port construction phases, finding that distinct communities resembled the dredging activities (Gutperlet et al. 2015). The current study expands upon this to i) characterise the habitats in this heterogeneous study area based on manual expert interpretation of the SSS data, sediment distribution and macrofaunal community structure, ii) compare spatial patterns of hydroacoustic classification, sediment composition and macrofaunal communities and test for pattern congruence, and iii) using multivariate statistical approaches, identify the natural and/or anthropogenic environmental factors (including dredging activities and grey values of the backscatter image derived by SSS) related to macrofaunal community compositions.

8.3. Material and methods

8.3.1. Study area

The research area lies in the central part of the Jade channel (Inner Jade, Figure 8.1a), a tidal inlet with the deep-water port of the German city Wilhelmshaven, the JadeWeserPort (JWP), within the German Bight (southern North Sea). The study area in front of the JWP is characterised by an upper mesotidal regime. Semi-diurnal tides range from 2.8 m at the northern entrance to 3.8 m in the southern Jade Bay (Kubicki and Bartholomä 2011). The study was conducted in the subtidal region of the Inner Jade (7.1-14.5 km of the old navigation channel) (Figure 8.1b).

Regular dredging of the old navigation channel by the local harbour authority WSA (Wasser- und Schifffahrtsamt Wilhelmshaven) guarantees a width of 300 m and a depth of 20.1 m (refer to the local chart datum, Normalhöhennull (NHN); Kubicki and Bartholomä 2011). Since March 2008, 46 million m³ of sand

has been used to create the 360 ha terminal area of the new deep-water port. Before piling, fine soft sediment was replaced by coarser material. In the process, sand was deposited both in the terminal area and also in front of the bulkhead (Figure 8.1b). The sand was mined from two sites north and south of the JWP, leading to deep depressions (approx. 50 m; Figure 8.1b) at both extraction sites. In 2012, land reclamation and the redirection of the navigation channel for access to the JWP were completed.

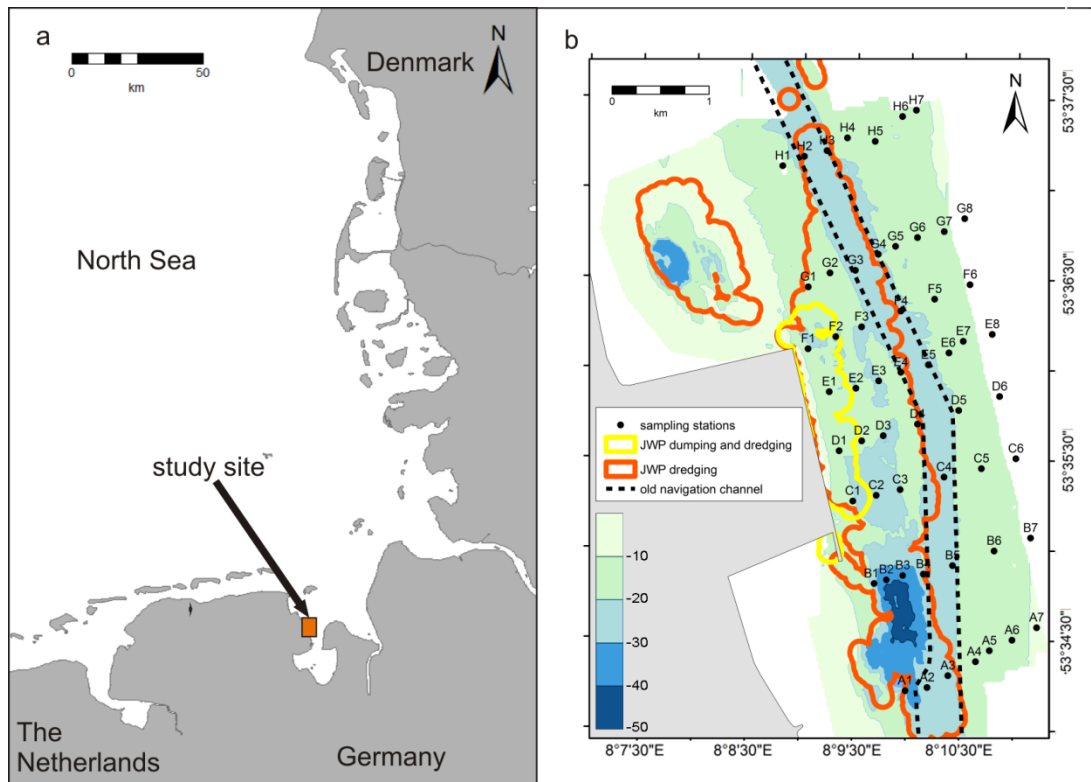


Figure 8.1. Location of a) the study area in the German Bight of the southern North Sea and b) bathymetry of the study area (depths in meter refer to Normalhöhennull (NHN)) and main features related to the new coastline (grey land), location of the sampling stations (black dots), the regularly dredged old navigation channel (dashed line), and the dredging (red line) and dumping (yellow line) activities for the JadeWeserPort (JWP).

8.3.2. Acoustic seafloor classification

In May 2010, a survey was carried out aboard the RV “Senckenberg”. A dual frequency Benthos™ 1624 SSS was deployed to map approx. 10.2 km² in front of the JWP construction site (6.1 km in north-south direction and 1.5 km in east-west direction). The north-west sector was not accessible at the time of the acoustic survey, and therefore 88% of the research area is covered with SSS data in this study. The Benthos 1624 SSS operates at two different frequency ranges: 110-130 kHz (low frequency, beam size 0.5° horizontal and 55° vertical) and 370-390 kHz (high frequency, beam size 0.5° horizontal and 35° vertical). A 200 m

swath width was used for data coverage. High resolution positioning was achieved by means of RTK-corrected DGPS data.

As the use of high frequency SSS data in such environment is more susceptible to external interferences, like engine noise (Collier and Brown 2005) or signal lost due to suspended mud (Schrottke et al. 2006), for the present study the low frequency data was processed and analysed. The recording and processing were carried out using SonarWiz™ software. Processing steps included both geometric and radiometric corrections. A final mosaic of the study area was exported (at 0.5 m resolution) and loaded into a GIS software (Global Mapper™ 13) for data analysis, mapping and interpretation.

Automated or semi-automated classification approaches of the Inner Jade SSS data could not entirely reflect the complexity of the sea bottom. In fact, the outputs of such classification tools did not show a segmentation of the SSS image in regions, but rather a fuzzy assemblage of classes with no clear meaningful correspondence to any morphological/sedimentological feature. This may be due to the high variability observed in sediment types and morphologies or the site-specific features (e.g. different generations of dredging marks, in some cases partially reworked by the highly dynamic sediments) leading to misclassifications. Therefore, manual expert classification was applied. Manual analysis and segmentation of the mosaic in regions (classification) was based on backscatter values (i.e. grey scale values) and seabed texture. The mapping process accounted for: intensity of the backscatter, presence/absence of seabed structures (e.g. dredging marks, dunes etc.), and morphological characteristics of such features (e.g. size, orientation, distribution, regularity, etc.). For each acoustic classes the mean grey level value was extracted from the raster image (by means of the QGIS2.8 Zone Statistics routine), and used for the identification of threshold values that grouped the classes into high- (HB), medium- (MB), and low- (LB) backscatter. Once defined the acoustic classes, bathymetry data from SBES (Furuno FCV 295) was combined with the backscatter from SSS to characterise the morphological features and to define the seabed roughness within each acoustic region.

8.3.3. *Sampling*

Following SSS data collection, 55 stations, with an average distance of approx. 250 m between stations, were sampled along eight west–east transects (A-H; Figure 8.1b). Around each JWP dredging and dumping position (midpoint coordinates were provided by the JWP Realization Company) a 100 m buffer was created. Within the 100 m radius around each sampling station, all buffers of

dredging and dumping activities before (measured since March 2008) and during the sampling (in May 2010) were summed. The eight sampling transects included 25 stations in the area that were directly affected by construction works for the JWP (Table 8.1).

Dredged stations	Dredging days	Days after
A2	25	263
A3	12	277
B1	4	342
B2	10	247
B3	30	139
B4	3	221
C1	3	382
C2	9	302
C3	19	341
D1	4	230
D2	3	387
D3	56	425
D4	2	322
E1	17	276
E2	26	375
E3	45	470
E4	5	274
F1	4	617
F2	11	381
F3	100	415
G1	3	56
G2	46	4
G3	22	259
H2	4	283
H3	2	252

Table 8.1. Number of dredging days for the JWP and number of days between the last dredging/dumping activity for the JWP and the sampling date for the JWP dredged stations (The regular dredging activities in the old navigation channel are not included here).

The local harbour authority WSA provided the total annual sediment volumes dredged from the old navigation channel (between 8 and 12 km) March 2008 – May 2010. 11 stations were placed in the regularly dredged old navigation channel.

At each station three samples were collected using a 0.1 m² Van Veen grab: two replicates for macrofauna and one sample for sediment analyses. At one station (G5) we were unable to collect a sediment sample. Stations E8, G1, G2, G8, H1, and H2 were not covered with SSS data.

8.3.4. Sediment sample procedure

After a macroscopic description of the recovered sediment sample, a subsample (approx. 200 ml) was taken for sediment grain size analysis. Sediments were split into mud fraction (<0.063 mm) and sand/gravel fraction by wet sieving over a 63 µm mesh in the laboratory. The sand and gravel fractions were separated by dry sieving over a 2 mm mesh. The sand content (0.063–2 mm) was weighed, treated with hydrochloric acid, and weighed again to determine the

content of sand sized shell debris. The gravel content (> 2 mm) was sorted into gravel and shell debris. For the total amount of shell debris in a sample, the shell debris of the sand sized and the gravel sized fraction were summed up. The samples were then classified in textural groups following Folk classification (1954).

8.3.5. *Macrofauna sample procedure*

Samples were sieved over a 1 mm mesh on board RV “Senckenberg”. The retained material was fixed with 4% buffered formaldehyde. In the laboratory, the samples were sieved again over 1 mm mesh and the organisms were stained with Rose Bengal. After sorting, all macrofaunal organisms were counted and identified to the lowest taxonomic level possible.

8.3.6. *Data analysis*

The effective number of taxa was chosen as the measure of community diversity, because it provides true diversity (opposed to entropy) with units representing number of taxa (Jost 2006). Other diversity indices can easily be converted into this linear number of equally-common taxa, e.g. the exponent of the Shannon-Wiener index gives the effective number of taxa (Jost 2006).

PRIMER™ v6 software (Plymouth Marine Laboratory) was used for multivariate statistical analyses (Anderson et al. 2008) of the macrofaunal community data. Taxa, not sampled quantitatively using the Van Veen grab (Hydrozoa, Bryozoa, Balanidae, Mysidacea, and large, mobile epifauna) were excluded from this analysis. Macrofaunal abundance was averaged from the two samples per station. After fourth root transformation, similarities between sampling stations were calculated using a Bray-Curtis coefficient (Bray and Curtis 1957) and then interpreted with the SIMPROF similarity profile test. SIMPROF tests the null hypothesis that a specific set of samples, not a priori divided into groups, do not differ significantly from each other (Clarke and Gorley 2006). The hierarchical agglomerative cluster analysis of the abundance data was used to identify macrofaunal community structure (Clarke and Warwick 2001). Ordination was conducted using MDS (non-metric multidimensional scaling) (Shepard 1962; Kruskal 1964). Differences between communities (clusters) were tested with a one-way PERMANOVA, which tests homogeneity using sample permutations (Anderson et al. 2008). The similarity percentage routine SIMPER was used to compare taxa abundance between the clusters and to identify characteristic taxa from distinct macrofaunal communities (Clarke and Warwick 2001).

Using ArcMap 10™, GIS maps were generated to overlay and compare the similarity of the spatial patterns of hydroacoustic classes, sediment composition, and macrofaunal communities. Using PRIMER, the RELATE routine matched the resemblance matrices of the macrofaunal abundance, the hydroacoustic classification and the sediment classes obtained from grab samples.

Distance-based linear models (DistLM) were carried out to assess the contribution of the environmental variables to the variability observed in the macrofauna community structure in PRIMER. DistLM is a multivariate multiple regression routine, in which a resemblance matrix of species abundance data is regressed against a set of explanatory (environmental) variables (Anderson et al. 2008). Prior to analysis, environmental variables were normalized to eliminate their physical units (Legendre and Birks 2012). Skewness of environmental data was inspected using draftsman plots (Anderson et al. 2008). The environmental variables were analysed individually (marginal tests), ignoring all other variables. This was followed by a sequential analysis where the “all specified” selection procedure based on the AIC (an information criterion) was used to include environmental variables. This selection procedure was chosen to explain the greatest degree of variation by fitting all the variables into the model (Clarke and Gorley 2006).

“Days after” (Table 8.1) included a dummy variable (10 000) for all stations not dredged or those in which the date of the last dredging activity is

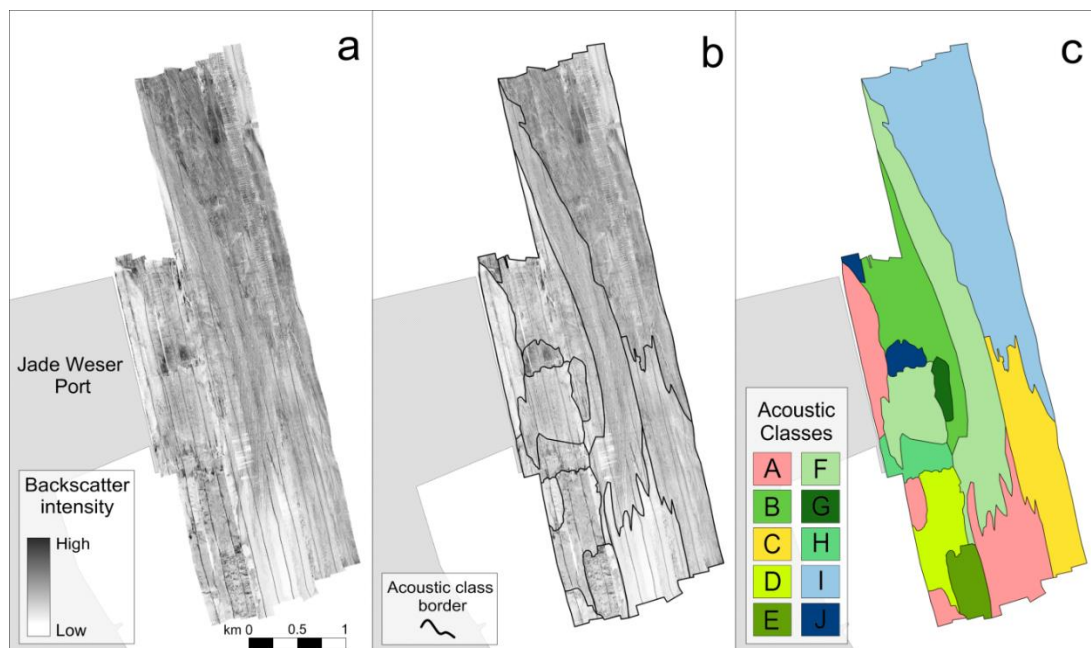


Figure 8.2. a) Sidescan sonar (SSS) mosaic (1 m resolution). High backscatter intensity in dark grey, low backscatter in white. b) Acoustic classes (black lines) on top of the SSS mosaic. c) Final classification of the SSS data in 10 acoustic classes (see Table 8.2 for the description).

unknown. The grey values were extracted from the backscatter image derived from the SSS data (Figure 8.2). To account for the heterogeneity of environment and uncertainties in absolute positioning due to variable offset of sampling gear (e.g. length and movements of the crane, shift of the sampler etc.) a buffer of 10 m was created around each sampling point. Grey level values were then extracted with the Zonal Statistics routine of QGIS for each buffer. The matrix of grey level values (including counts) was then combined with the threshold values used to group the HB, MB, and LB classes. Finally, the percentage of HB, MB, and LB were calculated for each station and used in the DistLM analysis. The model results were visualised through distance-based redundancy analysis routine (dbRDA; Legendre and Anderson 1999; McArdle and Anderson 2001; Anderson et al. 2004).

8.4. Results

8.4.1. *Classification of SSS backscatter data*

The mosaic was segmented into 10 acoustic classes (Figure 8.2), the characteristics of which are summarised in Table 8.2. Mean grey level values showed a grouping of the classes around three grey level intervals, separated by gaps (Table 8.2).

In fact, high greyscale values (lower backscatter intensity, LB) clearly differentiated one class (Class A) from a second group of seven classes (medium backscatter, MB), clustered around a narrow interval of grey values (189-195, using an 8-bit greyscale). In contrast, lower values (162-170, higher backscatter intensity) marked the transition toward two classes (Class I and Class J), which were labelled as HB classes. Two values (180 between HB and MB; 206 between MB and LB) were set as thresholds, and used for the computation of backscatter attributes for the dbRDA analysis.

Class A covered both the undisturbed area in the south and the western region close to the port bulkhead, where the disposal of sand took place. Here, the seabed surface appeared smooth, absent of relevant morphologies, either natural (bedforms) or human induced (dredging marks). It was characterised by the lowest grey scale values.

The whole eastern sector, less disturbed, presented medium-high backscatter values. Elongated structures (likely sand ribbons), parallel to the main channel and extending for hundreds of meters, were mapped on the mosaic from north to south, showing a sharp succession of HB and LB stripes. This eastern

region was subdivided in two acoustic classes. Class C presented a smooth bed surface, with no relevant features, except the aforementioned elongated structures, which did not produce evident morphologies on the single-beam data.

backscatter	mean greyvalue	acoustic class	characteristic sediments	description	sediments		roughness	SSS mosaic	
					ϕ	ϕ			
LB	216	A	mS to S	Both undisturbed (south) and dumping (JWP bulkhead) areas. Smooth surface, in general gently sloping. Absence of relevant seabed features (bedforms and dredging marks).					
	MB	195	B	S	Dredged area. Semicircular dredging marks (regularly spaced), with remobilised and reworked material (bedforms), partially superimposing the dredging marks				
		194	C	sM	Relatively undisturbed area. Scarce seabed features (elongated marks parallel to the channel, likely sand ribbons).				
		193	D	mS	Dredged area. Seabed texture relatively smooth, with steep ramps to the deeper sectors. Absence of dredging marks.				
		193	E	sM	Dredged area. Steep slopes separate the old seabed surface from the deeper, dredged sectors. Sharp morphologies (relict of the dredging activities) still visible, although single marks cannot be recognised.				
		191	F	mS	Dredged areas (old navigation channel and JWP area) with regularly shaped dredging marks (forming a characteristic, regular seabed textures). Scarce superimposed bedforms.				
		191	G	nn	Dredged area. Relicts of old dredging marks, partially overlaid by remobilized material (irregular bedforms).				
		189	H	nn	Dredged area. Steep cuts and slopes (irregularly spaced), relict of the dredging activities.				
HB	170	I	gS to sG	Relatively undisturbed area. Scarce seabed features (small dunes, perpendicular to the channel), a few elongated marks (sand ribbons?).					
	162	J	nn	Dredged areas. Regular dredging marks.					

Table 8.2. Acoustic classes and their characteristics, in relation with the sediment grain size composition and with the seabed roughness. A close up of the SSS image relative to each acoustic class is given in the last column, each box measuring approximately 90x120 m in size.

The backscatter intensity increased in class I (among the highest mean grey scale values), as well as the seafloor morphological complexity. In class I, scattered dune fields (from small to medium dunes, following Ashley 1990) and irregular morphologies in the north-eastern sector (transition between the eastern

tidal flat and the navigation channel) were observed. The north east corner of class I was located within a region of historical mussel farming.

All the seven remaining acoustic classes were located in the dredged areas. Three types of dredging marks could be recognised in the SSS data. In the old navigation channel (class F), they appeared as elongated, parallel, regularly shaped and spaced furrows. These were produced by the action of a trailing suction hopper dredger (TSHD), which was deployed both for regular channel maintenance and for sand pumping for land reclamation. Relicts of these dredging marks, usually reworked, could also be observed in other acoustic classes (class B and class G).

A second kind of dredging marks characterized class B, where a cutter suction dredger (CSD) was used to remove deeper layers of sand and mud. These marks occurred in stripes of semi-circular features. The high mobility of sediments in this area partially covered such dredging marks, especially in the eastern sector of class B. class J presented the highest mean grey level value among all the classes. It was also characterised by CSD marks.

The third type of dredging marks occurred in the eastern sector of class F, close to the bulkhead, where a different kind of dredger was deployed (a pontoon straddle dredger, BHD) to dig into the Pleistocene Lauenburger Ton formation. Sharp slopes bordered the area, cut through such very cohesive, semi-consolidated material, producing a flat depression with a very peculiar dredging-related texture

Medium backscatter and irregular seabed features defined the class H. Class D and class E contoured the southern mining pit. Class D presented smooth seabed texture and slopes. Class E corresponded to the deepest region of the research area, where dredging marks are still visible, although reworked and covered by more recent sedimentation.

8.4.2. Sediment composition and distribution

Sediments in the study site were mostly characterized by sand, to a lesser extent by gravel and shell debris (in the north-eastern region) and by mud-enriched fraction (Table 8.3; pie charts in Figure 8.3a).

Elevated mud contents (up to 86%) were observed in the old navigation channel, in some of the undisturbed eastern stations and in a few western, dredged stations. The highest content of gravel (35%) was located in the undisturbed north eastern region and in one station in the old navigation channel.

Station	Acoustic class	Mud <0.063 mm %	Sand 0.063–2 mm %	Gravel >2 mm %	Gravelly shells ca. %	Sandy shells ca. %	Total shell debris ca. %	Textural group (Folk, 1954)	Textural symbol
A1	A	17.96	79.16	0.00	0.00	2.87	2.87	Muddy sand	mS
A2	E	34.69	61.94	0.58	0.01	2.79	2.79	Slightly gravelly muddy sand	(g)mS
A3	E	80.41	19.09	0.12	0.02	0.35	0.37	Slightly gravelly sandy mud	(g)sM
A4	A	12.34	83.20	0.00	0.00	4.46	4.46	Muddy sand	mS
A5	A	15.27	81.11	0.00	0.00	3.61	3.61	Muddy sand	mS
A6	A	4.03	93.03	0.08	0.77	2.10	2.86	Slightly gravelly sand	(g)S
A7	C	59.28	36.44	0.42	2.23	1.63	3.86	Slightly gravelly sandy mud	(g)sM
B1	A	46.11	51.51	0.00	0.00	2.38	2.38	Muddy sand	mS
B2	D	37.34	56.58	1.95	0.00	4.12	4.12	Slightly gravelly muddy sand	(g)mS
B3	D	34.52	62.42	0.00	0.00	3.06	3.06	Muddy sand	mS
B4	D	35.13	61.95	0.00	0.00	2.93	2.93	Muddy sand	mS
B5	F	20.40	77.95	0.00	0.00	1.64	1.64	Muddy sand	mS
B6	C	27.44	65.25	2.06	0.70	4.55	5.25	Slightly gravelly muddy sand	(g)mS
B7	C	65.83	32.21	0.00	0.00	1.96	1.96	Sandy mud	sM
C1	F	10.57	82.09	5.12	1.42	0.81	2.23	Gravelly muddy sand	gmS
C2	F	70.21	27.16	2.47	0.00	0.16	0.16	Slightly gravelly sandy mud	(g)sM
C3	F	14.65	85.27	0.08	0.00	0.00	0.00	Slightly gravelly muddy sand	(g)mS
C4	F	38.97	35.37	25.60	0.07	0.00	0.07	Gravelly mud	gM
C5	C	86.49	12.85	0.00	0.00	0.66	0.66	Sandy mud	sM
C6	I	26.44	65.71	1.42	3.96	2.47	6.44	Slightly gravelly muddy sand	(g)mS
D1	A	10.66	88.28	0.00	0.01	1.05	1.06	Muddy sand	mS
D2	J	43.34	55.35	0.29	0.20	0.83	1.03	Slightly gravelly muddy sand	(g)mS
D3	J	14.16	84.79	0.05	0.00	1.00	1.00	Slightly gravelly muddy sand	(g)mS
D4	F	3.18	89.80	0.82	3.42	2.77	6.19	Slightly gravelly sand	(g)S
D5	I	50.54	46.73	0.07	0.05	2.61	2.67	Slightly gravelly sandy mud	(g)sM
D6	I	0.89	69.69	2.40	22.37	4.65	27.01	Slightly gravelly sand	(g)S
E1	A	1.61	97.59	0.01	0.00	0.78	0.78	Slightly gravelly sand	(g)S
E2	B	0.70	94.57	3.22	1.09	0.42	1.51	Slightly gravelly sand	(g)S
E3	B	21.45	76.95	0.77	0.32	0.51	0.83	Slightly gravelly muddy sand	(g)mS
E4	F	4.05	90.41	2.48	1.79	1.26	3.06	Slightly gravelly sand	(g)S
E5	F	68.56	28.87	0.00	0.00	2.57	2.57	Sandy mud	sM
E6	I	83.07	15.17	1.03	0.26	0.47	0.73	Slightly gravelly sandy mud	(g)sM
E7	I	62.76	34.48	0.04	0.08	2.64	2.72	Slightly gravelly sandy mud	(g)sM
E8	no data	7.22	86.26	0.01	3.22	3.29	6.51	Slightly gravelly sand	(g)S
F1	A	3.35	92.33	3.46	0.55	0.31	0.86	Slightly gravelly sand	(g)S
F2	B	1.29	97.75	0.29	0.21	0.45	0.66	Slightly gravelly sand	(g)S
F3	B	9.08	90.44	0.14	0.01	0.32	0.34	Slightly gravelly sand	(g)S
F4	F	36.00	60.39	0.00	0.05	3.57	3.62	Muddy sand	mS
F5	I	3.06	88.88	2.16	4.68	1.21	5.90	Slightly gravelly sand	(g)S
F6	I	4.89	63.53	0.01	26.38	5.19	31.57	Slightly gravelly sand	(g)S
G1	no data	2.48	94.78	2.21	0.06	0.46	0.52	Slightly gravelly sand	(g)S
G2	no data	7.20	90.87	1.38	0.03	0.53	0.56	Slightly gravelly sand	(g)S
G3	B	44.50	52.37	0.21	0.20	2.73	2.93	Slightly gravelly muddy sand	(g)mS
G4	F	45.37	52.15	0.00	0.03	2.45	2.48	Muddy sand	mS
G5	I	no data	no data	no data	no data	no data	no data	No data	no data
G6	I	3.39	77.52	2.80	13.54	2.75	16.29	Slightly gravelly sand	(g)S
G7	I	5.00	55.21	25.54	11.44	2.81	14.24	Gravelly sand	gS
G8	no data	14.82	62.42	4.19	15.85	2.72	18.57	Gravelly muddy sand	gmS
H1	no data	0.26	99.32	0.00	0.00	0.42	0.42	Sand	S
H2	no data	34.73	63.82	0.00	0.00	1.45	1.45	Muddy sand	mS
H3	I	50.35	45.99	0.30	0.58	2.78	3.36	Slightly gravelly sandy mud	(g)sM
H4	I	4.27	90.66	0.73	2.19	2.15	4.34	Slightly gravelly sand	(g)S
H5	I	0.37	84.78	3.95	7.46	3.44	10.90	Slightly gravelly sand	(g)S
H6	I	6.84	50.80	35.10	5.57	1.69	7.25	Muddy sandy gravel	msG
H7	I	10.68	70.79	4.88	11.49	2.16	13.65	Gravelly muddy sand	gmS

Table 8.3. Summary of the sediment grain size composition per station. For each sampling locations, the relative acoustic class is given.

According to Folk (1954) 10 sediment textural groups were present in the study area, ranging from sandy mud to muddy sandy gravel (Table 8.3; Figure 8.3a). Slightly gravelly sand (17 of 54 stations) dominated the north-western dredged sector and appeared at seven north-eastern stations and one station in the south-eastern area. The south-western dredged stations were dominated by muddy sand, which also occurred at two stations in the old navigation channel, one station in the north-western area and two stations in the undisturbed south-eastern area. Slightly gravelly muddy sand was found in the western dredged area and two stations in the undisturbed eastern area. Slightly gravelly sandy mud appeared at four stations in the eastern area, two stations in the old navigation channel, and one western dredged station. Sandy mud occurred at two south-eastern stations and one station in the old navigation channel. Gravelly mud was

found at only one station in the old navigation channel. Gravelly muddy sand was located at two stations in the undisturbed north-eastern area and in front of the JWP bulkhead. Pure sand occurred only at one north-western station. Gravelly sand was found at one station in the north-eastern area. Muddy sandy gravel also appeared at only one north-eastern station. The content of shell debris was particularly high (up to 32%) in seven stations, all located in the easternmost sector of the research site.

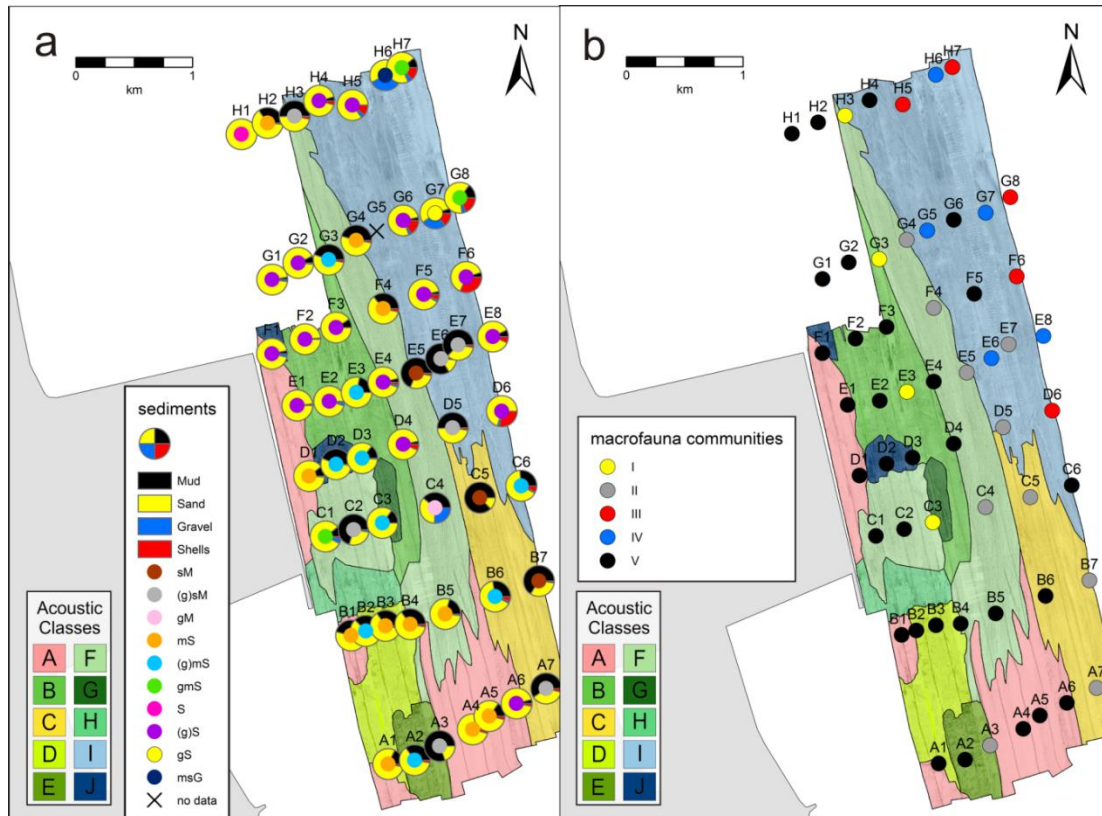


Figure 8.3. Sediment and macrofaunal composition in relation to the acoustic classification. a) the main sediment components (gravel, sand, mud, and shell lag) are represented by pie charts, overlapped by dots which correspond to the textural classification (after Folk, 1954) of the samples. b) Spatial distribution of the 5 macrofaunal communities, as derived by the statistical analysis.

8.4.3. Macrofauna

In total, 71 macrofauna taxa were identified. 50.7% of the organisms were polychaetes, 19.7% crustaceans, and 14.1% molluscs (15.5% belonged to Anthozoa and other groups). The SIMPROF test of the cluster analyses (Figure 8.4) revealed an “outlier” group (community I) and four communities (II-V). All communities were significantly different (PERMANOVA main test, $df = 4$, mean squares = 14166, Pseudo-F = 6.3289, $p = 0.001$, $p(\text{Monte Carlo}) = 0.001$; Table 8.4).

Macrofauna communities	df	PERMANOVA		PERMDISP	
		t	p	t	p
I, II	12	2.1574	0.002	6.9123	0.001
I, III	7	1.8193	0.009	7.4090	0.006
I, IV	7	1.7360	0.010	8.3622	0.004
I, V	33	1.5727	0.013	2.1731	0.208
II, III	13	3.1765	0.001	0.6723	0.566
II, IV	13	2.8661	0.002	0.2705	0.861
II, V	13	3.5894	0.001	4.3614	0.003
III, IV	8	1.6412	0.013	0.4604	0.643
III, V	34	2.3925	0.001	3.7020	0.005
IV, V	34	2.4478	0.001	3.4231	0.012

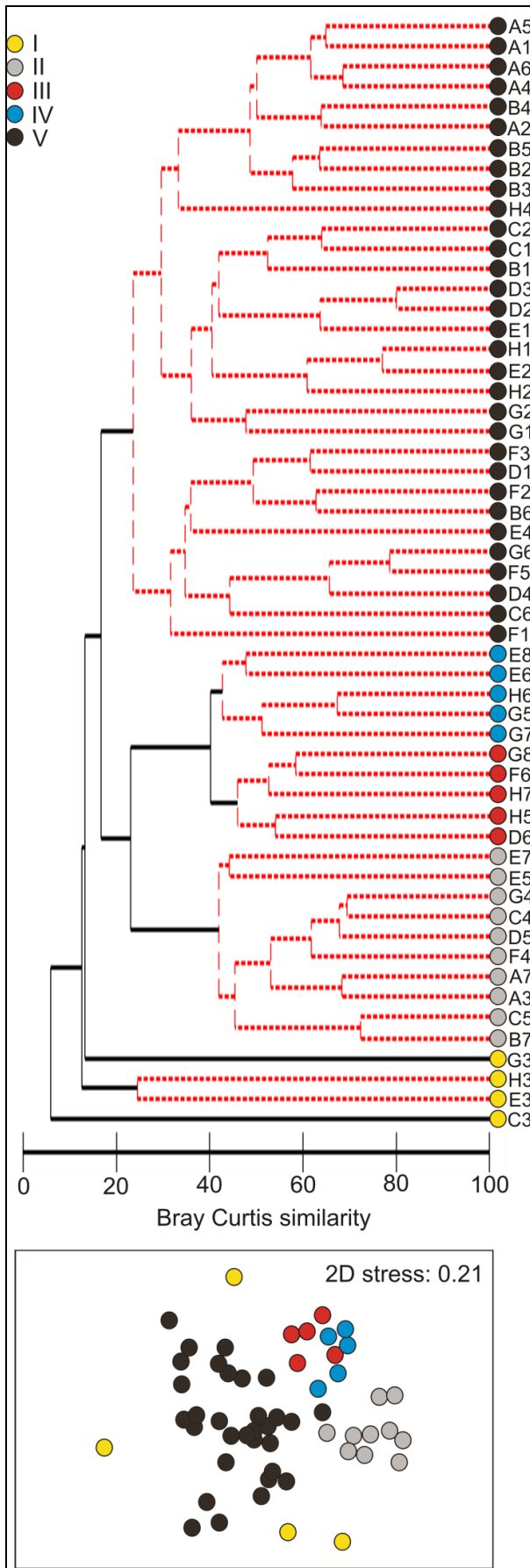
Table 8.4. Results of the PERMANOVA and PERMDISP pairwise test for all of the macrofauna communities, statistically significant ($p < 0.05$) are marked in bold.

The four stations exhibiting community I had the lowest mean taxa number, lowest mean abundance, and lowest biodiversity in the study area (Table 8.5). Community I was located within the old navigation channel and in the area dredged for the JWP (Figure 8.3b), associated with slightly gravelly muddy sand (75%) and slightly gravelly sandy mud (25%). The bivalve *Petricolaria pholadiformis*, which prefers fine sediments, was the characteristic species across the four stations (Table 8.6).

Community II appeared at stations with high mud content (40% with slightly gravelly sandy mud, 30% sandy mud, 20% muddy sand, and 10% gravelly mud) and located in the regularly dredged old navigation channel, the south eastern area and at one station (A3) in the south western dredged area (Figure 8.3b). Beside the mudphil amphipod *Corophium volutator*, the opportunistic spionids *Pygospio elegans* and *Polydora cornuta*, the bivalve *Petricolaria pholadiformis*, and juvenile mussels of the Mytilidae family characterised this community (Table 8.6).

Macrofauna community	I		II		III		IV		V	
	Mean	(sd)	Mean	(sd)	Mean	(sd)	Mean	(sd)	Mean	(sd)
Taxa number	3.5	(1.7)	7.3	(3.9)	11.2	(3.6)	17.6	(4.6)	4.8	(2.5)
Abundance [ind./m ²]	25.0	(12.9)	655.0	(855.9)	474.0	(271.5)	1682.0	(1499.5)	123.2	(135.8)
Effective number of taxa (Jost, 2006)	3.197	(1.468)	3.372	(1.502)	4.914	(2.711)	6.055	(1.473)	3.359	(1.518)
Mud content [%]	32.74	(17.35)	59.42	(16.84)	6.33	(6.29)	25.53	(38.37)	17.40	(17.34)
Sand content [%]	65.15	(18.92)	35.86	(14.38)	70.24	(8.92)	51.86	(29.11)	78.59	(17.16)
Gravel content [%]	0.34	(0.30)	2.62	(8.07)	3.09	(1.94)	15.42	(17.65)	1.09	(1.36)
Shell debris content [%]	1.78	(1.62)	2.10	(1.32)	20.34	(8.77)	7.18	(5.54)	2.93	(3.09)
Depth [m]	25.0	(0)	20.5	(6.0)	13.0	(4.5)	15.0	(4.1)	21.5	(5.2)
Dredging days	22.0	(17.7)	1.2	(3.8)	0	(0)	0	(0)	11.8	(21.6)

Table 8.5. Taxa number per station (0.1 m²), abundance (individuals/m²) and effective species number of all macrofaunal communities are given as mean with standard deviation (sd) with sediment categories (%), depth and number of dredging days for the JWP at the concerning stations.



Community III occurred in the north eastern area with elevated shell debris, slightly gravelly sand (60%) and gravelly muddy sand (40%; Figure 8.3b, Table 8.5). The polychaetes *Scoloplos (Scoloplos) armiger*, *Pygospio elegans*, *Nephtys caeca*, *Gattyana cf. cirrhosa*, *Nephtys* spp. juv., and *Eteone longa* and Anthozoa were characteristic of this community (Table 8.6).

	Mean abundance	Mean similarity	Contribution %
Community I		4.07	
<i>Petricolaria pholadiformis</i>	0.3	4.07	100
Community II		49.19	
<i>Corophium volutator</i>	26.6	19.94	40.53
<i>Pygospio elegans</i>	8.2	14.88	30.25
Mytilidae sp. juv.	1.1	5.8	11.79
<i>Petricolaria pholadiformis</i>	1.1	3.25	6.6
<i>Polydora cornuta</i>	24.7	2.54	5.15
Community III		49.36	
<i>Scoloplos (Scoloplos) armiger</i>	6.8	11.00	22.28
<i>Pygospio elegans</i>	23.7	9.89	20.03
<i>Nephtys caeca</i>	2.3	8.06	16.33
<i>Gattyana cf. cirrhosa</i>	1.1	6.92	14.02
Anthozoa	5.7	6.54	13.25
<i>Nephtys</i> spp. juv.	0.5	1.88	3.82
<i>Eteone longa</i>	0.5	1.67	3.39
Community IV		47.4	
Anthozoa	32.3	7.47	15.77
<i>Pygospio elegans</i>	12.5	5.97	12.6
Mytilidae sp. juv.	45.9	5.96	12.58
<i>Scoloplos (Scoloplos) armiger</i>	5.1	5.35	11.3
<i>Caprella</i> sp.	36.0	4.46	9.41
<i>Nephtys caeca</i>	0.8	3.8	8.01
<i>Gattyana cf. cirrhosa</i>	8.3	3.1	6.55
<i>Bivalvia</i> spp. juv.	1.1	2.76	5.82
<i>Tubificoides benedii</i>	3.5	1.31	2.77
<i>Dyopedos monacanthus</i>	2.2	1.12	2.35
Community V		31.32	
<i>Scoloplos (Scoloplos) armiger</i>	2.0	13.01	41.52
<i>Macoma balthica</i>	3.3	9.38	29.95
Mytilidae sp. juv.	1.4	2.24	7.16
<i>Peringia ulvae</i>	2.9	2.06	6.58
<i>Pygospio elegans</i>	0.3	1.24	3.97
<i>Nephtys hombergii</i>	0.3	0.95	3.02

Table 8.6. Characteristic macrofauna taxa with mean abundance of non-transformed data and mean similarity and percentage of their contribution to the community, based on Bray-Curtis similarity, using fourth-root-transformed taxa abundance data.

Community IV showed the highest mean taxa number, mean abundance, and biodiversity in the study area (Table 8.5). Similar to community III, community IV was situated in the north eastern area (Figure 8.3b). Community IV was associated with mixed sediments (sand with high gravel or high mud content; Table 8.5), slightly gravelly sandy mud (E6), slightly gravelly sand (E8), gravelly sand (G7) and muddy sandy gravel (H6; Figure 8.3). Community IV was characterised by Anthozoa, the polychaetes *Pygospio elegans*, *Scoloplos (Scoloplos) armiger*, *Nephtys caeca*, *Gattyana cf. cirrhosa*, the bivalves Mytilidae spp. juv. and

Bivalvia spp. juv., the amphipods *Caprella* sp., and *Dyopedos monacanthus* and the oligochaete *Tubificoides benedii* (Table 8.6).

Community V was also found in mixed sediments (41.9% with slightly gravelly sand, 29.0% muddy sand, 19.4% slightly gravelly muddy sand, 3.2% gravelly muddy sand, 3.2% slightly gravelly sandy mud, and 3.2% sand) mainly in the western area (dredged for the JWP), and in the southern transects A and B (Figure 8.3). In contrast to community IV, mean taxa number, mean abundance, and biodiversity were low in community V (Table 8.5). Community V was dominated by *Scoloplos (Scoloplos) armiger* and the bivalve *Macoma balthica*. Juvenile Mytilidae, the mud snail *Peringia ulvae*, and the polychaetes *Pygospio elegans* and *Nephtys hombergii* were characteristic of community V (Table 8.6).

8.4.4. Comparison of spatial patterns

The RELATE routine identified a low, yet significant similarity between macrofaunal abundance and the 10 acoustic classes (Rho = 0.093; $p = 0.008$). The similarity between macrofaunal abundance and sediment classes was higher and also significant (Rho = 0.211; $p = 0.001$). In contrast, there was no significant similarity between the patterns of sediments and the acoustic classification (RELATE, Rho = -0.007; $p = 0.496$). Nevertheless, Figure 8.5 shows some trends in the sediment distribution per acoustic class. In the area dredged for the JWP, classes A and B were characterised by muddy sand to sand with a sand content >90% for 83% of the samples belonging to class B. Classes C and F showed a similar composition (sandy mud to muddy sand) with a prevalence of coarser fractions in class F. Gravelly mud was only detected at one station (C4). Similar to class C, muddy sand prevailed in class D. Sandy mud characterised class E (sub-represented: one sample). Only one class (class I in the undisturbed north-eastern area) aligned along the sand-gravel axis. Classes G, H, and J were not covered by the sampling transect, therefore no sediment data was available.

8.4.5. Relationship between environmental variables and macrofauna community structure

In the marginal DistLM, differences in the spatial distribution of macrofaunal communities were best explained by the correlation with the number of days after the last dredging/dumping activity for the JWP (10.5%), followed by sediment characteristics (7.6–10.2%), high backscatter (7.4%), depth (6.3%), low backscatter (4.6%), and the number of dredging days for the JWP (3.7%). In the sequential tests, the number of days after the last

dredging/dumping activity explained the greatest proportion of variation in the macrofaunal community (10.5 %). After accounting for the variability associated with dredging/dumping activities, sand content (7.8%), mud content (5.9%), and shell debris (3.8%) still explained a significant, albeit lower variation in the macrofaunal community data (Table 8.7).

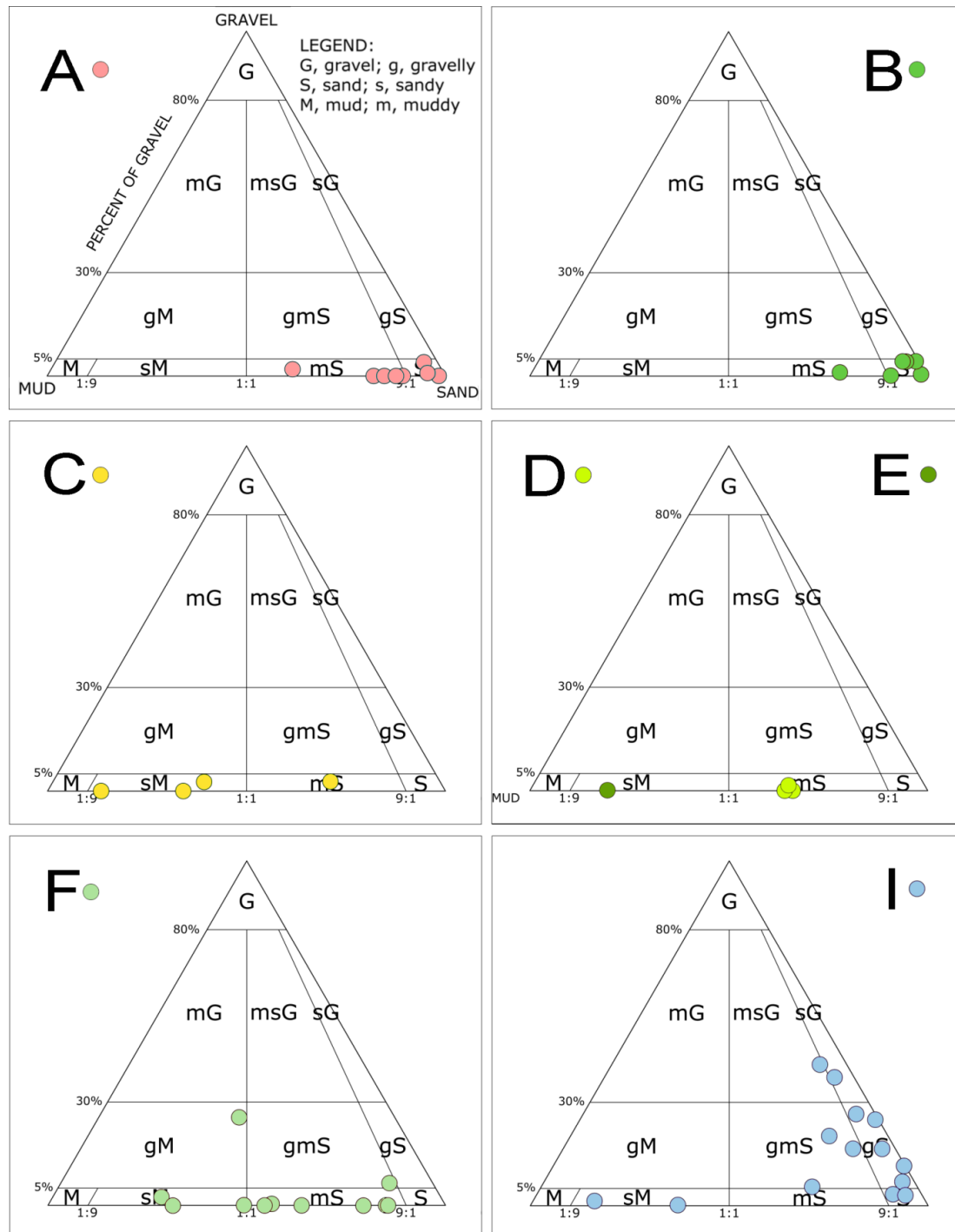


Figure 8.5. Sediment classification in textural groups (Folk, 1954) per acoustic class. Similar compositions can be observed between classes A and B (mS to S), and among classes C and E (sM) and D and F (mS). Only one

sample defines Class E, while three samples are plotted for Class D (although very similar, therefore not clearly visible). Classes G, H, and J were not sampled.

Environmental variables	Marginal tests			Environmental variables	Sequential tests			
	Pseudo-F	p	% Prop.		AIC	Pseudo-F	p	% Prop.
Days after	6.2089	0.001	10.49	Days after	439.44	6.2089	0.001	10.49
Sand content	6.0364	0.001	10.23	Sand content	436.45	4.9343	0.001	7.76
Mud content	5.3962	0.001	9.24	Mud content	434.36	3.9410	0.001	5.86
Shell debris content	4.3442	0.001	7.58	Shell debris content	433.57	2.6055	0.005	3.76
High backscatter	4.2593	0.001	7.44	Depth	433.84	2.4976	0.006	3.51
Depth	3.5748	0.001	6.32	Low backscatter	433.10	2.3986	0.010	3.27
Low backscatter	2.5586	0.011	4.61	Medium backscatter	434.34	1.6338	0.098	2.21
Dredging days	2.0404	0.027	3.71	High backscatter	434.63	0.8392	0.624	1.21
Medium backscatter	1.6726	0.106	3.06	Dredging days	434.30	0.6783	0.744	0.93
Gravel content	1.6134	0.095	2.95	Gravel content	435.57	0.6173	0.786	0.84

Table 8.7. Results of the multivariate regression analysis (DistLM). Environmental variables were analysed individually (marginal test) and sequentially using a step-wise forward selection procedure (AIC = an information criterion). % Prop. is the proportion of variance in macrofauna taxa explained by each variable. Significant (<0.05) values are indicated in bold (“days after” = the number of days after the last dredging/ dumping activity for the JWP).

The dbRDA-plot (Figure 8.6) illustrates these results and shows that communities I and V align at the axes of sand, dredging days and depth. In contrast, mud content was the most important structuring factor for community II. Communities III and IV coincided with elevated contents of gravel and shells and high backscatter. In total, the degree of variation explained by these environmental variables was rather low, at 40% ($R^2 = 0.39853$). (See Figure 8.6).

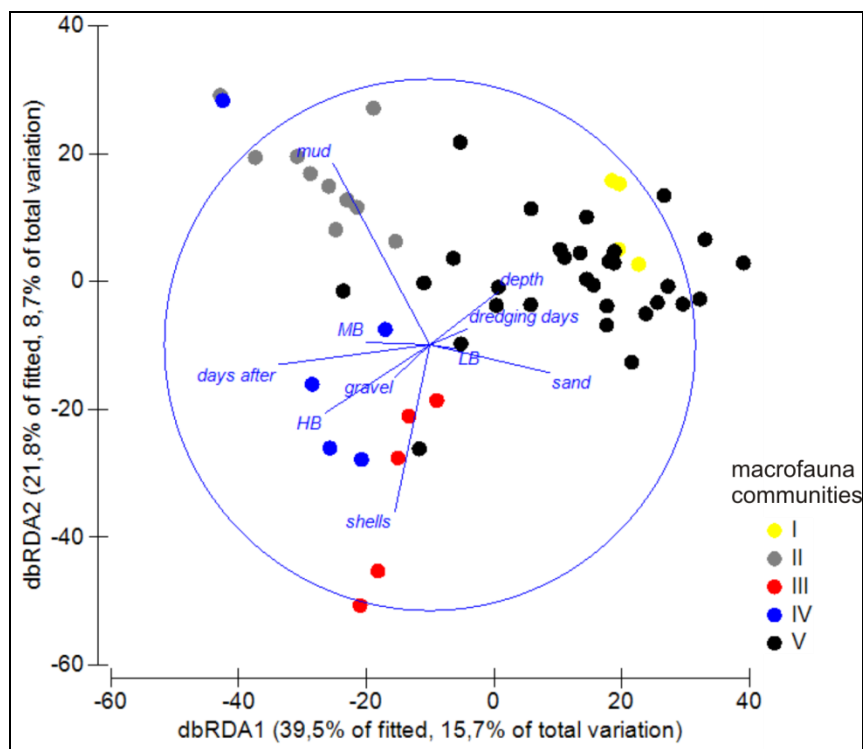


Figure 8.6. dbRDA plot representing the model of spatial variation in macrofaunal community structure and the relationship to environmental parameters (“days after” = number of days after the last dredging/ dumping activity for the JWP; HB = high backscatter, MB = medium backscatter, LB = low backscatter).

8.5. Discussion

The study area in the Inner Jade is a very heterogeneous environment, with multiple human activities, which had different degrees of impact (spatially and temporally) on the entire system. The western part and the old navigation channel have experienced frequent anthropogenic disturbances due to dredging and dumping activities. In contrast, the eastern and southern parts are less disturbed.

Many studies have demonstrated that acoustic seabed classification using SSS is a suitable tool for the identification of bed substrates and benthic habitats (Brown et al. 2004b, Ehrhold et al. 2006, Zajac et al. 2003, Franklin et al. 2003, Brown and Collier 2008). Soft bottoms (e.g., Markert et al. 2013), hard bottoms (e.g. Ojeda et al. 2004), and mixed environments with combination of hard- and soft- grounds (e.g. Cochrane and Lafferty 2002, Lucieer 2008, Holler et al. 2016), have been successfully classified by means of automatic and semi-automatic acoustic classification systems. Nevertheless, the classification of transitional environments with gradational changes in sediment and/or biological composition is still problematic (Pinn and Robertson 2003). In the present study, a manual expert approach for segmenting the SSS image into acoustic classes was preferred to automatic and semi-automatic methods, due to the poor preliminary results given by such techniques. In fact, the extreme variability in sediment composition and distribution, the meter-sized patchiness of the biological/sedimentological association, superimposed by many different morphological features, both natural (dune fields) and human induced (dredging marks and slopes), resulted in a fuzzy assemblage of acoustic classes, difficult to translate in terms of habitat.

In the attempt to produce habitat maps of a very heterogeneous region, Brown et al. 2004a described the problem of generalization (lumping) versus separation (over-splitting) of acoustic classes. In their study, the high degree of sediment heterogeneity was problematic for the identification of discrete boundaries between the physical habitats (Brown et al. 2004a).

Similarly, in this study the limited range of grey scale values would have brought to a very coarse classification (lumping effect, 3 classes summarized by the HB, MB and LB groups). On the other hand, the system-related decimetre-scaled resolution of the SSS, coupled with the general high quality of the recorded data and the vast catalogue of seabed features, in theory would have allowed the segmentation of the area in metric-sized polygons. Such a fragmentation (over-splitting effect) of the seabed, however, would not

correspond to the actual sedimentological and biological conditions and, at the end, would have no habitat meaning.

In this study, the manual expert acoustic classification reflected both the sea bottom roughness (mainly related to the anthropic activities) and, to a lesser extent, the complex pattern of the sediment distribution in the area. The end members among the 10 classes, in fact, reflected the degree of disturbance of the environment (class A in the southern region, class I in the north-eastern one), while for the majority of the remaining acoustic classes a complex interplay of sediment composition and topography drove the splitting process and the interpretation of the classification in habitat terms.

8.5.1. Hydroacoustic classification versus sediment distribution and seabed roughness

Strong links between sediments and acoustics have been demonstrated (e.g. Collier and Brown 2005), but the relationship between sediment and backscatter is not always straightforward (Ehrhold et al. 2006). Sedimentological factors (e.g. grain size, volumetric heterogeneity, fine-scale roughness and/or surface sediments) and significant slope variation may play an important role in interpreting acoustic responses (Urlick 1983).

The effects of the seabed morphology on the seafloor classification have been widely investigated in the last years (e.g., Briggs et al. 2001, Ferrini and Flood 2006, De Falco et al. 2010). Capperucci and Bartholomä (2012) distinguishes between topographic and sediment roughness, the first one reflecting the general geomorphological aspect of the seafloor (e.g. bedforms, slopes, etc.), the latter the sediment composition (grain size, sorting, etc.) and its spatial distribution on the seabottom.

The use of SSS data is somehow limited in assessing the influence of the topography on backscatter data, for which other systems (i.e. Multibeam or LiDAR) are usually preferred, alone or coupled with SSS data. Nevertheless, in the present study the combination of SSS and SB data allowed to compare and translate the backscatter texture into topographic and morphological features, including them in the definition of the different acoustic classes.

Although the statistical descriptors showed no significant similarity of the sediments with the 10 acoustic classes (Table 8.2), a trend could be found with the main backscatter groups (LB, MB, and HB), confirmed by the comparison with the seabed roughness. In fact, Class A (LB, mean grey level value: 216) was characterised by a smooth surface with sandy sediments and a few finer samples (muddy sand), whereas Class I (HB, mean grey level value: 170) was represented

by a rougher surface with coarser sediments (gravelly sand to sandy gravel, with a shell lag content up to 34%), reflecting the general relationship between backscatter intensity, grain size (Collier and Brown 2005), and topography (roughness).

The apparent contradiction of the MB acoustic classes (finer sediments but higher backscatter, in comparison to Class A; rougher surface but lower backscatter, in comparison to classes I and J) clearly shows the role of these two components (topographic and sediment roughness) on the backscatter intensity. An example is given by class E and D (Table 8.2), with the same mean grey level value (193) but a different combination of sediment composition and topography.

Such outcomes confirmed that in environments where the morphological and sedimentological heterogeneity occur at metric scale, the interplay between topography and sediments rule the SSS backscatter response, making unsuccessful the use of SSS image as a stand-alone method for sediment zonation and their associated benthic communities.

Brown and Collier (2008) concluded that in special environments it is not possible to extrapolate substrate maps into habitat maps based on acoustic signatures. The high anthropogenic impacts, combined with the high degree of natural variability appear to make the Inner Jade an ideal example of such an environment.

8.5.2. Hydroacoustic classification and sediments versus macrofauna community structure

The low, yet significant correlation between resemblance matrices of acoustic classification and macrofauna community structure emphasize the heterogeneity of the Inner Jade. Spatial heterogeneity of macrofaunal species is often linked to heterogeneity of sediments (Brown et al. 2004a), reported here relationship between macrofaunal community structure and sediment classes. Markert et al. (2015) also found a high heterogeneity of both sediment compositions and macrofaunal community structure in the shore-face connected ridges north of the nearby island of Spiekeroog (also in the German Bight, southern North Sea). The authors explained the small-scale spatial distribution of macrofaunal affinity groups by a heterogeneous surface sediment pattern, resulting from local hydrodynamics, which also influences the food availability (Markert et al. 2015).

However, in the current study, few taxa had known sediment preferences. The taxa with known sediment preferences observed in this study included

Anthozoa, *Corophium volutator* and *Petricolaria pholadiformis*. Anthozoa typically settle on gravel and shells, and were observed in the undisturbed north-eastern area (communities III and IV). In contrast, *Corophium volutator* and *Petricolaria pholadiformis* prefer fine sediments (Fenchel et al. 1975; Tebble 1976) and were found in the regularly dredged old navigation channel and at some stations in the undisturbed south-eastern area (communities I and II). Unlike the previously described taxa, *Scoloplos (Scoloplos) armiger* and *Pygospio elegans* cannot be used as indicators of sediment type. *Scoloplos (Scoloplos) armiger* (communities III, IV, V) is more cosmopolitan, without a real sediment preference (Coosen et al. 1994), and the opportunist *Pygospio elegans* (communities II, III, IV, V) also has a wide habitat tolerance (Bolam and Fernandes 2003). Although these taxa cannot be used as indicators of a particular sediment type, these species represent a tolerance for disturbance. It is likely that the impoverished macrofaunal abundance measured in the areas dredged for the JWP are the result of the physical disturbance due to dredging and not related to the bottom sediment characteristics. Overall, the macrofauna data indicated a rapid re-colonisation is possible after dredging cessation in highly dynamic areas (Borja et al. 2010), such as the Inner Jade. Nevertheless, community V showed still the characteristics of an early succession state (low taxa number, low abundance and dominance of cosmopolitan and opportunistic taxa).

8.5.3. Environmental factors structuring the macrofauna communities

The number of days after the last dredging/dumping activities for the JWP was the most important parameter describing the variability of macrofaunal communities in the Inner Jade, followed by sediment characteristics (content of sand, mud and shell debris). Depth, high and low backscatter grey values, and dredging intensity (expressed as the number of dredging days for the JWP) also played a significant role. Gravel content was less important, because only community IV appeared on undisturbed stations with elevated gravel content. Community V was the biggest group and occurred mainly in the area dredged for the JWP. This was also the deepest site of the study area and was dominated by sand. Community II showed an affinity for elevated mud contents, which predominately occurred in and close to the old navigation channel. In contrast, the spatial distribution of community III was best explained by the presence of shell debris in the undisturbed north-eastern area. Even with the multiple environmental parameters measured in this study, we were only able to explain 40% of the macrofaunal community data. This suggests that additional

environmental factors accounted in for this study are influencing the macrofaunal communities.

In the adjacent Jade Bay, Schückel et al. (2015) found that the macrofaunal species compositions were best explained by the variability of tidal current velocity and depth, followed by sediment characteristics (mud, total organic carbon, gravel and median grain size). Yet in their study Schückel et al. (2015) could also only explain 30% of the total variability in the macrofaunal community data using these parameters. They suggested that variables related to food availability (chlorophyll *a* content), predation or topographic characteristics could be responsible for the unexplained variability (Schückel et al. 2015). Based on our results we suggest that the unknown dredging intensity in the old navigation channel in the Inner Jade may helpful to explain re-colonisation in that area.

For future ecological assessments of human impacts, we recommend including a biological trait analysis. This technique can be used to investigate how ecosystem functions are altered by natural or human-mediated changes of species traits (Krumhansl et al. 2016).

8.6. Summary

The acoustic classification reflected the dredge marks and natural bedforms, but not the full heterogeneity of sediments and their associated benthic communities in the Inner Jade channel. Thus, this manual expert classification approach was successful in identifying anthropogenic disturbance of the seabed and in mapping natural bedforms. According to the different dredge marks, more acoustic classes in the disturbed area were generated than macrofauna communities were present. Thus, there were no strong links between the geological, biological and hydroacoustic patterns. Differences in the spatial distribution of macrofauna communities were best explained by the number of days after the last dredging/dumping activity, followed by sediment characteristics. Depth, backscatter grey values, and the number of dredging days played also a significant role as a structuring force.

8.7. Acknowledgement

This study was part of the international research training group INTERCOAST (“Integrated Coastal Zone and Shelf-Sea Research (IRTG1598)”), funded by the Deutsche Forschungsgemeinschaft (DFG). We thank Captain Karl Baumann and the crew of RV “Senckenberg” for their help

with sampling in 2010 and Corinna Schollenberger, Astrid Raschke, and Kerstin Thaler for their technical assistance. The local harbour authority (Wasser- und Schifffahrtsamt Wilhelmshaven (WSA)) provided data for dredging activities in the old navigation channel and the JadeWeserPort Realization Company provided data for dredging and dumping activities for the JWP and multibeam echosounder data, which are kindly acknowledged. Many thanks also to two anonymous reviewers for helpful comments on the manuscript and to Rachel J. Harris for English corrections.

8.8. References

- Anderson, M.J., Ford, R.B., Feary, D.A., Honeywill, C. 2004. Quantitative measures of sedimentation in an estuarine system and its relationship with intertidal soft-sediment infauna. *Mar. Ecol. Prog. Ser.*, 272, 33-48.
- Anderson, M.J., Gorley, R.N., Clarke, K.R. 2008a. PERMANOVA+ for PRIMER: guide to software and statistical models. PRIMER-E Ltd., Plymouth.
- Ashley, G.M. 1990. Classification of large-scale subaqueous bedforms; a new look at an old problem, *Journal of Sedimentary Research*, 60, 160-172.
- Auster, P.J., Langton, R.W. 1998. The effects of fishing on fish habitat. Paper presented at the Sea Grant Symposium on Fish Habitat - Essential Fish Habitat and Rehabilitation at the 1998 Annual Meeting, Hartford, Connecticut, 26-27 August 1998.
- Bolam, S.G., Fernandes, T.F. 2003. Dense aggregations of *Pygospio elegans* (Claparède): effect on macrofaunal community structure and sediments. *J. Sea Res.*, 49, 171-185.
- Borja, À., Chust, G., del Campo, A., González, M., Hernández, C. 2013. Setting the maximum ecological potential of benthic communities, to assess ecological status, in heavily morphologically-modified estuarine water bodies. *Mar. Pollut. Bullet.*, 71, 199-208.
- Borja À., Dauer, D.M., Elliott, M., Simenstad, C.A. 2010. Medium- and long-term recovery of estuarine and coastal ecosystems: patterns, rates and restoration effectiveness. *Estuar. Coast.*, 33, 1249-1260.
- Boyd, S.E., Cooper, K.M., Limpenny, D.S., Kilbridge, R., Rees, H.L., Dearnaley, M.P., Stevenson, J., Meadows, W.J., Morris, C.D. 2004. Assessment of the rehabilitation of the seabed following marine aggregate dredging. Science Series Technical Report, 154 pp.
- Boyd, S.E., Limpenny, D.S., Rees, H.L., Cooper, K.M. 2005. The effects of marine sand and gravel extraction on the macrobenthos at a commercial dredging site (results 6 years post-dredging). *ICES J. Mar. Sci.*, 62, 145-162.
- Boyd, S.E., Limpenny, D.S., Rees, H.L., Cooper, K.M., Campbell, S. 2003. Preliminary observations of the effects of dredging intensity on the re-colonisation of dredged sediments off the southeast coast of England Area, *Estuar. Coast. Shelf Sci.*, 57, 209-223.
- Bray, J.R., Curtis, J.T. 1957. An ordination of the upland forest communities of southern Wisconsin. *Ecol. Monogr.*, 27, 325-349.

- Briggs, K.B., Williams, K.L., Richardson, M.D., Jackson, D.R. 2001. Effects of changing roughness on acoustic scattering: (1) natural changes. In: Leighton, T.G., Heald, G.J., Griffiths, G., Griffiths, H.D. (Eds), *Proceedings of the Institute of Acoustics*, 23 (2), 343-390.
- Brown, C.J., Collier, J.S. 2008. Mapping benthic habitat in regions of gradational substrata: An automated approach utilising geophysical, geological, and biological relationships. *Estuar. Coast. Shelf Sci.*, 78, 203-214.
- Brown, C.J., Cooper, K.M., Meadows, W.J., Limpenny, D.S., Rees, H.L. 2002. Small-scale Mapping of Sea-bed Assemblages in the Eastern English Channel Using Sidescan Sonar and Remote Sampling Techniques. *Estuar. Coast. Shelf Sci.*, 54, 263-278.
- Brown, C.J., Hewer, A.J., Limpenny, D.S., Cooper, K.M., Rees, H.L. 2004a. Mapping seabed biotopes using sidescan sonar in regions of heterogeneous substrata: Case study east of the Isle of Wight, English Channel. *Int. J. Soc. Underwater Technol*, 26 (1), 27-36.
- Brown, C.J., Hewer, A.J., Meadows, W.J., Limpenny, D.S., Cooper, K.M., Rees, H.L. 2004b. Mapping seabed biotopes at Hasting Shingle Bank, eastern English Channel. Part I. Assessment using sidescan sonar. *J. Mar. Biol. Assoc. UK*, 84, 481-488.
- Capperucci, R., Bartholomä, A. 2012. Sediment vs. topographic roughness: anthropogenic effects on acoustic seabed classification. In: Leendert Dorst, L., van Dijk, T., van Ree, R., Boers, J., Brink, W., Kinneking, N., van Lancker, V., de Wulf, A., Nolte, H. (Eds), *Conference Proceedings of Hydro12, Taking care of the sea, the Hydrographic Society Benelux (HSB), on behalf of the International Federation of Hydrographic Societies (IFHS), Rotterdam, the Netherlands, 12-15 November 2012*, 23-28.
- Clarke, K.R., Gorley, R.N. 2006. *PRIMER v6: User Manual/Tutorial*. PRIMER-E, Plymouth.
- Clarke, K.R., Warwick, R.M. 2001. *Change in Marine Communities: An Approach to Statistical Analysis and Interpretation*. second edn. PRIMER-E, Plymouth.
- Cochrane, G.R., Lafferty, K.D. 2002. Use of acoustic classification of sidescan sonar data for mapping benthic habitat in the Northern Channel Islands, California. *Cont. Shelf Res.*, 22, 683-690.
- Collier, J.S., Brown, C.J. 2005. Correlation of sidescan backscatter with grain size distribution of surficial seabed sediments. *Mar. Geol.*, 214, 431-449.
- Cooper, K.M., Eggleton, J.D., Vize, K., Vanstaen, K., Boyd, S.E., Ware, S., Morris, C.D., Curtis, M., Limpenny, D.S., Meadows, W.J. 2005. Assessment of the rehabilitation of the seabed following marine aggregate dredging - Part II. Science Series Technical Report, 81 pp.
- Coosen, J., Seys, J., Meire, P.M., Craeymeersch, J.A.M. 1994. Effect of sedimentological and hydrodynamical changes in the intertidal areas of the Oosterschelde estuary (SW Netherlands) on distribution, density and biomass of five common macrobenthic species: *Spio martinensis* (Mesnil), *Hydrobia ulvae* (Pennant), *Arenicola marina* (L.), *Scoloplos armiger* (Muller) and *Bathyporeia* sp. *Hydrobiologia*, 282/283, 235-249.
- De Falco, G., Tonielli, R., Di Martino, G., Innangi, S., Simeone, S., Parnum, I.M. 2010. Relationships between multibeam backscatter, sediment grain size and *Posidonia oceanica* seagrass distribution. *Cont. Shelf Res.*, 30, 1941-1950.
- Degraer, S., Moerkerke, G., Rabaut, M., VanHoey, G., DuFour, I., Vincx, M., Henriët, J.P., VanLancker, V. 2008. Very-high resolution side-scan sonar mapping of biogenic reefs of the tube-worm *Lanice conchilega*. *Remote Sens. Environ.*, 112, 3323-3328.

-
- Diaz, R.J., Solan, M., Valente, R.M. 2004. A review of approaches for classifying benthic habitats and evaluating habitat quality. *J. Environ. Manage.*, 165-181.
- Eastwood, P.D., Souissi, S., Rogers, S.I., Coggan, R.A., Brown, C.J. 2006. Mapping seabed assemblages using comparative top-down and bottom-up classification approaches. *Can. J. Aquat. Sci.*, 63, 1536-1548
- Ehrhold, A., Hamon, D., Guillaumont, B. 2006. The REBENT monitoring network, a spatially integrated, acoustic approach to surveying nearshore macrobenthic habitats: application to the Bay of Concarneau (South Brittany, France). *ICES J. Mar. Sci.*, 63, 1604-1615
- Fenchel, T., Kofoed, L.H., Lappalainen, A. 1975. Particle size-selection of two deposit feeders: the Amphipod *Corophium volutator* and the Prosobranch *Hydrobia ulvae*. *Mar. Biol.*, 30, 119-128.
- Ferrini, V.L., Flood, R.D. 2006. The effects of fine-scale surface roughness and grain size on 300 kHz multibeam backscatter intensity in sandy marine sedimentary environments. *Marine Geology*, 228, 153-172.
- Folk, R.L. 1954. The distinction between grain size and mineral composition in sedimentary-rock nomenclature. *J. Geol.*, 62 (4), 344-359.
- Franklin, E.C., Ault, J.S., Smith, S.G., Luo, J., Meester, G.A., Diaz, G.A. 2003. Benthic habitat mapping in the Tortugas region, Florida. *Mar. Geod.*, 26, 19-34.
- Freitas, R., Rodrigues, A.M., Quintino, V. 2003a. Benthic biotopes remote sensing using acoustics. *J. Exp. Mar. Biol. Ecol.*, 285-286, 339-353.
- Freitas, R., Sampaio, L., Oliveira, J., Rodrigues, A.M., Quintino, V. 2006. Validation of soft bottom benthic habitats identified by single-beam acoustics. *Mar. Pollut. Bull.*, 53, 72-79.
- Freitas, R., Sampaio, L., Rodrigues, A.M., Quintino, V. 2005. Sea-bottom classification across a shallow-water bar channel and near-shore shelf, using single-beam acoustics. *Estuar. Coast. Shelf Sci.*, 65, 625-632.
- Freitas, R., Silva, S., Quintino, V., Rodrigues, A.M., Rhynas, K., Collins, W.T. 2003b. Acoustic seabed classification of marine habitats: studies in the western coastal-shelf area of Portugal. *ICES J. Mar. Sci.*, 60, 599-608.
- Gleason, A.C.R. 2009. Single-Beam Acoustic Seabed Classification in Coral Reef Environments with Application to the Assessment of Grouper and Snapper Habitat in the Upper Florida Keys, USA. Ph.D. Thesis, University of Miami, Florida.
- Gleason, A.C.R., Eklund, A.M., Reid, R.P., Koch, V. 2006. Acoustic Seabed Classification, Acoustic Variability, and Grouper Abundance in a Forereef Environment. NOAA Professional Papers NMFS, 5, 38-47.
- Gray, J.S. 1974. Animal-sediment relationships. *Oceanogr. Mar. Biol. Annu. Rev.*, 12, 223-261.
- Gutperlet, R., Capperucci, R.M., Bartholomä, A., Kröncke, I. 2015. Benthic biodiversity changes in response to dredging activities during the construction of a deep-water port. *Mar. Biod.*, 45, 819-839.
- Hitchcock, D.R., Bell, S. 2004. Physical impacts of marine aggregate dredging on seabed resources in coastal deposits. *J. Coast. Res.*, 20 (1), 101-114.
- Holler, P., Markert, E., Bartholomä, A., Capperucci, R., Hass, H.C., Kröncke, I., Mielck, F., Reimers, H.C. 2016. Tools to evaluate seafloor integrity: comparison of multi-device acoustic seafloor classifications for benthic macrofauna-driven patterns in the German

- Bight, southern North Sea. *Geo-Mar Lett.*, 37 (2), 1-17, doi: 10.1007/s00367-016-0488-9
- ICES 1992. Report of the ICES working group on the effects of extraction of marine sediments on fisheries. *ICES Coop. Res. Rep.*, 182, 78 pp.
- ICES 2001. Effects of extraction of marine sediments on the marine ecosystem. *ICES Coop. Res. Rep.*, 247, 84 pp.
- Johnson, R.G. 1972. Conceptual models of marine benthic communities. In: Schopf TJM (ed) *Models in paleobiology*. Freeman Cooper and Co., San Francisco, 148-159.
- Jost, L. 2006. Entropy and diversity. *Oikos*, 113, 363-375.
- Kenny, A.J., Cato, I., Desprez, M., Fader, G., Schüttenhelm, R.T.E., Side, J. 2003. An overview of seabed-mapping technologies in the context of marine habitat classification. *ICES J. Mar. Sci.*, 60, 411-418.
- Kenny, A.J., Rees, H.L. 1994. The effects of marine gravel extraction on the macrobenthos - early post-dredging recolonization. *Mar. Pollut. Bull.*, 28 (7), 442-447.
- Kenny, A.J., Rees, H.L. 1996. The effects of marine gravel extraction on the macrobenthos: Results 2 years post-dredging. *Mar. Pollut. Bull.*, 32 (8-9), 615-622.
- Kenny, A.J., Rees H.L., Greening, J., Campell, S. 1998. The effects of marine gravel extraction on the macrobenthos at an experimental dredge site off North Norfolk, UK (results 3 years post-dredging). *ICES Document CM*, 14, 7 pp.
- Kostylev, V.E., Todd, B.J., Fader, G.B.J., Courtney, R.C., Cameron, G.D.M., Pickrill, R.A. 2001. Benthic habitat mapping on the Scotian Shelf based on multibeam bathymetry, surficial geology and sea floor photographs. *Mar. Ecol. Prog. Ser.*, 219, 121-137.
- Kröncke, I. 2006. Structure and function of macrofaunal communities influenced by hydrodynamically controlled food availability in the Wadden Sea, the open North Sea and the Deep-sea. A synopsis. *Senckenb. marit.*, 36 (2), 123-164.
- Krumhansl, K., Jamieson, R., Krkosek, W. 2016. Using species traits to assess human impacts on near shore benthic ecosystems in the Canadian Arctic. *Ecological Indicators*, 60, 495-502
- Kruskal, J.B. 1964. Nonmetric multidimensional scaling: a numerical method. *Psychometrika*, 29, 115-129.
- Kubicki, A., Bartholomä, A. 2011. Sediment dynamics in the Jade tidal channel prior to port construction, southeastern North Sea. *J. Coast. Res.*, 64, 771-775.
- Legendre, P., Anderson, M.J. 1999. Distance-based redundancy analysis: testing multispecies responses in multifactorial ecological experiments. *Ecol. Monogr.*, 69, 1-24.
- Legendre, P., Birks, H.J.B. 2012. Chapter 8: from classical to canonical ordination. In: Birks HJB, Lotter AF, Juggins S, Smol JP (eds) *Tracking environmental change using Lake sediments*, vol 5: data handling and numerical techniques. Springer, Dordrecht, 201-248.
- Lucieer, V. 2008. Object-oriented classification of sidescan sonar data for mapping benthic marine habitats. *Int J Mar Sensing*, 29, 905-921.
- Markert, E., Holler, P., Kröncke, I., Bartholomä, A. 2013. Benthic habitat mapping of sorted bedforms using hydroacoustic and ground-truthing methods in a coastal area of the German Bight/North Sea. *Estuar. Coast. Shelf Sci.*, 129, 94-104.
- Markert, E. 2015. Habitat mapping of the seabed in the German Bight based on the study of small- and large-scale variability of macrofauna communities and their hydroacoustic signals. Dissertation, Carl von Ossietzky University, Oldenburg.

-
- Markert, E., Kröncke, I., Kubicki, A. 2015. Small scale morphodynamics of shoreface-connected ridges and their impact on benthic macrofauna. *J. Sea Res.*, 99, 47-55.
- McArdle, B.H., Anderson, M.J. 2001. Fitting multivariate models to community data: a comment on distance-based redundancy analysis. *Ecology*, 82, 290-297.
- Newell, R.C., Seiderer, L.J., Hitchcock, D.R. 1998. The impact of dredging works in coastal waters: a review of the sensitivity to disturbance and subsequent recovery of biological resources on the sea bed. *Oceanogr. Mar. Biol. Annu. Rev.*, 36, 127-178.
- Newell, R.C., Seiderer, L.J., Simpson, N.M., Robinson, J.E. 2002. Impact of marine aggregate dredging and overboard screening on benthic biological resources in the central North Sea: production licence area 408, coal pit. Marine Ecological Surveys Limited Technical Report No ER1/4/02 to the British Marine Aggregate Producers Association, 72 pp.
- Ojeda, G.Y., Gayes, P.T., Van Dolah, R.F., Schwab, W.C. 2004. Spatially quantitative seafloor mapping: examples from the southern North Carolina inner continental shelf. *Estuar. Coast. Shelf, Sci.*, 59, 399-416.
- Pinn, E.H., Robertson, M.R. 2003. Effect of track spacing and data interpolation on the interpretation of benthic-community distributions derived from RoxAnn™ acoustic surveys. *ICES Journal of Marine Science.*, 60, 1288-1297.
- Preston, J.M. 2006. Acoustic classification of seaweed and sediment with depth-compensated vertical echoes. In: *Proceedings of MTS/IEEE Oceans 2006*. Boston USA, 1-5.
- QuesterTangentCorporation 2003. Mapping Intertidal Oysters with QTC View, North Inlet - Winyah Bay, South Carolina. QTC Technical Report SR 41-03, 22 pp.
- Rhoads, D.C. 1974. Organism-sediment relations on the muddy sea floor. *Oceanogr. Mar. Biol. Annu. Rev.*, 12, 263-300.
- Robert, K., Jones, D.O.B., Huvenne, V.A.I. 2014. Megafaunal distribution and biodiversity in heterogeneous landscape: the iceberg-scoured Rockall Bank, NE Atlantik. *Mar. Ecol. Prog. Ser.*, 501, 67-88.
- Schrottke, K., Becker, M., Bartholomä, A., Flemming, B.W., Hebbeln, D. 2006. Fluid mud dynamics in the Weser estuary turbidity zone tracked by high-resolution side-scan sonar and parametric sub-bottom profiler. *Geo-Mar Lett*, 26, 185-198.
- Schückel, U., Beck, M., Kröncke, I. 2015. Macrofauna communities of tidal channels in Jade Bay (German Wadden Sea): spatial patterns, relationships with environmental characteristics, and comparative aspects. *Mar. Biodiv.*, 45, 841-855.
- Shepard, R.N. 1962. The analysis of proximities: multidimensional scaling with an unknown distance function. *Psychometrika*, 27 (125-140), 219-246.
- Shumchenia, E.J., King, J.W. 2010. Comparison of methods for integrating biological and physical data for marine habitat mapping and classification. *Cont. Shelf Res.*, 30, 1717-1729.
- Simonini, R., Ansaloni, I., Bonini, P., Grandi, V., Graziosi, F., Iotti, M., Massamba-N'Siala, G., Mauri, M., Montanari, G., Preti, M., De Nigris, N., Prevedelli, D. 2007. Recolonization and recovery dynamics of the macrozoobenthos after sand extraction in relict sand bottoms of the Northern Adriatic Sea. *Mar. Environ. Res.*, 64, 574-589.
- Snelgrove, P.V.R., Butman, C.A. 1994. Animal-sediment relationship revisited: cause versus effect. *Oceanogr. Mar. Biol. Annu. Rev.*, 32, 111-117.
- Tebble, N. 1976. British bivalve seashells - a handbook for identification. Second edn. Royal Scottish Museum, Edinburgh.

- Urlick, R. 1983. Principles of Underwater Sound. McGraw-Hill Book Company, New York.
- Van Dalfts, J.A., Essink, K., Madsen, H.T., Birklund, J., Romero, J., Manzanera, M. 2000. Differential response on macrozoobenthos to marine sand extraction in the North Sea and the Western Mediterranean. *ICES J. Mar. Sci.*, 57, 1439-1445.
- Van Overmeeren, R., Craeymeersch, J., Van Dalfts, J., Fey, F., Van Heteren, S., Meesters, E. 2009. Acoustic habitat and shellfish mapping and monitoring in shallow coastal water - sidescan sonar experiences in the Netherlands. *Estuar. Coast. Shelf Sci.*, 85 (3), 437-448.
- Warwick, R.M. 1993. Environmental impact studies on marine communities: pragmatical considerations. *Aust. J. Ecol.*, 18, 63-80.
- Wieking, G., Kröncke, I. 2005. Is benthic trophic structure affected by food quality? The Dogger Bank example. *Mar. Biol.*, 146 (2), 387-400.
- Zajac, R.N., Lewis, R.S., Poppe, L.J., Twichell, D.V., Vozarik, J., DiGiacomo-Cohen, M.L. 2003. Responses of infaunal populations to benthoscape structure and the potential importance of transition zones. *Limnol. Oceanogr.*, 48 (2), 829-842.

Page left intentionally blank

Chapter 9

Synthesis and future perspectives

The chapters presented in this doctoral thesis investigated specific aspects of seafloor habitat mapping based on hydroacoustic and in-situ sampling techniques, and examined the response of peculiar habitats to human disturbance, particularly regarding the construction of a deep water container terminal in the Jade area. The main goals of the thesis were a) to discriminate the influence of the seafloor roughness components (*topographic*, *sediment*, and *benthic roughness*) in modifying the acoustic backscatter intensity; b) to evaluate the performance of different acoustic systems (sidescan sonar, SSS; singlebeam, SBES; multibeam echo sounders, MBES), especially in mapping sharp and transitional habitat changes (i.e. characterized by “crisp” and “fuzzy” boundaries, Harris 2012) by means of both automatic and expert-based classification strategies; c) to estimate the impact on sediments and bio-communities caused by the dredging/dumping activities connected to the construction of a deep-water container terminal (JadeWeser Port). Five research sites within three areas of the German Bight (Jade, Norderney, Helgoland) were considered, characterized by highly dynamic tidal regimes and by different degrees of human disturbance.

9.1. Jade

In highly disturbed areas (like the inner Jade Channel), the presence of multiple generations of dredging marks dominated the automatic and semiautomatic classification outcomes more than the actual differences in sediment composition and distribution (*topographic roughness* >> *sediment roughness*). In fact, despite the presence of distinctive sediments (spanning from gravel content > 65% to sand > 95% to mud > 75%), the SSS, SBES, and MBES classifications largely corresponded to the morphological regions. In addition, the repetition of multiple sampling on the same location at different tidal stages (high water, ebb, low water, and flood) showed a high variability in sediment

composition. For instance, sediments with mud content difference $> 70\%$ were collected at the same sampling station. Such discrepancies could be linked both to patchy-like structures of the seafloor (as showed in the acoustic data) and/or to the influence of the tide-driven near-to-bed sediment movements.

The environmental impact due to the JadeWeser Port was also addressed. The results showed both a direct and indirect influence of dredging/dumping activities on the local bio-communities, seafloor morphologies, and sediments. The material spilled during the land reclamation produced a clear coarsening of the sediments nearby the construction site. The removal of the Holocene cover and the digging of Pleistocene clay deposits (Lauenburger Ton) introduced sediment types that used to be sub-represented in the area. The dredging connected to the new shipping route produced direct bathymetric changes and the mechanical removal of the existing bio-communities. As a consequence, opportunistic and highly mobile species quickly colonized the newly created ecological niches. This resulted in a general increase of the taxa number and abundance, if compared with the pre-disturbance setting. Even the areas not directly affected by digging/dumping works were impacted by higher suspension rates of remobilized material, with an increased abundance of suspension feeders.

Having considered the limits of acoustic-based classifications in such a complex environment, a SSS dataset was classified (using an expert based approach) and multivariate statistical descriptors were used for testing the pattern congruence among sediment types, benthic communities, and backscatter. The results showed a low, yet significant correlation between macrofauna abundance and both sediments and acoustic classes. Most important, the statistics indicated no correlation between sediments and acoustic classes, confirming that the *topographic roughness* is the most relevant backscatter drivers in this area.

The results pointed out the need of specific strategies for acoustic and sediment data collection in highly dynamic and disturbed habitats. In fact, as highlighted by Brown and Collier (2008), it is not always possible to extrapolate substrate types into habitat maps only based on acoustic data, both in natural and human disturbed environments. More specifically, the Jade area demonstrates that, where human activities produce direct changes in bathymetry and morphology of the seafloor, the backscatter intensity and texture (and, in particular, the relative automatic classification outcomes) are mostly driven by such features (*topographic roughness*) rather than by other seabed attributes (potentially relevant for habitat mapping), like sediments and benthic organisms. Therefore, in such environments the backscatter record should be always coupled at least with high resolution bathymetric data, in order to weigh the role of the

morphology. An expert-based approach is also recommended. In addition, in extremely dynamic environments where sediment transport and deposition processes change continuously, data gathered at a given time may not be representative of the actual seafloor properties; for instance, acoustic data and sediments not collected during the same tidal stage may differ significantly. The repetition of bottom sampling and acoustic data collection has to be considered, therefore, as a necessary step for assessing the variability of such environments and the quality of the related seafloor/habitat classification.

The Jade area offers the opportunity for assessing the ecological reaction of a system to port construction on a medium-long term time scale. A scientific survey should be carried out in the near future in order to investigate the rearrangement of sediments and benthic communities after their initial response to the human-induced stress. The hydrodynamic simulation produced during the container terminal planning phase (Kahlfeld and Schüttrumpf 2006) expected variations in current speed and suspended sediments only nearby the land-reclaimed site, due to the physical compensation effect of a reduced channel cross section and a deepening of the shipping channel. Further investigations about changes in sediments and bio-communities in the close area of the Jade Bay will point out possible effects of the port construction on undisturbed regions, where habitat composition was described before (for instance by Schückel and Kröncke 2013).

9.2. Norderney

In the backbarrier of Norderney, where the human disturbance is mainly expressed as a long term reaction of the ecosystem to the historical shaping of the whole coastal area (e.g. by diking, drainage of marshes and land reclamation, etc.), gentle seafloor morphologies were observed and the sediment composition reflected a typical tidal-flat sequence. The main morphological elements corresponded to the drainage system (intertidal and subtidal gullies and channels) and sediments ranged from mud to muddy sand, with the coarser fraction (mainly shell debris) occurring in the channels. The most prominent biological assemblage was represented by shellfish beds of different size (from $< 1 \text{ m}^2$ to $>100\text{m}^2$). In such complex system (where *topographic* \approx *sediment* \approx *benthic roughness*, and transitions among different substrate types were gradational), the attempt to classify the SSS record by means of automatic classification tools led to poor results. An expert-based classification was therefore preferred and the area was segmented in 10 classes depending on sediment characteristics, seafloor texture,

and the presence of shellfish beds. The collection of a second SSS dataset in bad sea conditions highlighted also the limits of such system, as the quality of the data was adversely affected and only the main elements (drainage network, shellfish beds, and tidal flat deposits) were identifiable. The research presented one of the first successful application of SSS for seafloor mapping of extremely shallow water intertidal and subtidal environments (min. water depth ≈ 70 cm), in which satellite/airborne remote sensing systems are usually preferred for their ability to cover large areas in a short time. The comparison with an existing classification based on RapidEye data (Jung et al. 2015) highlighted the superior ability of SSS in resolving seafloor structures, sediment classes, and shellfish beds.

For the future, a further step would be to test the use of the acoustic and sediment-based classes for training such satellite-based classification algorithms. A comparison with different satellite/airborne remote sensing systems would also represent an interesting research topic (e.g. Greene et al. 2018): in the last years Lidar and TerraSAR-X data have been used for classifying intertidal regions in the Wadden Sea (Schmidt et al. 2012, Adolph et al. 2016, Adolph et al. 2018), offering a horizontal resolution comparable to the SSS images. While the analysis of those data was mainly limited to the recognition of the water/land boundary, of the main morphological features (channels, bedforms), and to the detection of the shellfish beds, a further segmentation of the datasets on the basis of the sediment/acoustic classes could potentially allow to spatially extend the high-resolution classification of the SSS over a much larger area. In addition, the deployment of drone-mounted compact Lidar and imaging sensors (e.g. Murfitt et al. 2017; Coveney et al. 2018) will open new perspectives towards the integration of the upper intertidal and supratidal environments with the seafloor classification obtained by hydroacoustic systems and surface sediment data.

9.3. Helgoland

A combination of crisp and fuzzy boundaries characterized the less disturbed seafloor in the vicinity of Helgoland, in which the three hydroacoustic sources were used. The automatic classification tools were able to correctly identify and map the sharp contact between the soft- and the hard ground regions (*topographic roughness* \gg *sediment and benthic roughness*) in both research sites. A number of studies showed the ability of hydroacoustic systems to map rigid or semi-rigid biogenic structures and assemblages (mussel beds, coral reefs, reef-building tubeworms, etc., e.g. Allen et al. 2005, Degraer et al. 2008, van Overmeeren et al. 2009, Flores and Siringan 2017). This research was able to

prove that dense communities of soft, centimeter-sized benthic organisms (devoid of rigid structures) modify the intensity of the acoustic backscatter, in regions characterized by homogeneous sediment composition and by the absence of dominant seafloor morphologies (*benthic roughness* >> *topographic and sediment roughness*). The gradual increase in backscatter intensity recorded in the soft ground area west of Helgoland, in fact, was attributed to the high density of the brittle star *Amphiura filiformis* (> 1700 individuals/m²) with their upstanding feeding arms. The interaction between the different roughness components played also an important role in the segmentation of the hard ground region in the “Helgoland Steingrund” site, where the acoustic systems alone could not discriminate between the colonized and non-colonized substrata and between the two different populations of bryozoan (*topographic roughness* >> *benthic roughness*).

The Norderney and Helgoland areas offer a good example of how the subdivision of the seafloor roughness into three main components is, to some degree, flexible and their definition is, at least in part, overlapping. For instance, the shellfish beds on the Norderney tidal flat produced a topographic relief on the seafloor. Similarly, the cobbles and boulders (sediments) in the “Steingrund” research site (Helgoland) created a morphological change in the seafloor topography. In such contexts, the seafloor roughness could be referred to as either *benthic* or *topographic roughness* (shellfish beds), and as either *sediment* or *topographic roughness* (hard ground deposits).

The research presented in this doctoral thesis provided new understanding of specific aspects in the field of the acoustic seafloor classification techniques. The outcomes of the present work were included in the recommendations and specification of scientific projects for habitat mapping and monitoring of German waters (WIMO Project; Bartholomä, Capperucci et al. 2016).

9.4. References

- Allen, Y., Wilson, C., Roberts, H., Supan, J. 2005. High resolution mapping and classification of oyster habitats in nearshore Louisiana using sidescan sonar. *Estuaries and Coasts*, 28, 435-446, doi: 10.1007/BF02693925.
- Adolph, W., Farke, H., Lehner, S., Ehlers, M. 2018. Remote sensing intertidal flats with TerraSAR-X. A SAR perspective of the structural elements of the tidal basin for monitoring the Wadden Sea. *Remote Sensing*, 10(7), 1085, doi: 10.3390/rs10071085.
- Adolph, W., Jung, R., Schmidt, A., Ehlers, M., Heipke, C., Bartholomä, A., Farke, H. 2016. Integration of TerraSAR-X, RapidEye and airborne lidar for remote sensing of intertidal

-
- bedforms on the upper flats of Norderney (German Wadden Sea). *Geo-Marine Letters*, 37(2), 193–205, doi: 10.1007/s00367-016-0485-z.
- Bartholomä, A., Capperucci, R.M., Haas, C., Kröncke, I., Mielck, F., Reimers, H.C., 2016. Hydroakustische Methoden im Habitatmonitoring. In: Winter, C., et al. 2016. WIMO – Wissenschaftliche Monitoringkonzepte für die Deutsche Bucht – Abschlussbericht, 29-41.
- Brown, C.J., Collier, J.S. 2008. Mapping benthic habitat in regions of gradational substrata: An automated approach utilising geophysical, geological, and biological relationships. *Estuar. Coast. Shelf Sci.*, 78(1), 203-214, doi: 10.1016/j.ecss.2007.11.026.
- Coveney, S., Butler, D., Monteys, X. 2018. Intertidal Feature Mapping from Sentinel and Drone (INTREPID), Technical Report, Geological Survey of Ireland, 2017-SC-031, doi: 10.13140/RG.2.2.19502.36163.
- Degraer, S., Moerkerke, G., Rabaut, M., Van Hoey, G., Du Four, I., Vincx, M., Henriët, J.-P., Van Lancker, V. 2008. Very-high resolution side-scan sonar mapping of biogenic reefs of the tube-worm *Lanice conchilega*. *Remote Sensing of Environment*, 112(8), 3323-3328, doi: 10.1016/j.rse.2007.12.012.
- Flores, P.C., Siringan, F. 2017. Mapping coral reefs using low-cost side scan sonar and satellite imagery in Masinloc, Zambales, Philippines. doi: 10.13140/RG.2.2.12653.08164.
- Harris, P.T. 2012. Biogeography, benthic ecology, and habitat classification schemes. In: Harris, P.T. and Baker, E.K. (Eds), *Seafloor geomorphology as benthic habitat*, Elsevier, 61-92, doi: 10.1016/B978-0-12-385140-6.00004-9.
- Greene, A., Rahman, A., Kline, R., Rahman, M. 2018. Side scan sonar: a cost-efficient alternative method for measuring seagrass cover in shallow environments. *Estuarine, Coastal and Shelf Science*, 207, 250-258, doi: 10.1016/j.ecss.2018.04.017.
- Jung, R., Adolph, W., Ehlers, M., Farke, H. 2015. A multi-sensor approach for detecting the different land covers of tidal flats in the German Wadden Sea — A case study at Norderney. *Remote Sensing of Environment*, 170, 188-202, doi: 10.1016/j.rse.2015.09.018.
- Kahlfeld, A. Schüttrumpf, H., 2006. UnTRIM modelling for investigating environmental impacts caused by a new container terminal within the Jade-Weser Estuary, German Bight. *Proceedings of the 7th International Conference of HydroScience and Engineering (Philadelphia, USA, ICHE)*.
- Murfitt, S.L., Allan, B.M., Bellgrove, A., Rattray, A., Young, M.A., Ierodiaconou, D. 2017. Applications of unmanned aerial vehicles in intertidal reef monitoring. *Nature Scientific Reports*, 7, 10259, doi: 10.1038/s41598-017-10818-9.
- Schmidt, A., Winny, A., Klonus, S., Ehlers, M., Farke, H., Soergel, U. 2012. Potential of airborne laser scanning data for classification of Wadden Sea areas. *Proceedings of the 32nd Earsel Symposium, Mykonos Island*, 495-502.
- Schückel, U., Kröncke, I. 2013. Temporal changes in intertidal macrofauna communities over eight decades: A result of eutrophication and climate change. *Estuarine, Coastal and Shelf Science*. 117, 210–218, doi: 10.1016/j.ecss.2012.11.008.
- van Overmeeren, R., Craeymeersch, J., van Dalfsen, J., Fey, F., Heteren, S., Meesters, E. 2009. Acoustic habitat and shellfish mapping and monitoring in shallow coastal water - Sidescan sonar experiences in The Netherlands. *Estuarine, Coastal and Shelf Science*, 85, 437-448, doi: 10.1016/j.ecss.2009.07.016.